Genetic analysis of the role of Epstein-Barr virus nuclear antigen leader protein (EBNA-LP) in B cell transformation.

Agnieszka Szymula

A thesis submitted for the degree of Doctor of Philosophy

2016

Imperial College London

Department of Medicine

Section of Virology

I. ABSTRACT

Epstein-Barr virus (EBV) is a gammaherpesvirus that causes infectious mononucleosis and is associated with several human malignancies. *In vitro*, EBV induces the activation and continuous proliferation of primary human B cells, which carry the viral genome as a latent episome. One of the latency-associated proteins is the EBV nuclear antigen leader protein (EBNA-LP). EBNA-LP is strongly expressed at the initiation of the transformation process and has been previously reported to assist the activation of genes by EBNA-2.

To investigate the role and mechanism of action of EBNA-LP in the context of viral infection and B cell transformation, I have generated EBNA-LP knockout EBVs (LP-KO ^{i}) and their revertants (LP-REV ^{i}) by recombineering in the B95.8 bacterial artificial chromosome (BAC). We found that B cells infected with LP-KO ^{i} were able to undergo limited proliferation. However, we were not able to establish LCLs after infection of EBV-negative B cells. We also found that LP-REV ^{i} was somewhat impaired in its transforming ability. We identified four nucleotide changes in EBNA-LP's introns in both LP-KO ^{i} and LP-REV ^{i} that may influence transforming abilities.

Therefore, new EBNA-LP knockouts (LP-KO ^{w}) containing wild-type intronic sequences were constructed. LP-KO ^{w} initially induced proliferation of adult B cells but then slowed around 5-14 days post infection, after which the cells recovered and established LCLs. However, in cord blood, LP-KO ^{w} failed to establish LCLs. Transcript level analysis in primary B cell infections showed that EBNA-LP can regulate the EBNA-2-regulated viral genes *LMP-1* and *LMP-2*, as well as the *EBER-2* gene, which is EBNA-2-independent. EBNA-LP has also a more limited role in modulating the EBNA-2-targeted host gene *HES-1*.

II. ACKNOWLEDGMENTS

First and foremost, I would like to thank my supervisor Dr. Rob White for his invaluable insight, unfailing support, endless enthusiasm and for making my Ph.D. experience productive and stimulating. My sincere contrafibularities on having me as your first Ph.D. student. It's been an honour!

I would also like to thank Prof. Martin Allday for valuable suggestions during the lab meetings and Prof. Paul Farrell for the support that allowed me to survive in London while I was writing this thesis.

Many thanks to all members of the Allday group, especially Ph.D. students: Jens Kalchschmidt, Guiyi Ho and Adam Gillman. Thank you so much for being my true friends, both in and outside of the lab! I am sure that I would have struggled without you. Jens, thanks for being such a great Robot, I hope that your basement is nice, and please remember: it wasn't Mr. Onion! Also, thank you to Gill Parker, who always kept everything and everyone organized.

And of course a big thank you to the White group: Dr. Richard Palermo and Mohammed Ba Abdullah. Richard, thanks for being my companion in the LP-misfortune; we both know that the "L" in EBNA-LP doesn't really stand for "leader" (if anything it's: lunatic, loser or licentious and libertine as it interacts with anything that's around… in a weird way…). We truly earned our nicknames of Weird and Crazy, as you have to be one of these to work on EBNA-LP with such excitement.

Last but not least, many thanks to my family and friends for constant support.

III. DECLARATION OF ORIGINALITY

All the work presented in this thesis is the result of my own work (except where indicated). This work was carried out at the Section of Virology, Faculty of Medicine, Imperial College London under the supervision of Dr. Rob White and co-supervision of Prof. Martin Allday.

IV. COPYRIGHT DECLARATION

V. ABBREVIATIONS

ADAR	Adenosine Deaminase Acting on RNA
ADP	Adenosine Diphosphate
AID	Activation-Induced Cytidine Deaminase
APS	Ammonium Persulphate
ATF4	Activating Transcription Factor 4
BAC	Bacterial Artificial Chromosome
BART	BamHI A Rightward Transcripts
BCR	B Cell Receptor
BL	Burkitt Lymphoma
BSA	Bovine Serum Albumin
CaHV	Callitrichine Herpesvirus
CAT	Chloramphenicol Acetyltransferase
CD	Cluster of Differentiation
CDKN2A	Cyclin-Dependent Kinase Inhibitor 2A
CeHV	Cercopithecine Herpesvirus
CF	Calibrator Factor
ChIP	Chromatin Immunoprecipitation
CIII	Complex III
Cm	Chloramphenicol

CMV	Cytomegalovirus
Cp	C Promoter
CR	Conserved Region
CRM1	Chromosome Region Maintenance 1
CtBP	C-Terminal Binding Protein
DAPI	4',6-Diamidino-2-Phenylindole
DLBCL	Diffuse Large B Cell Lymphoma
DMSO	Dimethyl Sulfoxide
DS	Dyad Symmetry
EBER	Epstein–Barr virus-Encoded small RNA
EBF1	Early B-Cell Factor 1
EBNA	Epstein-Barr virus Nuclear Antigen
EBV	Epstein-Barr Virus
ECL	Enhanced Chemiluminescence
EDTA	Ethylenediamine Tetra-Acetic Acid
EdU	5-Ethynyl-2'-Deoxyuridine
ELISA	Enzyme-Linked Immunosorbent Assay
ERK	Extracellular signal-Regulated Kinase
FBS	Foetal Bovine Serum
FSC	Forward Scatter
GaC	Gastric Carcinoma

GC	Germinal Centre
GFP	Green Fluorescent Protein
HAX-1	HCLS1-Associated Protein X-1
HCLS1	Hematopoietic Cell-specific Lyn Substrate 1
HDAC	Histone Deacetylase
HEK	Human Embryonic Kidney
HES1	Hairy and Enhancer of Split-1
HIF1α	Hypoxia-Inducible Factor 1-Alpha
HL	Hodgkin Lymphoma
HLA	Human Leukocyte Antigen
HP1	Heterochromatin Protein 1
HRP	Horseradish Peroxidase
HRS	Hodgkin Reed Sternberg
HSP	Heat Shock Protein
HSV	Herpes Simplex Virus
HT	4-Hydroxytamoxifen
IFI16	Interferon Inducible Protein 16
IFN	Interferon
Ig	Immunoglobulin
IL	Interleukin
IM	Infectious Mononucleosis

IR	Internal Repeat
IRF7	Interferon Regulatory Factor 7
JNK	C-Jun N-Terminal Kinase
Kan	Kanamycin
KO	Knockout
KSHV	Kaposi's Sarcoma-associated Herpesvirus
LAT	Latency-Associated Transcript
LB	Luria Broth
LCL	Lymphoblastoid Cell Lines
LCV	Lymphocryptovirus
LDHA	Lactate Dehydrogenase A
LMB	Leptomycin B
LMP	Latent Membrane Protein
LP	Leader Protein
MAD	Matrix-Associated Deacetylase
MBP	Maltose Binding Protein
MHV	Mouse Hepatitis Virus
miRNA	Micro RNA
MOI	Multiplicity Of Infection
MS	Multiple Sclerosis
NCoR	Nuclear receptor Co-Repressor

ND10	Nuclear Domains 10
NEB	New England Biolabs
NF-κB	Nuclear Factor Kappa-light-chain-enhancer of activated B cells
NHSBT	National Health Service Blood and Transplant
NK	Natural Killer cell
NLS	Nuclear Localization Signal
NOD	Non-Obese Diabetic
NoDS	Nucleolar Detention Sequence
NoLS	Nucleolar Localization Signal
NPC	Nasopharyngeal Carcinoma
OD	Optical Density
ORF	Open Reading Frames
OriLyt	Origin of Lytic replication
OriP	Origin of Plasmidial replication
PAGE	Poly-Acrylamide Gel Electrophoresis
PAMP	Pathogen-Associated Molecular Pattern
PARP	Poly ADP Ribose Polymerase
PBL	Peripheral-Blood Lymphocyte
PBS	Phosphate-Buffered Saline
PCA	Principal Component Analysis
PCR	Polymerase Chain Reaction

PDL	Population Doubling Level
PFA	Paraformaldehyde
PHD	Prolylhydroxylase
PI	Propidium Iodide
PML NB	Promyelocytic Leukemia Protein Nuclear Body
PMSF	Phenyl Methyl Sulphonyl Fluoride
PP2A	Protein Phosphatase 2A
PTLD	Post-Transplant Lymphoproliferative Disease
Qp	Q Promoter
RA	Rheumatoid Arthritis
RBPJ	Recombination Binding Protein-J
REV	Revertant
RIPA	Radioimmunoprecipitation Assay
RPS3A	Ribosomal Protein S3A
RT	Reverse Transcription
SB	Super Broth
SCID	Severe Combined Immunodeficiency
SDS	Sodium Dodecyl Sulphate
SIM	SUMO Interaction Motif
sisRNA	Stable Intronic Sequence RNA
sLCL	Spontaneous LCL

SLE	Systemic Lupus Erythematosus
SNP	Single Nucleotide Polymorphisms
SS	Sjögren's Syndrome
SSC	Side Scatter
STET	Sucrose Triton EDTA Tris
SUMO	Small Ubiquitin-like Modifier
TBE	Tris-Borate-EDTA
TE	Tris-EDTA
TEMED	NNN'N'-Tetramethylethylenediamine
Tet	Tetracycline
TGF-β	Transforming Growth Factor-Beta
TPA	12-O-Tetradecanoylphorbol-13-Acetate
TR	Terminal Repeat
UPR	Unfolded Protein Response
VCA	Virus Capsid Antigen
WB	Western Blotting
Wp	W Promoter
WT	Wild Type

VI. TABLE OF CONTENTS

VII. TABLE OF FIGURES

VIII. TABLE OF TABLES

1 INTRODUCTION

1.1 Overview of Epstein-Barr virus

Epstein-Barr virus (EBV) is a gamma-herpesvirus that asymptomatically infects up to 95% of the human population. Primary infection of EBV usually occurs in early childhood and causes a self-limiting proliferation of B cells, partially controlled by an elevated T cell response (Bakacs et al., 1978). The virus persists in a latent form for the rest of the person's life and is shed almost continuously. However, EBV infection during or after adolescence, can cause infectious mononucleosis (Balfour et al., 2015). EBV is also associated with several B cell lymphomas including endemic Burkitt lymphoma (Rowe et al., 2014), Hodgkin lymphoma (Vockerodt et al., 2014), diffuse large B cell lymphoma (Heslop, 2005), and the epithelial malignancies: nasopharyngeal carcinoma and gastric carcinoma (Chen, 2011). EBV-associated cancers occur most frequently in immunosuppressed individuals. For instance, EBV has been implicated in the majority of cases of post-transplant lymphoproliferative disease (Hopwood and Crawford, 2000).

1.2 Genetics of EBV

The Epstein–Barr virus is composed of a double-stranded approximately 172-kb long DNA genome that encodes more than 80 genes and non-coding RNAs (Baer et al., 1984). The genome is linear in a virus particle but circularized as an episome in the nucleus of infected cells (Lindahl et al., 1976); the circularization occurs by an unknown mechanism, but is due to the presence of variable number of tandemly arranged, approximately 0.5 kb long terminal repeat units (TRs) at the ends of the linear form (Zimmermann and Hammerschmidt, 1995). The EBV genome was first mapped using Southern blot

hybridization of radioactively labelled restriction fragments that were named from A to Z and then on to a, b, c, etc. based on their size, where A is the largest (Skare and Strominger, 1980) (Fig.1.1). The mapping was interpreted to show that the EBV genome is divided into two unique regions (short and long) by the major internal repeat (IR) consisting of variable numbers of W units, where each is 3 kb long (Fig.1.1). In contrast to alpha- and beta-herpesviruses, these two unique regions are placed in a specific orientation relative to each other (no genomic isomerization). The genome contains both polymerase II and III transcribed genes. Candidate open reading frames have been systematically named based on their position in BamHI restriction fragments (i.e. BARF1 is starting in BamHI A with rightward reading frame no1) (Skare and Strominger, 1980).

There is not yet a defined wild type EBV sequence, as there is significant variation in both the sequence and the copy numbers of many of the repeat arrays between different strains. However, the best characterized strain variation- based on EBV nuclear antigen 2 (EBNA-2) sequence- led to the classification of EBV into type 1 and type 2. These two variants have a clear phenotypic difference *in vitro*: type 1 is much more transforming than type 2 (Rickinson et al., 1987). The distinction between those two strains extends also to the family of EBV nuclear antigen 3 variations (Rowe et al., 1989) but the degree of change is smaller than in case of EBV nuclear antigen 2.

The first EBV strain that had its genome cloned and sequenced was type 1 EBV: B95.8 (Baer et al., 1984). This strain was obtained from an infectious mononucleosis patient's blood leukocytes and used to infect marmoset blood leukocytes in order to produce high titres of infectious virus, because human leukocytes infected with EBV produced very small amounts of EBV in an irregular manner (Miller and Lipman, 1973). Sequencing was based on previously generated EcoRI and BamHI restriction fragments. The B95.8 strain is widely used in laboratories worldwide; however, it is missing a 13.6 kb segment of its genome (Baer

et al., 1984) (Fig.1.1). This deleted fragment was subsequently sequenced from Raji strain (Parker et al., 1990) and an updated EBV genome consensus combining these was published several years later (de Jesus et al., 2003).

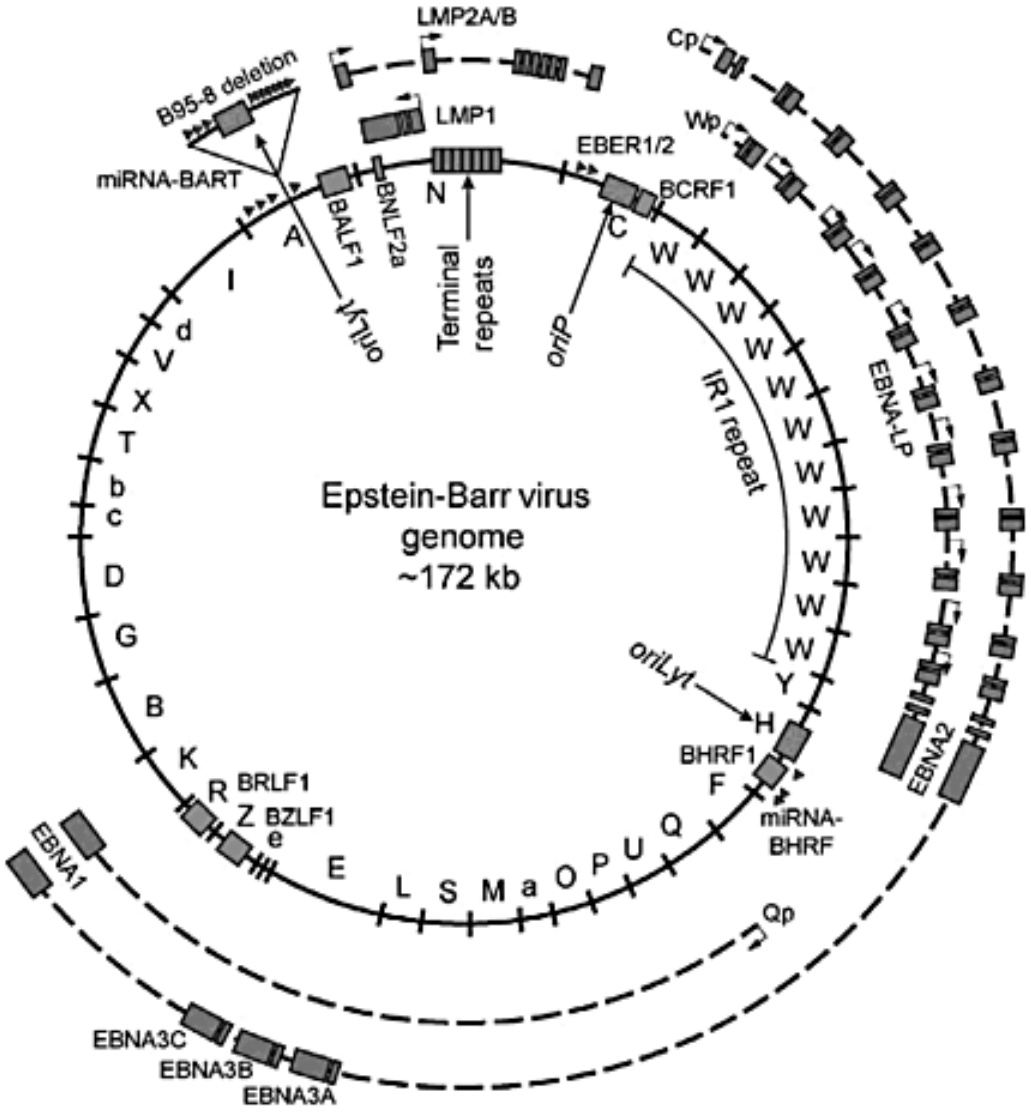

Fig. 1.1 Schematic of the EBV genome. Letters on the inner side of the circular genome describe the BamHI digestion fragments. The origin of plasmid replication (oriP), two origins of lytic replication (oriLyt) and the terminal repeats are indicated by arrows from the inner side of the circle. Lytic genes are shown in boxes placed in the inner circle. Dashed lines indicate intronic regions that are excised during splicing. Coding exons for the latent genes are shown in boxes on the dashed lines outside of the circle. Different promoters are marked by small arrows on the dotted line outside of the circle. The LMP promoters and the B95.8 deletion indicated outside of the circle. (Modified from Price and Luftig 2014).

1.3 Model of EBV persistence *in vivo*

In healthy individuals infected with EBV, the virus persists within memory B cells in a transcriptionally quiescent form. The current model proposed by Thorley-Lawson suggests that to establish persistence, EBV infects naïve B cells, activating them to become proliferating B-blasts using the growth transcription programme (also called latency III) (Thorley-Lawson and Babcock, 1999) (Fig.1.2). During latency III all six Epstein-Barr virus nuclear antigens (EBNAs) as well as latent membrane proteins (LMPs), EBV-associated small nuclear RNAs (EBERs), BHRF1 miRNAs and some of BamHI A rightward transcripts (BARTs) are expressed (Xing and Kieff, 2007) (Table 1.1). EBNAs are predominantly regulators of transcription, while LMPs activate signal transduction pathways, mainly helping to ensure cell survival (Found and Thorley-Lawson, 2001). This complex system of viral latent gene expression makes the EBV infected B cells morphologically and phenotypically very similar to normal B blasts, much like when naïve B cells have been activated by antigens and T cell help (Found and Thorley-Lawson, 2001).

These highly immunogenic EBV-activated B-blasts are a transient form *in vivo* and they are thought to migrate to a germinal centre (GC) following the gradient of lipid (7alpha,25-dihydroxycholesterol) produced by follicular lymphoid stromal cells. This lipid is recognized by chemokine receptor EBI2, which is up-regulated on the surface of both antigen- and EBV-activated B blasts (Gatto and Brink, 2013). Once in the GC, EBV-infected B-blasts undergo an initial expansion and differentiate into centroblasts, thereafter into centrocytes, mimicking affinity maturation of antigen-activated B cells (Roughan and Thorley-Lawson, 2009). In the GC, EBV-infected B cells switch from the growth transcription programme (latency III) into latency II, where most of the latent EBV nuclear antigen genes are shut-down such that only EBNA-1, LMP-1, LMP-2, EBERs and miRNAs are expressed (Found and Thorley-Lawson, 2001) (Fig.1.2; Table 1.1). In this state, EBNA-1

is still needed to maintain the viral genome as an episome. LMPs are thought to mimic the B cell receptor (BCR) and T-helper signals required for survival and thereafter permit differentiation into memory B cells (for details about LMP-1 and LMP-2 see section 1.8.2). EBNA-2 has to be turned off because its expression transactivates promoters of the latent genes, including those responsible for progression in the cell cycle (for details about EBNA-2 see section 1.8.1.2) (Thorley-Lawson and Babcock, 1999).

Infected centrocytes differentiate further into quiescent memory B cells, leaving the follicles and entering "true latency" in the peripheral blood (Thorley-Lawson and Babcock, 1999) (Fig.1.2). Once this latency in memory compartment is established, the expression of the latent proteins is not required anymore. Therefore, this transcription programme where no EBV proteins can be detected is called latency 0 (Thorley-Lawson and Babcock, 1999) (Table 1.1).

Occasionally EBV infected memory B cells re-enter the cell cycle to divide. This division is proposed to not to be driven by the virus but by the normal memory cell's homeostatic mechanisms. In this case EBNA-1 is the only EBV protein expressed, to support episome replication and segregation- this transcriptome profile is called as latency I (Thorley-Lawson and Babcock, 1999) (Fig.1.2; Table 1.1). Expression of EBNA-1 does not trigger a cytotoxic T cell response (Levitskaya et al., 1995), which makes the EBV-infected memory B cell not susceptible to immune surveillance.

Latently infected memory B cells can return to lymph nodes and receive signals to differentiate into plasma cells and produce the virus (for lytic cycle reactivation see section 1.5) (Laichalk and Thorley-Lawson, 2005) (Fig.1.2).

This model is based on evidence that some of the latent proteins (especially LMPs) can mimic the signals required for activation and differentiation of normal B cells, and the

observation that the EBV in peripheral circulation is restricted to memory B cells, whereas in tonsils the virus is detected in the presence of both naïve and memory B cells (Thorley-Lawson and Babcock, 1999). It has been also demonstrated that EBV-positive B cells found in the GC within tonsils, express functional and phenotypic markers of GC cells and they are in latency II stage (Roughan and Thorley-Lawson, 2009).

The model is supported by many different studies but there are still some issues that need resolving. For example, there is no evidence that expression of the full growth programme (latency III) is required to established latency. It has been also shown that naïve and memory B cells are equally susceptible to EBV infection (Ehlin-Henriksson et al., 2003) so either or both populations could theoretically be infected *in vivo*.

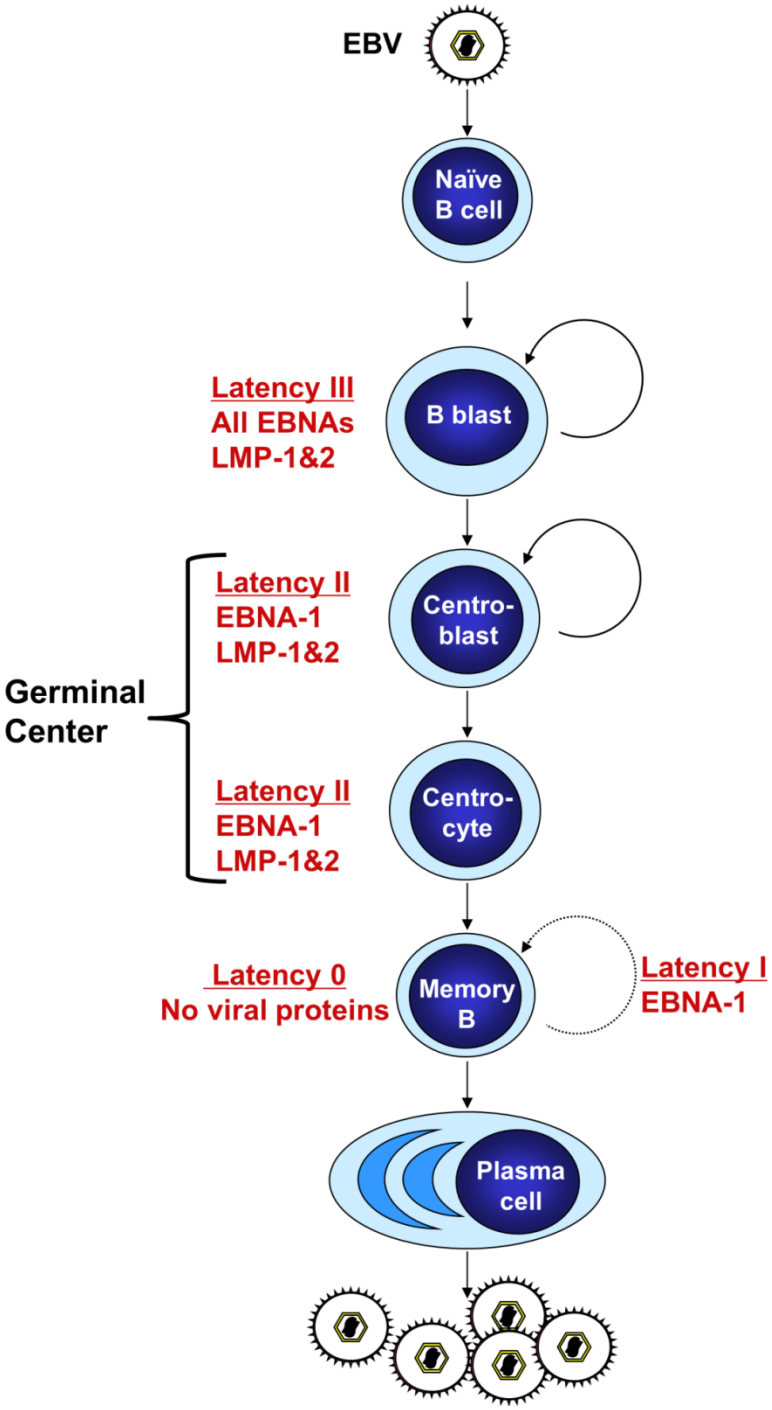

Fig. 1.2 Graphical representation of the Thorley-Lawson model of *in vivo* EBV life cycle. B cell differentiation states (white text within cells) is accompanied by distinct EBV gene expression profiles (red text), round arrows indicate stage where cells can proliferate. (Modified from Allday, 2009).

Latency Programme	Expressed EBV Genes	Used EBV Promoters	Occurrence during EBV life cycle	Occurrence in EBV-associated diseases
0	EBERs BARTs		Memory B cells in peripheral blood	
I	EBNA-1 EBERs BARTs	Qp	Dividing memory B cells	Burkitt lymphoma
II	EBNA-1 LMP-1 LMP-2 EBERs BARTs	Qp	Centroblasts and centrocytes	Hodgkin lymphoma and Nasopharyngeal carcinoma
III	EBNA-1 EBNA-2 EBNA-3A EBNA-3B EBNA-3C EBNA-LP LMP-1 LMP-2 EBERs BARTs	Wp Cp	Activated B-blasts and lymphoblastoid cell lines (LCLs)	Post-transplant lymphoproliferative disease

Table 1.1 EBV latency programmes. EBV latent gene expression and promoters' usage during different latency programmes and their occurrence in EBV life cycle and EBV-associated diseases.

1.4 Early EBV infection and transformation *in vitro*

Because the target for EBV infection is the naïve resting B cell (it expresses a marker of B cell lineage (CD19) and a marker of naïve B cells (IgD) but lacks a marker of germinal center cell (CD10) and a marker of memory B cell (CD27)) (Joseph et al., 2000), the virus has to initiate B cell entry from G0 state into the cell cycle to replicate its genome. The virus binds to B cells via gp350/220 expressed on the virion to complement receptor 2 (CR2 or CD21) present on the B cell, resulting in activation of signal transduction pathways and leading to efficient infection (for detailed EBV entry and tropism see section 1.6) (Sinclair and Farrell, 1995).

Within a few hours after infection, synthesis of EBV nuclear antigen 2 is initiated (Allday et al., 1989), which drives the cell into G1 phase of the cell cycle (Sinclair et al., 1994). Expression of EBV nuclear antigen 2 is accompanied by EBV nuclear antigen leader protein (detectable levels of both proteins are reached between 12h and 24h) (Allday et al., 1989, Sinclair et al., 1994), and followed by the expression of other EBV nuclear antigens (detectable between 24h and 40h post infection) and latent membrane proteins (detectable by western blot between 48h and 72h) (Allday et al., 1989). At this stage (72h) all of the EBV latent proteins are expressed. While the EBV nuclear antigens reach expression levels similar to those in established cell lines around 40h after infection (Allday et al., 1989), the latent membrane proteins are expressed at very low levels early after infection which increase rapidly with time post infection (Price et al., 2012).

Not only latent but also some lytic immediate early genes such as BZLF1 and BHRF1 are expressed early after infection of naïve B cells. Expression of these genes fails to induce the lytic cycle at that point. However, it has been shown that BZLF1 has also a crucial role in driving the proliferation of early infected B cells (Kalla et al., 2010).

The complete list of viral genes expressed within the first days after infection of primary B cells has not yet been systematically characterised. This pre-latent state of transcription lasts for about a week after infection and seems to end when EBV DNA acquires cellular nucleosomes and becomes methylated later during infection (Woellmer and Hammerschmidt, 2014).

After a few days of infection with EBV, the morphology of B cells changes dramatically; cells become large and irregular in shape, they develop short villipodia and start adhere to other infected B cells forming clumps of cells (Rowe, 1999).

EBV infection of naïve B cells results in their transformation into continuously proliferating lymphoblastoid cell lines (LCLs) which usually leads to their immortalization (a state when cells continue proliferating beyond 160 population doubling levels (PDLs) and express strong telomerase activity that is exceeding the average level of mortal LCLs 50 to 100 times) (Sugimoto et al., 1999). LCLs express all of the proteins/RNAs present during latency III (for latency see section 1.3). The virus production in LCLs is typically minimal or undetectable.

1.5 Lytic cycle reactivation

To produce infectious virus, EBV has to switch from the latent to the lytic phase. This transition is triggered by expression of the viral encoded transcription factors, BZLF1 (Hicks et al., 2003) and BRLF1 (Ye et al., 2007). The immediate early transcripts encoding BZLF1 and BRLF1 originate from two different promoters: Zp and Rp respectively. Rp transcripts however are bicistronic and can potentially make both BRLF1 and BZLF1 proteins (Manet et al., 1989). BZLF1 is the master regulator of lytic cycle; it induces BRLF1 and its own expression and initiates a cascade of viral lytic gene activation. These genes then work

together to create and shed fully formed viral progeny, completing the lytic cycle (Ragoczy and Miller, 1999).

The promoters that regulate expression of BZLF1 and BRLF1 are strongly repressed during latency. It has been shown that latent EBV DNA is unmethylated at active latency genes and fully methylated at completely repressed lytic promoters. BZLF1 can bind to methylated motifs in viral promoters to initiate their activation (Bhende et al., 2004). Upon BZLF1 binding, nucleosomes are removed, polycomb repression is lost, and RNA polymerase II is recruited to the activated early promoters, initiating lytic viral gene expression (Woellmer et al., 2012).

There are two origins of EBV DNA lytic replication (oriLyt) located approximately opposite each other in the EBV genome (Hammerschmidt and Sugden, 1988). Seven binding sites for BZLF1 are located within oriLyt. Transcription and DNA replication of oriLyt are two independent processes but they are both activated by similar combinations of BZLF1-binding sites (Schepers et al., 1996).

The lytic cycle can also be triggered by the differentiation of latently infected B cells into plasma cells. The key mediator of this differentiation- BLIMP1- has been identified as a contributing factor of EBV latent-to-lytic switch in some of EBV-positive B cell types by inducing transcription from Rp and Zp (Reusch et al., 2015).

In cell culture *in vitro*, methods of induction of the lytic cycle vary between independent cell lines. However, the most commonly used stimuli are: a combination of phorbol ester (i.e. TPA) and histone deacetylase inhibitor (i.e. sodium butyrate) as well as calcium ionophores (Falk and Ernberg, 1999), Ig cross-linking in Akata (Takada and Ono, 1989) and transforming growth factor-beta (TGF-β) (Liang et al., 2002).

1.6 EBV tropism

EBV requires at least 5 viral envelope glycoproteins for its efficient entry into a B cell: gp350, gp42 and gB (as gB homotrimer) are involved in attachment to the B cell, while gH and gL (as gHgL heterodimer) work with gB in inducing cell fusion: these last three are known as a core fusion machinery (Borza and Hutt-Fletcher, 2002). After attachment mediated by an interaction between EBV glycoprotein gp350 and the complement receptor type 2 (CR2) also known as cluster of differentiation 21 (CD21), the virus is endocytosed into a low pH compartment where the fusion occurs. Glycoprotein gp42 binds directly to gH and turns dimeric gHgL into a trimeric gHgLgp42 complex. This interaction changes the conformation of gp42 which induces its binding to the human leukocyte antigen (HLA) class II molecule. This interaction in turn, activates the core fusion machinery allowing for efficient infection of B cells. Additionally, gH can bind cellular integrins. The amount of gp42 in the virion is lower than the amount of gHgL, which results in more heterodimers without gp42 as a third partner, making the heterodimers more accessible for integrins.

Epithelial cells do not express HLA class II constitutively, which makes gp42 useless in the fusion process. However, the interaction of dimeric gHgL complexes with integrins replaces the cell fusion triggered by the interaction of gp42 with HLA class II. When the virus is produced in B cells, the number of trimeric gHgLgp42 complexes is reduced, because gp42 interacts with HLA class II in the secretory pathway during virus assembly, targeting the gp42/HLA complex to the peptide loading compartment, where they are then degraded by proteases. In contrast, virus produced in epithelial cells, which lack HLA class II, is enriched for trimeric gHgLgp42 complexes, as there is no gp42 degradation (Borza and Hutt-Fletcher, 2002). This use of dimeric gHgL complexes to trigger epithelial cell fusion and trimeric gHgLgp42 complexes to trigger B cell fusion is thought to cause the virus to switch its tropism between B cells and epithelial cells: the increase in gp42 in epithelial-derived virus

particles makes it 100-fold more infectious for a B cell than B-cell-derived virus. The opposite situation is not as dramatic: B-cell-derived virus is 5-fold more infectious for an epithelial cell than epithelial-derived virus (Chesnokova and Hutt-Fletcher, 2014).

The infection of epithelial cells by cell-free virus is generally inefficient. However, the rate of epithelial cell infection can be significantly increased by co-culture with EBV negative B cells (Shannon-Lowe et al., 2006): after binding to primary B cells, most of the virions are not internalized. These virions remain on the B cell surface and can be transferred to CD21-negative epithelial cells through the formation of an intracellular synapse. This transfer process requires the gp350-CD21 interaction and the gH and gB viral glycoproteins but is independent of gp42. It has been suggested that this mechanism allows EBV to simultaneously access both lymphoid and epithelial cells (Shannon-Lowe et al., 2006). There are also strain-specific differences in the ability of viruses to infect epithelial cells. For instance, cell-free M81 strain virus is much more efficient at infecting epithelial cells than B95-8 (Tsai et al., 2013).

1.7 EBV-associated diseases

EBV is associated with many malignant diseases such as lymphomas, carcinomas and also more benign ones such as infectious mononucleosis. EBV has also been proposed as a trigger/cofactor for some autoimmune diseases. Overall around 1-1.5% of worldwide cancer burden is estimated to be EBV-attributable (Parkin, 2006).

1.7.1 Infectious mononucleosis (IM)

A delay in primary EBV infection (most commonly where infection occurs after adolescence) can result in infectious mononucleosis (IM). Approximately 80% of primarily

infected adults develop symptoms like: sore throat, cervical lymphadenopathy (enlarged lymph nodes in the neck), fatigue, upper respiratory inflammation, headache, decreased appetite, fever and myalgia (muscle aches) (Balfour et al., 2013). The disease is characterized by the appearance of large number of lymphocytes, mostly CD8+ T cells, which can reach five to ten fold higher numbers in blood in comparison to healthy individuals (Strang and Rickinson, 1987). It is not clear, what drives such expansion of T cells in IM but factors like: failure of innate immune control by natural killer (NK) cells (Chijioke et al., 2013), EBV activation of pre-existing cross-reactive memory CD8+ T cells (Clute et al., 2005) or genetic background (Hwang et al., 2012) have been suggested.

The age-associated differences in the symptoms of primary infection, lead to questions about the differences between immature and adolescent/adult immune systems that might trigger the more severe symptoms. One theory that may account for this is that of heterologous immunity (Selin et al., 1998). This theory suggests that responses to new infections early in life are mostly triggered by naïve T cells, which then become memory T cells. With age the naïve T cell population decreases and each individual becomes more dependent on the diversity of potentially cross-reactive memory T cells (Clute et al., 2013).

A recent study in Gambian children has shown that asymptomatic EBV infection in children triggers a virus-specific CD8+ T cell response that can control the infection without over-expansion. These children were monitored for circulating EBV loads, antibody status against virus capsid antigen (VCA) and both total and virus-specific CD8+ T cells. Many children retained high virus loads comparable to IM patients and had detectable EBV-specific T cells expressing activation markers without IM-like symptoms. This response decreased over time and the cells lost activation markers in a similar way as seen in IM. However, in contrast to IM, the infections in children occurred without high expansion of total CD8+

numbers. Therefore, it has been suggested that the CD8+ T cells' over-expansion, rather than virus load per se, causes the symptoms of IM (Jayasooriya et al., 2015).

1.7.2 Burkitt lymphoma (BL)

Burkitt lymphoma (BL) is the tumor in which EBV was first discovered (Epstein et al., 1965). The defining feature of BL is translocation of the proto-oncogene MYC, usually into one of the immunoglobulin loci which results in deregulation (constitutive activation) of *MYC* transcription (Bemark and Neuberger, 2000). Burkitt lymphomas can be classified into three groups based on geographic distribution and EBV association: endemic, sporadic and HIV-associated (Brady et al., 2007). Sporadic Burkitt lymphoma is rarely associated with EBV and accounts for 1–2% of adult lymphomas in Western Europe and America. Endemic Burkitt lymphoma however, is associated with EBV in more than 95% cases and is mostly distributed in the equatorial part of Africa and other places with hyperendemic malaria. AIDS-associated BLs are approximately 30% EBV-positive (Brady et al., 2007). BL exhibits the same profile of immunoglobulin gene class switching and hypermutation as germinal center and memory B cells (Klein et al., 1995) and has a latency I EBV transcription program (Table 1.1). According to Thorley-Lawson model, this suggests that Burkitt lymphoma originates from a MYC translocation probably in a germinal centre centroblast that is on its way to become a memory B cell. Because of activated MYC, this cell remains in a proliferating state and therefore constitutively expresses EBNA-1 (Thorley-Lawson and Gross, 2004).

1.7.3 Hodgkin lymphoma (HL)

Approximately half of Hodgkin lymphomas (HL) are EBV-positive and for those, infectious mononucleosis is a predisposing factor (Hjalgrim et al., 2003). EBV-positive HLs express the latency II program (Table 1.1), which is normally found in latently infected germinal-center B cells (Thorley-Lawson and Gross, 2004). Hodgkin Reed Sternberg (HRS) cells are the hallmark of Hodgkin lymphoma. HRS cells are large, often multinucleated and do not resemble the phenotype of any normal cells in the body. The immunoglobulin genes of HRS cells are class-switched and hypermutated to the same extent as immunoglobulin genes of germinal center B cells (Küppers and Rajewsky, 1998), but EBV-positive Hodgkin disease is often characterized by non-functional Ig rearrangements or mutations (Kanzler et al., 1996). These data support the hypothesis that Hodgkin disease originates from EBV-infected germinal-center B cells. The Thorley-Lawson model proposes that HRS cells are centrocytes with inadequate antibody signaling that have been rescued from apoptosis by LMP-l and LMP-2A expression, but are prevented from exiting the cell cycle and becoming memory B cells (Thorley-Lawson and Babcock, 1999).

1.7.4 Post-transplant lymphoproliferative disease (PTLD)

Post-transplant lymphoproliferative disease (PTLD) is term given to a heterogeneous group of B-cell tumors that arise as a result of therapeutic immunosuppression. These tumors usually carry EBV and often express the latency III program (Thorley-Lawson and Gross, 2004) (Table 1.1). The major contributor to PTLD is an impaired cytotoxic T-cell response, which permits uninhibited growth of EBV-infected cells in their blast-like state (Found and Thorley-Lawson, 2001). To develop such a lymphoma, the EBV-infected cell must also fail in exiting the cell cycle and differentiating to become a resting memory B cell. These lymphoblasts continue to proliferate and are not killed because the cytotoxic T-cell response

is impeded (Thorley-Lawson and Gross, 2004). Based on Thorley-Lawson model of persistence (for the model see section 1.3), EBV infected B blasts expressing latency III should be restricted to the lymphoid tissue as their escape into the peripheral circulation would be atypical for B blast behavior (Thorley-Lawson and Babcock, 1999). The majority of PTLD is limited to the lymph nodes (extra nodal PTLD are less common and associated with genetic anomalies) and often resolves when immunosuppression is reduced, restoring more normal T cell function (Knowles et al., 1995).

1.7.5 Carcinomas

The mechanistic association of EBV with epithelial cell tumors such as nasopharyngeal carcinoma (NPC) and gastric carcinoma (GaC), is less clear than in case of lymphomas. It is currently thought to be caused by the establishment of virus latency in epithelial cells which display premalignant genetic changes (Young and Dawson, 2014). Almost all cases of non-keratinising nasopharyngeal carcinoma are EBV positive; the virus is present in all tumor cells (Niedobitek, 2000) and almost 10% of the gastric carcinomas are monoclonal proliferations of EBV-carrying tumor cells (Iizasa et al., 2012).

1.7.6 Autoimmunity

Epidemiologically, EBV is the most closely implicated infectious agent associated with autoimmune disorders such as multiple sclerosis (MS), systemic lupus erythematosus (SLE), Sjögren's syndrome (SS) and rheumatoid arthritis (RA). Associations of EBV with these diseases includes elevated titers of EBV antibodies, reduced T cell response against EBV and elevated EBV viral load. It is not clear if and how EBV triggers or increases autoimmunity. However it is known that it can influence the activation status of the immune

system by stimulating the production of pro-inflammatory mediators and this could potentially play a role in autoimmune pathogenesis (Draborg et al., 2013).

1.8 EBV latent genes

Latent EBV infection has a crucial role in causing many disorders. The pattern of EBV latent gene expression varies between different tumor types and highlights the impact of EBV latent proteins on cell growth and survival. The EBV latent proteins have different functions allowing for the maintenance of EBV in infected cells and the controlling of multiple signaling and transcriptional pathways leading to proliferation and survival of infected cells.

1.8.1 Epstein-Barr nuclear antigens (EBNAs)

1.8.1.1 EBNA-1

EBNA-1 is expressed in all dividing EBV-infected cells. The protein consists of a short N-terminal domain, which is separated from the rest of the protein by a long glycine-alanine repeat unit. This repeat interferes with the processing and MHC class I-restricted presentation of EBNA-1 peptides by the infected cells and as a result there is no CD8+ T cell-mediated response to latently infected cells, which express only EBNA-1 to maintain the virus (Levitskaya et al., 1995).

EBNA-1 is responsible for the replication and persistence of EBV episomes during latency. It mediates replication in synchrony with the host genome (Adams, 1987) via binding to the dyad symmetry (DS) element of the plasmid origin of replication (oriP) (Yates et al., 2000). EBNA-1 also binds to the family of repeats (FR) element of oriP, which

facilitates stable and even mitotic segregation of EBV episomes into daughter cells during cell division (Lupton and Levine, 1985). Binding of both elements by EBNA-1 results in the formation of a loop between them and allows EBV for long-term stable persistence in latently infected cells (Mackey and Sugden, 1999). It has been shown that at least seven repeats in the FR are needed for the optimal function of the oriP (Wysokenski and Yates, 1989). Additionally, another region within BamHI C called Rep* has been identified in B95.8 EBV as an element that can independently contribute to the replication of episomes in the absence of the DS element of oriP (Kirchmaier and Sugden, 1998), and a region adjacent to oriP containing the EBERs contributes to matrix attachment and improves episome stability (White et al., 2001), indicating that the EBV latent origin of replication is more complex than previously assumed.

Additionally, in the presence of EBNA-1 and the FR element, the increased expression of reporter genes encoded in plasmids can be observed in a manner typical for enhancer elements (Lupton and Levine, 1985). For instance, in cis it increases expression from the viral Cp (Sugden and Warren, 1989) and LMP-1/LMP-2B promoters (Gahn and Sugden, 1995) suggesting that EBNA-1 is important for the transcriptional activation of latent genes. However, these experiments were performed using either co-transfection or luciferase assay and have not been confirmed in the context of viral infection.

EBNA-1 regulates its own expression by binding near the Qp promoter of the EBV genome, which is used to express EBNA-1 when other EBNAs are not present (during latency I and II) (Nonkwelo et al., 1996). EBNA-1 has a higher affinity for the DS and FR elements than for its recognition sites downstream of Qp, so it only binds to the Qp sites when its level is high and able to saturate the other binding sites. This may acts as a feedback mechanism to restrict EBNA-1 expression levels to the minimum required for episome maintenance and any host gene regulation (Ambinder et al., 1990).

1.8.1.2 EBNA-2

EBNA-2 is the major oncogene responsible for B cell transformation in vitro (Cohen et al., 1989). Based on the sequence of EBNA-2, EBV has been categorized into two distinct strains: type 1 and type 2 (also called type A and B). These two strains differ in their ability to transform B cells into LCLs: type 1 is much more transforming than type 2 (Rickinson et al., 1987).

EBNA-2 transactivates many cellular and viral genes. EBNA-2 does not bind to DNA directly; rather it interacts with cellular binding proteins to activate the transcription of its target genes. The most studied DNA-binding protein that interacts with EBNA-2 is the recombination binding protein-J kappa (RBPJ), also known as Cp binding factor 1 (CBF1) (Grossman et al., 1994). Until recently it was thought that in the absence of EBNA-2, RBPJ recruits a co-repressor complex to the promoters or enhancers to which it is bound, which prevents histone acetylation and promotes trimethylation, resulting in repressing transcription of target genes (Lai, 2002). When EBNA-2 is present however, it was suggested that it interacts with RBPJ at those binding sites, displacing the co-repressor complex and recruiting transcriptional co-activators instead (Hsieh et al., 1996). This model, however, has been recently challenged. Rather than moving to pre-bound RBPJ complexes, it was shown that EBNA-2 can induce the formation of new chromosome binding sites for RBPJ and another cellular protein; early B-cell factor 1 (EBF1) (Lu et al., 2016). These newly induced binding sites occupied by complexes of EBNA2-EBF1-RBPJ correlate with transcriptional activation of genes required for B cell proliferation and survival (Lu et al., 2016).

The major EBV latent promoter (Cp) and the promoters for LMP-1, LMP-2A and LMP-2B carry at least one RBPJ binding site and are strongly activated by EBNA-2 (Abbot et al., 1990). One of the best characterized host genes to have been defined as a target for EBNA-2 is the proto-oncogene MYC. The interaction between EBNA-2 and the

promoter/enhancers of MYC was recently shown by chromatin conformation capture: in the presence of EBNA-2, a chromatin loop links an upstream enhancer bound by EBNA-2 to the MYC transcription start site (Zhao et al., 2011). Activation of MYC by EBNA-2 is the major step for initiation of the proliferation of EBV-infected B cells. Deregulated MYC expression is associated with numerous cancers, including Burkitt lymphoma, resulting from the MYC translocation (Wilda et al., 2004). Constitutive expression of MYC in the B-cell compartment of transgenic mice predisposes these animals to develop lymphoma within a few months of birth (Adams et al., 1985). MYC expression is closely followed by expression of the cell cycle regulator cyclin D2. This cyclin however, does not seem to be a direct target gene for EBNA-2 (Kaiser et al., 1999).

Additionally, it has been reported that EBNA-2 can act as a transcriptional repressor. For instance it can suppress the expression of immunoglobulin M (IgM) in LCLs and Burkitt lymphoma cell lines (Jochner et al., 1996). It also inhibits expression of highly mutagenic activation-induced cytidine deaminase (AID) during EBV-driven B cell growth (Tobollik et al., 2006). This correlates with the observation that no ongoing mutation can be seen in proliferating EBNA-2 positive B cells during IM, while EBNA-2-negative Burkitt lymphoma B cells (latency I) are characterized by substantial hypermutation (Tobollik et al., 2006) (Table 1.1).

1.8.1.3 The EBNA-3 family

EBNA-3A, EBNA-3B, EBNA-3C (historically also called EBNA-3, EBNA-4 and EBNA-6, respectively) are a family of proteins encoded by tandemly arranged genes. Despite having similar gene structures and partial sequence homology, they have distinct functions. Early EBV genetic studies indicated that EBNA-3A and EBNA-3C are essential for B cell

transformation (Tomkinson et al., 1993), while EBNA-3B is dispensable (Tomkinson and Kieff, 1992). However, recent studies have shown that EBNA-3A is not absolutely required for B cell transformation and LCLs can be established by EBNA-3A knockout EBV (Hertle et al., 2009).

A third of the genes identified by microarrays to be regulated by EBNA-3s, require more than one EBNA-3 for their regulation, mostly EBNA-3C co-operating with either EBNA-3A, EBNA-3B or both (White et al., 2010). The transcriptome data have been backed up by ChIP-seq data that also show similar combinations of co-localization of EBNA-3s on the genome (Paschos, Ho and Allday; unpublished data). All three EBNA-3 proteins can bind to the RBPJ at the same site as EBNA-2 (Robertson et al., 1996).

Because transient reporter assays have shown that EBNA-3s can inhibit EBNA-2 activation of viral promoters (e.g. the Cp promoter), it was suggested that EBNA-3s may act as a functional antagonists that negatively regulate those genes activated by EBNA-2 (Radkov et al., 1997). This concept is supported by the fact that the EBNA-3s can counteract the transcriptional function of EBNA-2 on cellular promoters like MYC, through competition for RBPJ binding (Cooper et al., 2003). Additionally, it has been reported that EBNA-3A and EBNA-3C interact with various repressive transcription co-factors like histone deacetylases (HDACs) and C-terminal binding protein (CtBP) (Touitou et al., 2001). However, further studies have shown that in some circumstances, EBNA-3C can activate (rather than repress) transcription from viral promoters like LMP-1 (Jiménez-Ramírez et al., 2006). It can also directly induce expression of activation-induced cytidine deaminase (AID) (Kalchschmidt et al., 2016a). Both of these studies complicated the previously proposed transcription-repression model.

Additionally, recent studies have shown that RBPJ accumulates at the EBNA-3C-binding sites on the genome only when EBNA-3C is functional (Kalchschmidt et al., 2016b),

which mirrors the observations made by Lu et al., (2016), where EBNA-2 induces the binding of RBPJ to genome loci (see section above).

Importantly, EBNA-3A and EBNA-3C have been shown to cooperate to repress two major tumor suppressor genes: Bcl-2-interacting mediator of cell death (Bim) (Anderton et al., 2008) and cyclin-dependent kinases $p16^{INK4A}$ (Skalska et al., 2010), contributing to B cell survival and increasing the likelihood of lymphomagenesis. Specifically, the repression of $p16^{INK4A}$ was found to be essential for the outgrowth of LCLs lacking EBNA-3C, while methylation of the Bim gene (*BCL2A11*) is a feature of EBV-positive Burkitt lymphoma. EBNA-3C has also been reported to play a role in the disruption of the cell cycle by modulating a G1 arrest checkpoint in B cells through the effects of $p16^{INK4A}$ (Maruo et al., 2006).

In contrast, EBNA-3B has been shown to act like a tumor suppressor *in vivo* as infection of humanized NOD/SCID/γc–/– mice with EBNA-3B knockout EBV led to aggressive, immune-evading monomorphic diffuse large B cell lymphoma (DLBCL)-like tumors, with EBNA-3B mutations being identified in several EBV-positive human lymphomas (White et al., 2012).

1.8.1.4 EBNA-LP

Because Epstein-Barr nuclear antigen leader protein (EBNA-LP) is the subject of this thesis, it will be discussed extensively in section 1.9.

1.8.2 Epstein-Barr latent membrane proteins (LMPs)

1.8.2.1 LMP-1

Expression of LMP-1 can be initiated from two different promoters: a proximal promoter within the BamHI N-EcoRI D fragment of the EBV genome (ED-L1) (Hudson et al., 1985) and a distal promoter within the first terminal repeat of the EBV genome (TR-L1) (Sadler and Raab-Traub, 1995) (Fig.1.3). Expression of LMP-1 in latency III is induced by activation of the LMP-1 transcription by EBNA-2 (Wang et al., 1990) but is EBNA-2-independent in latency II. LMP-1 levels are balanced by positive and negative auto-regulatory loops: when the levels of LMP-1 are low, the unfolded protein response (UPR) pathway is triggered at the transmembrane domain of LMP-1, which then up-regulates activating transcription factor 4 (ATF4). The ATF4 then induces transcription from the LMP-1 promoter (Dong and Sugden, 2008). Additionally, cellular transcription factors (such as NF-κB or interferon regulatory factor 7 (IRF7)), which are activated by LMP-1, play a role in the positive autoregulation of LMP-1 as well (Demetriades and Mosialos, 2009, Ning et al., 2003). It has also been shown that LMP-1 expression can be induced by EBNA-3C (in an EBV-positive cell line with doxycycline-inducible EBNA-3C) (Jiménez-Ramírez et al., 2006), by EBNA-1/FR (using luciferase assay in LCLs) (Gahn and Sugden, 1995) and EBNA-LP alongside EBNA-2 (for EBNA-LP co-activation see section 1.9.8).

LMP-1 has been found to be essential for B cell transformation both *in vitro* (Kaye et al., 1993) and in transgenic mice, where it is able to cause lymphomas (Kulwichit et al., 1998). LMP-1 is able to mimic the signals that are induced by the activation of the co-stimulatory B cell receptor CD40 by T helper cells (which in physiological environments leads to B cell activation) (Kilger et al., 1998); this activates the transcription factor NF-κB and supplies essential survival signals required for B cell transformation (Cahir-McFarland et

al., 2004). It has also been published that LMP-1 by activation c-Jun N-terminal kinase (JNK) pathway can up-regulate the kinases Cdc2 and Cdk2, which drive the cell cycle (Kutz et al., 2008). LMP-1 suppresses the activation of BZLF-1 and thereby inhibits entry into the lytic cycle (Adler et al., 2002). High levels of LMP-1 can be toxic and cause cytostasis and autophagy (Hammerschmidt et al., 1989). Additionally, the transmembrane domains of LMP-1 can activate apoptosis in B cells via the UPR pathway (Pratt et al., 2012).

The transition from newly infected B cells to long term outgrowth of EBV-infected B cells requires NF-κB activity, and the high (LCL-like) levels of LMP-1 and NF-κB activity are not seen until approximately 3 weeks after infection (in comparison to much lower levels that can be seen early after infection) (Price et al., 2012). Because NF-κB is activated by LMP-1, it has been hypothesized that the delay in NF-κB activation may be due to direct attenuation of NF-κB activity (and consequently LMP-1 levels) by high MYC activity early after infection (as it has been reported that high levels of MYC can inhibit an LMP-1/NF-κB feed-forward loop) (Price et al., 2012).

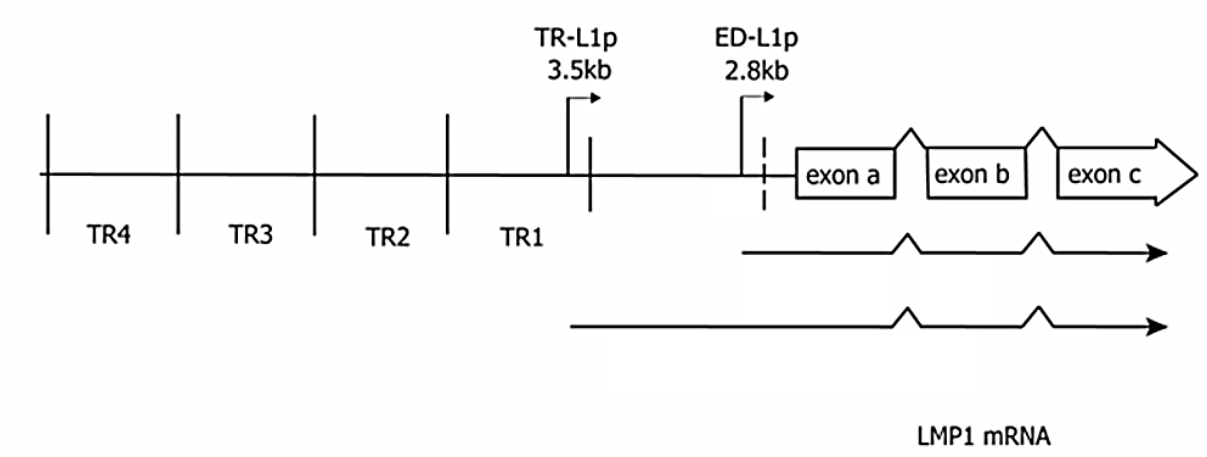

Fig. 1.3 Schematic of LMP-1 gene and transcripts. LMP-1 has three exons. There are two promoters: ED-L1p and TR-L1p that generate the 2.8-kb and 3.5-kb LMP-1 mRNAs respectively. (Modified from Noda et al., 2011).

1.8.2.2 LMP-2

Previously, two LMP-2 isoforms (LMP-2A and LMP-2B) that are expressed from two separate promoters have been identified (Fig.1.4). Both promoters have RBP-J binding sites and can be regulated by EBNA-2. The LMP-2B promoter is also shared with LMP-1 promoter, but LMP-1 is transcribed in the opposite direction to LMP-2B (Fig.1.1). LMP-2A exon 1 contains a start codon whereas LMP-2B exon 1 does not. Therefore protein coding for LMP-2B starts in exon 2, which means that LMP-2A has an extended N-terminus relative to LMP-2B (Sample et al., 1989). LMP-2A localizes to the cellular plasma membrane, while LMP-2B localizes to a perinuclear region in the infected cells (Lynch et al., 2002). Recently, additional promoter was identified within the TR, which also encodes LMP-2B (Fox et al., 2010) (Fig.1.4). Transcripts generated from the TR promoter are found at high levels in primary NK/T cell lymphoma tissue, which have undetectable levels of conventional LMP-2A and LMP-2B transcripts (Fox et al., 2010). Expression of LMP-2 is regulated by EBNA-2 at both the LMP-2A and LMP-2B promoters (Bornkamm and Hammerschmidt, 2001). However, it has been suggested that LMP-2A can also be regulated by the Notch signaling pathway (Anderson and Longnecker, 2008) and that transcription of LMP-2B may be co-activated by EBNA-LP (see section 1.9.8 for more detail).

LMP-2A and LMP-2B are dispensable for B cell transformation *in vitro* (Longnecker et al., 1993). LMP-2A modifies cellular signaling by recruiting proteins to its N-terminal domain. When Lyn and Syk kinases bind to LMP-2A, they are activated, assembling the same complex that assembles on the B cell receptor (BCR), and providing a constitutive activation of a BCR-like signaling (Fruehling et al., 1998). LMP-2B is not able to interact with Lyn and Syn, because it lacks the N-terminal domain. However it has been suggested that LMP-2B can form aggregates with LMP-2A and thereby negatively regulate expression of LMP-2A (Rovedo and Longnecker, 2007).

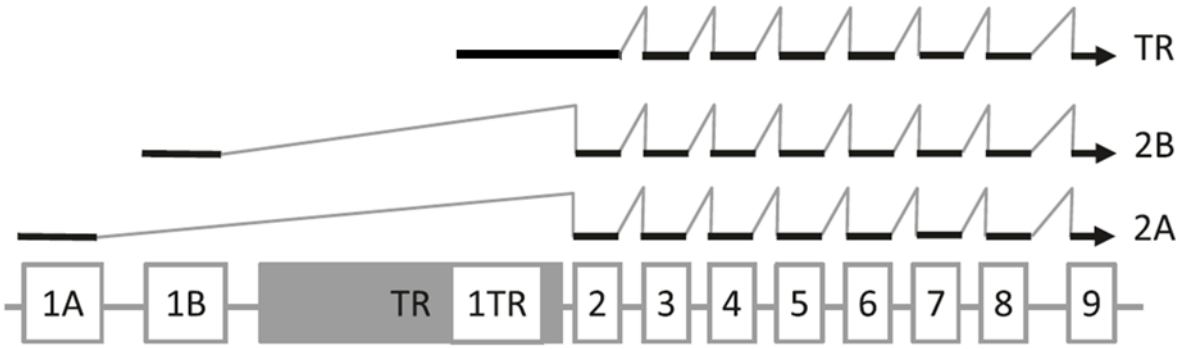

Fig. 1.4 Schematic of LMP-2 gene and transcripts. LMP-2 has nine exons. There are three promoters that generate distinct first exons: 1A (in LMP-2A), 1B (in LMP-2B), 1TR (in LMP-2TR). (Modified from Cen and Longnecker 2015).

1.8.2.3 The combined action of LMP-1 and LMP-2A in cell survival in the germinal centre

LMP-1 and LMP-2A together are thought to be able to provide the growth and survival signals that are required to initiate germinal center reaction (Thorley-Lawson and Babcock, 1999). These signals in normal B cells are usually provided by T cell help and antigen-binding during the primary immune response. Normally, B cells activated by an antigen migrate into the follicles of lymph nodes and form (or join) germinal centers, where they undergo proliferation, antibody class switching and somatic hypermutation, accompanied by positive selection for cells with higher-affinity antibodies (Liu et al., 1989). LMP-1, as a functional homologue of CD40, is able to mimic T helper cell stimulation and rescue B cells from apoptosis and drive their proliferation. In parallel, LMP-2A mimics B cell antigen receptor signaling, which is also required for survival in germinal center. This combined effect of LMPs provides the two signals required for the survival of EBV-infected cells in the germinal center (regardless of their ability to detect antigen). After the maturation in GC, the cells are thought to become memory B cells and enter latency 0.

1.8.3 Epstein-Barr RNAs

1.8.3.1 Epstein-Barr virus-Encoded RNAs (EBERs)

The Epstein-Barr virus-Encoded RNAs are two individually expressed non-polyadenylated RNAs: EBER-1 and EBER-2. Both *EBER*s contain RNA polymerase III intragenic transcription control regions and are transcribed by RNA polymerase III (Howe and Shu, 1989). Additionally, each *EBER* gene contains three upstream promoter elements (that are more typical of polymerase II-transcribed genes) that are essential for efficient transcription (Howe and Shu, 1989). The EBER transcripts are highly expressed which makes them the most abundant viral RNA present in EBV-infected cells (Lerner et al., 1981). EBERs are thought to be expressed in all EBV infected cells. As a result, detection of EBERs (EBER in-situ hybridization) is the primary method for identifying EBV-positive clinical malignancies.

The function of EBERs is still controversial and unclear. Recombinant viruses derived from Akata strain deleted for functional EBERs, exhibited a 100-fold decrease in their transformation efficiency compared to the wild type virus (Yajima et al., 2005). However, recombinant viruses derived from B95.8 or P3HR1 strains that are also lacking EBERs, show no measurable difference from the wild type virus in B cell transformation (Gregorovic et al., 2011, Swaminathan et al., 1991). These phenotypic differences are probably due to the strains that were used and the fact that Akata-derived viruses contain additional viral transcripts and miRNAs, which are not present in the B95.8 or P3HR1 viruses.

The EBERs are also dispensable for the lytic replication of EBV as the inducibility of both early and late lytic antigens was similar in EBER-positive and -negative cell lines (Swaminathan et al., 1991).

It has been published that deletion of each of EBER from B95.8 strain, results in changes of gene expression in LCL (Gregorovic et al., 2011), which indicates a role of EBERs in gene regulation at the level of RNA abundance.

Recently it has been shown that EBER-2 interacts with PAX5, a transcription factor which plays a role in regulation of LMP-1 (Lee et al., 2015). EBER-2 is required for the localization of PAX5 to a binding site in the terminal repeats, which exhibits sequence homology to an EBER-2 loop (Lee et al., 2015). Knockdown of EBER-2 in an EBV-positive Burkitt lymphoma cell line has been shown to have a similar effect on LMP transcription as depletion of PAX5 in LCLs, namely the up-regulation of LMP-1 and LMP-2 expression (Lee et al., 2015). The EBERs can also form ribonucleoprotein complexes with the La protein (Lerner et al., 1981) and the ribosomal protein L22 (Toczyski et al., 1994).

Both EBER-1 and EBER-2 have been recently found to be present in the purified exosome fractions of EBV-infected cell lines (Ahmed et al., 2014). This exosome-mediated release could provide stability to EBERs from degradation by nucleases and a transport to uninfected cells (Pegtel et al., 2010).

1.8.3.2 BamHI-A Rightward Transcripts (BARTs)

BamHI-A Rightward Transcripts (BARTs) are another group of abundant RNAs present in EBV-infected cells. Several open reading frames (ORFs) have been identified within the BART transcripts (Smith et al., 2000). However, proteins encoded by these ORFs remain undetected in sera of EBV-associated cancer patients, patients with infectious mononucleosis or EBV-positive healthy donors (van Beek et al., 2003). The B95.8 strain carries a 10 kb deletion which removes most of the BART region. B95.8 is still fully able to

transform B cells in vitro, which indicates that BARTs are dispensable for B cell immortalization (Robertson et al., 1994).

1.8.3.3 EBV-encoded microRNAs (miRNAs)

It is now thought that the major functional components of the BART transcripts are the 22 miRNAs that they encode (Skalsky and Cullen, 2013). In addition, latency III cells also produce three microRNAs (miRNAs) from the BHRF1 transcript (Cai et al., 2006). Most of the BART miRNAs are missing from the B95.8 EBV strain as a result of its 10 kb deletion, leaving only 5 BART miRNAs (1, 2, 3, 4 and 15) still present. This suggests that the majority of BART miRNAs are not required for B cell transformation *in vitro*.

The BHRF1 miRNAs are expressed at high levels in latency III but are undetectable or present at very low levels in latency I and II (Cai et al., 2006). The BART miRNAs are expressed at high levels in latently infected epithelial cells and at lower levels in B cells (Cai et al., 2006).

Some of miRNAs have been shown to have viral targets. For example, BART miRNA-2 can target a lytic gene BALF5 mRNA for degradation which suggests that BART miRNA-2 may contribute to suppressing the switch from latent to lytic replication by preventing premature BALF5 expression (Barth et al., 2008). Other EBV miRNAs have been demonstrated to have cellular targets. For example, BHRF1 miRNA-3 can down-regulate the interferon-inducible T-cell attracting CXC-chemokine ligand 11 (CXCL11) suggesting its role in an immunomodulatory mechanism in EBV-positive lymphomas (Xia et al., 2010).

1.8.3.4 Stable intronic sequence RNAs (sisRNAs)

Recently (after this project had begun) sequencing analysis of nuclear RNAs from B cells latently infected with EBV identified conserved and stable RNA structures that arise from intronic sequences within the W repeats (stable intronic sequences- sisRNAs) (Moss and Steitz, 2013).

The 81-nucleotide sisRNA-1 originates from the intron between exons W1 and W2 of EBNA-LP. Using computational modelling, it has been predicted to form a small conserved stem-loop structure at its 5' end, but is generally predicted to be unstructured (Fig.1.5). SisRNA-1 is detectable by Northern blotting, and quantitation by qPCR suggests that it is expressed at very high levels- at a similar abundance to EBER-2 (Moss and Steitz, 2013). No function has- as yet- been ascribed to sisRNA-1. The sisRNA-1 sequence is ~100% conserved in EBV strains. This homology extends to other lymphocryptoviruses: 91% conserved in mouse hepatitis virus 4 (MHV4), 98% in Pongine herpesvirus 1, 94% in Pongine herpesvirus 3, 91% in Cercopithecine herpesvirus 12 (CeHV12), and 60% in Callitrichine herpesvirus 3 (CaHV3) (Moss et al., 2014).

SisRNA-2 arises from the long introns of the W repeats of EBNA-LP, but is less well defined (Moss and Steitz, 2013). SisRNA-2 has a very long region (586 nt) that is predicted to form a stable hairpin (Moss et al., 2014) (Fig.1.6). Canonically paired regions of sisRNA-2 are separated by internal loops that are structurally conserved across the lymphocryptoviruses (Moss et al., 2014). Additionally, sisRNA-2 is predicted to contain residues that could be substrates for adenosine deaminase acting on RNA (ADAR), which converts adenosine to inosine (A-to-I) in double-stranded RNA that could alter and perhaps destabilize the RNA hairpin (Moss and Steitz, 2013) (Fig.1.6).

Large stable introns are found in other herpesviruses (Burton et al., 2003). In herpes simplex virus 1 (HSV1), a long (~2000 nt) intron, known as the latency-associated transcript

(LAT), is able to suppress apoptosis by inhibiting cellular apoptotic pathways (Henderson et al., 2002). SisRNA-2 resembles the LAT in size, therefore it may be possible that LAT and sisRNA2 play analogous roles in preventing infected cell from undergoing apoptosis.

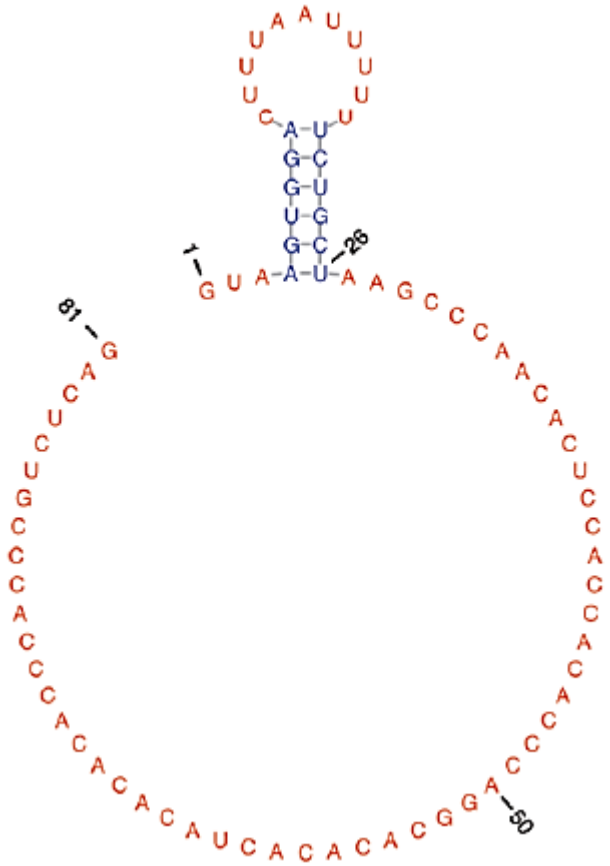

Fig. 1.5 Predicted structure of sisRNA-1. The structure is predicted as a conserved loop with one hairpin close to its 5'. (Modified from Moss et al., 2014).

Fig. 1.6 Predicted structure of the hairpin region of sisRNA-2. A reported A-to-I editing site is indicated with a red "I". (Modified from Moss and Steitz, 2013).

1.9 Epstein-Barr virus nuclear antigen leader protein (EBNA-LP)

Because EBNA-LP is the subject of this project, its biology will be described in more depth in the following sections.

EBNA-LP is also known as EBNA-5 (Dillner et al., 1986). In rare cases it can be found as EBNA-4 (Rogers et al., 1990), but this name was only used before the nomenclature was agreed.

1.9.1 The structure of EBNA-LP gene and its transcripts

All of the six EBNAs are produced from one extensively spliced long transcript generated during latency III. EBNA-LP is encoded at the 5' end of this polycistronic transcript (Woisetschlaeger et al., 1989). Each transcript is generated from one of two types of promoters: either the W promoter (Wp), which is present in multiple copies (one within each of the BamHI W repeat units), or the C promoter (Cp), which is present upstream of the repeat, within the BamHI C fragment (Fig.1.7).

The EBNA-LP gene consists of the repetitive W region and the C terminal unique region. There are three types of non-coding exons: single C1, single C2, multiple copies of W0 (part of the repeat region) and four types of coding exons: multiple copies of exons W1 and W2 (both part of the repeat region) and single Y1 and Y2 (both part of a unique region) (Fig.1.7). The W1 and W2 exons are divided by a short intron (processed into sisRNA-1), while W1W2 exon pairs are separated by longer intronic sequence (from which sisRNA-2 is made). The longer intron is present at the beginning of each BamHI W repeat unit and contains one of EBV's largest (1149 nucleotides long) open reading frames (BWRF1 ORF) (Jenson et al., 1987). The BWRF1 has no ATG start codon; so it is not clear whether it is a

functional ORF. Also it is not intact in all strains (Ba Abdullah et al; manuscript in preparation).

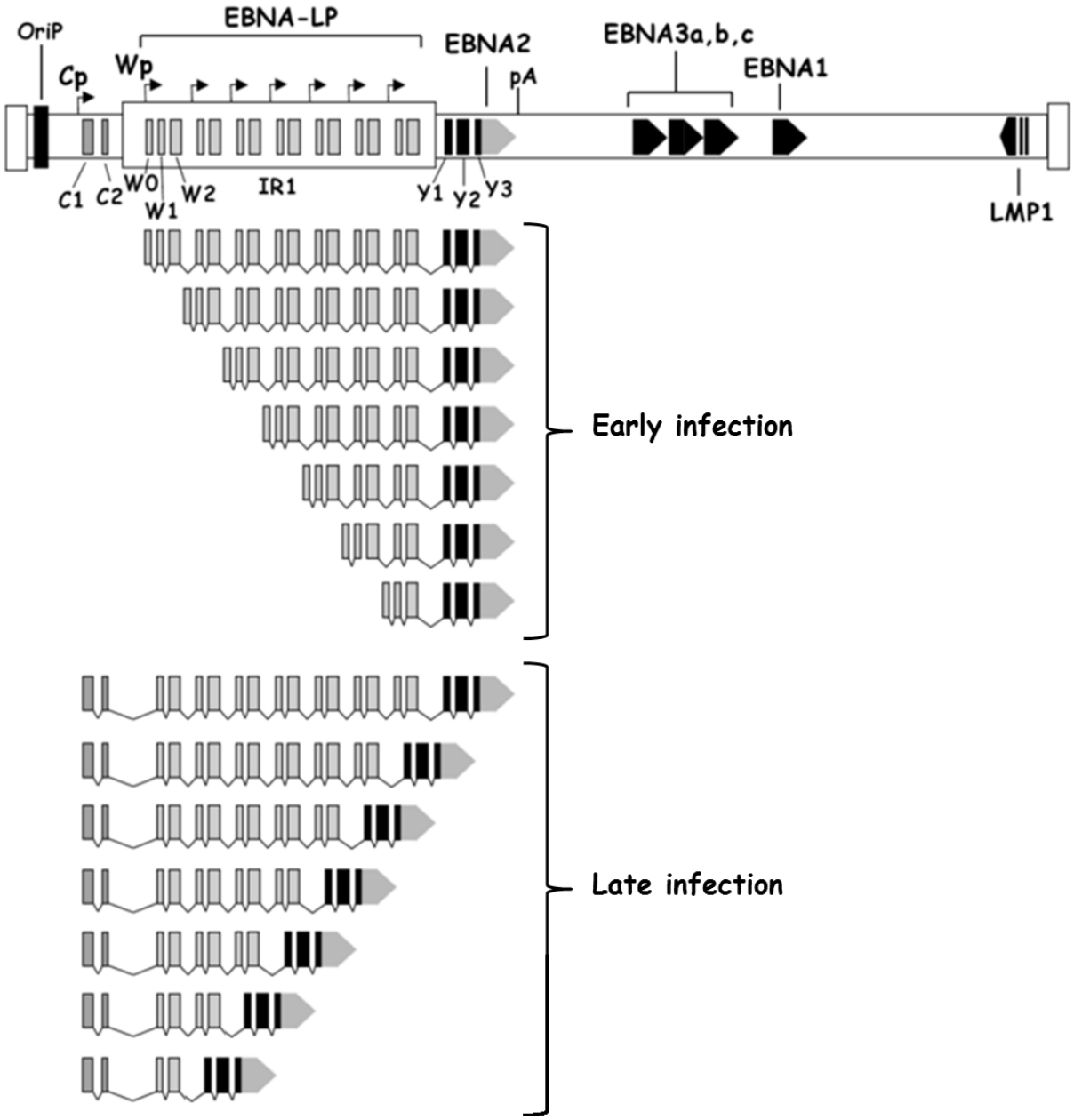

Fig. 1.7 Exon organization of EBNA-LP gene transcripts. Transcription of EBNA-LP is initiated from the Wp promoter (early infection) or the Cp promoter (established latency). The viral latent origin of replication (OriP), the polyadenylation site (pA) for EBNA-LP/EBNA-2 transcripts and location of other EBNA and LMP genes are shown. There are three non-coding exons: C1, C2, W0 and four coding exons: W1, W2, Y1, Y2. The schematic shows how transcription could result in the production of variable EBNA-LP isoforms. The other EBNA genes are encoded by additional alternative splicing of this long polycistronic transcript from the Y2 or from within the YH exon, generating the shorter Y3 exon to the downstream U exon (not shown). (Modified from Ling et al., 2009).

Initially after infection, promoters within the W repeats (Wp) initiate transcripts that encode various combinations of the EBNAs through alternative splicing. These transcripts have a short (27 nucleotide) first exon (W0) that is spliced to exon W1. The W1 exon is then spliced to W2. Exon W2 is spliced either to exon W1 in a subsequent repeat unit or to exon Y1. The Y1 exon is spliced to the final EBNA-LP exon, Y2 (Sample et al., 1986) (Fig.1.7). The Y2 exon then splices to either Y3/YH splice acceptor or to the U exon to generate downstream EBNAs. During later stages of infection, the C promoter (Cp) is activated and becomes the dominant promoter producing latency-associated transcripts (Woisetschlaeger et al., 1989, Hutchings et al., 2006). These transcripts do not contain the W0 exon; instead the 5'UTR consists of exon C1 spliced to exon C2. This is then spliced directly to exon W1. Downstream splicing is then thought to be the same as for Wp transcripts (Sample et al., 1986) (Fig.1.7).

In order to allow this long, complex transcript to produce either EBNA-2 or EBNA-LP by (presumably) cap-mediated translation from the 5' end of the transcripts, there are two variants of the W1 exon: W1 and W1'. These exons differ only in their 5' splice acceptors, which are 5 bases apart (Fig.1.8) and the splice site selection defines whether the transcript encodes EBNA-2 or EBNA-LP: if the splice occurs to the shorter W1' exon (from either of exons C2 or W0), a methionine initiation codon for EBNA-LP is generated across the splice junction. In contrast, splicing to the longer W1 exon does not generate an AUG start codon, such that the transcript's first initiation codon is the one that initiates translation of EBNA-2 (Rogers et al., 1990) (Fig.1.8). All EBNA transcripts contain the *EBNA-LP* ORF in their 5'UTR, but vary in whether they contain its start codon (Woisetschlaeger et al., 1990). However, the EBNA-2 ORF is spliced out through the splicing from the Y2 exon or Y3 exon to the splice acceptor within U fragment in transcripts encoding the EBNA-3s or EBNA-1 (Fig.1.9).

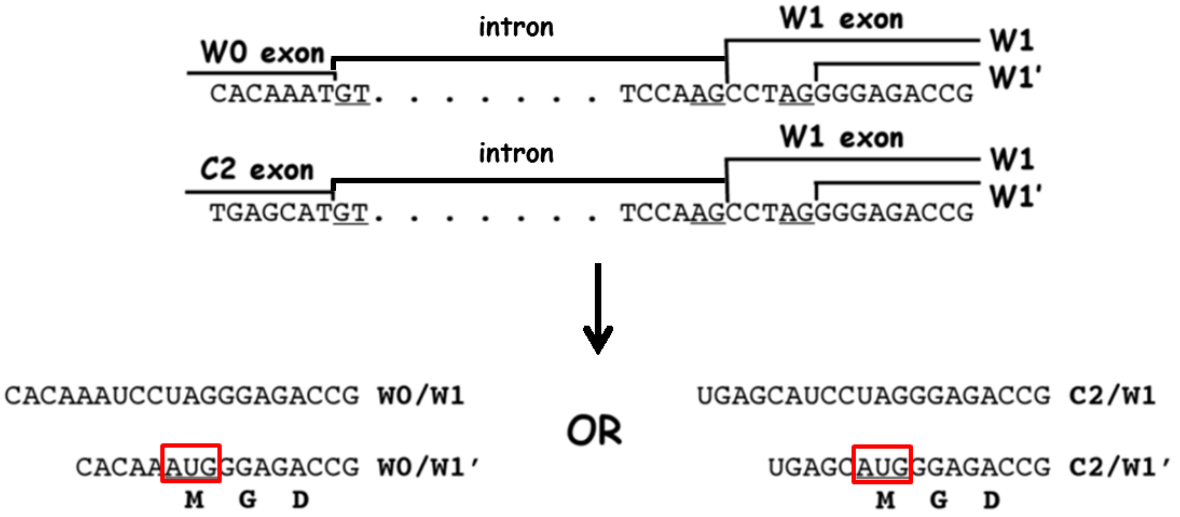

Fig. 1.8 Alternative splicing initiating the EBNA-LP ORF. Alternative splicing to the W1' exon (either from Wp or Cp promoter) generates an AUG codon (red box) for EBNA-LP, while splicing to the W1 exon does not. (Modified from Ling et al., 2009).

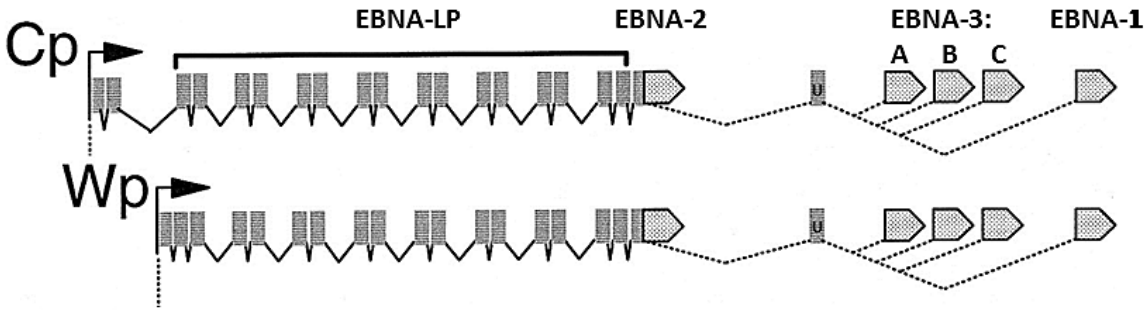

Fig. 1.9 Schematic of EBNA genes transcription during latency III. Type III latency involves expression of all six EBNAs, that are generated by alternative splicing of long primary transcripts initiated from either Cp or Wp. (Modified from Paulson and Speck, 1999).

The number of W1W2 exon pairs in the transcript determines the size of EBNA-LP (Sample et al., 1986) (Fig.1.7). One probable mechanism for the generation of multiple different sized EBNA-LP isoforms is a direct consequence of using the Wp promoter. For example, in a virus with 6 repeats, if each of the 6 repeats contains an active Wp, then the virus will produce transcripts starting in each repeat unit, and if those transcripts include

every downstream W1W2 exon pair, then there will be equal numbers of each protein size, containing between 1 and 6 repeats, and this would explain the variable numbers of repeat domains in EBNA-LP (Fig.1.7). However, transcripts initiated from the single Cp promoter also contain variable numbers of W repeats (Bodescot and Perricaudet, 1986) (Fig.1.7). With Cp-derived transcripts, generation of EBNA-LP has additional levels of complexity, probably as a result of alternative splicing between repeats resulting in variable numbers of W1W2 exons and therefore different sizes of EBNA-LP (Sample et al., 1986). It has not been established how the skipping of W1W2 exons occurs in shorter EBNA-LP transcripts (i.e. if the EBNA-LP transcripts from Cp always contain the first W repeat, or if the last repeat is always spliced to Y1 exon or if the splicing and joining the repeats is more random, and whether exon skipping occurs in the W1-W2 or W2-W1 splice junctions). Additionally, some of the transcripts derived from B95.8 cells have been found to lack single W2 exons (Bodescot and Perricaudet, 1986) resulting in protein size shifts by the size of single W2 exon (for EBNA-LP protein see section 1.9.3).

1.9.2 Expression of EBNA-LP

EBNA-LP is expressed during the pre-latent stage and latency III (for latency see section 1.3). Expression of EBNA-LP in diseased tissues/cells has not been exhaustively investigated (partly due to lack of broad applicability of anti-EBNA-LP antibodies) but it is assumed to match the expression of EBNA-2, which has been assessed.

In B95.8 EBV-infected B cells *in vitro*, EBNA-LP is first detectable around 12h post-infection (Allday et al., 1989, Sinclair et al., 1994), reaches maximal levels early after infection and decreases over time but is still expressed at a detectable level in established LCLs (Sinclair et al., 1994, Thorley-Lawson and Gross, 2004).

1.9.3 The structure of EBNA-LP protein

As a result of its repetitive nature (through variation in the exon usage described in section 1.9.1), the EBNA-LP protein consists of variable repeat segments of the W1/W2 exons that encode 22 and 44 amino acids respectively at the N-terminus, and a unique segment of the Y1 and Y2 exons that encode 11 and 34 amino acids respectively at the C-terminal end (Fig.1.10). A comparison of EBNA-LP sequences originating from human and non-human primate lymphocryptoviruses (LCVs) identified the five most conserved regions (CR1- CR5) and conserved amino acids (Fig.1.10) (McCann et al., 2001).

In newly infected B cells and freshly infected EBV-negative B cell tumor lines, multiple isoforms of EBNA-LP are usually expressed, while established B95.8 LCLs and older established cell lines seem to express fewer isoforms (Finke et al., 1987). It has also been demonstrated (by cloning EBV-transformed cord blood-derived LCLs by limiting dilution) that different LCL clones, 8 weeks after transformation, differ in their predominant EBNA-LP isoform(s), indicating that a single cell is able to produce a ladder of different EBNA-LP protein sizes (rather that each EBNA-LP isoform being produced by a single cell) and that expression of fewer isoforms in established cell lines may be a result of clonal selection (Finke et al., 1987).

Analysis of the EBNA-LP proteins produced in several B95.8-carrying cell lines, observed that the spacing between the different EBNA-LP bands separated by SDS-page gel electrophoresis is more complex than the 6 kDa increments corresponding to the size of each additional repeat encoded by the W1/W2 exon pairs. The predominant spacing of 6 kDa to 8 kDa was confirmed but in addition, the shifts of 2 kDa to 4 kDa were observed (Finke et al., 1987). The size of these shifts corresponds to the deletion of either the W1 or W2 exon and supports the observation made by Bodescot and Perricaudet, (1986), of a B95.8-derived cDNA lacking the W2 exon (for EBNA-LP transcripts, see section 1.9.1).

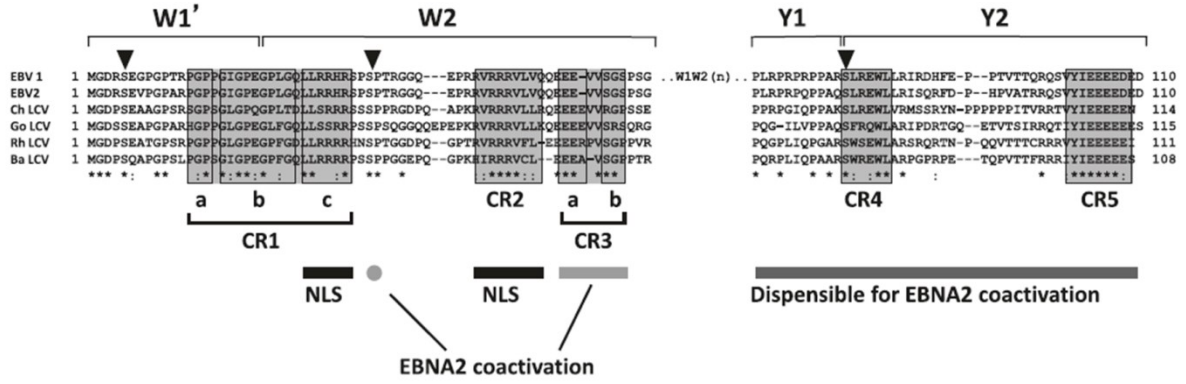

Fig. 1.10 Sequence comparison between EBNA-LP proteins from different EBVs and LCVs. For simplicity only one W repeat is presented. Conserved amino acids are marked with asterisks, similar amino acids are marked with dotted lines and conserved serines are marked with arrowheads. The conserved regions are indicated by grey boxes. The black and grey bars below indicate regions responsible for nuclear localization (NLS), EBNA-2 co-activation, and not required for co-activation. (Modified from Peng et al., 2000a).

There are two main variants of EBNA-LP: variant 1 and variant 2. They were defined based on the monoclonal antibody detection, which was first linked to type 1 and type 2 EBV (Finke et al., 1987) but later reported to be due to a pair of amino acid variations in the W1 exon (Peng et al., 2000b) (Fig.1.11). The most widely used monoclonal antibody against EBNA-LP (JF186) can only detect variant 1 of EBNA-LP (Finke et al., 1987), as its epitope lies within exon W1, across the 2 amino acid SNPs that distinguish variant 1 from variant 2 (Fig.1.11). Also, diversity in exon Y1 (2 SNPs) and Y2 (8 SNPs) has been reported, however, this diversity is semi-independent from variation in the W1 exon (Peng et al., 2000a) (Fig.1.10). All known EBNA-LP variants however, are detectable by another monoclonal antibody 4D3 (Shaku et al., 2005), as its epitope lies somewhere within highly conserved exon W2 (Fig.1.11). Based on recent EBV genome sequence analysis performed in our lab (Ba Abdullah et al.; manuscript in preparation), there are more EBNA-LP variants than was previously considered (Fig.1.12). The two known variants of the W1 exon were validated although variant 1 of exon W1 has an additional nucleotide sequence variant that does not change the protein sequence (renamed 1.2). The W2 exon is completely conserved in all but

one of 71 analysed EBV strains. There are two major variants of the Y1 exon (distinguished by 2 aa difference) that segregate with type 1 and type 2 EBV. The Y2 exon is the most variable between different EBV strains and has 4 major variants (that we have renamed A, B, C and Z), and there are further amino-acid variants within these groups (Fig.1.12). This analysis has shown that the different variants of EBNA-LP exons are only partially co-inherited (i.e. variant 2 of W1 can be present in a virus with any of the major subtypes of Y1 and Y2, whereas variant 1 of exon W1 appears to be restricted to exon Y2 subtype A) (Fig.1.12).

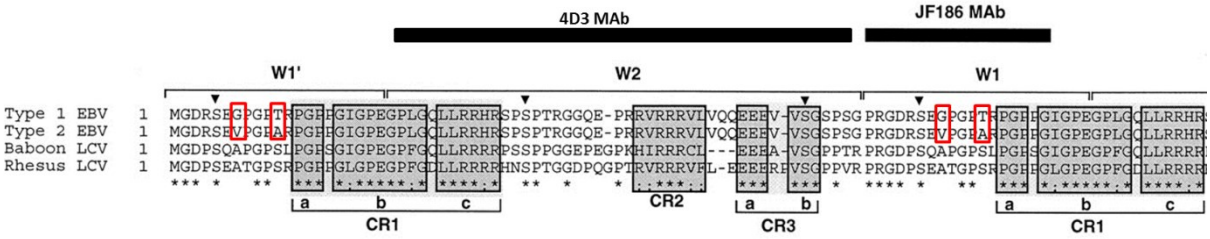

Fig. 1.11 Alignment of one and a half W repeat from EBNA-LP proteins from different EBVs and LCVs . Conserved amino acids are marked with asterisks, similar amino acids are marked with dotted lines and conserved serines are marked with arrowheads. The conserved regions are indicated by grey boxes. Differences in amino acids residues between type 1 and type 2 are marked by red boxes. The epitopes recognizable by the JF186 and 4D3 monoclonal antibodies are indicated by the black bars above the sequence alignments. (Modified from Peng et al., 2000b).

a

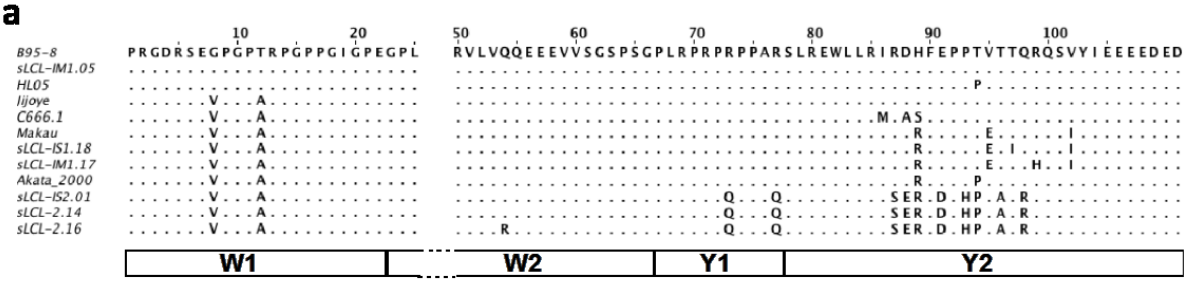

b

Example strain	W1	W2	Y1	Y2	Overall subtype	Number (/71)
B95-8	1.1	1	1.1	A	1A	13
sLCL-IM1.05	1.2	1	1.1	A	1A	3
HL05	1.2	1	1.1	A-P	$1A^{P}$	1
Jijoye	2	1	1.1	A	2A	2
C666.1*	2	1	1.1	A-M	$2A^{M}$	2
Makau1	2	1	1.1	B	2B	29
sLCL-IS1.18	2	1	1.1	B-I	$2B^{I}$	2
sLCL-IM1.17	2	1	1.1	B-H	$2B^{H}$	1
Akata	2	1	1.2	C	2C	11
sLCL-2.14†	2	1	2.1	Z	2Z	4
sLCL-IS2.01	2	1	2.2	Z	2Z	3
sLCL-2.16	2	1^{R}	2.2	Z	$2^{R}Z$	1

Fig. 1.12 Recently identified variation in EBNA-LP. a. Alignment of single W repeat and Y1/Y2 unique region. Names of example strains are present on the right. Conserved amino acids are marked with dotted line. Exons names are under the alignment. **b.** Table showing the combination of different EBNA-LP exon variants in different example EBV strains. Adjacent shaded rows are identical at the protein level. Lines separate more closely related EBNA-LP types. "*" includes M81 strain. "†" includes prototype type 2 EBV strain AG876. (Modified from Ba Abdullah et al, manuscript in preparation).

1.9.4 Localization of EBNA-LP

EBNA-LP protein localizes to the nucleus due to a bipartite nuclear localization signal (NLS) in exon W2 (Peng et al., 2000b) (Fig.1.10). Early after infection of primary B cells, EBNA-LP exhibits a diffuse localization in the whole nucleus (Ling et al., 2005). From day 4 after infection (and in established LCLs) EBNA-LP is associated mostly with promyelocytic

leukemia nuclear bodies (PML NBs) also known as nuclear domains 10 (ND10) (Ling et al., 2005, Bandobashi et al., 2001). Most of the PML NB-associated proteins contain SUMO interaction motifs (SIMs) and are post-translationally sumoylated, which is thought to help PML NB assembly or co-localization (Lallemand-Breitenbach and de Thé, 2010). Interestingly, EBNA-LP is lacking a SIM and there is no evidence so far that it can be SUMO-modified. However, it has been shown that EBNA-LP can bind to another protein that localizes to PML NBs, Sp100 (see section 1.9.9.1 for more detail).

Using cell fractionation and Western blot analysis, it has been reported that low molecular weight (27kDa and 34kDa) EBNA-LPs lacking the Y1Y2 domain (expressed by P3HR1 and Daudi cell lines) localize mainly to the cytoplasm (Garibal et al., 2007). Immunofluorescence analyses after transfection of both HeLa and DG75 cells have shown that EBNA-LP with a single W repeat localizes exclusively in the cytoplasm (Peng et al., 2000b). In a heterokaryon assay, transiently expressed isoforms of EBNA-LP with four or two W repeat domains were able to shuttle between nuclei, whereas isoforms with seven W repeats were not (Ling et al., 2009). However, addition of leptomycin B (LMB), which blocks chromosome region maintenance 1 (CRM1)-dependent nuclear export was unable to inhibit EBNA-LP nuclear-cytoplasmic shuttling (Ling et al., 2009). Also, no EBNA-LP domain that mediates nuclear export has been identified (Ling et al., 2009). This led to suggestion that the shuttling of shorter isoforms was due to diffusion.

1.9.5 Phosphorylation of EBNA-LP

EBNA-LP is a phosphoprotein (Petti et al., 1990). Analysis of the radioactively-labelled EBNA-LP protein immunoprecipitated from drug-synchronized EBV-positive Burkitt lymphoma cell line in latency III, which were verified additionally for cell cycle phase by flow cytometry, has shown that while the phosphorylation of EBNA-LP can be

detected throughout the cell cycle, it is hyperphosphorylated during G2/M and hypophosphorylated during G1/S (Kitay and Rowe, 1996a). Analysis of phosphoamino acids has shown that all phosphorylation was only on serine residues (Kitay and Rowe, 1996b). Three serine residues are highly conserved within EBNA-LP homologs between different species (Peng et al., 2000a) (black arrows in Figure 1.10). Mass-spectrometric analysis of EBNA-LP identified the serine residue at position 36 in the W2 domain as the major phosphorylation site of EBNA-LP, and the existence of another weaker phosphorylation site in W2 domain (Yokoyama et al., 2001). Substitutions of serine 36 with alanine in each W2 domain (of EBNA-LP with three W repeats) significantly reduced the ability of EBNA-LP to enhance EBNA-2-dependent co-activation of viral gene, LMP-1 (for co-activation function see section 1.9.8). In contrast, substitution of S36 with glutamic acid (which structurally mimics phosphorylated serine) retained EBNA-LP's co-activating phenotype. This indicates that the phosphorylation may be involved in (or required for) the co-activation function of EBNA-LP (Yokoyama et al., 2001).

1.9.6 The role of EBNA-LP in B cell transformation

Relatively little is known about the function or mechanism of action of EBNA-LP in transformation. In a P3HR1 background co-complemented with a type 1 EBNA-2, EBV mutants lacking exons Y1 and Y2 were less efficient at transforming B cells than the wild-type virus (Hammerschmidt and Sugden, 1989) and they were able to establish LCLs only when infected B cells were plated on irradiated feeder cells (Mannick et al., 1991). Also, studies determining transforming abilities of EBVs with EBNA-LP made of different numbers of W repeats (0W-6W) have shown that there is no transformation detected for EBV with 0W or 1W repeat, and that the yield of transformed cells increases progressively with the number of W repeats (from the minimum transformation by EBV with 2W repeats to the

maximum transformation by EBV with 5W and 6W repeats, indicating that 5W repeats are needed for optimal B cell transformation (Tierney et al., 2011). The transformation efficiency for EBV with 2W repeats is around 5- and 20-fold lower than for EBV with 3W and 4W repeats respectively, and around 100-fold lower than for EBV with 5W and 6W repeats (Tierney et al., 2011). However, the reason for this difference is not clear. It may be due to the reduced size of EBNA-LP, the reduced transcriptional activity from the reduced number of Wp promoters or a dose effect of some other component of the W repeats.

1.9.7 The role of EBNA-LP in apoptosis

While there is no report of full length EBNA-LP modulating apoptosis, it has been shown that Y1Y2-truncated low-molecular weight (27kDA and 34kDa, which correspond to EBNA-LP with fewer than five W1W2 domains) isoforms of EBNA-LP may protect cells from apoptosis induced by the drugs vertoxin 1 and staurosporine in a caspase-dependent manner (Garibal et al., 2007). These reported isoforms are expressed by Wp-restricted Burkitt lymphoma cell lines P3HR1 and Daudi; both of these cell lines lack the EBNA-2 gene and the C-terminal domain of EBNA-LP gene and transcribe the EBNA genes from Wp, rather than Qp or Cp, leading to the production of EBNA-1, EBNA-3s, and truncated EBNA-LP. The Y1Y2-truncated low-molecular weight isoforms are localized to the cytoplasm in these cells. It has also been shown that after infection of EBV-negative Burkitt lymphoma cells with the P3HR1 virus strain, the sensitivity to verotoxin 1 was strongly decreased, whereas infection with the B95.8 virus strain had little effect (Garibal et al., 2007). The Y1Y2-truncated EBNA-LPs were localized to the cytoplasm also in breast cancer cells (MCF7), and were much more protective against staurosporine-induced apoptosis (based on sub-G1 cells on a cell cycle profile) than the full-length protein with 4 repeats (Garibal et al., 2007). Verotoxin 1 induced activation of the serine-threonine protein phosphatase 2A (PP2A) in cell

lines expressing full-length EBNA-LP but not in cell lines expressing short Y1Y2-truncated form of EBNA-LP (P3HR1 and Daudi) and co-immunoprecipitation performed in all of these cell lines, demonstrated that Y1Y2-truncated (but not full length) forms of EBNA-LP are able to co-precipitate with catalytic subunit of PP2A (Garibal et al., 2007). The authors proposed that the interaction between truncated EBNA-LP and PP2A prevents PP2A activation and therefore results in resistance to apoptosis, but offered no additional experimental evidence to support this. However, Wp-restricted Burkitt lymphoma cell lines also produce transcripts, where (probably due to the missing Y1 and Y2 exons) W2 is spliced directly to BHRF1 gene (Kelly et al., 2009). The BHRF1 protein is a viral bcl2 homologue, and is associated with the lytic cycle. The expression of this protein was confirmed using western blotting in Wp-restricted Burkitt lymphoma cell lines (Kelly et al., 2009) and shown to provide partial protection against ionomycin- and staurosporine-induced apoptosis in EBV-converted BL31 cell lines (Yee et al., 2011).

1.9.8 The role of EBNA-LP as EBNA-2 co-activator in gene regulation

One of the first indications that EBNA-LP can play a role in regulating gene transcription came from a study on cyclin D2 done in primary B cells co-transfected with EBNA-2 and EBNA-LP expression plasmids. Cyclin D2 protein begins to be detectable in primary B cells sometime between 12 and 30 hours after infection with EBV (Sinclair et al., 1994). This timing correlates with the expression of EBNA-2 and EBNA-LP. Electroporation of gp340-primed primary B cells with expression plasmids vectors (priming was performed to mimic the viral entry and to increase expression efficiency of introduced plasmids), neither EBNA-2 nor EBNA-LP alone were able to induce transcription of the cellular cyclin D2 gene. However, when EBNA-2 and EBNA-LP were electroporated together, cyclin D2 transcripts were detectable (Sinclair et al., 1994). Therefore, it was suggested that the

combined action of EBNA-2 and EBNA-LP, is sufficient (and perhaps required) to cause resting B cells primed with gp340 to enter the G1 phase of the cell cycle. Additionally, no detectable cyclin D2 RNA can be found in Burkitt lymphoma cell lines Daudi and P3HR1, both of which have a deletion in the viral genome that disrupts the coding regions for EBNA-2 and EBNA-LP (Sinclair et al., 1994).

Other studies- using transient transfection in latency I Burkitt lymphoma cell lines- have reported EBNA-LP as an enhancer of EBNA-2's activation of the viral *LMP-1* gene: transfection of the EBNA-2 vector alone had no effect (in Akata-BL cell line that carries type 1 EBV strain) or led to up-regulation (in Eli-BL cell line that carries type 2 EBV strain) of LMP-1 protein (however, LMP-1 levels were lower than that observed in LCLs); LMP-1 up-regulation was never observed after transfection of the EBNA-LP vector alone; co-transfection of both EBNA-2 and EBNA-LP vectors resulted in LMP-1 expression at levels 5- to 10-fold higher than those induced by EBNA-2 alone (Nitsche et al., 1997). A similar EBNA-LP co-activation effect was observed when type 2 EBNA-2 was used (Nitsche et al., 1997). Additionally, there was no difference in the induction of LMP-1 using EBNA-LPs with 2, 4 or 7 W exon domains co-transfected with EBNA-2, showing that EBNA-LP with only two W repeats is sufficient for optimal activity (Nitsche et al., 1997). Similarly, Y1Y2-deleted EBNA-LP was as efficient as the full length EBNA-LP at enhancing the EBNA-2-mediated up-regulation of LMP-1 expression, indicating that Y1Y2 domain is not required for the co-activation function of EBNA-LP in *LMP-1* regulation both from the virus genome in Burkitt lymphoma cells (Nitsche et al., 1997) and using a reporter gene (chloramphenicol acetyltransferase- CAT) driven by an LMP-1 promoter construct transfected into an EBV-negative BL cell line (Harada and Kieff, 1997). By using a construct with synthetic RBPJ sites positioned upstream of the HSV-1 thymidine kinase promoter in a similar experimental setup, they also showed that RBPJ sites are sufficient for EBNA-LP co-activation of EBNA-2

(Harada and Kieff, 1997). Furthermore, extensive mutagenesis studies identified conserved region CR3 and serine 36 (in the W2 exon) to be required for enhancing the activation of an LMP-1 promoter construct by EBNA-2 in Akata cells (Peng et al., 2000b), and demonstrated the importance of EBNA-LP phosphorylation on serine 36 (see section 1.9.5) (Yokoyama et al., 2001). Conserved regions CR1 and CR2 are not required for the EBNA-LP co-activation function (Peng et al., 2000b), and neither are CR4 or CR5, which are present in the Y1 and Y2 exons respectively (Nitsche et al., 1997).

More studies based on plasmid co-transfection into Burkitt lymphoma cells harbouring EBV in latency I, found the native *LMP-2B* promoter to also be stimulated by EBNA-LP co-activation of EBNA-2 (Peng et al., 2005). The same study reported that, in contrast, *LMP-2A* and the cellular genes *CD21* and *HES1* were induced by EBNA-2 but showed no further induction after co-expression of EBNA-LP, either in EBV-positive or -negative Burkitt lymphoma cell lines (Peng et al., 2005). Conflicting observations were later reported by Portal et al., (2011), who found that co-expression of EBNA-LP together with EBNA-2, enhanced *HES1* transcription two-fold compared to EBNA-2 alone. EBNA-LP alone has never been shown to regulate gene expression independently of EBNA-2.

Together these data raise the question whether or not EBNA-LP is a global transcriptional co-activator. The transient expression assays described above do not clearly answer this question: therefore genetic analysis of the EBNA-LP co-activation function in the context of virus infection is needed.

1.9.9 Proposed mechanisms of the EBNA-LP co-activation function

The data on EBNA-LP co-activation function strongly suggest that the cooperation between EBNA-LP and EBNA-2 happens through a mechanism that requires cellular co-

factors. However, different studies have implicated different cellular cofactors in this process, without formally demonstrating that any one of them is truly essential.

1.9.9.1 Co-activation via Sp100

The only cellular cofactor that is known to interact with the CR3 co-activation domain of EBNA-LP (which is essential for enhancement of EBNA-2) is the Sp100 protein (Ling et al., 2005). Sp100 is one of the proteins associated with PML NBs (Everett et al., 2006), which is where EBNA-LP is localized in established LCLs (for EBNA-LP localization see section 1.9.4).

PML NBs are nuclear substructures defined by the presence of the PML protein (which is essential for the assembly of other PML NB components in normal cells). PML, Sp100 and several other proteins that can be recruited to PML NBs are substrates for SUMO-modification, which is thought to play a role in PML NBs dynamics (Everett, 2006). PML NBs have been hypothesized to perform a cellular defense against DNA viruses by inhibition of viral gene expression, because they are manipulated or targeted for degradation by a number of DNA viruses, and viral mutations that prevent their disruption of PML NBs, reduce viral fitness (Everett et al., 2006). All herpesvirus families target PML NBs in the early stages of lytic replication. For instance, PML NBs are targeted and disrupted by the herpes simplex virus (HSV) protein ICP0, which induces degradation of PML and Sp100 (Everett, 2001), by the cytomegalovirus (CMV) proteins IE1 and IE2, which displace PML and Sp100 from PML NBs (Ahn et al., 1998) and by EBV protein BZLF1, which disperses PML NBs (Adamson and Kenney, 2001). As a result of these interactions, herpesviruses initiate more robust lytic infection. Sp100 is also known to associate with the transcriptional repressor heterochromatin protein 1 (HP1). HP1 plays a role in organizing of chromatin

structure and therefore may enhance transcription of genes that lie within heterochromatic regions (Hayakawa et al., 2003).

Several Sp100 splice variants have been identified (Guldner et al., 1999). These different Sp100 splice variant proteins localize to different parts of the nucleus (one of them localizes to PML NBs and others are mostly dispersed) (Guldner et al., 1999). Moreover, it has been reported that these mostly dispersed isoforms of Sp100 (but not the isoform that localizes to PML NBs) are able to suppress the expression of HSV-1 IE proteins (Negorev et al., 2006). Additionally, different forms of Sp100 based on their sumoylation can be detected in cells, and it has been shown that HSV ICP0 and CMV IE1 proteins specifically abrogate the SUMO modification of Sp100 (either by preventing the formation or by degrading of the SUMO-modified forms) (Müller and Dejean, 1999).

It has been reported that the transient expression of EBNA-LP can displace Sp100 but not PML from PML NBs after transfection of EBV-negative DG75 B cells (Ling et al., 2005). Western blot analysis of Sp100 comparing DG75 cells with DG75 transfected with EBNA-LP, found no difference in levels, indicating that EBNA-LP induced Sp100 displacement from PML NBs, rather than Sp100 degradation (Ling et al., 2005). However, another group claimed that after EBNA-LP transfection into EBV-negative DG75 B cells, EBNA-LP forms nuclear dots which do not co-localize with PML NBs (Szekely et al., 1996).

Ling et al. (2005) also reported that EBV infection causes the displacement of Sp100 but not PML from PML NBs shortly after infection of primary B cells: at day 2 Sp100 was dispersed in about 90% of infected cells (Ling et al., 2005). The percentage of infected cells lacking Sp100 foci decreased with time and by 5 days after infection only about 4% of infected cells were observed to have displaced Sp100 (Ling et al., 2005). The timings of Sp100 re-localization to foci correspond with the re-localization of EBNA-LP from the whole nucleus to the PML NBs (Ling et al., 2005, Bandobashi et al., 2001).

The binding of EBNA-LP to Sp100 has not been comprehensively mapped, but an EBNA-LP carrying a triple alanine substitution in CR3 that was not able to enhance activation by EBNA-2, also did not interact with Sp100 or displace it from NBs (Ling et al., 2005). This supported the idea that Sp100 is important in assisting EBNA-2 gene regulation, and was strengthened by co-transfection experiments in latency I Burkitt lymphoma cell lines (and using promoter constructs in EBV-negative DG75 cells), where expression of Sp100 mutant with a deletion of the N-terminus (the domain responsible for localization to PML) or overexpression of wild type Sp100 was able to replace EBNA-LP in enhancing EBNA-2 induction of the *LMP-1* promoter, suggesting that the presence of Sp100 outside of PML NBs may be required for sufficient co-activation (Ling et al., 2005). In contrast, no enhancement of EBNA-2 activation was seen after overexpression of N-terminally truncated Sp100 mutants from which the domain responsible for interaction with HP1 was also deleted, which suggests that HP1-induced chromatin modification may be involved in the process of enhancing EBNA-2 activation (Ling et al., 2005).

Other studies have shown that although latent EBV infection does not disrupt PML NBs in the EBV-positive Burkitt lymphoma cell lines, Akata and Raji (Raji cells do not express EBNA-LP despite being in latency III) as well as in latently EBV-infected LCLs, the lytic reactivation of EBV in all of these cell lines (variously using anti-IgG antibodies, BZLF1 transfection or TPA and butyrate to induce lytic cycle) results in complete Sp100 dispersion and only partial dispersion (approximately 50%) of PML from PML NBs (Bell et al., 2000). It was therefore hypothesized that expression of lytic gene, BZLF1 is responsible for Sp100 displacement. After transfection of BZLF1 into EBV-negative human epithelial Hep-2 cells, BZLF1 did not affect the integrity of PML NBs; however, in cells in which BZLF1 was overexpressed at very high levels, the Sp100 as well as PML became dispersed (Bell et al., 2000). Co-transfection of BZLF1 and another lytic gene BRLF1 into Hep-2 cells

did not result in PML NB disruption, suggesting that interaction of BZLF1 with other EBV protein is required to disrupt PML NBs during the lytic cycle (Bell et al., 2000). Another group also reported that expression of BZLF1 or BRLF1 in latently infected EBV-positive cell line results in PML dispersion (Adamson and Kenney, 2001). However, in contrast to the previous group they showed that BZLF1 but not BRLF1 expression is sufficient to disrupt PML NBs in EBV-negative HeLa cell line (Adamson and Kenney, 2001). Additionally, they reported that BZLF1 itself is SUMO-modified and (using co-transfection of PML, BZLF1 and HA-SUMO into EBV-negative DG75 cell lines) they showed that it competes with PML for limiting amounts of SUMO (Adamson and Kenney, 2001). Interestingly, after expression of BZLF1 mutant lacking its SUMO-modification site in HeLa cells, the disruption of PML was still observed, suggesting that BZLF1 uses additional (to competition for SUMO) mechanism in disrupting PML NBs (Adamson and Kenney, 2001).

1.9.9.2 Co-activation via HDAC4 and HDAC5

Shortly after Sp100 was proposed as the mechanism for EBNA-2 activation, it was also proposed that EBNA-LP may co-activate EBNA-2 through its interaction with histone deacetylases (HDACs) 4 and 5 (Portal et al., 2006). HDAC activity is associated with gene silencing (Ropero and Esteller, 2007). EBNA-2 and EBNA-LP were shown to immunoprecipitate with HDAC4 from nuclear (EBNA-2) and both nuclear and cytoplasmic (EBNA-LP) extracts of LCLs and the authors concluded that EBNA-LP associates with HDAC4 in both the nucleus and cytoplasm of LCLs (Portal et al., 2006). Additionally, in the EBV-negative B cell lymphoma cell line BJAB, engineered to stably express EBNA-LP, there was a decrease in nuclear HDAC4 concentration and increase in cytoplasmic HDAC4 concentration in comparison to EBNA-LP-negative BJAB (Portal et al., 2006). However, transfection of BJAB cells with wild type or a co-activation-incompetent EBNA-LP mutant

(with alanine substitution of all three conserved serines in the W1W2 domain), showed that while wild type EBNA-LP co-precipitated with HDAC4, the mutated EBNA-LP was not able to do so (Portal et al., 2006). In contrast, overexpression of 14-3-3 gamma (a protein that re-localizes HDACs from the nucleus to the cytoplasm) in BJAB cells did not affect EBNA-2 activation of the LMP-1 promoter and doubled the enhancement of transcription by EBNA-LP (Portal et al., 2006). Based on this observation, the authors proposed a model whereby EBNA-LP re-localizes HDAC4 and HDAC5 away from the promoters targeted by EBNA-2 and into the cytoplasm, leading to the enhancement of transcription (despite the fact that re-localization of HDACs by 14-3-3 gamma had no effect on LMP-1 promoter activation by EBNA-2 but increased co-activation by EBNA-LP, suggesting that role of EBNA-LP is not to re-localize HDACs and that HDACs repress co-activation function of EBNA-LP).

1.9.9.3 Co-activation via NCoR

It has also been reported that EBNA-LP co-activation depends on the displacement of NCoR-repressive complex from enhancers (Portal et al., 2011). EBNA-LP, EBNA-2 and RBPJ can be immunoprecipitated by endogenous NCoR from EBV-negative Burkitt lymphoma cell lines stably expressing either EBNA-2, EBNA-LP or both EBNA-2 and EBNA-LP. Based on this experiment, the authors concluded that EBNA-LP can associate with NCoR (Portal et al., 2011). Co-repressors such as NCoR are stored in spherical foci in the nucleus called matrix-associated deacetylase (MAD) bodies, whereas co-repressor complexes interact with target genes in widely dispersed subnuclear domains (Voss et al., 2005). To determine whether EBNA-LP could alter NCoR localization, GFP fusions of EBNA-LP, NCoR, RBPJ and EBNA-2 were overexpressed in EBV-negative Burkitt lymphoma cell line. GFP-NCoR localized to the MAD bodies. GFP-RBPJ was diffuse in the nucleus when expressed alone or with EBNA-2, but overexpression of NCoR caused GFP-

RBPJ and EBNA-2 to re-localize to the MAD bodies as well. In each case, overexpression of EBNA-LP re-distributed all three proteins away from MAD bodies to become diffuse in the nucleus (Portal et al., 2011). The authors therefore proposed that EBNA-LP dismisses NCoR-RBPJ-EBNA-2 complexes from MAD bodies to the nucleoplasm, a site of active transcription. Additionally, an EBNA-LP mutant with a deletion of the Y1Y2 domain (which has previously been shown to be dispensable for EBNA-2 co-activation (Nitsche et al., 1997)) was able to associate with NCoR but failed to dismiss NCoR from MAD bodies (Portal et al., 2011). However, EBNA-LP mutants that fail to co-activate EBNA-2 (and had been used by this group in their HDAC experiments (Portal et al., 2006)) were not tested for their ability to change NCoR localization. Chromatin immunoprecipitation (ChIP) assays of overexpressed EBNAs showed that EBNA-LP can dismiss native NCoR from RBPJ-EBNA-2 enhancer and promoter sites of *HES1*, *CD21* and *CD23* (Portal et al., 2011).

1.9.9.4 Co-activation via heat shock proteins

Immunoprecipitation experiments performed in LCL cell lines showed that EBNA-LP co-precipitates with heat shock proteins: hsp72 and hsp73 (Mannick et al., 1995). The co-precipitation occurred regardless of whether Y1Y2 domain is present, suggesting that hsp72 and hsp73 associate with W repeats of EBNA-LP (Mannick et al., 1995). However, when another group generated fusion proteins containing maltose binding protein (MBP) fused to various EBNA-LP mutants, they showed that only MBP-tagged proteins containing the Y2 exon precipitated the hsp73, concluding that Y1Y2 domain is required for binding (Kitay and Rowe, 1996a).

Co-expression of hsp72 with EBNA-LP and/or EBNA-2 in EBV-negative Burkitt lymphoma cell lines, significantly increased EBNA-2 and EBNA-LP co-activation of an

LMP-1 promoter construct, and was dependent on the Y1Y2 domain (Peng et al., 2007). Western blot analysis in latency I Akata cells showed increased induction of LMP-1 protein expression when hsp72 was overexpressed together with EBNA-2 and EBNA-LP in comparison to cells in which only EBNA-2 and EBNA-LP were overexpressed (Peng et al., 2007). Based on these data the authors proposed a model in which hsp72 chaperones EBNA-LP in shuttling of repressors (Sp100 and/or HDAC4) from EBNA-2-activated promoters (Peng et al., 2007).

1.9.9.5 Co-activation via direct interaction with EBNA-2

A single study reported that in transient expression in EBV-negative Burkitt lymphoma cell lines, EBNA-2 and a mutant FLAG-EBNA-LP lacking last ten amino acids of Y2 domain are able to co-precipitate. However co-precipitation was not observed with full length FLAG-EBNA-LP or a mutant FLAG-EBNA-LP lacking the whole Y1Y2 domain (Peng et al., 2004). Based on this observation, the authors concluded that EBNA-2 and EBNA-LP directly interact with each other (Peng et al., 2004), even though this was not shown for the WT EBNA-LP. Other groups have been unable to detect any direct interaction between full length EBNA-LP and EBNA-2 proteins, and no co-localization has been observed between the EBNA-2 and EBNA-LP in established LCLs using high-resolution deconvolution confocal microscopy (Peng et al., 2005).

1.9.10 Interaction of EBNA-LP with other proteins

A large number of proteins have been shown to interact with EBNA-LP but few of them have been shown to have significance in the biology of the whole virus.

1.9.10.1 Interaction with pRb and p53

Co-immunoprecipitation experiments performed in EBV-negative Burkitt lymphoma cell lines overexpressing EBNA-2 and EBNA-LP reported that EBNA-LP co-precipitates with two major tumor suppressor proteins: retinoblastoma (pRb) and p53 (Szekely et al., 1993). The pRb protein is responsible for regulation of the E2F cellular transcription factor family and progression through the cell cycle. However, EBNA-LP expression in this context had no significant effect for repression of E2F-1 activity by pRb (Inman and Farrell, 1995). Also, co-transfection experiments performed in the latency I Akata cell line, which contains a frame shift mutation on one allele of the p53 gene and expresses very low levels of p53, demonstrated that EBNA-LP does not prevent p53-mediated transactivation of reporter gene expression (Inman and Farrell, 1995). Therefore, whether there is any biological relevance for EBNA-LP's interaction with pRb and p53 remains unclear.

1.9.10.2 Interaction with HAX-1

HAX-1 is found in the cytoplasm (mainly associated with mitochondria) and is thought to be involved in a variety of signal transduction processes (reviewed by Fadeel and Grzybowska, (2009)). Co-immunoprecipitation experiments performed in EBV-negative Burkitt lymphoma cell line co-transfected with HAX-1 and EBNA-LP vector that contains seven W repeats (long forms of EBNA-LP localize to the nucleus) or only one W repeat (short forms of EBNA-LP were found in the cytoplasm and therefore could form complexes with HAX-1), showed that both long and short forms of EBNA-LP co-precipitated with HAX-1 (Dufva et al., 2001). Mutational analysis of EBNA-LP revealed that the interaction is mediated by the W1W2 domain (Kawaguchi et al., 2000).

1.9.10.3 Interaction with p14ARF and MDM2

EBNA-LP has also been reported to interact with the tumor suppressor protein p14ARF (Kashuba et al., 2003). The p14ARF protein binds to MDM2 inhibiting its E3 ubiquitin ligase activity and preventing p53 to be targeted for degradation. In both yeast 2-hybrid and GST pull-down, it was shown that EBNA-LP can interact with p14ARF (Kashuba et al., 2003). Overexpression of p14ARF in multiple cell lines with different p53 statuses (wild type, deleted, mutated) led to cell cycle arrest and cell death. However, co-expression of EBNA-LP in these cell lines reduced the effect triggered by overexpression of p14ARF resulting in increased survival of those cells (Kashuba et al., 2003). A few years later, the same group reported that EBNA-LP forms tri-molecular complexes with MDM2 and p53, and in this way (not via p14ARF binding) inhibits the function of p53 (Kashuba et al., 2011).

1.9.10.4 Interaction with fte-1 (RPS3A)

EBNA-LP has been reported to associate with fte-1, also known as RPS3A (Kashuba et al., 2005). The fte-1 protein is the v-fos transformation effector that has many biological functions; it enhances v-fos mediated cellular transformation and is a part of the small ribosomal subunit. It also interacts with the apoptosis regulator, poly ADP ribose polymerase (PARP). The overexpression of fte-1 has been associated with a rapid cell proliferation and predisposition to apoptosis. Using the yeast 2-hybrid system, it was shown that EBNA-LP interacts with fte-1 (Kashuba et al., 2005). The interaction was confirmed by GST pull-down assay using recombinant fusion proteins and lysate from LCLs. A mutant EBNA-LP containing four W repeats and lacking the Y1Y2 domain, as well as an EBNA-LP with only two W repeats, were not able to precipitate fte-1 in this experiment, suggesting that at least three/four W repeats and Y1Y2 domain are required for this interaction (Kashuba et al., 2005). It was shown that endogenous fte-1 in breast cancer cell line MCF7 localizes to the

nucleoli. When EBNA-LP was transfected into these cells, it co-localized with fte-1, and led to the enrichment of endogenous fte-1 in the nucleoli (Kashuba et al., 2005). However, in primary B cells fte-1 seems to localize to the cytoplasm (Kashuba et al., 2005).

1.9.10.5 Interaction with PHD1

PHD1 is one of three prolylhydroxylases that can hydroxylate hypoxia-inducible factor 1 alpha (HIF1α) under normoxic conditions. The hydroxylated HIF1α is recognized by an E3 ubiquitin ligase and degraded on proteasomes. A GST pull-down assay performed using LCLs lysates has shown that EBNA-LP binds PHD1, while EBNA-3A binds PHD2, which suggested that HIF1α may be stabilized in LCLs because of a lack of hydroxylation (Darekar et al., 2012).

HIF1α is highly expressed in most solid tumors, where the access to oxygen is limited and instead of oxidative phosphorylation to generate the energy needed for cellular processes, cells rely on aerobic glycolysis, a phenomenon termed “the Warburg effect” (reviewed by Xie et al. (2014)). HIF1α is known to activate aerobic glycolysis resulting in production of high levels of lactate, lactate dehydrogenase A (LDHA) and pyruvate. It has been reported that the concentrations of lactate, pyruvate and the catalytic activity of LDHA were significantly higher in the LCLs than in mitogen-activated B cells (Darekar et al., 2012). Early EBV-infected B cells showed intermediate values (in comparison to LCLs and mitogen-activated B cells) for lactate, pyruvate and lactate dehydrogenase (Darekar et al., 2012).

1.10 Genetic manipulation of the EBV genome

Because of the large size of herpesvirus genomes, homologous recombination (rather than conventional cloning strategies) is the method that has been used to introduce mutations into the viral genome. Recombination efficiency (with exogenous DNA) in EBV however is several times lower than in the α-herpesviruses. Additionally, isolation of the recombinant virus from mixed populations of mutants and wild-type viruses is much more difficult because cells infected with EBV do not produce progeny virus (no plaque formation) in contrast to α-herpesviruses (Delecluse and Hammerschmidt, 2000).

Therefore, initially, the immortalising attributes of EBV were used to select and purify recombinant EBVs: recombinant EBV was generated by recombination of the type 1 EBNA-2 gene (and the adjacent EBNA-LP Y1 and Y2 exons) into the genome of the P3HR1 viral strain, in which the EBNA-2 gene is deleted and therefore the virus is incapable of immortalising B cells. Recombinant P3HR1 genomes into which EBNA-2 had recombined regain their transforming potential. As a result, infection of primary B cells results in proliferating cell lines that carry the recombinant EBV genome. Limiting dilution is then performed to isolate the EBV-infected immortalised cell clones that contain only the recombinant virus (Hammerschmidt and Sugden, 1989). Recombination of the P3HR1 genome with plasmids that contain EBNA-2 and the region targeted for modification allows for the alteration of these genes. However, this strategy only works for modifications that do not severely compromise the transforming potential of the virus.

Over the past years, the cloning of the B95.8 strain of EBV into a bacterial artificial chromosome (BAC) (Delecluse et al., 1998) has made it possible to modify the EBV genome through recombineering in bacteria, to design specific mutants of interest (Feederle et al., 2010). This permits the generation of any mutant without requiring essential virus genes to be functionally intact. There are two main methods used to construct mutants of the EBV BACs.

Both of them are based on homologous recombination between wild type and a mutant gene of interest which has to be flanked by identical DNA sequences to allow for initiation of recombination. One method uses a linearized targeting vector with an antibiotic resistance cassette (flanked by Flp-recombinase target (frt) sites) inserted next to the mutated gene. In this way, the mutation of interest is introduced along with antibiotic resistance cassette, which allows for the selection of recombinants. The antibiotic resistance cassette is then removed by transient transduction of the Flp recombinase into the cells (reviewed in Feederle et al. (2010)). The second approach uses a circular targeting vector that carries a mutated version of a gene of interest, recombinase (i.e. RecA) gene and multiple selection markers which usually include a temperature-sensitive origin of replication, an antibiotic resistance gene such as kanamycin. During transcription of RecA, the recombination is initiated via one of the homology regions. This results in generation of co-integrants that carry both the wild type and the mutated sequence with two identical sets of the homology flanks. The presence of chloramphenicol resistance gene in the BAC allows for the selection of co-integrants by growing the bacterial cells in the presence of chloramphenicol and kanamycin. Finally, in order to remove the targeting vector from the bacterial cells, cells are cultured at non-permissive temperature in the presence of a negatively selecting agent (reviewed in Feederle et al. (2010)). After modification in E. coli, the viral DNA is transfected into EBV negative (i.e. HEK 293) cells to establish EBV-producing cell lines.

Since the original cloning of the B95-8 strain into a BAC, the Burkitt lymphoma-derived strain Akata (Kanda et al., 2004) and the more epitheliotrophic NPC-derived M81 strain (Tsai et al., 2013) have been cloned. These systems allow for the reverse genetic analysis of EBV gene function in the context of virus infection to help in understanding of EBV biology. Knockouts of a variety of EBV latency genes such as LMP-1 (Dirmeier et al., 2003), LMP-2 (Mancao and Hammerschmidt, 2007), EBNA-1 (Humme et al., 2003), EBNA-

2 (Kelly et al., 2005), EBNA-3A (Hertle et al., 2009), EBNA-3B and EBNA-3C (Anderton et al., 2008), using the BAC system have been produced. However, the recombineering technology also allows for the generation of more sophisticated recombinants, including amino-acid-targeting mutations (Skalska et al., 2010), EBNA-2 type 2 point mutant (Tzellos et al., 2014), and gene fusions with modified estrogen receptors (Maruo et al., 2006). However, there are limitations of the B95.8 BAC such as the unreliable GFP expression from the virus in infected primary B cells and LCLs and the missing 10 kb of the BART region, meaning that this is not a true wild-type EBV strain.

1.11 Aims of the thesis

Knockouts of most of the EBV latency genes have been already generated, allowing for the assessment of their function in the context of viral infection. However, the function of EBNA-LP in the biological relevant environment is still not characterized.

The aims of this thesis were therefore to generate the virus lacking EBNA-LP protein and to assess the role of EBNA-LP in the context of B cell infection. This was to be achieved by:

- Construction of EBNA-LP knockout EBV (and its revertant) without disruption of other viral genes' expression.
- Assessment of the role of EBNA-LP in B cell transformation (cell activation, proliferation, establishment of LCLs).
- Investigation of host and viral gene regulation by EBNA-LP.
- Assessment of the role of EBNA-LP-Sp100 interaction in EBV infection.
- Assessment of the contribution of EBNA-LP to resistance to drug-induced cell death.

2 MATERIALS AND METHODS

2.1 Solutions, buffers and reagents used

2.1.1 Solutions and buffers

Luria broth (LB):

0.5% NaCl, 1% BactoTryptone, 1% Yeast extract, made up in dH_2O and autoclaved.

Superbroth (SB):

2.4% Yeast extract, 1.2% BactoTryptone, 0.4% glycerol, made up in dH_2O and autoclaved, 20x KPB added to 5% final concentration before use.

LB Agar:

0.5% NaCl, 1% BactoTrypton, 1% Yeast extract, 1.5% agar, made up in dH2O and autoclaved. If required, cool down to 50°C after autoclaving and add 10% sucrose.

KPB (20x stock):

340 mM KH_2PO_4, 1.4 M K_2HPO_4, made up in dH_2O.

STET:

8% sucrose, 5% Triton X-100, 50 mM EDTA, 50 mM Tris-HCl pH=8.0, made up in dH_2O.

TE:

10 mM Tris-HCl pH=8.0, 1 mM EDTA pH=8.0, made up in dH_2O.

TBE (20x stock):

2 M Tris, 40 mM EDTA, 2 M boric acid, made up in dH_2O.

GTE:

50 mM glucose, 50 mM Tris-HCl pH=8.0, 50 mM EDTA pH=8.0, made up in dH2O.

Alkaline SDS (P2):

0.2 M NaOH, 1% SDS, made up in dH_2O.

Sucrose DNA loading buffer (6x):

50% sucrose, 0.1 M EDTA, bromophenol blue and xylene cyanol, made up in dH2O.

Ficoll DNA loading buffer (6x):

25% ficoll-400, 25 mM EDTA, bromophenol blue and xylene cyanol, made up in dH2O.

Radioimmunoprecipitation assay (RIPA) buffer (5x):

0.25 M Tris-HCl pH=8.0, 0.5% SDS, 5% IGEPA CA630, 0.75 M NaCl, 2.5% sodium deoxycholate (DOC), made up in dH2O.

RIPA lysis buffer:

1x RIPA buffer, 4% protease inhibitor cocktail, 1 mM PMSF, made up in dH2O.

SDS sample buffer (5x):

50 mM Tris-HCl pH=6.8, 2% SDS, 10% glycerol, 1% 2-mercaptoethanol, bromophenol blue, made up in dH_2O.

SDS running buffer (10x stock):

0.25 M Tris, 192 mM glycine, 0.1% SDS, made up in dH_2O.

Transfer buffer:

1x SDS running buffer, 23% ethanol, made up in dH_2O.

Triton X-100 block/perm buffer:

10% fetal bovine serum (FBS), 100 mM glycine, 0.2% Triton X-100, made up in PBS.

MACS running buffer:

PBS pH=7.2, 2mM EDTA, 0.5% BSA.

MACS rinsing buffer:

PBS pH=7.2, 2mM EDTA.

2.1.2 Antibiotics

Antibiotic	Stock	Working concentration
Ampicillin	100 mg/ml in 70% ethanol	0.1 mg/ml
Kanamycin	50 mg/ml in distilled water	50 µg/ml
Chloramphenicol	12.5 mg/ml in 70% ethanol	12.5 µg/ml
Tetracycline	5 mg/ml in 70% ethanol	10 µg/ml
Hygromycin B	50 mg/ml in PBS	100-200 µg/ml

Table 2.1 Antibiotics.

2.1.3 Antibodies

Antigen	Clone ID	Species	Source	Application
EBNA-2	PE2	Mouse	Hybridoma culture supernatant	WB: 1:50, Flow Cyt: 1:5
EBNA-2	R3	Rat	Merck Millipore	IF: 1:200
EBNA-3A	ab16126	Sheep	Abcam	WB: 1:1000
EBNA-3B	6C9	Rat	Hybridoma culture supernatant	WB: 1:10
EBNA-3C	A10	Mouse	Hybridoma culture supernatant	WB: 1:10
EBNA-LP	JF186	Mouse	Hybridoma culture supernatant	WB: 1:500, IF: 1:20
EBNA-LP	4D3	Mouse	Kind gift from Prof. Y. Kawagushi	WB: 1:1000, IF: 1:200
HIF1alpha	C429	Mouse	Invitrogen	IF: 1:50
IFI16	C18	Goat	Santa Cruz Biotechnology	IF: 1:100
PML	pABah	Rabbit	Jena Bioscience	IF: 1:1000
p21	12D1	Rabbit	Cell Signaling	WB: 1:1000
Sp100	PL	Rabbit	Kind gift from Prof. P. Ling	IF: 1:500
Sp100	SpGH	Rabbit	Kind gift from Prof. R. Everett	IF: 1:2000
γ-tubulin	T6557	Mouse	Sigma	WB: 1:10000

Table 2.2 Primary antibodies.

Antigen	Fluorophore	Source	Application
CD19	PE-Texas Red	Invitrogen	Flow Cyt: 1:10
CD20	PE-Vio770	Invitrogen	Flow Cyt: 1:20
CD23	PE-Vio770	Miltenyi	Flow Cyt: 1:20
CD38	PE	Biolegend	Flow Cyt: 1:20
CD58	647 AlexaFluor	BD Bioscience	Flow Cyt: 1:20
HIF1alpha	647 AlexaFluor	Biolegend	Flow Cyt: 1:10

Table 2.3 Fluorophore-conjugated primary antibodies for flow cytometry.

Specificity	Species	Source	Application
Mouse IgG	Sheep	GE Healthcare Life Sciences	WB: 1:2000
Rabbit IgG	Goat	Dako	WB: 1:2000
Rat IgG	Rabbit	Dako	WB: 1:2000
Sheep IgG	Rabbit	Dako	WB: 1:2000

Table 2.4 HRP-conjugated secondary antibodies.

Specificity	Fluorophore	Species	Source	Application
Mouse IgG	488 FluoProbe	donkey	Cheshire	IF: 1:100
Mouse IgG	547 FluoProbe	goat	Cheshire	IF: 1:100
Mouse IgG	647 FluoProbe	donkey	Cheshire	IF: 1:100
Mouse IgG	488 AlexaFluor	goat	Life Technologies	IF: 1:1000
Mouse IgG	594 AlexaFluor	goat	Life Technologies	IF: 1:1000
Mouse IgG	647 AlexaFluor	goat	Life Technologies	IF: 1:1000
Rabbit IgG	488 FluoProbe	goat	Cheshire	IF: 1:100
Rabbit IgG	547 FluoProbe	donkey	Cheshire	IF: 1:100
Rabbit IgG	647 FluoProbe	donkey	Cheshire	IF: 1:100
Rabbit IgG	594 AlexaFluor	goat	Life Technologies	IF: 1:1000
Rabbit IgG	647 AlexaFluor	goat	Life Technologies	IF: 1:1000
Rat IgG	488 FluoProbe	donkey	Cheshire	IF: 1:100
Rat IgG	547 FluoProbe	donkey	Cheshire	IF: 1:100
Rat IgG	647 FluoProbe	goat	Cheshire	IF: 1:100
Rat IgG	488 AlexaFluor	goat	Life Technologies	IF: 1:1000
Goat IgG	546 AlexaFluor	donkey	Life Technologies	IF: 1:1000
Mouse IgG	RPE	goat	Dako	Flow Cyt: 1:100

Table 2.5 Fluorophore-conjugated secondary antibodies.

2.1.4 Primers and TaqMan assays

Primer name	Primer sequence
Cp forward	5'-AATCATCTAAACCGACTGAAGAAACAG-3'
T3 reverse	5'-ATTAACCCTCACTAAAGGGA-3'
T7 forward	5'-TAATACGACTCACTATAGGG-3'
U reverse	5'-GGTCTATGATGCGACGATCAC-3'
W1W2 reverse	5'-GAGGGGACCCTCTGGCC-3'
Wp forward	5'-CGCCAGGAGTCCACACAAAT-3'
Y1Y2del forward	5'-GAATTCGCATCCAGTGAGCCGACCCAGCGCCAATCTGTCTACATAG-3'
Y1Y2del reverse	5'-CGGCTCACTGGATGCGAATTCTCAGTGGCCGTAGTGGCTTGGTTGTAAG-3'
Y2end reverse	5'-CCTGTGACTTAGTCTTCATCCTCTTC-3'
Yh reverse	5'-GCTTAGAAGGTTGTTGGCATG-3'

Table 2.6 Primers for regular polymerase chain reaction (PCR).

Primer name	Primer sequence
ALAS1 forward	5'-GGATTCGAAACAGCCGAGTG-3'
ALAS1 reverse	5'-TGACATCATTGTGGCGGAAG-3'
Cp-C2 forward	5'-AAGAAACAGCCTCCTGCACG-3'
GNB2L1 forward	5'-GAGTGTGGCCTTCTCCTCTG-3'
GNB2L1 reverse	5'-GCTTGCAGTTAGCCAGGTTC-3'
RPLP0 forward	5'-ACTCTGCATTCTCGCTTCCT-3'
RPLP0 reverse	5'-GGACTCGTTTGTACCCGTTG-3'
sisRNA-1 forward	5'-GTAAGTGGACTTTAATTTTTTCTGCTAAGCCC-3'
sisRNA-1 reverse	5'-TGGGTGTGTGTAGTGTGTGC-3'
W0 forward	5'-CAGAGCGCCAGGAGTCCACAC-3'
W2 reverse	5'-GGTGCCTTCTTAGGAGCTGTCC-3'

Table 2.7 Primers for Real-Time polymerase chain reaction (qPCR).

TaqMan assay name	Assay ID
CCND2	HS00153380_m1 CCND2
EBER-2	AID1TA4 EBER2
EBNA-2	AIY9X8V EBNA2
EBNA-3A	AI20SZ2 EXON U-3A_152
HES1	HS00172878_m1 HES1
LMP-1	LMP1 EXON 2-3
LMP-2	LMP2 EXON 2-9
MYC	HS00153408_m1 MYC

Table 2.8 TaqMan assays (Applied Biosystems).

2.2 DNA analysis and cloning

2.2.1 Restriction digestion

Digests were performed using restriction endonucleases from New England Biolabs (NEB) and buffers were selected according to their recommendations. Analytical digestions were performed in 15 µl reactions (using 1 µl plasmid DNA or 5 µl BAC miniprep) while preparative digestions were performed in 30 µl reactions (1-5 µl of plasmid DNA to correspond to approximately 500-2000 ng of DNA).

2.2.2 Cloning

Digested DNA bands were excised from an agarose gel and purified using QIAquick spin DNA gel extraction kit (QIAGEN). Purified DNA fragments were ligated using T4 DNA ligase (NEB) in 10x T4 DNA ligase buffer (NEB).

To transform ligated DNA into bacteria, DNA (typically the whole ligation reaction) was added to 50 µl of chemically competent DH5α E. coli and incubated on ice for 15 minutes. A heat shock was then performed (bacteria were incubated in a water bath for 1 minute at 42°C and immediately transferred into ice). 900 µl of LB was added and bacteria left to recover for 1 hour in a shaking incubator at 37°C (1.5 hours at 30°C for temperature-sensitive or unstable plasmids). Either 100 µl of the bacteria or a pellet of all the transformed bacteria (resuspended in 100 µl) was spread on agar plates containing the appropriate antibiotic and incubated overnight at 37°C or 30°C.

2.2.3 Plasmid miniprep

A bacterial colony transformed with a plasmid of interest was grown overnight at 37°C (30°C for temperature sensitive plasmids) with shaking in 1.5 ml of Super Broth (SB) containing the appropriate selective antibiotic (see table 2.1). The next day bacteria were pelleted by centrifugation at 4000 rpm for 5 minutes in a microcentrifuge. The bacterial pellets were resuspended by vortexing in 70 µl of STET, lysed by addition of 200 µl alkaline SDS, neutralised by addition of 150 µl 7.5 M ammonium acetate and incubated on ice for 15 min. After that time debris was removed by centrifugation at 13000 rpm in a microcentrifuge for 15 minutes at 4°C. The supernatant was poured into a fresh tube and the DNA was precipitated by addition of 240 µl of isopropanol and pelleted by centrifugation at 10000 rpm in a microcentrifuge for 5 min. The DNA pellet was washed in 200 µl of 70% ethanol, allowed to air dry for 10 minutes and resuspended in TE containing 5 µg/ml RNase A, using 50 µl (for low copy plasmids/BACs) or 120 µl (for high copy plasmids).

2.2.4 Agarose gel electrophoresis

DNA fragments were separated by migration in a 0.8-1.5% agarose gel containing SybrSafe (Invitrogen) in 1x TBE under 80 V for 1-2 h using a Hoeffer HE33 horizontal submarine gel system.

2.2.5 Gel extraction

DNA gel extraction was performed using the QIAquick gel extraction kit (Qiagen). The appropriate DNA fragment was excised from the gel with a clean scalpel, mixed with 3 volumes (typically 450 µl) of Buffer QG (Qiagen) and incubated at 50°C for 10 min. After dissolving, 1 volume (150 µl) of isopropanol was added. The mixture was applied to the

QIAquick column and spun in a microfuge at 13000 rpm for 1 min. Flow-through was discarded, 0.5 ml of Buffer QG (Qiagen) was added to the column and spun again. The column was washed with 0.75 ml of Buffer PE (Qiagen) and centrifuged twice in a microfuge at 13000 rpm for 1 min. The column was placed into a clean tube and DNA was eluted by addition of 30 µl of nuclease-free water that was allowed to stand for a minute before centrifugation at 13000 rpm for 1 min in microfuge.

2.2.6 Deletion mutagenesis using In-Fusion cloning

The plasmid vector was amplified using inverse PCR with oligonucleotides designed to contain a primer sequence specific to the 25 nucleotides of sequences outside of region to be deleted at their 3' ends and 24 bases of shared homology (that do not include the bases to be deleted) at their 5'ends (that allows for joining the fragments and circularization of the PCR product).

To perform inverse PCR, 1 ng of plasmid vector was mixed with 400 nM of each Y1Y2del forward and Y1Y2del reverse primer (see table 2.6) and 12.5 µl of CloneAmp HiFi PCR premix (Clontech) in a final volume of 25 µl. The cycling conditions were as follows: 10 cycles of 98°C for 10 s, 60°C for 15 s, 72°C for 45 s and then 25 cycles of 98°C for 10 s, 68°C for 15 s, 72°C for 45 s.

The PCR product was gel purified and circularized by mixing 50 ng of the PCR product with 4 µl of In-Fusion HD enzyme premix (Clontech) in final volume of 20 µl. The reaction was incubated at 50°C for 15 min and placed on ice. 2.5 µl of reaction was transformed into 50 µl of chemically competent DH5α E. coli. As a negative control, an additional reaction (without the In-Fusion enzyme) was prepared and similarly transformed into competent DH5α E. coli. Colonies from the experimental plate were miniprepped, extracted plasmids

were analyzed by restriction digestion, and the DNA sequence checked by Sanger sequencing (CSC genomics) using T7 forward and T3 reverse primers (see table 2.6).

2.2.7 Generation of recombinant EBV-BACs

Competent E.coli (see section 2.2.8) containing the EBV-BAC that is to be modified were defrosted on ice. One µl of a temperature sensitive kanamycin resistant shuttle vector (pKovKan) containing the desired insert and 5 µl of a plasmid expressing the RecA gene and tetracycline resistance (pDF25-Tet) were added to the bacteria, mixed, kept on ice for 30 min and then heat shocked at 42°C for 1 min. 1 ml of LB was added to the BAC and shaken for 1.5 hours at 30°C. 100 µl of cells were plated on Cm+Kan+Tet plates and incubated at 30°C o/n to select for colonies that contain both plasmids and the EBV-BAC. The next day 10-50 colonies were picked and pooled in 1ml LB. 100 µl of this was plated on Cm+Kan plates and incubated at 43°C o/n, to select for BACs that had recombined with the pKovKan plasmid (and allowing unintegrated pKovKan and pDF25-Tet to be lost due to their temperature-sensitive replication origins). The next day colonies were picked into 1.5 ml SB and grown overnight at 37°C. BAC DNA was isolated by miniprep and analyzed using restriction digestion and pulsed field gel electrophoresis. Colonies containing intact co-integrants (where possible two independent co-integrants that use different recombination half-sites for the integration) were made competent (see section 2.2.8).

Competent E.coli containing cointegrants were transformed with 2 µl of pDF25-Tet. After recovery for 1.5 hour at 30°C, bacteria were plated on Cm+Tet plates and incubated at 30°C o/n. The next day colonies were picked and pooled in 1 ml LB containing 5% Sucrose+Cm+Tet and incubated at 30°C with shaking for 8 h to enrich for colonies that have removed the KovKan backbone from the BAC. Twenty microliters of culture was streaked onto 14 cm diameter LB agar plates containing Cm+5% Sucrose and incubated at 43°C o/n to

select for recombinants (and against co-integrants). To identify and exclude colonies that have survived sucrose selection through mutation of the SacB gene, colonies were replica plated onto Cm+Kan and then Cm alone plates. Plates were incubated at 37°C o/n. BAC DNA was isolated from colonies that grew on the Cm only plate but not on the Cm+Kan plate, and screened by restriction digestion and pulsed field gel electrophoresis. AgeI and EcoRI are used to assess EBV genome integrity; other enzymes are used to establish whether the recombination has reverted to the parental virus or incorporated the change carried by the pKov-Kan shuttle vector.

2.2.8 Preparation of competent bacteria for recombineering

E.coli cells containing EBV-BAC were grown o/n at 37°C in 1 ml LB containing antibiotic (chloramphenicol for EBV-BAC, chloramphenicol+kanamycin for co-integrants). Next day 100 µl of the overnight culture was diluted in 10 ml of LB with antibiotic, grown at 37°C for 3 hours in a 50 ml falcon tube and then placed in an ice slurry for 30 minutes. After that time cells were spun at 1137 rcf for 15 minutes at 4°C. The cell pellet was resuspended in 2 ml of 100 mM $CaCl_2$. The suspension was left on ice for 30 minutes and then centrifuged at 1137 rcf for 15 minutes at 4°C. Pellets were resuspended in 200 µl of 100 mM $CaCl_2$ with 15% glycerol. Cells were split into 50 µl aliquots, snap-frozen and stored at -80°C.

2.2.9 Pulsed-field gel electrophoresis

Larger (10-100 kb) DNA fragments were separated by migration in a 1% agarose gel in 0.5x TBE using the Bio-Rad contour-clamped homogeneous electric field (CHEF-DR II) with chiller system at 14°C, at 6 V/cm with the following settings: initial switch = 1 s and final switch = 10 s (for undigested BAC: initial switch = 2 s, final switch = 16 s).

Electrophoresis was run for 13 h (for undigested BAC: 16 h). After running, DNA was stained by soaking the gel in 0.5x TBE supplemented with 0.5 µg/ml ethidium bromide (EtBr) for >30 minutes. Gels were then imaged using the Bio-Rad Gel Doc XR+ imaging system.

2.2.10 CsCl maxiprep

To isolate larger quantities of supercoiled DNA suitable for transfection, single colonies of E.coli containing wild type and modified BAC were cultured in 1 ml of SB with antibiotic at 37°C. After 8 hours cultures were diluted into 500 ml of SB with 12.5 µg/ml chloramphenicol and grown at 33°C o/n. Next day, cells were transferred to centrifuge bottles and spun down for 15 min in an SLA3000 rotor at 2702 rcf. Pellets were resuspended in 30 ml of GTE buffer, lysed by adding 60 ml of alkaline SDS, inverted to mix and neutralised immediately by adding 45 ml of 7.5 M ammonium acetate. After 15 min of incubation on ice, the lysate was spun for 10 min at 4303 rcf at 4°C. The supernatant was filtered using 70 µm cell strainers. DNA was precipitated by adding 0.6-0.7 volumes (typically 75 ml) of isopropanol, mixing by inversion and spinning for 10 min at 2702 rcf. The pellet was washed with 5 ml of 70% ethanol, briefly air dried and then dissolved in 6 ml of TE_{25} (10 mM Tris-HCl, 25 mM EDTA). The DNA solution (made up to 10 g with TE) was transferred into tubes with 10.55 g of CsCl. After gently dissolving the CsCl, 50 µl of EtBr was added. The DNA/CsCl was transferred into Beckman 13.5 ml centrifuge tubes using an unplugged syringe with blunt 19G needle as a funnel. Tubes were filled up to the top with TE, sealed using the Beckman heat-sealer and spun in an ultracentrifuge for at least 16 h at 60000 rpm at 20°C using 70.1Ti rotor. The lower band (of two visible bands) containing BAC DNA was removed using 1 ml syringe and 19G needle. The extracted DNA was transferred into fresh CsCl solution (36.9 g of CsCl resuspended in 37.7 ml of TE) and spun again for at least 16 h

at 60000 rpm at 20°C in a 70.1Ti rotor. Next day, the visible lower band was removed using a 1 ml syringe and 19G needle, transferred into 1.5 ml eppendorf tubes and ethidium bromide was extracted six times by mixing with 1 ml of TE saturated butanol. DNA was precipitated by adding 0.5 volumes of 7.5 M ammonium acetate, 2.5 volumes of 100% EtOH and 1 µl of linear polyacrylamide (LPA; GenElute, Sigma-Aldrich). The pellet was washed with 70% EtOH and resuspended in 100 µl of TE.

2.3 Cell culture

HEK293-SL cells (a kind gift from Dr. C. **S**hannon-**L**owe), Raji cells and LCLs were cultured in RPMI 1640 medium (Gibco) supplemented with 10% foetal calf serum (FCS) (Gibco), penicillin, streptomycin and 2 mM L-glutamine at 37°C, 5% CO_2.

BL31 cells were cultured in RPMI 1640 medium (Gibco) supplemented with 10% FCS (Gibco), penicillin, streptomycin, 1 mM sodium pyruvate (Sigma) and 50 µM α-thioglycerol (Sigma) at 37°C, 5% CO_2.

EBV-infected primary B cells and PBLs were cultured in RPMI 1640 medium (Gibco) supplemented with 15% FCS (tested for suitability for EBV transformation of primary B cells: PAA or Gibco), penicillin, streptomycin at 37°C, 5% CO_2.

MRC5 cells were cultured in DMEM (Gibco) supplemented with 10% FCS, penicillin, streptomycin at 37°C, 5% CO_2.

Establishment of EBV-HEK293-SL producer cell lines was performed in complete media for HEK293-SL cells described above but supplemented with previously tested FCS that is suitable for outgrowth of virus producer cell lines (PAA or GE healthcare).

HEK293-SL or BL31 cell lines that carry EBV genome were cultured in complete media additionally supplemented with 100 μg/ml of hygromycin B (Roche).

2.4 Isolation of leucocytes from human blood products

2.4.1 Isolation of PBLs from human buffy coat residues

Buffy coat residues ordered from National Health Service Blood and Transplant (NHSBT) (usually around 120 ml) were transferred from the blood bag into a sterile cell culture flask and topped up with cold PBS to 200 ml. After mixing, 25 ml of diluted blood was slowly layered onto 25 ml Ficoll-Paque (GE Healthcare Life Scences) in each of eight 50 ml centrifuge tubes. Tubes were spun at 400 rcf for 30 mins at room temperature with the brake off. After centrifugation, lymphocytes (creating a grey-white interface between the ficoll and the diluted plasma layer) were collected using a 5 ml pipette. Cells from the eight tubes were combined in 100 ml of wash buffer (RPMI with 1% FCS) in bullet tubes on ice. To wash off the ficoll, bullet tubes were spun at 400 rcf for 5 min. Supernatant was removed into waste container and 200 ml of wash buffer was added, the cell pellet resuspended and spun again. After removing supernatant, cell pellet was resuspended in 50 ml wash buffer, and strained through a 70 μm cell strainer (BD Falcon).

2.4.2 Isolation of PBLs from human leukodepletion cones

Leukodepletion cone ordered from National Health Service Blood and Transplant (NHSBT) was flushed with 50 ml of RPMI using a syringe and 19G needle to inject through the tube at the top of the cone and the overflow from the tube at the bottom of the cone was

collected. The blood cells were layered on ficoll in two 50 ml centrifuge tubes and processed in a same way as buffy coat residues.

2.4.3 Isolation of PBLs from human cord blood

The cord blood was obtained thanks to collaboration with Dr. Beth Holder and Prof. Beatte Kampmann through the MatImms@Imperial study, and the research midwives and technicians who consented the patients and collected the samples: Dr. Beverly Donaldson, Ms. Marielle Bouqueau, and Mr. Thomas Rice. PBLs from cord blood were isolated in a same way as adult PBLs scaling down all of the reagents because of the very small volume of obtained cord blood.

2.4.4 Isolation of primary B cells from previously purified PBLs population

B cells were isolated using AutoMACS separator (Miltenyi Biotec): 10^9 PBLs were spun at 400 rcf for 5 minutes in a 50 ml centrifuge tube. The supernatant was removed, cells were resuspended in 8 ml MACS running buffer and 500 µl of CD19 microbeads (Miltenyi Biotec) were added. After mixing, cells were incubated in the fridge for 15 minutes. Meanwhile, the AutoMACS separator was set up: outlet ports were wiped with 70% ethanol; MACS running and MACS rinsing buffer were installed; column exchange programme was run. After 15 min of cell incubation with CD19 beads, 40 ml of MACS running buffer was added, cells were centrifuged and supernatant removed to wash off excess beads. Cells were resuspended in 5 ml of fresh MACS running buffer and placed under the input port of the separator. Collecting tubes (15 ml centrifuge tubes) were placed under the negative and positive ports. The positive selection programme was run to purify CD19-positive B cells. Cells were resuspended in fresh growth medium for primary B cells and counted.

2.5 Virus production, analysis and infection

2.5.1 Generation of EBV-producer cell lines

2.5.1.1 Transfection of HEK293-SL cells

HEK293 cells were seeded in a 6-well plate at a density of 20-40%. After 36 h cells were transfected with 1 μg of BAC DNA mixed with 0.75 μl lipofectin (Invitrogen) and 40 μl of 0.1 mg/ml peptide 6 (Hart et al., 1997), diluted into 1 ml Opti-MEM (Invitrogen) and incubated for 6 h. After that time media was replaced with growth media (RPMI). After 48 h, growth media was replaced with media containing 200 μg/ml of hygromicin B. The next day cells were trypsinized, split between four 10 cm dishes each containing 12 ml RPMI with 10% FCS (batch tested for its ability to support establishment of EBV-HEK293-SL clones), P/S, 2 mM L-glutamine, 200 μg/ml hygromycin B and incubated at 37°C, 5% CO_2 for 10 days. Media was then changed every 5 days until colonies were large enough to ring clone.

2.5.1.2 Ring cloning of transfected cells

Colonies were picked once they were around 3-5 mm in diameter, using "cloning rings" stuck to the base of the dish with sterilized vacuum grease. Colonies were trypsinized with 40 μl fresh trypsin for five minutes and then neutralised with fresh media in situ and transferred into 6-well plates and serially expanded until growing in 75 cm flasks in RPMI 1640 whose concentration of hygromycin B was reduced to 100 μg/ml. Cell lines were screened for their ability to produce virus and for the integrity of the viral episome (see below).

2.5.2 Assessment of virus production

The stable EBV-HEK293-SL producer cell lines were co-transfected with BZLF1 and BALF4 (1 μg of a 1:1 mix of plasmids for cells seeded in 6 well plate, or 12 μg of a 1:1 mix of plasmids for cells seeded in 10 cm dish for large scale virus production) using the lipofectin and peptide 6 transfection method described in section 2.5.1.1, to induce the lytic cycle of EBV and produce virus. BZLF1 is an immediate early transactivator of the lytic cycle (see section 1.5), BALF4 is a viral glycoprotein which is transfected because it has been shown that it significantly enhances the ability of the produced EBV to infect human cells (Neuhierl et al., 2002). After 4 days, the virus supernatant was harvested and filtered through a 0.45 μm filter (NALGENE), and stored at 4°C.

Later on during the project the lipofectin and peptide 6 were replaced by the GeneJuice reagent (Novagen). In this case cells were co-transfected with BZLF1 and BALF4 (6 μg 1:1 mix of plasmids for cells seeded in 10 cm dish) mixed with 18 μl GeneJuice (Novagen), diluted into 5 ml of Opti-MEM (Invitrogen) and incubated for 6-8h. After that time media was replaced with growth media (RPMI).

To assess the titer of the virus, 0.5 ml Raji cells ($2x10^5$ cells/ml) were infected with serial 10-fold dilutions of virus in 1.5 ml in wells of a 24 well plate. After 48 h, 0.5 ml media containing 20 nM TPA (Sigma) and 5 mM N-butyrate (Sigma) was added to infected cells to activate the CMV promoter-driven GFP to allow infected cells to be more clearly identified. The next day the cell clumps were disrupted by pipetting and after the cells had settled, virus was quantified using fluorescent microscopy to count the number of GFP-positive Raji cells per well.

2.5.3 Low molecular weight DNA extraction from mammalian cells

To obtain BAC DNA for episome rescue, EBV-BAC-carrying HEK293 cells were scraped from the dish, spun down, washed in PBS and centrifuged at 3000 rpm for 5 min in a microfuge. Pellets were resuspended in 60 µl of STET, lysed by addition of 130 µl alkaline SDS, neutralised by addition of 110 µl 7.5 M ammonium acetate and incubated on ice for 10 min. After that time cells were centrifuged at 13000 rpm for 30 minutes at 4°C in microfuge. DNA was extracted against phenol/chloroform/isoamyl alcohol (24:24:1 ratio) and then twice with chloroform using MaXtract gel tubes (Qiagen) to separate the aqueous and organic phases and DNA was precipitated by addition of 670 µl of 100% ethanol and centrifugation. Then DNA was washed with 200 µl of 70% ethanol, and resuspended in 50 µl of TE containing 5 µg/ml RNase A.

2.5.4 Episome rescue

Low molecular weight DNA isolated from EBV positive cell lines (1 µl) was electroporated into 20 µl of Electromax DH10B bacteria (Life Technologies) in a 1 mm electroporation cuvette (Bio-Rad). The electroporation was performed using a Bio-Rad Gene Pulser electroporator at 1.8 kV, 200 Ω and a capacitance of 25 µF. After electroporation, 400 µl of SOC medium (Life Technologies) was added. Bacteria were transferred into the shaking incubator at 37°C for 1 h. After that time the whole volume was plated on 14 cm agar plates containing Cm. BAC DNA was isolated from colonies by miniprep and screened by restriction digestion.

2.5.5 BL31 infection

BL31 cells (10^5 cells in 0.5 ml of growth media in 24-well plate) were infected with 0.5 ml of virus. After approximately 16 h, 800 µl of media was exchanged for fresh BL31 growth media. Two days after infection, 800 µl of media was exchanged for BL31 media with 200 µg/ml of hygromycin B (to select for infected cells).

2.5.6 Primary B cell and PBL infection

Primary B cells or PBLs (typically 10^6-$2x10^6$ cells per viral infection) were infected with different mutant viruses at the same MOI (typically MOI=1-2 rgu/B cell, depending on experiment) diluted to the same volume. Infection was carried out at 37°C for 3 h, shaking. After three hours, the cells were spun down and media replaced with primary B cell media supplemented with 50 ng/ml (isolated B cells, cord blood PBLs) or 500 ng/ml (adult PBLs) of cyclosporine A. Cells were plated in 24-well or 48-well plates either alone or in a presence of MRC5 feeder cells irradiated for 8 min which corresponds to dose of 50 Gy..

2.6 RNA analysis

2.6.1 RNA extraction

RNA was extracted using the RNeasy mini kit (Qiagen). Harvested cells were washed with PBS and resuspended in an appropriate volume of RLT buffer containing 10 µl of β-mercaptoethanol per 1 ml of RLT buffer. These lysates could be stored at -80°C until required. Cells were homogenized by passing the lysate 8 times through a blunt 25G needle fitted to a 1 ml syringe. One volume of 70% ethanol was added to the homogenized lysate and mixed by pipetting. Samples were transferred to RNeasy spin columns placed in a 2 ml

collection tube and centrifuged for 15 s at 10000 rcf. Flow through was discarded and 700 µl of buffer RW1 was added to RNeasy spin column to wash the membrane. Columns were spun for 15 s at 10000 rcf. Flow through was discarded, 500 µl of buffer RPE was added to RNeasy spin column and samples were spun again for 15 s at 10000 rcf. The flow through was discarded, another 500 µl of buffer RPE was added to RNeasy spin column and samples were spun again for 15 s at 10000 rcf. Again, the flow through was discarded. RNeasy spin columns were then placed in a new 2 ml collection tubes and centrifuged at 10000 rcf for 1 min to eliminate any possible carryover of buffer RPE. After that the RNeasy spin columns were placed in a new 1.5 ml collection tubes, an appropriate volume of RNase-free water was added directly to the spin column membrane and the samples were spun at 10000 rcf for 1 min to elute RNA.

2.6.2 DNase treatment of RNA samples

RNA samples were treated with DNase using Precision DNase kit (PrimerDesign). Samples were incubated with appropriate volume of DNase for 10 min at 30°C. To inactivate DNase, samples were incubated for 5 min at 55°C.

2.6.3 Reverse transcription

RNA samples were reverse transcribed to cDNA using SuperScript III First-Strand Synthesis SuperMix for qRT-PCR (Invitrogen). RNA was mixed with appropriate volume of 2x RT Reaction Mix and RT Enzyme Mix and incubated first at 25°C for 10 min and then at 50°C for 30 min. To terminate the reaction, samples were incubated at 85°C for 5 min and then chilled on ice. To remove the RNA template from the cDNA:RNA hybrid molecule after

first-strand synthesis, 1 µl of RNase H (Invitrogen) was added to all samples, mixed and incubated at 37°C for 20 min.

2.6.4 Polymerase Chain Reaction (PCR) analysis of EBNA-LP/EBNA-2 transcripts

RNA was extracted from established EBV-BAC-BL31 cell lines with the RNeasy kit (Qiagen) and reverse transcribed using SuperScript Supermix (Invitrogen). To amplify EBNA-LP transcripts from infected cells, we used a reverse primer in the Yh exon and forward primers in either W0 exon (Wp primer) or spanning the sequence of C1 and C2 exons (Cp primer) to allow transcripts initiated in both Cp and Wp to be analysed (see table 2.6). 0.05 µg of cDNA was mixed with 0.5 µl 10 mM dNTP, 0.5 µM of forward and reverse primers, 0.25 µl Q5 polymerase (NEB) in a final volume of 25 µl. For the Cp primer 5µl of GC enhancer was also added. The cycling conditions were as follows: 98°C for 30s, and then 30 cycles of 98°C for 10s, 65°C for 30s, 72°C for 55s, with a final cycle of 72°C for 2 min.

2.6.5 Real-Time PCR

Real-Time PCR was performed on a ViiA™ 7 Real-Time PCR system with a 384-well block (Applied Biosystem) using either SYBR Green Low Rox kit (Kapa Biosystems) or Takyon Probe Low Rox kit (Eurogentec) (for primers' sequences and the TaqMan details see table 2.7 and 2.8). The cycling conditions were: 95°C for 3 min, followed by 40 cycles of 95°C for 3s and 60°C for 25s. Dissociation curve analysis was performed for SYBR Green assays at the end of each run to ensure the absence of non-specific products. Quantification of mRNA levels was carried out using the Delta-Delta Ct method. Results were analyzed using DataAssist Software v3.01 (Thermo Fisher Scientific). mRNA levels for each target gene

were normalized to 2 houskeeping genes: ALAS1 and RPLP0 (these were identified as the best ones based on DataAssist Software analysis out of the 4 different housekeeping genes tested). Data were expressed relative to the sample from WT-infected cells harvested on day two. The statistical difference between LP-KO/Y1Y2-KO group and WT/REV group was calculated using two sample unequal variance (heteroscedastic) t-test.

2.6.6 Microarrays

Transcriptome analysis using Affymetrix Exon microarrays (Human Exon 1.0ST) was performed by University College London Genomics on RNAs obtained from BL31 cell lines (the same methodology as has been done in our lab by Ian Groves for EBNA-2 KO- infected BL31). The data was analyzed using Partek Genomics software.

2.7 Protein analysis

2.7.1 Protein extraction

Seventy µl of RIPA lysis buffer with protease inhibitor cocktail and 100 mM PMSF was added to the cell pellet (usually 10^5-10^6 cells) and pipette up and down to lyse the cells. The cell lysate was incubated on ice for 10 min and spun at 14000 rpm for 10 min at 4°C in a microfuge. Supernatant was collected, transferred to a fresh tube and stored at -70°C.

2.7.2 SDS PAGE gel electrophoresis

Protein separation was performed using sodium dodecyl sulphate-polyacrylamide gel electrophoresis (SDS-PAGE). The gel consisted of resolving gel (7.5%-12% acrylamide

(Sigma), Tris pH=8.8, 0.1% SDS) and stacking gel (5% acrylamide (Sigma), Tris pH=6.8, 0.1% SDS). Gels were polymerized using 24 µl of 10% ammonium persulphate (APS) and 10 µl of NNN'N'-tetramethylethylenediamine (TEMED) per 1.5 mm gel. Prior to loading, protein samples were mixed with 5x SDS sample buffer, boiled for 5 min and loaded in equal amounts (typically 20-30 µg per lane). The gel was run at 150 V for 75 min in SDS running buffer.

2.7.3 Transfer of proteins from a gel to a membrane

Proteins separated by SDS-PAGE electrophoresis were electrotransferred onto a nitrocellulose membrane at 100 V for 1 h in transfer buffer cooled by an ice pack.

2.7.4 Western blotting

The nitrocellulose membrane blotted with protein was blocked in 5% milk diluted in 0.1% PBST (PBS, 0.1% Tween) solution for 1 h on a shaker at room temperature. After that time, the blocking solution was discarded and a primary antibody diluted in 10 ml blocking solution was added. The membrane was incubated with primary antibody over night at 4°C, shaking. The following day, the membrane was washed 3 times for 10 min with 0.1% PBST. The appropriate secondary antibody conjugated to horseradish peroxidase (HRP) diluted 1:2000 in blocking solution was added to the membrane and incubated for 1 hour at room temperature, shaking. After that time, the membrane was washed again 3 x 10 min with 0.1% PBST. To visualize proteins, the membrane was incubated for 5 minutes with ECL solutions A and B (GE Healthcare Life Sciences) mixed in a 1:1 ratio and exposed on autoradiography film (VWR).

2.8 Flow cytometry

2.8.1 Extracellular staining

Harvested cells were spun down for 3 min at 3000 rpm using a microcentrifuge, washed with PBS containing 0.5% BSA, then incubated with 60 µg of human IgG (Sigma) for 10 min. After blocking with IgG, 50 µl of fluorescent antibody (or antibodies) at an appropriate dilution (see table 2.3) in PBS + 0.5% BSA was added to the cells and incubated for 30 min-1 h (depends on antibody) at 4°C in the dark. After incubation with antibody, cells were washed twice with PBS + 0.5% BSA, then resuspended in 300 µl PBS containing a live/dead stain (0.2 µl/ml of Sytox Blue (Invitrogen) or 10 µl/ml DRAQ7 (BioStatus)) and after >10 min analyzed by flow cytometry.

2.8.2 Intracellular staining using PFA/Triton as fixation/permeabilization

Harvested cells were spun down for 3 min at 3000 rpm using microcentrifuge, washed with PBS containing 0.5% BSA and stained with 1 µl/ml of fixable live/dead stain (Fixable near IR dead cell stain (Invitrogen)) resuspended in PBS for 10 min in the dark. After staining, cells were washed again with PBS + 0.5% BSA and fixed using 4% PFA (ThermoFisher) in PBS for 15 min at room temperature in the dark. After fixing, cells were washed with PBS + 0.5% BSA and incubated with 200 µl of blocking/permeabilization buffer (PBS + 10% FCS + 100 mM Glycine (Sigma) + 0.2% Triton-X100 (Sigma)) for 30 min at room temperature in dark. After that time, the primary antibody at an appropriate dilution (see table 2.2) in blocking/permeabilization buffer was added and incubated for 30 min at 4°C in dark. Cells were washed again and the fluorescent secondary antibody at an appropriate dilution (see table 2.5) in blocking/permeabilization buffer was added and

incubated again for 30 min at 4°C in dark. After that cells were washed with PBS + 0.5% BSA and analyzed by flow cytometry.

2.8.3 Intracellular staining using ethanol fixation/permeabilization

Harvested cells were spun down for 3 min at 3000 rpm using microcentrifuge, washed with PBS containing 0.5% BSA and stained for 10 min in the dark with 1 µl/ml of Fixable near-IR dead cell stain (Invitrogen) resuspended in PBS. After staining, cells were washed again with PBS + 0.5% BSA and fixed with 200 µl of ice cold 80% ethanol for 30 min at 4°C in the dark. After fixing, cells were spun for 5 min at 2000 rpm using microfuge. To rehydrate the cells PBS + 0.5% BSA was added, cells were resuspended and incubated for 15 min. After that time, the cells were spun for 5 min at 5000 rpm using a microfuge and resuspended in 200 µl of PBS + 0.5% BSA. Primary antibody at an appropriate dilution (see table 2.2) in PBS + 0.5% BSA was added and incubated for 30 min at 4°C in dark. Cells were washed again and the secondary fluorescent antibody at appropriate dilution (see table 2.5) in PBS + 0.5% BSA was added and incubated again for 30 min at 4°C in dark. After that cells were washed with PBS + 0.5% BSA and analyzed by flow cytometry.

2.8.4 Cell Trace Violet staining

Primary cells were resuspended at 10^6 cells/ml in PBS. One µl of 5 mM CellTrace Violet stock solution (Invitrogen) in DMSO (Invitrogen) was added per ml of cell suspension and incubated for 20 min at 37°C in dark. After that time, 5 times volume the original staining volume of complete B cell media was added to the cells and incubated for 5 min at room temperature in dark to remove any free dye remaining in the solution. Cells were pelleted by centrifugation and resuspended in fresh pre-warmed complete B cell media.

2.8.5 Staining for cell cycle analysis

After fixing cells with 80% ethanol (see section 2.8.3), 300 µl of DAPI/Triton-X100 solution (PBS + 0.1% Triton-X100 (Sigma) + 1 µg/ml DAPI (Chemometec) was added to the cells, which were then analyzed by flow cytometry.

2.8.6 Smart Flare experiment

Cells were plated at $5x10^4$ cells/well in 96-well plate. Smart Flare probes (Uptake control, Scrambled control and Housekeeping probe) were resuspended by adding 50 µl of nuclease-free water to obtain an initial Smart Flare concentration of 100 nM. Fifteen µl of this solution was then further resuspended in 135 µl of PBS to obtain intermediate Smart Flare concentration. To obtain working Smart Flare concentration (200 pM - 800 pM), intermediate solutions were resuspended in cell culture media. The working solution was then added to previously plated cells and incubated for 16 h at 37°C, 5% CO_2. After that time, cells were harvested, washed with PBS and analyzed using flow cytometry.

2.8.7 Flow cytometry procedure

Flow cytometry was performed using either Fortessa B (Beckton Dickinson) or LSRII (BD) flow cytometers. For each experiment compensation controls were prepared and compensation was performed using Diva software (BD). The same number of total events was recorded for each sample (using Diva software) and the following gating strategy was performed: 1) gating for intact cells in forward scatter area (FSC-A) vs side scatter area (SSC-A); 2) gating for singlets first in FSC width (FSC-W) vs FSC height (FSC-H) and then in SSC-W vs SSC-H; 3) gating for live cells (based on live/dead stain) if needed.

2.9 Immunofluorescence for microscopy

2.9.1 Staining using PFA/Triton-X100 as a fixation/permeabilization

Cells were seeded in a 12-well sterile removable chamber attached to a glass slide (Ibidi). At appropriate time points media was gently removed from the chambers and cells were very gently washed with PBS. After washing, cells were fixed with 4% PFA (Invitrogen) for 15 min and washed twice with PBS. After fixing, cells were incubated with 200 µl of blocking/permeabilization buffer (PBS + 10% FCS + 100 mM Glycine (Sigma) + 0.2% Triton-X100 (Sigma)) for 30 min at room temperature. After that time, primary antibody at an appropriate dilution (see table 2.2) in blocking/permeabilization buffer was added and incubated for 1 hour at room temperature with gentle rocking. After that time the antibody solution was removed, cells were washed 3 times with PBS and the appropriate secondary fluorescent antibody at an appropriate dilution (see table 2.5) in blocking/permeabilization buffer was added and incubated again for 1 h at room temperature gently rocking in the dark. Antibody was then removed and cells were washed 3 times with PBS. After washing, the chamber was detached from the slide, the slide was briefly washed in dH_2O and the coverslip was mounted onto the slide using Prolong Gold Antifade mountant with DAPI (Life Technologies), and left for 24 h in dark to set. Images were taken using Zeiss LSM5 Pascal confocal microscope: 63x objective, 4 x zoom and a projection of z-stacks of 1µm sections.

2.9.2 Staining using PFA/acetone as a fixation/permeabilization

Cells were seeded in a 12-well sterile removable chamber and fixed with 4% PFA as described in section 2.9.1 above. After fixing with PFA, cells were incubated with 200 µl of

ice cold acetone for 2 min at 20°C. After that time acetone was quickly removed from wells and the chambers were washed with PBS. After washing, PBS with 1% BSA was added for 15 min to block unspecific binding. The primary antibody at appropriate dilution (see table 2.2) in PBS with 1% BSA was then added and incubated for 1 h at room temperature, gently rocking. After that time the antibody solution was removed, cells were washed 3 times with PBS and the appropriate secondary fluorescent antibody at an appropriate dilution (see table 2.5) in PBS with 1% BSA was added and incubated again for 1 h at room temperature gently rocking in the dark. Antibody was then removed and cells were washed 3 times with PBS. After washing, the chamber was detached from the slide, which was briefly washed in dH_2O and the coverslip was mounted to the slide using Prolong Gold Antifade mountant with DAPI (Life Technologies) and left for 24 h in dark to set. Images were taken using Zeiss LSM5 Pascal confocal microscope: 63x objective, 4 x zoom and a projection of z-stacks of 1µm sections.

2.10 Drug treatment and analysis of cell viability and death

Different BL31 cell lines were plated at $3x10^5$ cells/ml in a 24-well plate. After 24 h the cells were treated either with 0.062 µM staurosporine (Sigma), 0.3 µM camptothecin (Sigma), 1 µg/ml of ionomycin (Sigma) or an appropriate volume of DMSO as a control. After 24 h (for staurosporine, camptothecin and DMSO) or 48 h (for ionomycin and DMSO), 44 µl of cells from each well were transferred into microcentrifuge tube. The dead cell stain propidium iodide (PI) at a final concentration of 500 µg/ml and live cell stain VitaBright43 at a final concentration of 100 µM were both added to the tube of cells and mixed. Stained cells were then loaded into an 8 chamber slide (NC-Slide A8 (Chemometec)) and the apoptosis protocol (Chemometec) was run using NC-3000 cell analyzer.

2.11 Treatment of cells with proteasome inhibitor (MG-132)

Cells were treated with DMSO alone or with MG-132 (Sigma) resuspended in DMSO and diluted in culture media to final concentration of 10 μM. After 8 hours of treatment, cells were harvested by centrifugation, washed with PBS and the cell pellet stored at -80°C for further analysis.

2.12 EBV VCA IgG ELISA

To isolated serum for EBV- ELISA, 1 ml of buffy coat residue was transferred to a 1.5 ml microcentrifuge tube, left at room temperature for more than 1 h to allow blood clotting and spun down at 1200 rcf for 10 min. Serum was collected and transferred to a fresh microcentrifuge tube and stored at -20°C.

To detect EBV in human serum, the Epstein Barr virus VCA IgG ELISA kit KA2254 (Abnova) was used. Human serum samples collected from buffy coat residues were diluted 1:21 in Sample Diluent (Abnova) and mixed well. 100 µl of diluted sera, Calibrator (Abnova) and Negative and Positive Controls (Abnova) were dispensed into the appropriate ELISA wells coated with EBV-VCA antigen. For the reagent blank, 100 µl of Sample Diluent was dispensed into one of the wells. Samples were incubated in wells for 20 minutes at room temperature. After that time liquid from all wells was removed, wells were washed three times with 300 µl of 1x Wash Buffer (Abnova) and blotted on paper towel. 100 µl of Enzyme Conjugate (Abnova) was dispensed into each well and incubated for 20 minutes at room temperature. After that time, Enzyme Conjugate was removed, wells were washed three times with 300 µl of 1x Wash Buffer and blotted on paper towels. 100 µl of TMB Substrate (Abnova) was added to the wells and incubated for 10 minutes at room temperature. After that time, 100 µl of Stop Solution (Abnova) was added to all wells. Optical density (O.D.)

was read at 450 nm using a FLUOstar Omega plate reader within 15 min after adding Stop Solution.

The results were calculated using protocol provided by the kit (Abnova) and the Calibrator Factor (CF) value displayed on the Calibrator bottle (Abnova). First, the cut-off value was established: Calibrator O.D. x Calibrator Factor (CF). Then the Antibody (Ab) Index of each sample was calculated by dividing the O.D. value of each sample by the cut-off value. The experiment was considered valid based on the following criteria: the O.D. of the Calibrator was greater than 0.25, the Ab index for Negative Control was less than 0.9 and the Ab Index for Positive Control was greater than 1.2. The EBV status of each donor was established based on Antibody Index, where results <0.9 mean that there is no detectable antibody to EBV-VCA IgG by ELISA, results of 0.9-1.1 mean that the sample is borderline positive and that the follow-up testing is required, results >1.1 mean that there is detectable antibody to EBV-VCA IgG by ELISA.

3 RESULTS I: PRODUCTION AND ANALYSIS OF THE FIRST GENERATION EBNA-LP MUTANTS EBV

3.1 Generation of the initial set of recombinant EBVs

The major challenge with genetic analysis of EBNA-LP arises from its complex splicing and repetitive nature (see section 1.9.1). EBNA-LP is encoded at the 5' end of the polycistronic transcripts from which other EBNAs are translated. Therefore, simple removal of the EBNA-LP gene from the EBV genome would result in the lack/disruption of other EBNAs' transcripts and of non-coding RNAs that are expressed from the introns present in this region. Also, introduction of a single STOP codon at the beginning of the EBNA-LP sequence would not generate an EBNA-LP knockout, because of the multiple numbers of W repeats (and the fact that each repeat unit contains a promoter, Wp that could initiate an EBNA-LP-encoding transcript) and the alternative splicing that skips W repeat units. As a result the W repeat unit with the STOP codon would be spliced out of some transcripts and EBNA-LP protein isoforms, albeit shorter by this one W repeat, could still be expressed.

Because of the above reasons, a different approach to generate EBNA-LP knockout (or any other EBNA-LP mutant) virus has been taken. This consisted of introducing a STOP codon (or any other desired mutation) into a single W repeat and using this mutated repeat to generate an array of W repeats, where each W repeat has the STOP codon. Thus despite the alternative splicing, no single W repeat unit could be used to produce EBNA-LP protein. Obtained in this way an array of W repeat units each containing a mutated EBNA-LP gene/exon was introduced into the EBV genome by RecA-mediated recombination in bacteria as described in section 3.1.2.

This approach can be taken to alter any position in the W repeats and consists of following steps: generation of mutant W repeat unit; building this unit into an array; addition of the non-repetitive parts of the genome either side of the array (unique flanks); cloning into a recombineering vector (pKovKan); deletion of W repeats from the EBV BAC (to prevent recombination events between recombinant repeat array and the repeat in the virus genome); introduction of the repeat array into the W knockout EBV by homologous recombination.

3.1.1 Construction of EBNA-LP-KO ^{i} and EBNA-LP-REV ^{i} shuttle vector

To generate a shuttle vector containing an array of mutated W repeats, the desired mutation (two STOP codons and a PvuI restriction site for diagnostics) was introduced into the W1 exon (Fig.3.1a) by de novo synthesis of W1 exon. To facilitate the cloning (see the paragraph below), the BsmBI restriction site that lies within the W1-W2 intron was also mutated as part of the synthesized fragment). Because of this additional intronic mutation, the EBNA-LP knockout was called LP-KO ^{i} (where "i" stands for intronic mutation). Figure 3.1b shows the general strategy for generation of EBNA-LP mutant shuttle vectors. The EBNA-LP-KO ^{i} shuttle vector (p8267) was generated by Dr. Rob White. The mutated exon was cloned into a single W repeat unit (BWRF1 between BamHI) that had been subcloned from the B95.8 EBV BAC (named HB9, for **H**ammerschmidt **B**AC p208**9**) that is used by our group. This BAC clone contains 6 copies of the W repeat, which is typical of wild-type viruses (Palser et al., 2015).

To generate the array of W repeats, type IIS compatible restriction endonucleases (BsmBI and BtgZI) were used following a strategy devised by Grundhoff and Ganem (2003). These enzymes recognize and bind to the DNA at a defined distance from their cleavage site, thus enabling them to cut and extend repetitive regions while retaining a single binding site for the enzyme. We have a vector (p8247/pASz001 with a pBR322-based replication origin)

in which the BamHI sites at either side of a single Bam W repeat unit can be cut by BsmBI (left flank) or BtgZI (right flank) (Fig.3.1b). There are other unique restriction sites including an MluI site outside these flanks. This allows us to cut with Mlu/BsmBI and Mlu/BtgZI to combine one repeat unit into two, while retaining a unique copy of each restriction site. From here we can combine two repeat units into four and then add another two to generate 6 repeat units. However, there was also a restriction site for BsmBI within the intron between exons W1 and W2. Because the BsmBI restriction endonuclease was required for this cloning strategy, the intronic BsmBI restriction site was mutated (from CGTCTC to CG**A**CTC). After obtaining an array of six W repeats, homology regions (portions of the EBV genome containing the C2 exon- upstream, and the Y1 and Y2 exons- downstream) were cloned on each end of the synthetic W repeat array (Fig.3.1b).

To control for second site mutations, and for any effect of the BsmBI mutation, I also generated a revertant construct in which the BsmBI mutation is retained, while the sequence of exon W1 is restored to wild type. Because of this additional intronic mutation, the EBNA-LP revertant was called LP-REV ^{i} (where "i" again stands for intronic mutation).

The strategy for generating the EBNA-LP revertant shuttle vector was based on the same general strategy of construction of EBNA-LP mutants (Fig.3.1b). This involved introducing the BsmBI mutation into a single Bam W repeat unit (pASz001). After that, using the type IIS restriction endonucleases BsmBI and BtgZI as described above, W repeats were joined creating two W repeats (pASz002), which were joined further into an array of four (pASz004). At the same time the genome region containing the C2 exon and the start of the W repeat region (C2 flank) was cloned into pASz002 (the vector with one pair of W repeats) to generate pASz003. These two constructs (pASz003 and pASz004) were joined together, generating an array of six W repeats with the C2 flank (pASz005). Finally, the genomic region containing the end of the W repeats and the Y1 and Y2 exons (Y1Y2 flank) was added

at the end of repeats (pASz006). The whole array flanked by non-repeat regions was then cloned into the temperature sensitive kanamycin resistant shuttle vector pKOV-Kan-ΔCm (White et al., 2003) to generate pASz007.

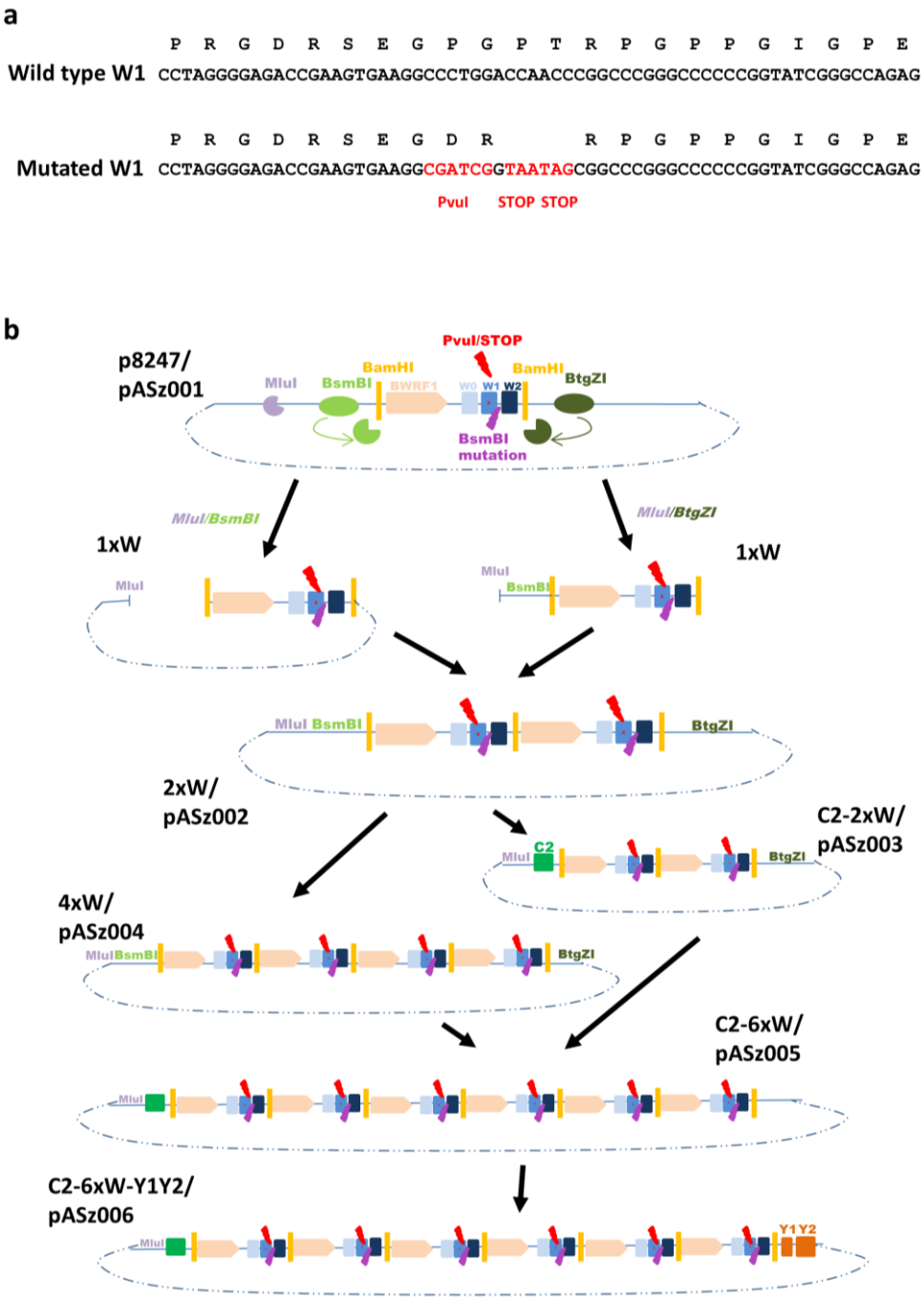

Fig. 3.1 Generation of EBNA-LP mutant shuttle vector. a. Generation of EBNA-LP-KO [i] single W repeat: two STOP codons (red) and a PvuI restriction site (red) were introduced into exon W1 of a BamW repeat unit. Nucleotide sequences of the wild type and mutated W1 exons are shown aligned to each other. Encoded amino acids are shown above the corresponding nucleotide sequences. **b.** Generation of an array of mutated repeats: The W repeat unit carrying a mutation (not present in case of LP-REV [i]: pASz001) and the additional BsmBI mutation is introduced into the vector (p8247/pASz001). Methodology for building from a single W repeat to 6 repeats flanked by homology regions is shown. BWRF1 open reading frame is represented by the pink arrow; W exons are represented by blue (light blue to dark blue) squares; BamHI sites are represented by yellow lines; mutations introduced into exon W1 are shown as red lightning (not present in LP-REV [i] constructs: pASz); the BsmBI mutation introduced into the intron between W1 and W2 exon is shown as a purple lightning bolt. The binding sites of restriction enzymes are indicated by green ovals, while their digestion sites are indicated by ¾ of a circle in corresponding colours. Homologous flanks: C2 exon and Y1Y2 exons are represented by green and orange squares respectively.

3.1.2 Construction of EBNA-LP-KO ^{i} and EBNA-LP-REV ^{i} EBV-BACs

The generation of EBNA-LP-KO was achieved by first deleting the W repeats from a wild type B95.8 BAC (Fig.3.2a) as this avoids unwanted recombination between the W repeats of the virus and the modified repeat in the shuttle vector.

To introduce the mutated EBNA-LP-KO repeat array, the shuttle vector containing the mutated W repeats flanked by homology regions and a plasmid expressing the RecA gene (pDF25-tet) were co-transformed into competent Escherichia coli (DH10B) cells containing the B95.8 EBV BAC with deleted W repeats (schematic in Fig.3.2b). Co-integrants were selected and resolved as described in section 2.2.7.

A revertant of the EBNA-LP-KO carrying the BsmBI mutation (EBNA-LP-REV) was produced in the same way: by recombineering first to delete the mutated W repeat region from LP-KO ^{i} (p8366), and then to introduce the wild type (with BsmBI mutation) W repeats by recombineering with pASz007.

Using above strategy, we have generated two independent EBNA-LP-KO ^{i} BACs: LP-KO ^{i} 2.6 and LP-KO ^{i} 1.28, and their corresponding revertants: LP-REV ^{i} 2.6 and LP-REV ^{i} 1.28 (Fig.3.3).

The integrity of the recombinants (in terms of them having the same genome structure and number of W repeats as in wild type) and the presence of the introduced mutation(s) were confirmed using four different restriction digestions analyzed by pulsed field gel electrophoresis (Fig.3.4a). The quality of BAC maxiprep (isolated by CsCl gradient centrifugation (see section 2.2.10) was confirmed by analyzing undigested DNA by pulsed field gel electrophoresis (Fig.3.4b), as BAC DNA preparations containing a high proportion of supercoiled DNA appear to more consistently give rise to good quality virus producer cell lines.

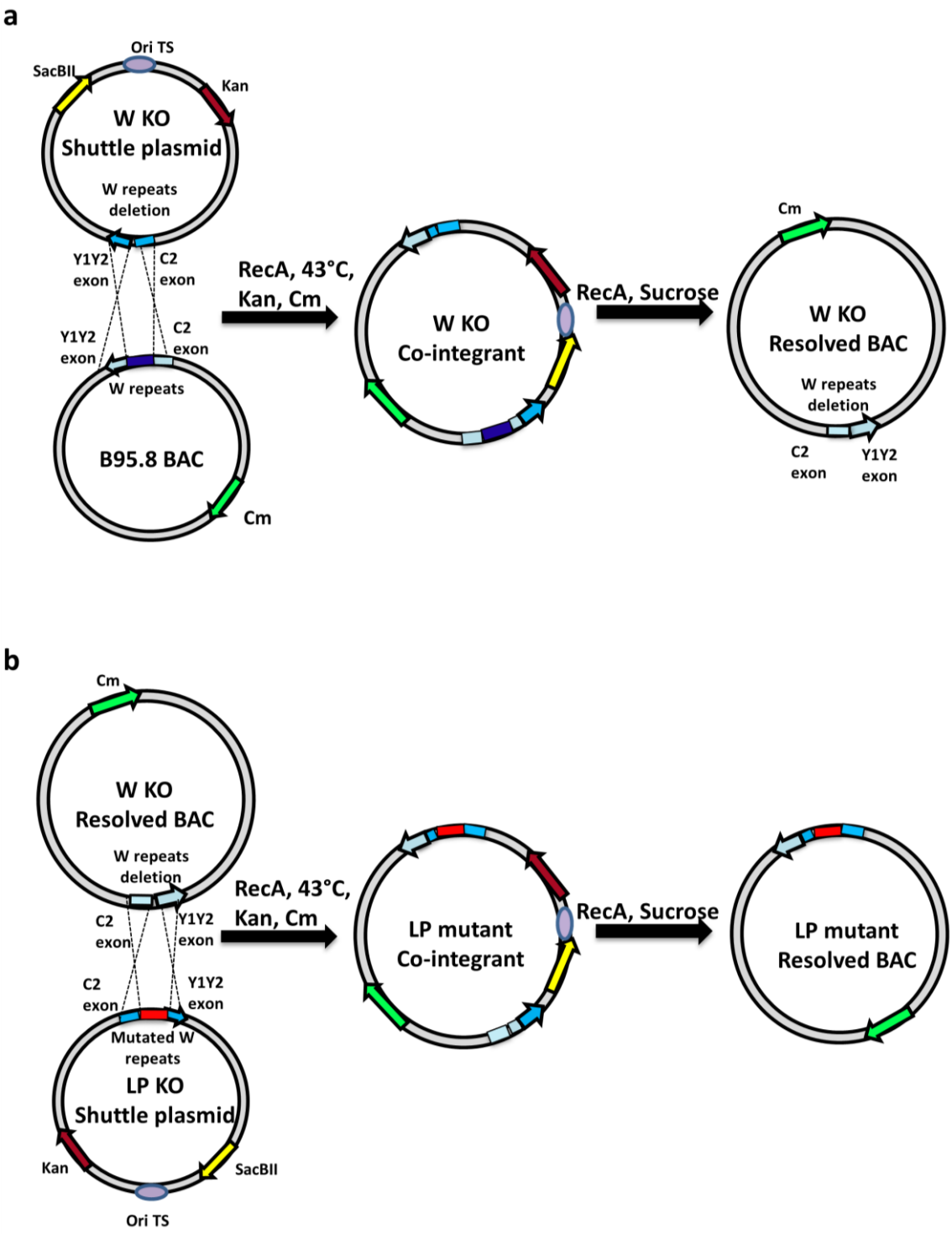

Fig. 3.2 Generation of EBNA-LP recombinants in EBV-BAC. Process of introducing mutations into W repeat region involves first **(a)** deleting the W repeats and then **(b)** restoring a modified W repeat array. **a.** Removal of W repeats from a wild type B95.8 BAC. Shuttle plasmid with W repeats deletion was recombined into the wild type BAC (HB9), generating co-integrants which were further resolved using sucrose plates. **b.** Introduction of mutated W repeats into BAC with W repeats deletion; shuttle plasmid with mutated W repeats was recombined in BAC with deleted W repeats, generating co-integrants which were further resolved using sucrose plates. Chloramphenicol and kanamycin resistance cassettes are represented by green and dark red arrows respectively, temperature sensitive origin of replication (oriTS) represented by purple oval, SacBII as a yellow arrow. Homologous flanks for recombination are shown in light blue, wild type W repeats in dark blue and mutated W repeats in red.

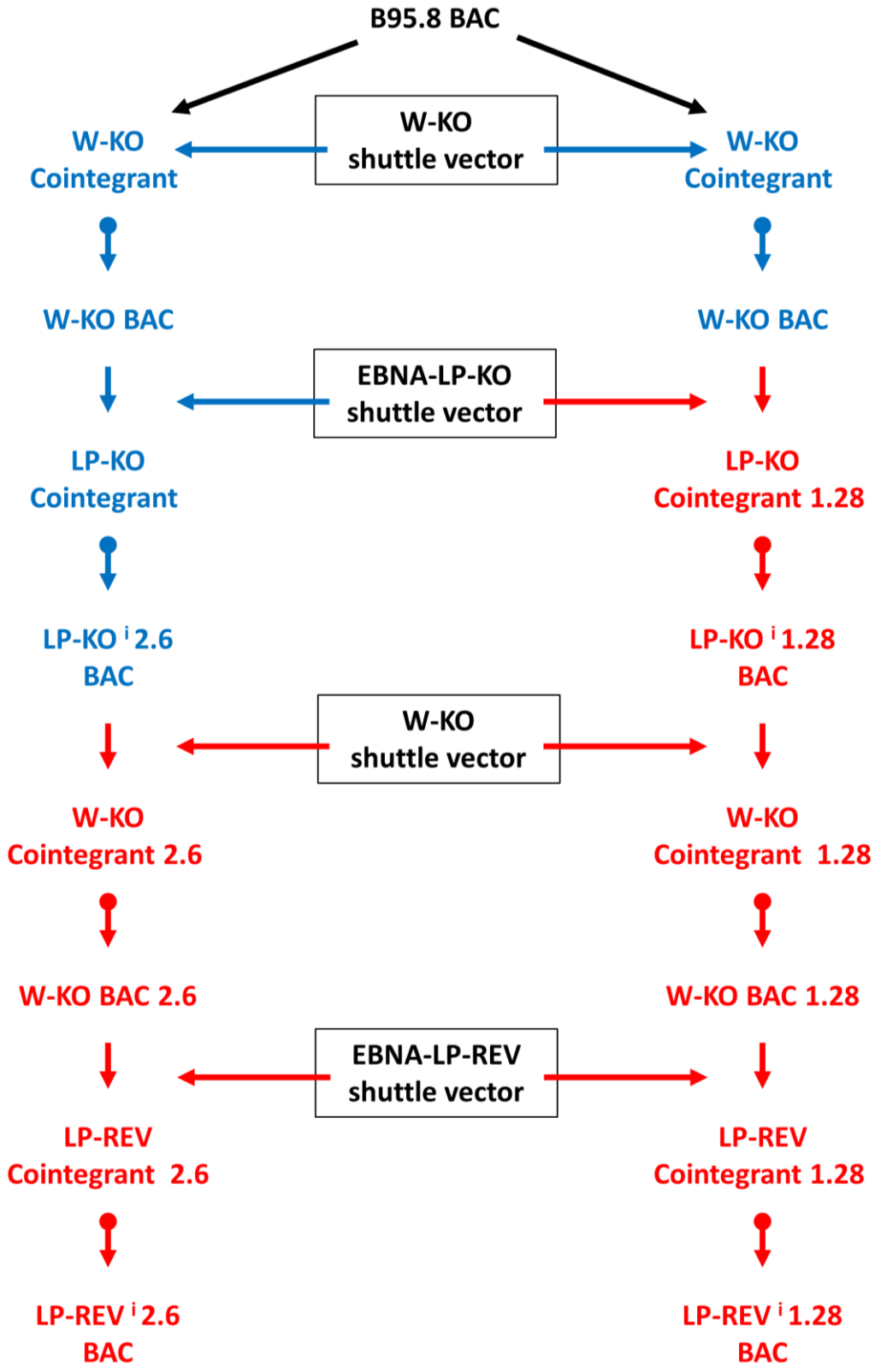

Fig. 3.3 Schematic of generation of independent LP-KO ^{i} and LP-REV ^{i} BACs. Shuttle vectors used in recombination are in black rectangles. Recombination is represented by regular arrows; the cointegrant resolution step is represented by arrows with a round start. Recombination steps that were performed by Dr.White are shown in blue, while steps performed by me are in red.

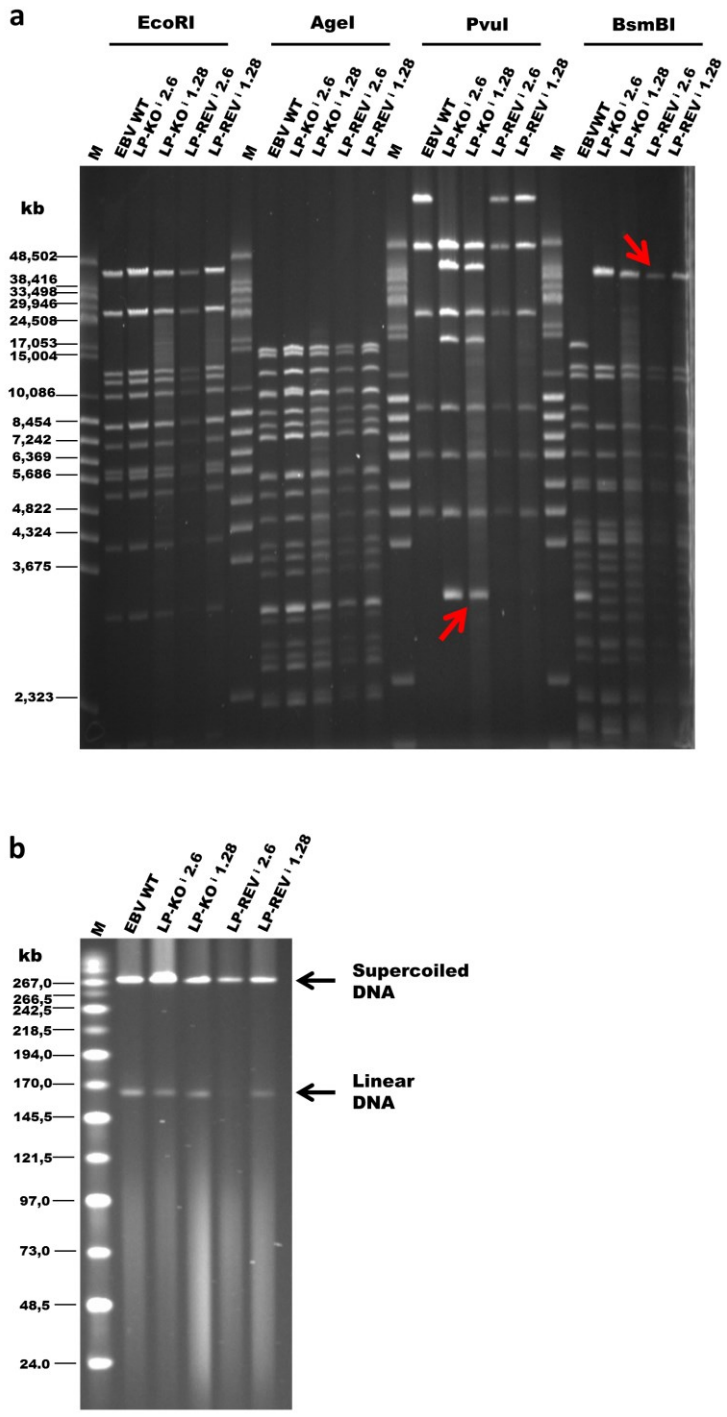

Fig. 3.4 Pulsed field gel analysis showing EBV-BAC maxiprep DNA of EBNA-LP knockouts and their revertants. a. Digested BAC maxipreps; EcoRI and AgeI digests show that all BACs have the same genome structure and number of W repeats as the parental EBV-BAC HB9 (EBV WT). The EBNA-LP KO sequence includes a PvuI restriction site in each W repeat unit. As a result PvuI cuts the W repeats only in knockouts, generating the 3kb W repeat units (lower red arrow). Due to the introduced BsmBI mutation in the W1W2 intron in both knockouts and revertants, BsmBI fails to cut within the W repeats in EBNA-LP-KO ^{i} and EBNA-LP-REV ^{i}. As a result the 3kb W repeat units (lower red arrow), are replaced by a 40kb band (upper red arrow). **b.** Undigested BAC maxiprep; The EBV-BAC DNA is approximately 170 kb in length. A linear DNA band migrates at this size in the gel (lower arrow). However, most of the purified BAC DNA is in an undamaged (supercoiled) form and migrates much more slowly in the gel (upper arrow).

3.1.3 Construction of Y1Y2-KO and Y1Y2-REV EBV-BACs

Because previous research (see section 1.9.6) reported the reduced transformation efficiency of EBV lacking exons Y1Y2 (which encode the unique C-terminus of EBNA-LP), I also generated a knockout of the Y exons in the EBV BAC (Y1Y2-KO) and its revertant (Y1Y2-REV).

Previously, Y1Y2-KO EBVs had been generated in both the Sugden and Kieff labs based on recombination into P3HR1 strain (Hammerschmidt and Sugden, 1989). P3HR1 virus lacks the last two exons (Y1 and Y2), the end of the W repeat and all of the EBNA-2 gene. To generate a Y1Y2-KO mutant, they introduced a plasmid that was lacking the last two exons of EBNA-LP but inserted a complete W repeat and a functional EBNA-2 gene into the P3HR1 genome. The virus was induced into the lytic cycle and confirmed to be a recombinant Y1Y2-KO EBV (Hammerschmidt and Sugden, 1989). It is possible, however, that the deletion of the whole Y1 and Y2 exons may have affected the splicing and therefore expression of other viral genes (for details of EBNA-LP splicing see section 1.9.1).

Therefore, in my Y1Y2-KO, removal of Y1 and Y2 exons was designed to retain the Y1 splice acceptor and Y2 splice donor, while introducing a STOP codon, and a restriction site for EcoRI to facilitate further analysis (Fig.3.5). This was achieved by In-Fusion cloning (see section 2.2.6) using a plasmid vector containing the Y1 and Y2 exon sequence and oligonucleotides designed to contain a primer sequence specific to the part of the EBV genome and the first 13 nucleotides of exon Y1 (reverse primer) or 25 middle nucleotides of Y2 (forward primer) at their 3' ends (outside of the sequence to be deleted) and 24 bases of shared homology at their 5'ends (that allows for joining the fragments and re-circularization of the PCR product) (Fig.3.5). The modification was confirmed by sequencing, and the modified region cloned into a temperature sensitive kanamycin resistant shuttle vector. Using RecA-based recombineering (section 2.2.7), I have generated two independent Y1Y2-KO

BACs: Y1Y2-KO 3.1 and Y1Y2-KO 4.2 and the latter of which was then reverted to wild type to make Y1Y2-REV 4.2 (Fig.3.6).

To confirm the integrity of recombinants (the same genome structure and number of W repeats as in the wild type) and the presence of the introduced mutation(s), five different restriction digestions were analyzed by pulsed field gel electrophoresis (Fig.3.7).

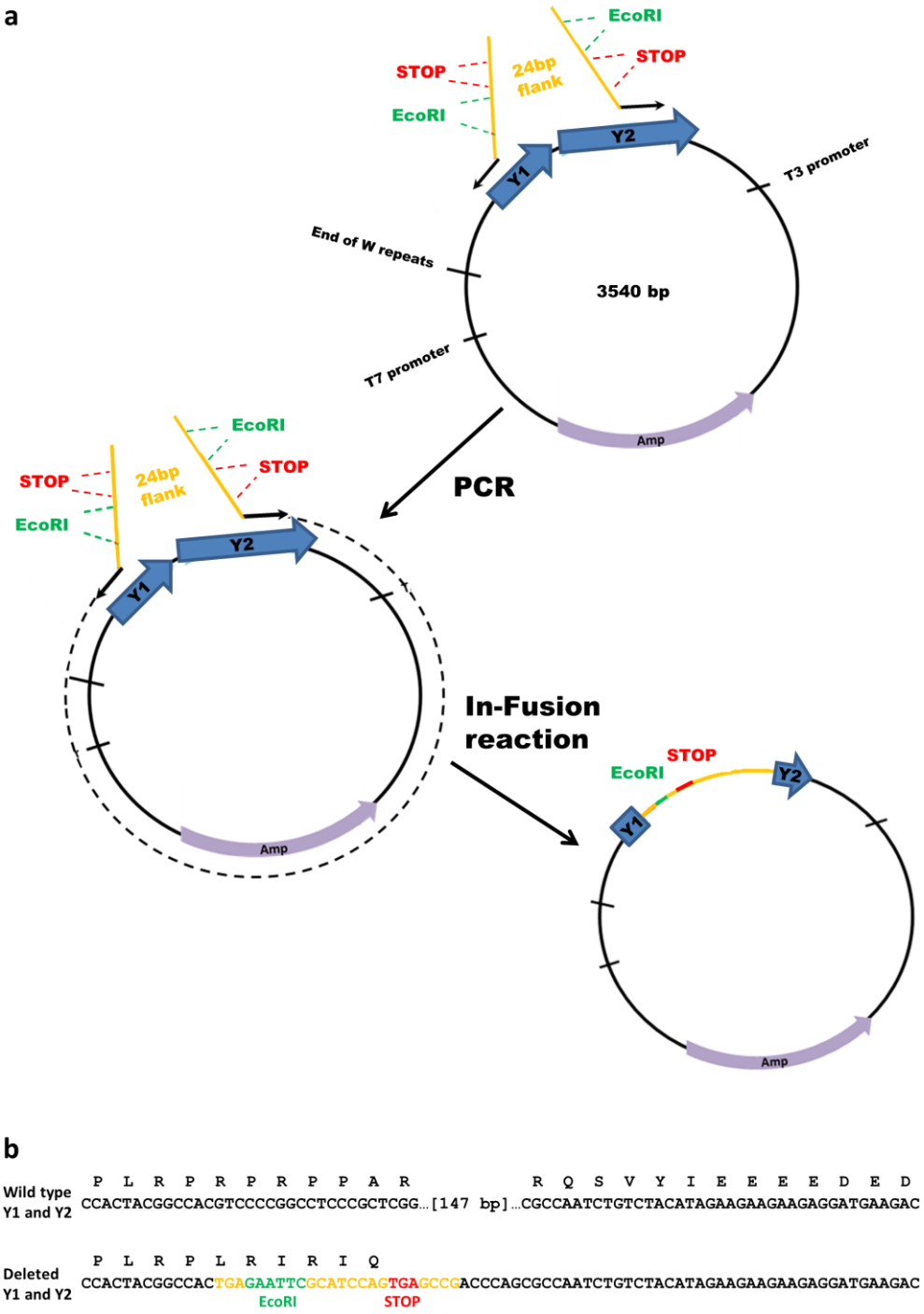

Fig. 3.5 In-Fusion deletion of Y1Y2 exons. a. In-Fusion mutagenesis is performed in two major steps: 1. amplification of the vector using PCR (represented by dotted line outside of the vector) with primers partially specific to retained sequence of exons (black arrows outside of the vector) and partially homologous to each other (yellow lines), where the homologous fragments contain introduced mutations (STOP codon (red) and EcoRI site (green)), 2. re-circularization of the vector using In-Fusion reaction. Ampicillin resistance cassette represented by light purple arrow, T3/T7 promoters and end of W repeats marked by black lines on the vector. Y1 and Y2 exons represented by big blue arrows. **b.** Comparison between wild type and partially deleted sequence of the Y1 and Y1 exons and the intron in between them. Introduced EcoRI site in green, STOP codon in red and the rest of 24 bp flank in yellow. Nucleotide sequences of the wild type and deleted exons are aligned to each other. Encoded amino acids are shown above the corresponding nucleotide sequences.

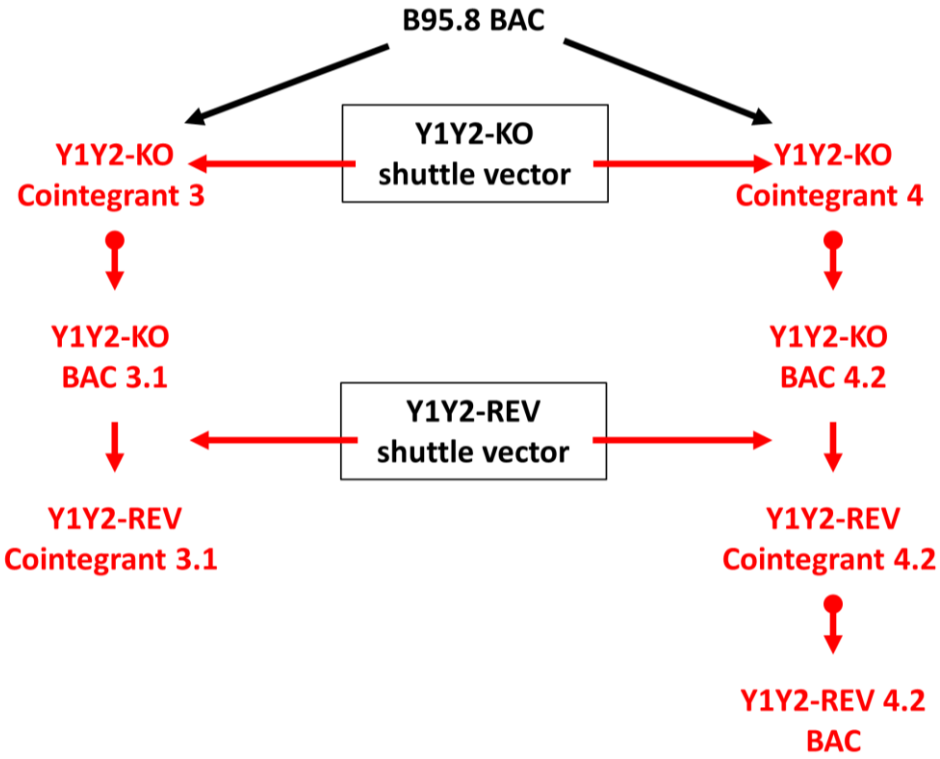

Fig. 3.6 Schematic of generation of independent Y1Y2-KO and Y1Y2-REV BACs. Shuttle vectors used in recombination in black rectangles. Recombination represented by regular arrows, cointegrants resolving step represented by arrows with round start. Recombination performed by me in red.

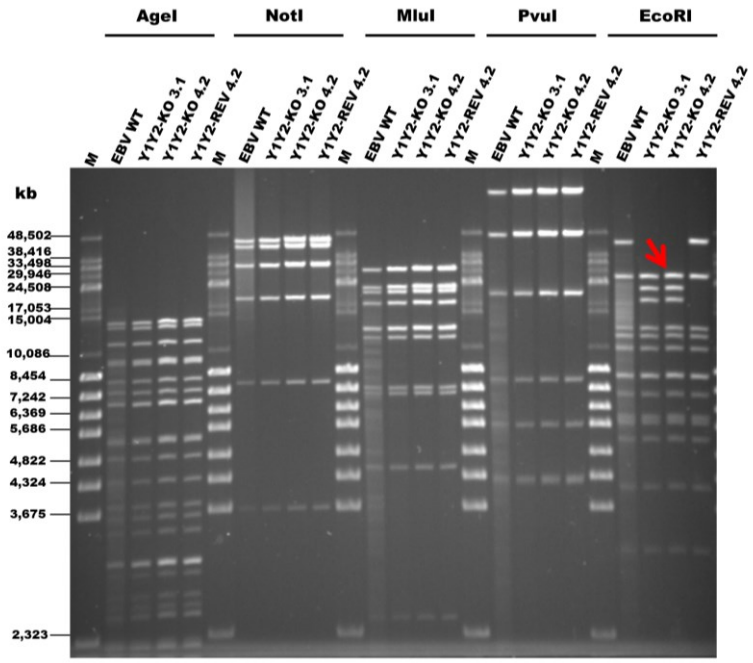

Fig. 3.7 Pulsed field gel analysis showing EBV-BAC maxiprep DNA of Y1Y2-KO and Y1Y2-REV. Digested BAC maxipreps; AgeI, NotI, MluI, PvuI digests show that all BACs have the same genome structure and number of W repeats as the parental EBV-BAC (EBV WT). Y1Y2-KO sequence includes an EcoRI restriction site. As a result the longest band in WT is cut into 2 shorter fragments in Y1Y2-KOs (red arrow).

3.1.4 Generation of HEK 293 producer cell lines and virus production

In order to generate EBV-producing cell lines, the recombinant BAC DNAs (maxiprepped and purified by cesium chloride density gradient centrifugation to maximize the proportion of intact, supercoiled DNA as shown in Fig.3.4b) were transfected into HEK-293 cells. To provide the opportunity to assess the importance of EBNA-2 cooperation with EBNA-LP in B cell transformation, I also transfected cells with an EBNA-2 knockout (E2-KO) and its revertant (E2-REV), (both recombineered by Ian Groves in a way to retain the splice donor of exon Y3 (Fig.1.7); unpublished data), as the producer cell lines that had previously been established in the lab did not produce sufficiently high titers of virus to obtain a high percentage of infected B cells. Colonies of cells were grown out and producer cell lines established (see section 2.5.1). To validate these cell lines, low molecular weight DNA (see section 2.5.3) isolated from 5 producer cell lines for each of the 10 recombinant viruses (EBV WT, LP-KO ^{i} 2.6, LP-REV ^{i} 2.6, LP-KO ^{i} 1.28, LP-REV ^{i} 1.28, Y1Y2-KO 3.1, Y1Y2-KO 4.2, Y1Y2-REV 4.2, E2-KO and E2-REV) was transformed into bacteria by electroporation to recover the viral episome from the cells for analysis. Four episomes from each cell line were analysed, using 2 different digests (400 digests). Representative digests can be seen in Figure 3.8. Cell lines with all episomes correct were tested for their ability to produce virus (Table 3.1). The best cell lines for most of recombinant viruses produced reasonable to high titers of virus- typically >100 Raji green units/µl (Fig.3.9). Cell lines transfected with LP-KO ^{i} 1.28 and LP-REV ^{i} 1.28 produced consistently lower titers of virus than the other recombinants (which was not improved despite repeating the maxiprep, transfection and outgrowth of new colonies two more times).

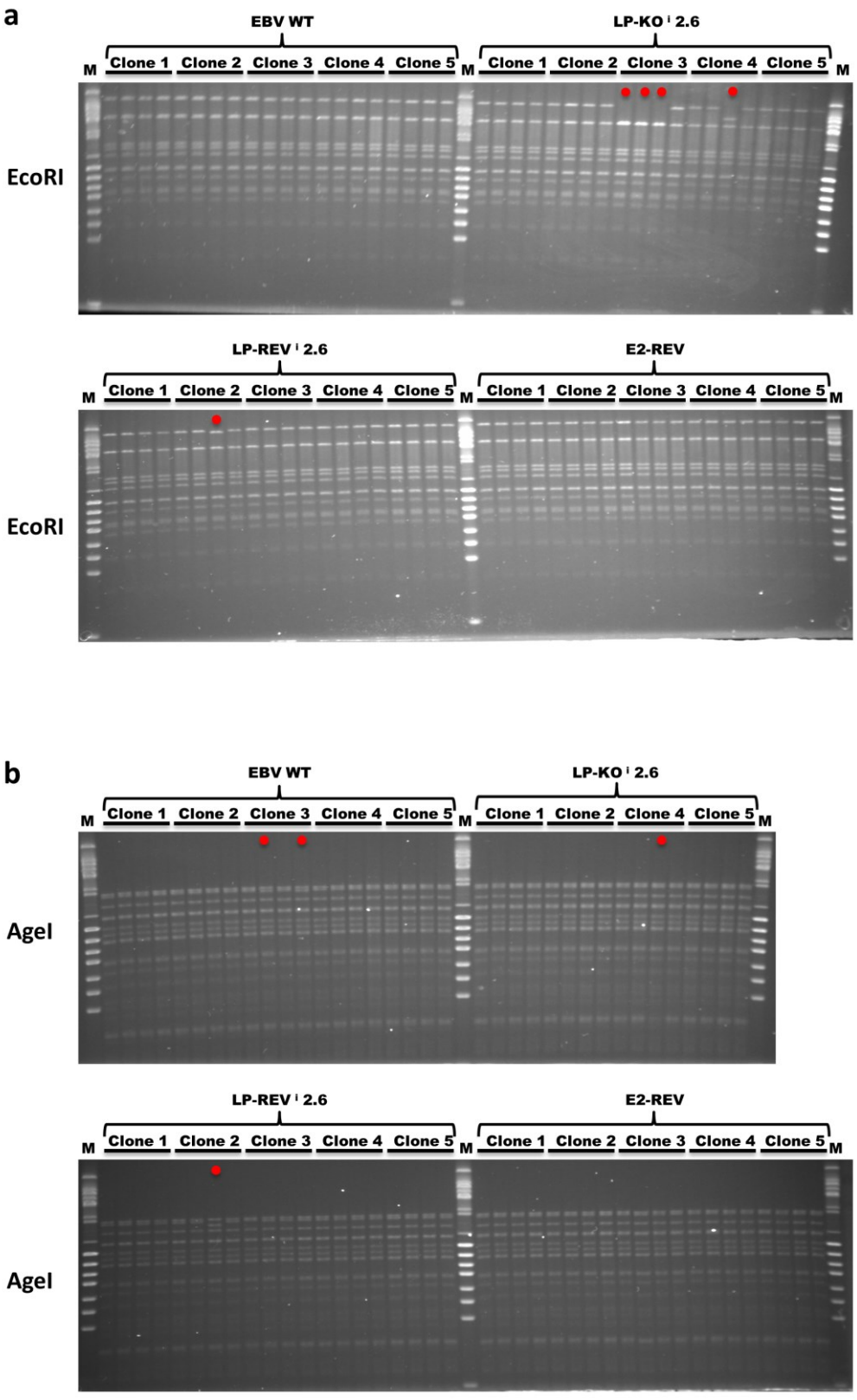

Fig. 3.8 Pulsed field gel picture after episome rescue. Digestion with either **a.** EcoRI or **b.** AgeI of episomes rescued from representative HEK-293 cell clones for 4 different recombinant viruses. Digests which show that episomes are not correct are marked with red dots. Cell line (clone) number 3 for LP-KO 2.6 was omitted from the AgeI digests as it was not intact according to EcoRI digestion.

Cell line	Virus producing ability
WT A1	0
WT A2	+
WT A3	+ + +
WT A4	0
WT A5	+ +
LP-KO ^{i} 2.6 A1	0
LP-KO ^{i} 2.6 A2	+ + +
LP-KO ^{i} 2.6 A4	+
LP-KO ^{i} 2.6 A5	+ +
LP-REV ^{i} 2.6 A1	0
LP-REV ^{i} 2.6 A2	+ +
LP-REV ^{i} 2.6 A3	+
LP-REV ^{i} 2.6 A4	+
LP-REV ^{i} 2.6 A5	+ + +
LP-KO ^{i} 1.28 A1	+
LP-KO ^{i} 1.28 A2	+
LP-KO ^{i} 1.28 A3	0
LP-KO ^{i} 1.28 A4	0
LP-KO ^{i} 1.28 A5	0
LP-REV ^{i} 1.28 A1	0
LP-REV ^{i} 1.28 A2	+
LP-REV ^{i} 1.28 A3	0
LP-REV ^{i} 1.28 A4	+
LP-REV ^{i} 1.28 A5	0
E2-KO A1	+
E2-KO A2	+ + +
E2-KO A3	+ + +
E2-KO A4	0
E2-REV A1	+
E2-REV A2	+
E2-REV A3	+ +
E2-REV A4	+ +
E2-REV A5	+ + + +
Y1Y2-KO 3.1 A1	0
Y1Y2-KO 3.1 A2	+ +
Y1Y2-KO 3.1 A3	+ + +
Y1Y2-KO 3.1 A4	+
Y1Y2-KO 4.2 A1	+
Y1Y2-KO 4.2 A2	+ +
Y1Y2-KO 4.2 A3	0
Y1Y2-KO 4.2 A4	+ +
Y1Y2-REV 4.2 A1	+
Y1Y2-REV 4.2 A2	+ +
Y1Y2-REV 4.2 A3	+ + +
Y1Y2-REV 4.2 A4	+ + +
Y1Y2-REV 4.2 A5	+ +

Table 3.1 Ability to produce virus by established HEK 293 producer cell lines. The producing ability was assessed based on the green Raji units, and scored from 0 to + + + + (where "0" represents no virus production observed and "+ + + +" represents high virus titers).

To try to improve the production of virus, I tested other methods (in addition to the lipofectin/peptide 6 transfection method that had previously been used in our lab (see section 2.5.2). We found that transfection of the BALF4 and BZLF1 plasmids using the GeneJuice reagent consistently improved the virus production from most of the cell lines (Figure 3.9) and gave more consistent virus titers across different users (not shown). Additionally to our regular harvest of virus from the media, I tested the harvest from the producer cell lines using a freeze/thaw method to release intracellular virus. This form of virus production resulted in more concentrated virus stocks, but these were unstable, as after a few months of storage in the fridge (where titers of viruses harvested from the media do not change significantly) there was almost no infectious virus left in these stocks.

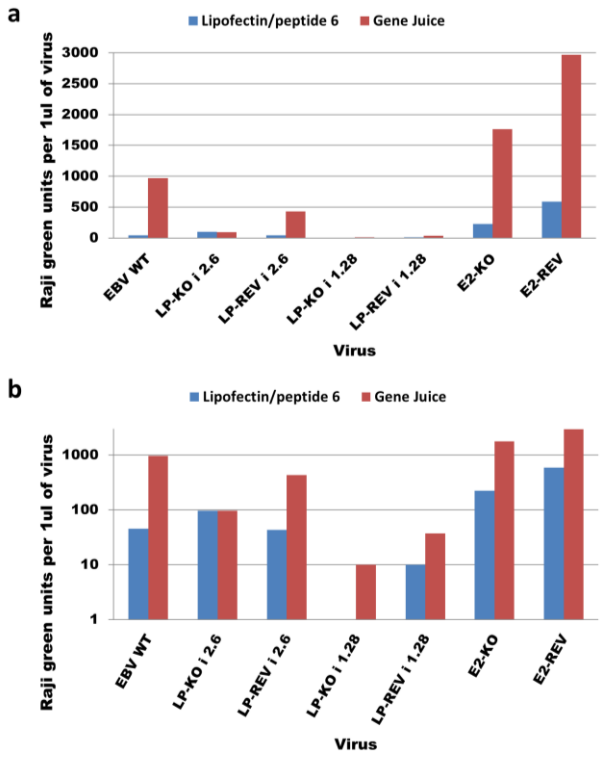

Fig. 3.9 Virus production using different transfection methods. Virus-producing cell lines were transfected with BZLF1 and BALF4 plasmids using either lipofectin and peptide 6 or GeneJuice reagent. The virus was harvested and ten-fold dilutions used to infect Raji cells. Titration was performed based on GFP as a marker of infected cells (section 2.5.2). Titers are represented as green Raji units per µl of virus. The x-axis represents different virus producer cell line. The y-axis represents the titer. Lipofectin + peptide 6 method in blue bars, while GeneJuice method in red bars. **a.** To show the scale of difference in virus titers, the data are represented in linear scale. **b.** To represent the relative values of low titers, the data are also presented in logarithmic scale.

3.2 Analysis of virus function in BL31 cells

To identify genes regulated by EBNA-LP, the WT, LP-KO ^{i} (2.6 and 1.28), E2-KO, Y1Y2-KO (3.1 and 4.2) viruses and their revertants were used to infect the EBV-negative Burkitt lymphoma cell line, BL31 (each infection in duplicate). These cells are useful for studying mutants of essential transforming genes, as the cells are already transformed (by Myc translocation, p53 mutation and cyclin-dependent kinase inhibitor 2A (CDKN2A) deletion amongst others) so they do not require EBV's transforming capabilities in order to establish EBV-positive cell lines. It therefore offers a platform to study the behavior of mutant viruses that are defective in otherwise essential virus functions. This approach has been previously used to study genetic mutants of the EBNA-3 genes (White et al., 2010, Anderton et al., 2008) and the BHRF1 locus (Yee et al., 2011).

3.2.1 The splicing of transcripts in EBNA-LP-KO ^{i} BL31 cells appears the same as wild-type

To test whether the introduction of either the BsmBI mutation or the LP knockout mutation had affected EBNA-LP transcript splicing, cDNA was obtained from BL31 cell lines and PCR amplification across the spliced region of EBNA-LP was performed. To check which promoter is active in the BL31 cell lines, two different forward primers were used: one spanning the C1/C2 exon junction and one present in exon W0 (Table 2.6), along with a reverse primer in the YH exon (Fig.3.10).

As analyzed by PCR and electrophoresis (Fig.3.11), the lengths and variety of EBNA-LP transcripts is similar for most of the cell lines (except that in Y1Y2-KOs the transcripts are shorter by the size of the Y1Y2 deletion). Additionally, transcripts from both latency

promoters (Cp and Wp) were detectable in all EBV-BL31 cell lines, although their relative activity was not assessed.

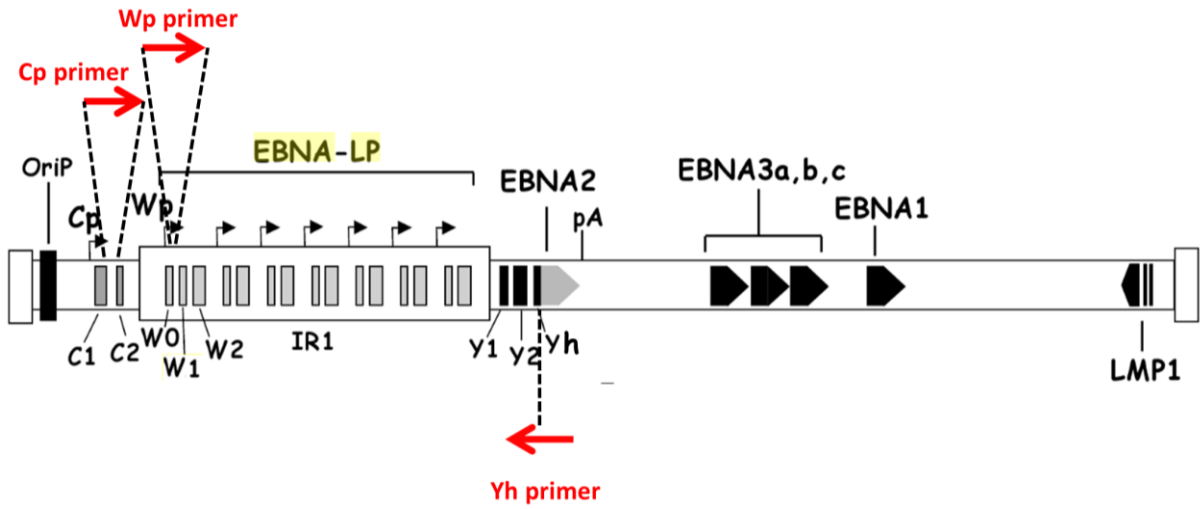

Fig. 3.10 Schematic of a fragment of EBV genome that contains EBNA-LP gene. Little rectangles represent EBNA-LP exons, while "triangles" represent exons for other latency genes. Black arrows represent promoters (Cp or Wp). The localization of primers used in in PCR is marked with red arrows. Note that the Wp primer may bind to exon W0 transcripts originating from any of the repeat units, depending on which Wp promoter initiated transcription, rather than exclusively to the first W0 exon shown in the schematic above. (Modified from Ling et al., 2009).

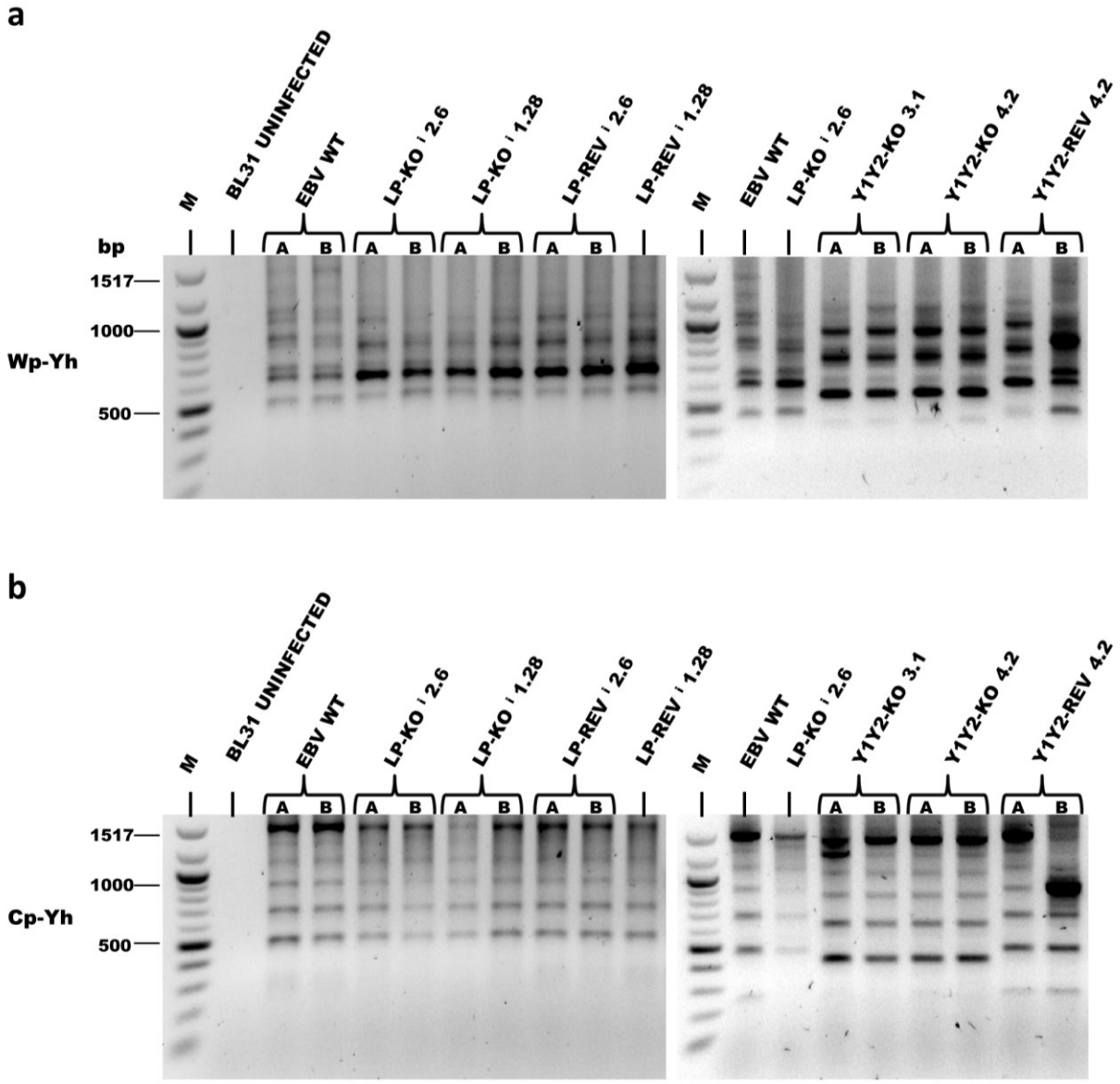

Fig. 3.11 Agarose gel electrophoresis of PCR-amplified cDNA obtained from BL31. PCR amplification of cDNA from transcripts across spliced regions initiated at either **a.** the Wp promoter or **b.** the Cp promoter, with a reverse primer in the YH exon. Expected size for DNA bands for normal Wp transcripts [bp]: 1505, 1307, 1109, 911, 713, 515. The predicted size for DNA bands containing between 1 and 6 W repeats initiated at the Cp promoter are [bp]: 1530, 1332, 1134, 936, 738, 540. Characteristic ladder of differently sized DNA bands is visible in both cases, indicating variable numbers of W repeats. Sizes of bands in the marker (100bp ladder, NEB) are indicated to the left of each gel.

3.2.2 Latent gene expression in BL31 cell lines is normal in LP-KO ^{i} EBV, but truncated EBNA-LP is barely detectable in Y1Y2-KO-BL31

To confirm that EBNA-LP protein is not produced from LP-KO ^{i}, and to test whether introduced mutations affect protein levels of other EBV latency genes, Western blots were performed using protein extracted from BL31 cells infected with different EBV mutants. Figure 3.12 shows that there is no detectable EBNA-LP in any LP-KO ^{i} cell line, and that there are no consistent differences in expression of most of other viral genes between different viruses. An exception is the higher EBNA-2 protein level in all four Y1Y2-KO-infected BL31 cell lines, and also in one Y1Y2-REV-infected and E2-REV-infected cells. Since there is no obvious connection between the cell lines with higher/lower EBNA-2 levels, I speculate that this may be due to a clonal selection during outgrowth. Diversity in EBNA-LP expression was notable, with larger EBNA-LP isoforms in the LP-REV ^{i} cell lines and one of the Y1Y2-REV lines (4.2 A), but shorter isoforms in E2-KO and Y1Y2-REV 4.2 B cell lines. Additionally, expression of these shorter EBNA-LP isoforms corresponds with the increased levels of EBNA-2. Since diversity of EBNA-LP sizes is typical of LCLs, it is assumed to be due to clonal selection where that clone exhibits a preferred EBNA-LP splice variant in culture (Finke et al., 1987). More strikingly, EBNA-LP is barely detectable in both Y1Y2-KO cell lines; it is detectable only after long exposures of the film.

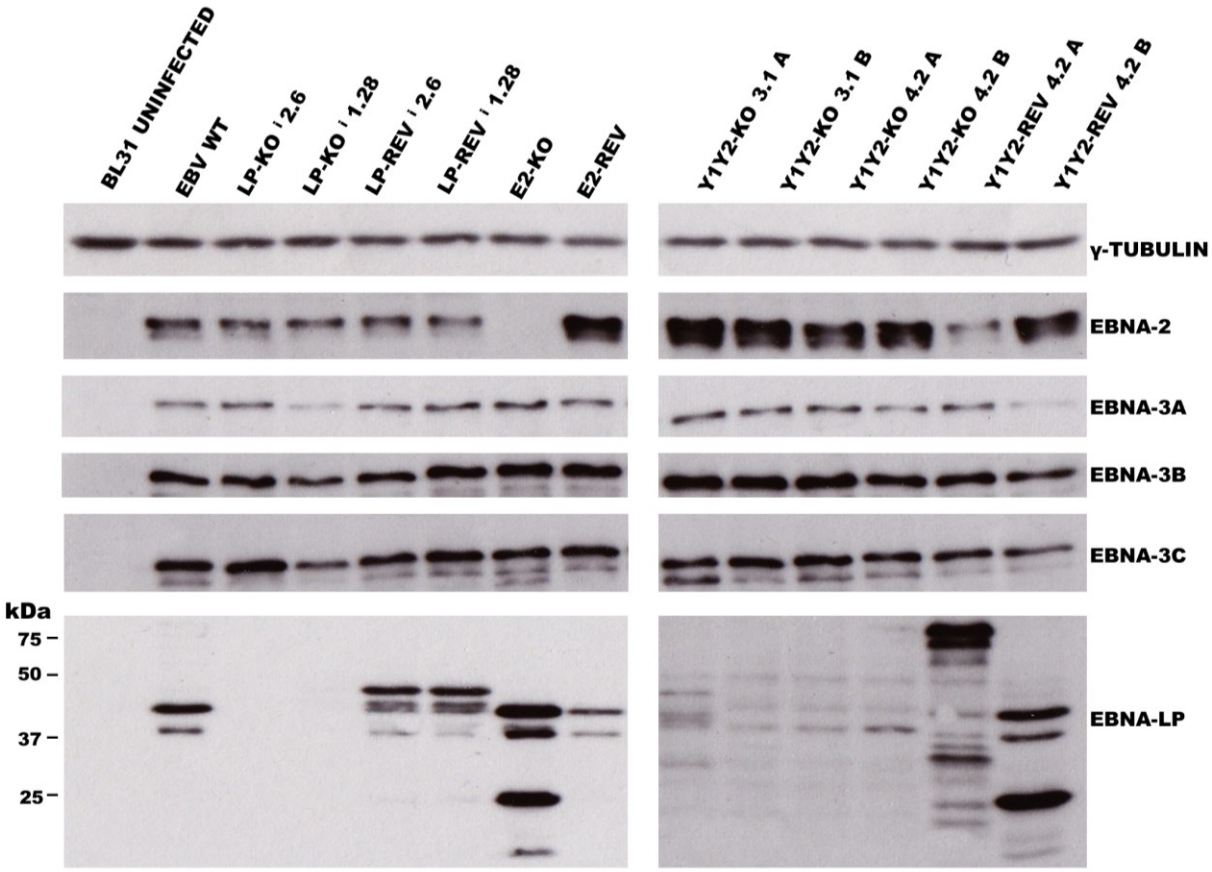

Fig. 3.12 Western blot analysis of protein extract obtained from BL31 cell lines infected with different EBV mutants. 20 μg of protein extracted from BL31 cell lines using RIPA buffer (see section 2.7.1) was separated by SDS–PAGE (12% gel for EBNA-LP and 7.5% gels for the other proteins) followed by Western blot and detection with antibodies against EBV latent proteins. γ-tubulin was used as a loading control.

3.2.3 EBNA-LP may be involved in regulation of mitochondrial genes but is not required for host gene activation by EBNA-2 in established BL31 cell lines

Previous studies have shown (through various co-transfection experiments) that EBNA-LP can enhance the induction of genes by EBNA-2 (see section 1.9.8). To investigate the extent to which EBNA-LP co-operates in host gene regulation with the other EBNAs (especially with EBNA-2) in the context of normal virus gene expression, and to identify the genes on which it acts independently, transcriptome analysis using Affymetrix Exon microarrays (Human Exon 1.0ST) was performed on a panel of infected BL31 cell lines, and

a subset of genes previously reported to be regulated by EBNA-2 and EBNA-LP was assessed by qPCR. Data from the Exon microarrays were analyzed and compared to previously undertaken and validated arrays for EBNA-2 KO EBV in BL31 cells (Groves, White & Allday; unpublished data) (Fig. 3.13a). Principal component analysis (PCA) was used to draw the major differences between samples. PCA is a statistical algorithm, which transforms the data to a new coordinate system, where the highest variances are emphasized and the smallest are omitted. As can be seen from Figure 3.13a, there is a systematic difference between the previously undertaken microarrays on E2-KO BL31 cells (cubes) and the new set (triangles) of microarrays, which makes the comparison between these two sets more difficult, therefore, the previously undertaken microarrays were excluded from the subsequent statistical analyses. Within the new data set, LP-KO ^{i} and Y1Y2-KO cluster together, along with the E2-REV cell line, and one of the Y1Y2-REV cell lines (Fig.3.13). Interestingly these revertants are the ones found to lack longer isoforms of EBNA-LP and to express higher amounts of EBNA-2 (Fig.3.13c).

When we looked for EBNA-LP regulated genes, we discovered that many of these genes are related to mitochondria (e.g. *MRPS17*- responsible for protein synthesis within the mitochondrion, *LYRM7*- assembly factor in mitochondria) (Fig.3.13b). However, in all of the cases of apparently EBNA-LP regulated genes, we observed the clustering of LP-KO ^{i} and Y1Y2-KO together with E2-REV and one Y1Y2-REV that are in the same PCA cluster (Fig.3.13). This indicates that the size of EBNA-LP (specifically where cell lines express only the short isoforms) or the amount of EBNA-2 can affect the regulation of genes by EBNA-LP (Fig. 3.13b). The Multi-Mapping Bayesian Gene eXpression (MMBGX) algorithm, which disaggregates the signal at probes matching multiple transcripts located in different parts of the genome or isoforms of the same gene (Turro et al., 2010), was used to generate gene expression level estimates for each gene (performed by Ernest Turro). The

MMBGX-processed data was used to perform analysis of variance (ANOVA) model (incorporating virus type as a variable), and within this model we contrasted two groups: the WT versus the LP-KO i- infected cells. During analysis all data are used in the ANOVA model, but the statistical comparison is only done between the two chosen groups. The genes were sorted based on the fold-change difference (LP-KO i-infected BL31 vs WT-infected BL31). The most altered genes (after removal of pseudogenes, and TCR genes) are shown in Table 3.2. As can be seen, the link between the ten most regulated genes in the list is that three of them are involved in mitochondrial function (Table 3.2).

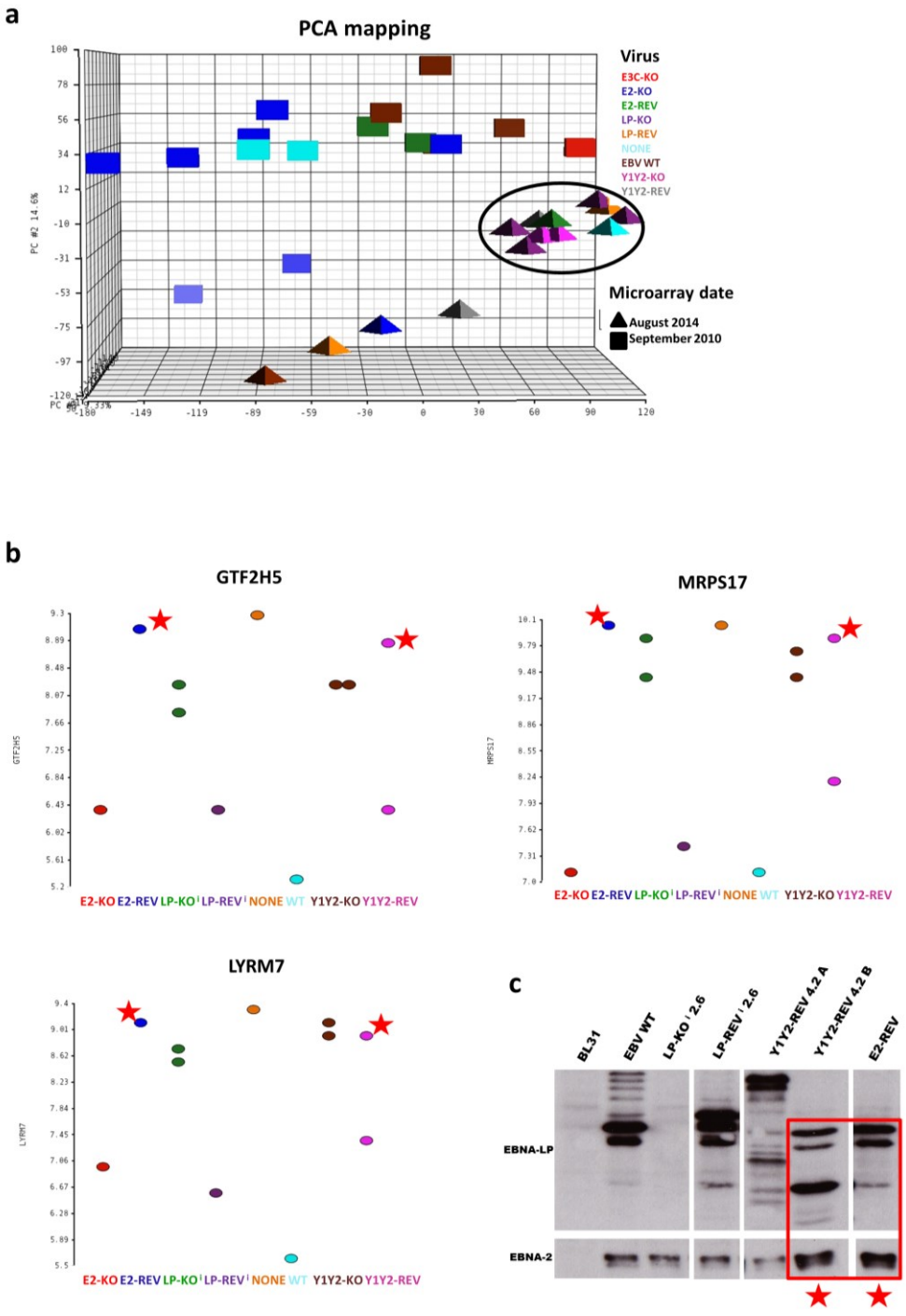

Fig. 3.13 Host gene regulation by EBNA-LP in BL31 cells. a. Principal Component Analysis (PCA) on microarray data using Partek Genomic Suite. BL31 cell lines established with different types of recombinants are represented by different colours. Data obtained from the new (mainly LP-KO and WT/REV) cell lines are represented by triangular pyramids. Data obtained previously (by Groves, White and Allday) are represented by cubes. The black circle indicates clustering of mutants either lacking EBNA-LP or expressing mutated or only short isoforms of EBNA-LP and higher amounts of EBNA-2. **b.** Microarray-derived expression data for 3 examples of genes that may be regulated by EBNA-LP: *GTF2H5*, *MRPS17*, *LYRM7*. The x-axis represents different cell BL31 cell lines, the y-axis represents microarray gene intensity in $\log_2$ values (where <3 is considered as no expression and >8 is considered as robust gene expression). Red stars indicate mutants expressing only short forms of EBNA-LP and higher amounts of EBNA-2. **c.** Western Blotting analysis of EBNA-2 and EBNA-LP expression from the cell lines used in the microarray (harvested simultaneously to the RNA analysed). Red stars indicate the same mutants as analysed on the microarray plot.

Gene Name	Full name	p-value (LP-KO vs. WT)	Fold-change (LP-KO vs. WT)	Change (LP-KO vs. WT)
EXTL3	Exostosin Like Glycosyltransferase 3	0.00252877	4.01467	LP-KO up vs WT
SLC25A13	Solute Carrier Family 25 Member 13	0.0184975	3.56856	LP-KO up vs WT
MME	Membrane Metalloendopeptidase	0.0574703	3.05022	LP-KO up vs WT
MRPS17	Mitochondrial Ribosomal Protein S17	0.00590704	2.99999	LP-KO up vs WT
IL7R	Interleukin 7 Receptor	0.00945657	2.86605	LP-KO up vs WT
OGFRL1	Opioid Growth Factor Receptor Like 1	0.0139549	2.78345	LP-KO up vs WT
RAB4A	RAB4A, Member RAS Oncogene Family	0.0406741	2.67574	LP-KO up vs WT
RPP14	Hydroxyacyl-Thioester Dehydratase Type 2, Mitochondrial	0.0485922	2.67169	LP-KO up vs WT
GTF2H2	General Transcription Factor IIH Subunit 2	0.049881	2.46737	LP-KO up vs WT
VENTX	VENT-Like Homeobox Protein 2	0.0257095	-2.54893	LP-KO down vs WT

Table 3.2 Genes regulated by EBNA-LP in BL31 infected cell lines. Ten the most regulated genes after applying MMBGX algorithm and comparing LP-KO [i]- against WT- infected BL31. Genes related to mitochondria are shadowed in grey.

Additionally, we have analyzed genes regulated by EBNA-2 that have been reported to be additionally enhanced by EBNA-LP, like *CR2/CD21* (which is a B cell/T cell receptor for EBV involved in the complement system and B cell activation), and also genes that are clearly regulated by EBNA-2 based on previously undertaken arrays (Groves, White & Allday; unpublished data), like *ELL2* (an elongation factor for RNA polymerase II), *BCL2A* (regulator of apoptosis) or *MLLT3* (responsible for transcription dysregulation in cancer) to assess whether there is co-activation effect by EBNA-LP in any other case. However, these analyses do not support a role for EBNA-LP in increasing transcription of EBNA-2 target genes (Fig. 3.14) as the transcript levels for genes regulated by EBNA-2 do not show any difference between LP-KO-infected and WT-infected cell lines (in contrast to E2-KO infected cells, which have much lower levels).

Data from qPCR of EBNA-2 regulated genes (*HES1*, *BCL2A1*, *ELL2*, *MLLT3*) supported the observation that LP-KO-infected BL31 cells have similar transcript levels to wild type-infected cell lines rather than to E2-KO-infected lines (Fig. 3.15), which suggests that in established BL31 cell lines, EBNA-2-dependent gene activity may not require EBNA-LP, as EBNA-2 regulated genes could have reached a stable equilibrium state that is the same regardless of the presence or absence of EBNA-LP.

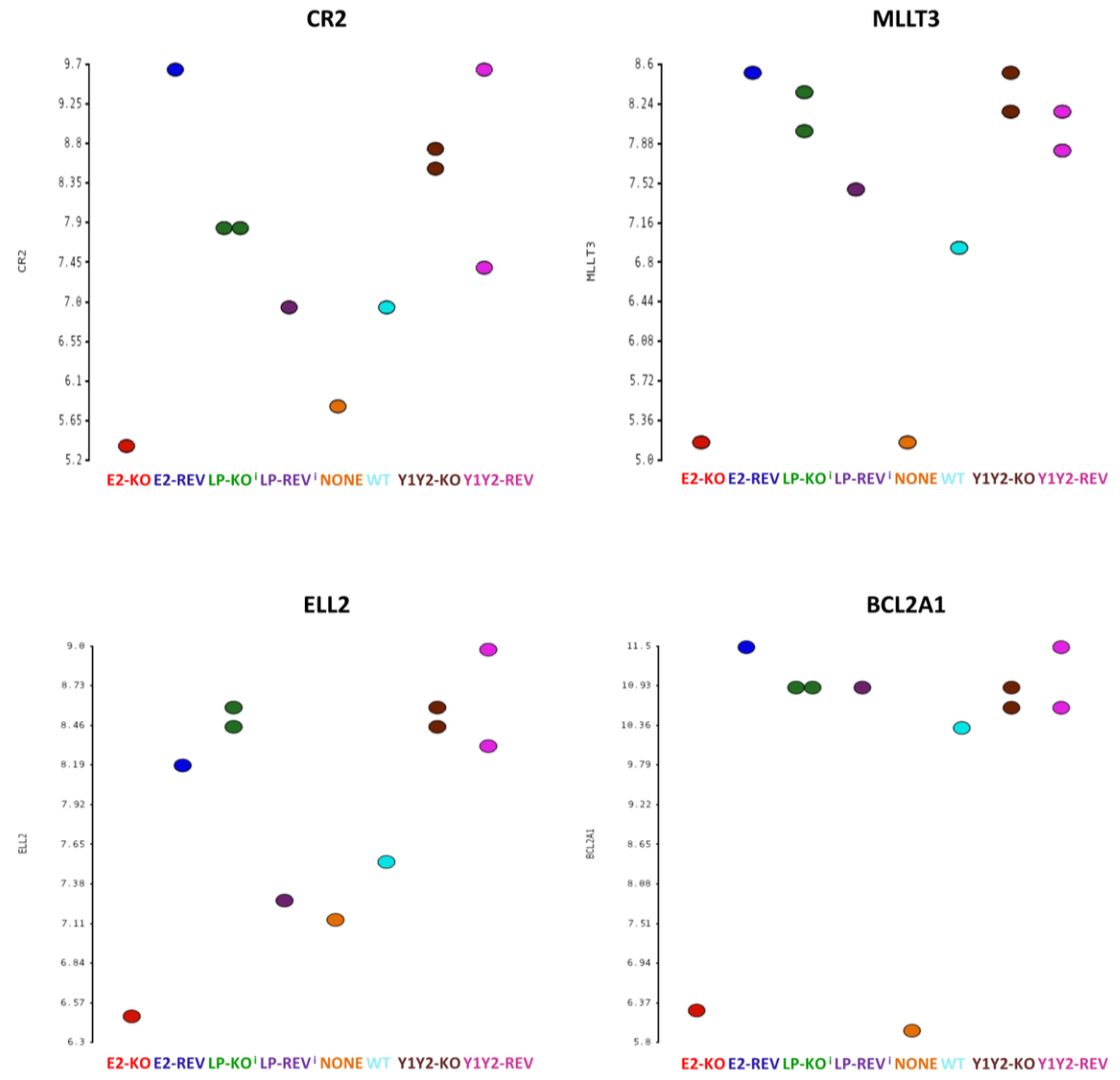

Fig. 3.14 Microarray analysis showing 4 representative examples of genes regulated by EBNA-2. Different types of mutant virus are represented by different colours. The x-axis represents different cell BL31 cell lines, the y-axis represents microarray gene intensity in log2 values (where <3 is considered as no expression and >8 is considered as robust gene expression).

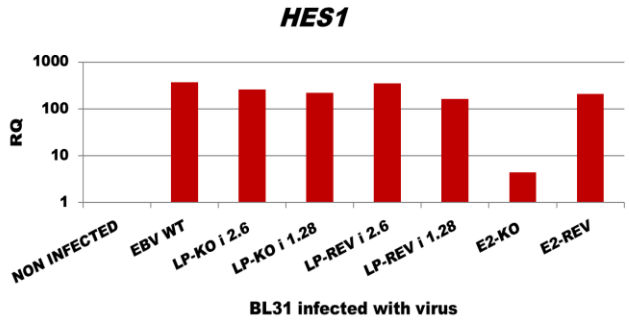

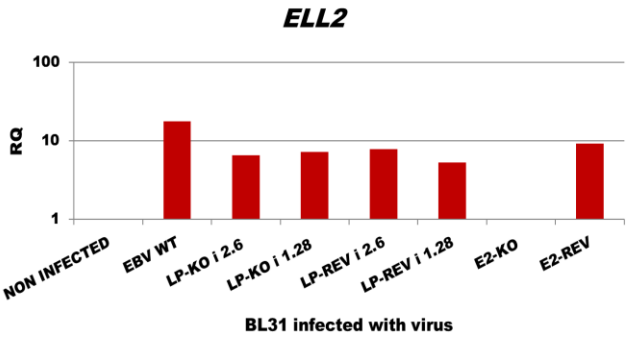

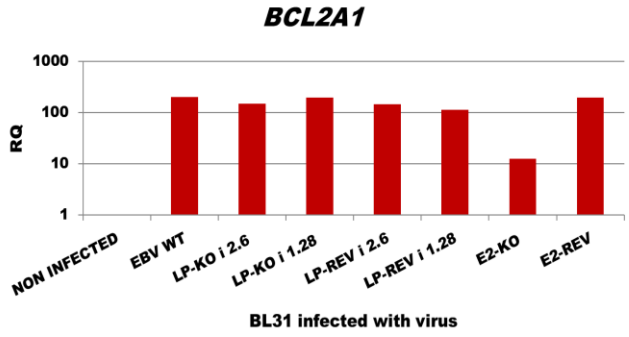

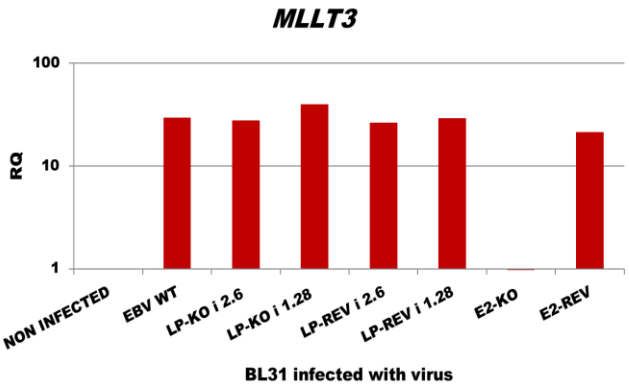

Fig. 3.15 qPCR on genes regulated by EBNA-2. Expression normalized to uninfected BL31. RQ- relative quantification.

3.2.4 EBNA-LP does not play a role in resistance to drug induced apoptosis

Latent EBV in B cells can inhibit apoptosis induced by ionomycin (calcium-ionophore) and staurosporine (inhibitor of protein kinases) whose effect is mediated by the accumulation of the pro-apoptotic protein, NOXA (Yee et al., 2011). This protection is not dependent on tumor suppressor p53, which is mutated in the BL31 cell line. A study using BL31 cell lines infected with different EBV mutants has shown that the BHRF1 locus (which encodes BHRF1 (an anti-apoptotic BCL2 homologue) and 3 microRNAs) partially protects against ionomycin-induced apoptosis, while an unidentified factor was responsible for suppressing Noxa induction. Analysis of knockouts showed that the mechanism does not require the EBNA-3s, EBNA-2, LMPs or EBERs, and latency I cells are not protected, likely ruling out EBNA-1 and the BART miRNAs (Yee et al., 2011). Latency III lines and Wp-restricted cell lines P3HR1 and Daudi (which express a truncated, low molecular weight isoform of EBNA-LP) retain protection against apoptosis induced by staurosporine (for details see section 1.9.7). To check whether EBNA-LP (either full length or truncated) may be involved in this protection, LP-KO [i] and Y1Y2-KO BL31 cell lines were treated with ionomycin, staurosporine and another pro-apoptotic drug, the topoisomerase inhibitor, camptothecin (after initial experiments to establish suitable drug doses and lengths of treatment; not shown). As controls, uninfected BL31 (which should have no protection), BHRF1-KO-infected BL31 (which should have partial protection) and WT-infected BL31 (which should have full protection) were used. To assess the viability of cells, propidium iodide (PI) uptake (which stains dead cells) was measured using a chamber-based fluorescence cell counter NucleoCounter NC-3000 system (Chemometec) to analyze a much higher number of cells without bias triggered by personal assessment of the color of stained cells (in contrast to the trypan blue method). Different BL31-infected cell lines after treatment with drugs (or DMSO as a control) were stained with PI, plotted on fluorescence graphs and the gates were set to

count dead and live cells (Fig.3.16). After gating, the percentage of live cells after drug treatment was calculated relative to the live cell percentage after DMSO control treatment, and plotted as bar graphs (Fig.3.17). There was no consistent increase in cell death after drug treatment of BL31 infected with EBV lacking EBNA-LP in comparison to revertants, whereas the BHRF1 knockout and uninfected cell lines consistently exhibited a reduced resistance to cell death (Fig.3.17). However, an increased background level of cell death was observed for uninfected BL31 and BHRF1-REV-infected BL31 in comparison to all of the other mutants, as seen after control treatment with DMSO (Fig.3.16a). The experiment was repeated using trypan blue method and Countess cell counter (Invitrogen) with similar results (not shown).

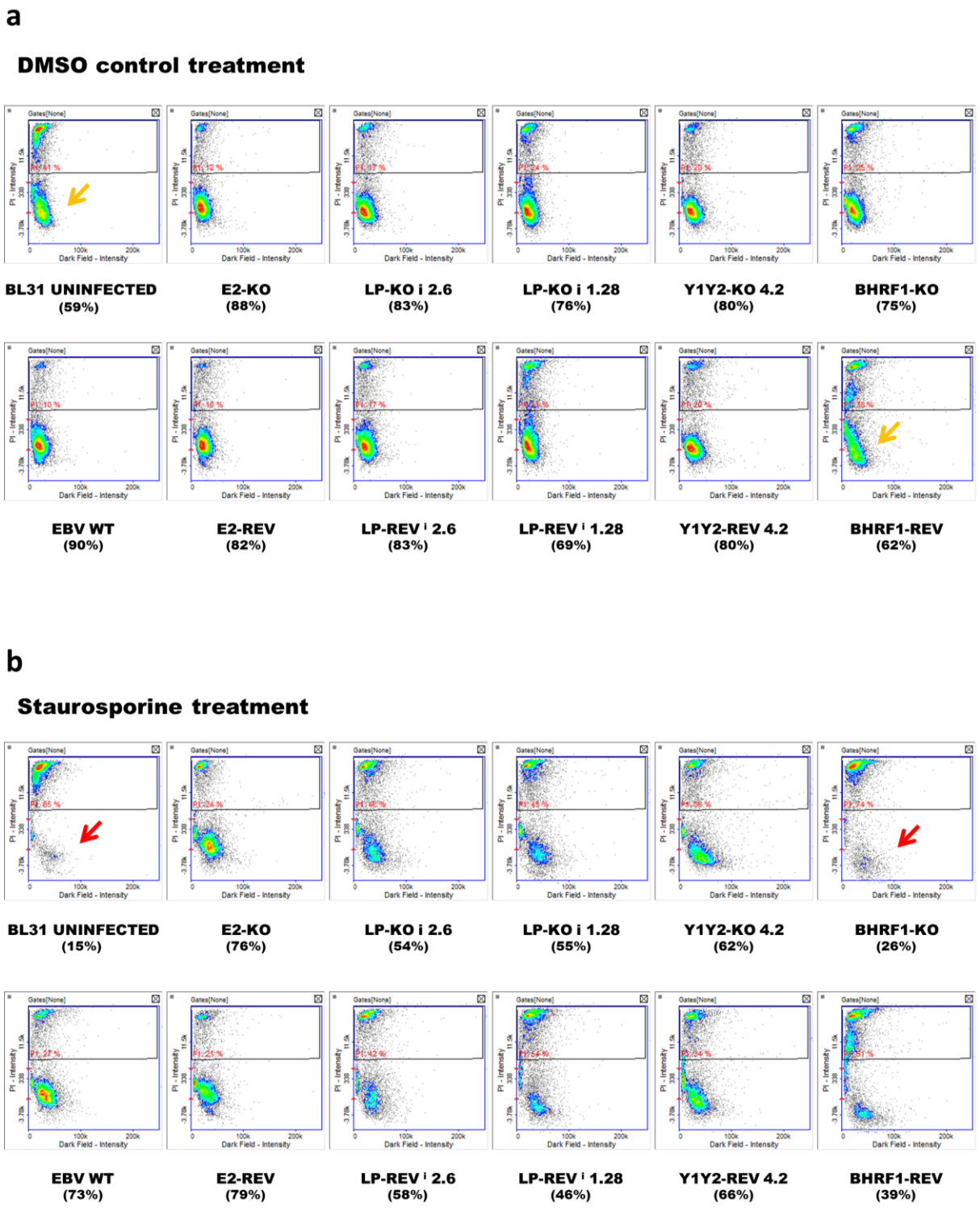

Fig. 3.16 Analysis of cell death after treatment with drugs (staurosporine as an example). Different BL31 cell lines were treated for 24h with **a.** DMSO as a control or **b.** 0.062 uM Staurosporine. The cell viability was assessed using propidium iodide (PI) staining and measured using the NC-3000. The x-axis represents dark field intensity, the y-axis represents PI intensity. Gates (black boxes) measure the percentage of dead cells (red text). The percentage of live cells is indicated in brackets under each graph. Yellow arrows indicate the two cell lines with reduced viability in the DMSO control treatment in comparison to other mutants. Red arrows indicate decreased proportion of live cells after Staurosporine treatment in comparison to other mutants.

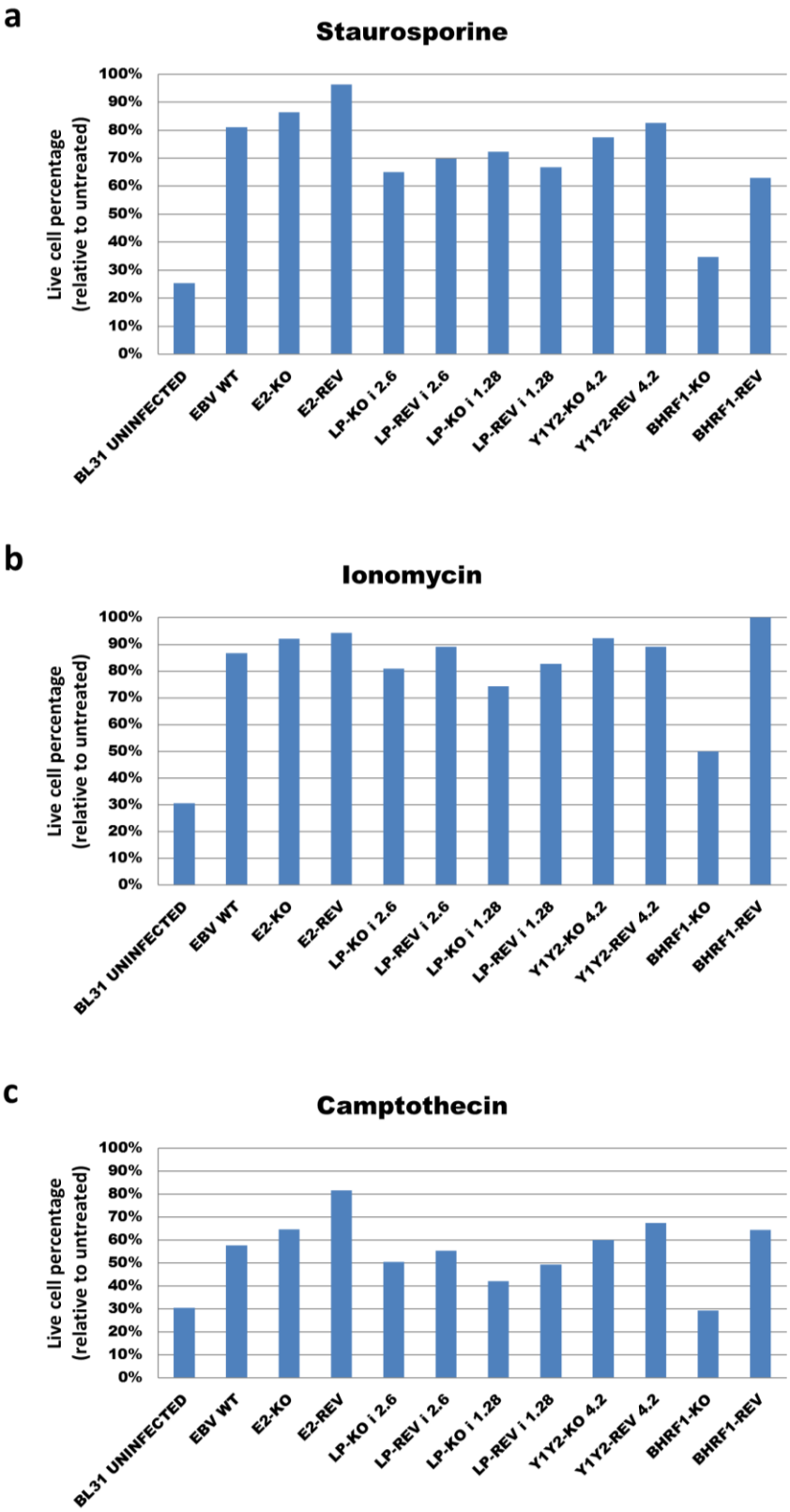

Fig. 3.17 Analysis of cell death after treatment with staurosporine, ionomycin and camptothecin. Different BL31 cell lines were treated with **a.** 0.062 uM Staurosporine for 24h , **b.** 1ug/ml Ionomycin for 48h, **c.** 0.3 uM Camptothecin for 24h**.** DMSO data are included in both cases (24h and 48h) as a control. The percentage of live cells (established based on analysis shown in Figure 3.16) after drug treatment was divided by the percentage of live cells after DMSO control treatment and plotted as bar graphs.

3.3 Behaviour of LP-KO ^{i} in primary B cells

To assess whether EBNA-LP knockouts are able to transform B cells, and to determine what role is played by EBNA-LP during transformation, either CD19-isolated primary B cells or total peripheral blood lymphocytes (PBLs) (both isolated from buffy coat residues) were infected with the same set of mutant viruses that had been used for BL31 infections. To make sure that the rate of infection was same for all of the recombinant EBVs, all the infections in this chapter were performed at an MOI=1 (based on the green Raji unit titration of each stock of produced virus- see section 2.5.2).

3.3.1 LP-KO ^{i} 2.6-infected B cells are not able to establish continuously proliferating LCLs

To establish whether EBNA-LP is essential for the transformation of B cells into LCLs, primary B cells derived from adult blood donation products and isolated by magnetic sorting (positive selection for CD19 expression) were infected with different recombinant viruses. Cells were assessed by microscopy (see figures 3.18 and 3.19 for pictures taken at 40x and 10x magnification respectively) to investigate any visible signs of B cell activation/expansion. B cells infected with WT EBV become activated (Fig.3.18) and clump together (Fig.3.19). B cells infected with LP-KO ^{i} virus initially show signs of activation, as some cells become bigger, and more irregular (Fig.3.18), they clump together in an equivalent to WT-infected cells way at day 3 (Fig.3.19a) and the clusters enlarge and accumulate until approximately 7 days after infection but much slower than WT-infected cells (Fig.3.19b and c). However, by 10 days post infection, WT-infected cells have extensively proliferated, whereas the clusters of LP-KO ^{i}-infected cells seem to have dispersed (Fig.3.19d). E2-KO-infected B cells are completely devoid of activation, and are indistinguishable from the uninfected control (Fig.3.18 and 3.19), indicating that LP-KO ^{i}-

infected cells are less defective than E2-KO-infected. B cells infected with Y1Y2-KO change their appearance and expand slightly slower than WT-infected cells (not shown) but are able to establish LCLs (with or without feeder cells), which confirms that the Y1Y2 domain is not essential for B cell transformation in our BAC, as was previously reported by Mannick et al. (1991) for the P3HR1-derived Y1Y2-KO virus (see section 1.9.6). As expected, cells infected with E2-REV and Y1Y2-REV behave indistinguishably from WT-infected cells. However, cells infected with LP-REV ^{i} 2.6 expand consistently slower than those infected by the WT and other revertant viruses (Fig.3.19).

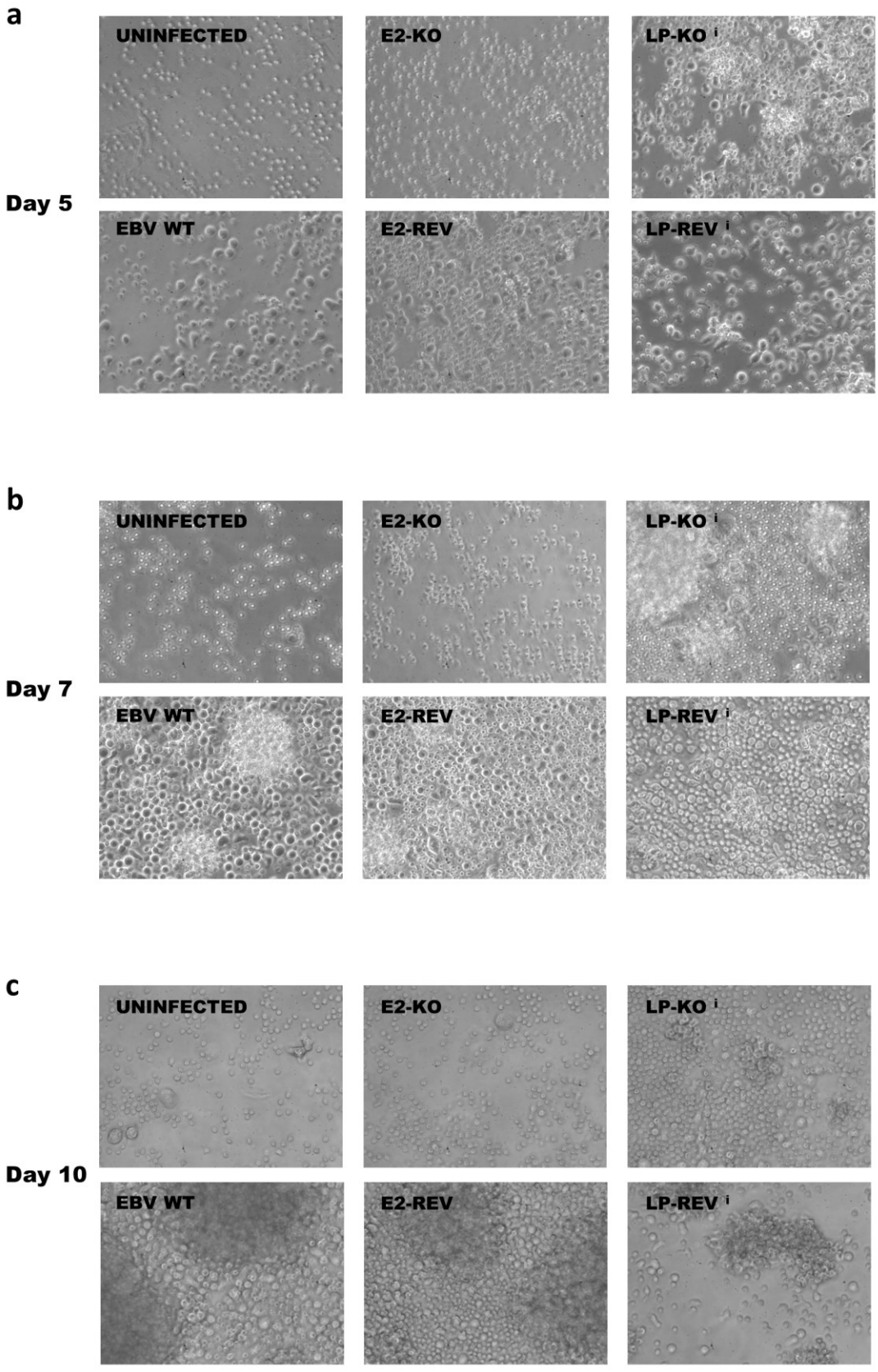

Fig. 3.18 Morphology of primary B cells infected with recombinant EBVs. CD19-isolated human B cells were infected with different EBV recombinants at MOI=1. Pictures of cells in the wells were taken at **a.** day 5, **b.** day 7, and **c.** day 10, under 40x magnification.

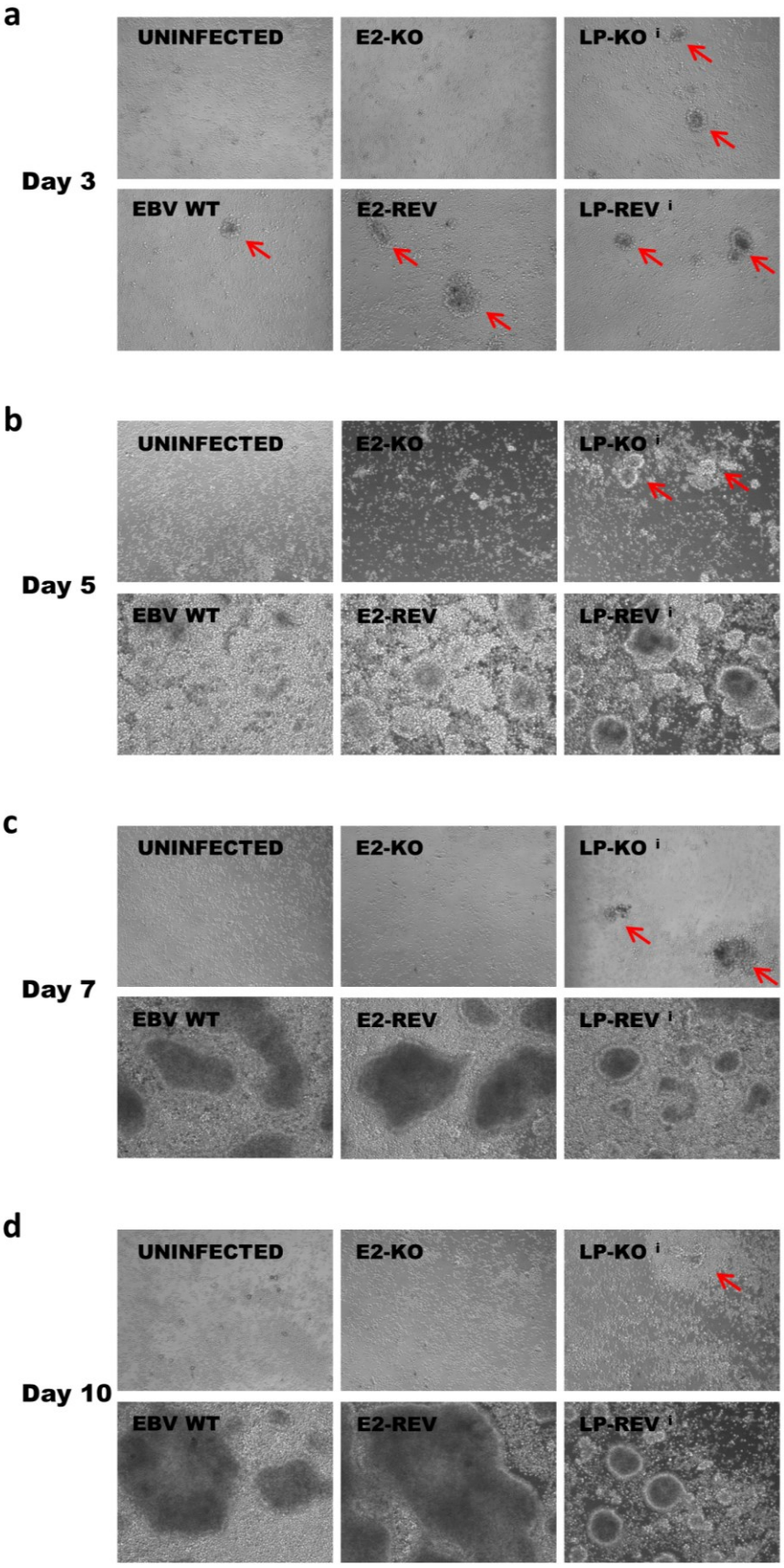

Fig. 3.19 Expansion of primary B cells infected with recombinant EBVs. CD19-isolated human B cells were infected with different EBV mutants at an MOI=1. Pictures of cells in the wells were taken under 10x magnification, at **a.** day 3, **b.** day 5, **c.** day 7 and **d.** day 10. Red arrows indicate clusters of activated cells.

The outgrowth experiment was repeated approximately 30 times using CD19-positive B cells or PBLs (to assess whether the initial failure of LP-KO ^{i}-infected B cells to establish LCLs could be supported by higher cell density) with the same result: failure of LP-KO ^{i} virus to establish LCLs.

To test whether this failure of LP-KO ^{i}-infected B cells to establish LCLs could be rescued by external signals that might support growth, infected B cells were also co-cultured with irradiated MRC5 cells as feeder cells. This experiment was repeated using 12 different donors. In two of these twelve infections, LP-KO ^{i}-infected cell populations were able to establish LCLs. However, for one of these two, the uninfected B cells also produced an LCL (termed sLCL, where "s" stands for spontaneous).

Analysis of the sLCL and matched LP-KO ^{i}-derived cell line (sLCL-LP-KO ^{i}) showed that both expressed not only EBNA-LP but also a shorter form of EBNA-2, a longer form of LMP-1 and a longer form of EBNA-3C than other B95.8-BAC-infected LCLs (not shown). This implies that most of the viral latency proteins originate from the endogenous virus that gave rise to the sLCL, rather than from the LP-KO ^{i} BAC and that LP-KO ^{i}-infected cells were transformed by endogenous virus rather than LP-KO ^{i} virus. Despite this, sLCL-LP-KO ^{i} contained some GFP-positive cells, which suggests co-infection with both, endogenous and LP-KO ^{i} virus or that the culture is a mix of BAC-infected and endogenous-infected cells that somehow support each other.

In the second case (from a different donor), there were no spontaneous LCLs evident in the uninfected control. No EBNA-LP was detected in this LP-KO ^{i}-LCL using JF186 antibody, which detects only a subset of EBNA-LP isoforms- see section 1.9.3 (Fig.3.20a). However, EBNA-LP was readily detected by 4D3 antibody, which detects all known EBNA-LP isoforms (Fig.3.20a). This shows that these LCLs do express EBNA-LP, and that this EBNA-LP must come from a non-B95.8 strain. Other EBV latency proteins were

indistinguishable from B95.8 (Fig.3.20). We speculate that this EBNA-LP derives from the blood donor's endogenous EBV. To test whether the *EBNA-LP* gene has recombined into the LP-KO ^{i} BAC, or is derived from a complementing virus, the viral DNA from these LCLs was isolated by episome rescue (recovery into bacteria) from a low molecular weight DNA preparation. Since this process relies on the viral genome containing a BAC element for propagation in bacteria, this will only recover original BAC-LP-KO ^{i} genomes. Enzymatic digestions and pulsed-field gel electrophoresis of rescued virus genomes clearly showed that all of the recovered genomes carried the LP-KO ^{i} mutations (addition of the PvuI site and removal the BsmBI site) in each W repeat, and no other unexpected rearrangements (Fig.3.20b). This implies that the EBNA-LP derives from complementation with an endogenous EBV, rather than a recombination between the two virus strains.

To attempt to avoid this sort of contamination from endogenous virus, I additionally performed infection of PBLs from three different EBV-negative donors and two umbilical cord blood samples, all cultured both with and without the presence of feeder cells. I was unable to establish LCLs after infection with LP-KO ^{i} in any of these experiments, whereas LP-REV ^{i} consistently established LCLs, albeit more slowly than WT and other revertant viruses.

Overall, this shows that LP-KO ^{i} is unable to establish LCLs (although is able to contribute to the establishment of an LCL when complemented by a (presumably) non-transforming EBV strain).

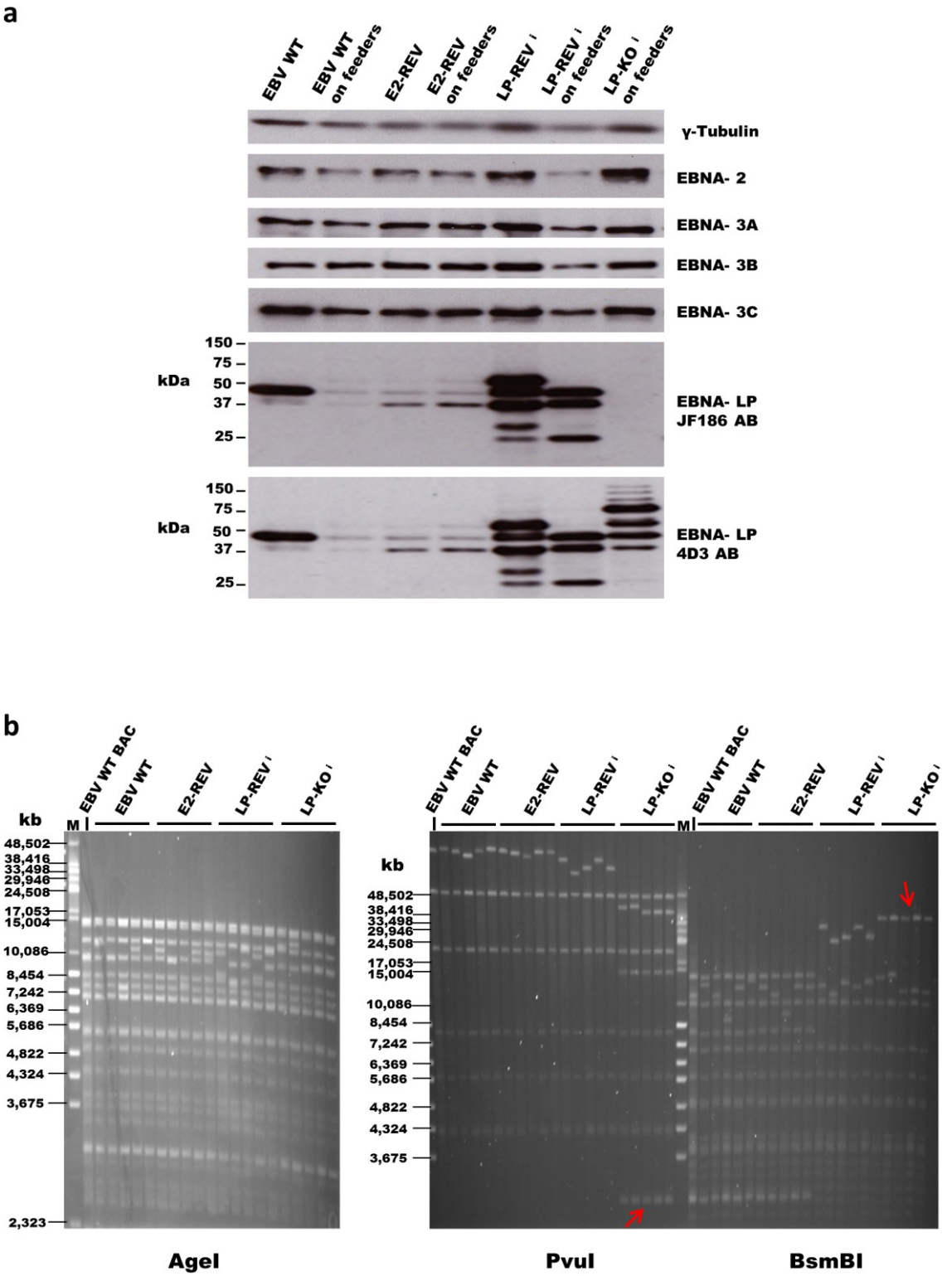

Fig. 3.20 Analysis of LCLs obtained after primary B cells infection with different EBV mutants (including LP-KO ^{i}). a. Proteins extracted from LCLs (RIPA lysate) were separated by SDS–PAGE (12% polyacrylamide gel for EBNA-LP and 7.5% polyacrylamide gels for other proteins) blotted and probed with antibodies as indicated. γ-tubulin was used as a loading control. **b.** Pulsed-field gel electrophoresis of DNA after episome rescue. Five different episomes from each cell line were digested as indicated and analyzed by pulsed field electrophoresis. As a control WT BAC EBV was used. Red arrows indicate the retained mutations that were introduced to modified BACs.

3.3.2 Analysis of EBV infection in different blood donors

In order to find an EBV-negative source of B cells (so that we could be certain that LCLs would not grow out spontaneously from infection by the donor's latent EBV strain) as well as assessing which PBLs could be transformed with highest efficiency (which would allow for optimization of different assays in the most efficient way), PBLs from 8 different donors were isolated, frozen down and tested for different properties (EBV positivity by ELISA, percentage of CD20-positive cells, LCLs outgrowth efficiency, percentage of infected cells by EBNA-2 expression, proliferation efficiency etc.). Results can be seen in Table 3.2. Out of the 8 donors tested, one of them was EBV-negative by VCA ELISA (donor AD35) and for one them the EBV status was inconclusive (donor AD37). There was no case of spontaneous outgrowth or apparent activation in any of these donors (either with or without feeder cells). The transformation efficiency after WT EBV infection- as measured by percentage of EBNA-2 positive cells on day 7, and the degree of proliferation- as measured by using CellTrace violet on days 5 and 7, varies a lot between different donors (Table 3.2). The percentage of B cells in the PBL population also varied between donors as well but did not really correspond with the variation in transformation efficiency (not shown). The percentage of cells expressing GFP is lower than the percentage of cells expressing EBNA-2 and these two properties do not correspond with each other, confirming previous observations that the GFP expression is unreliable in primary B cells infected with recombinant virus. Most of the assays used in primary CD19-isolated B cell experiments were established and optimized using the frozen PBLs stocks described in table 3.2.

Donor	EBV status (ELISA)	CD20+ cells Non-infected day 5	CD20+ cells E2-REV infected day 5	Proliferated of CD20+ cells day 5	GFP+ of all live cells day 7	Proliferated of all live cells day 7	EBNA-2 positive day 7	Proliferated of EBNA-2+ day 7	Outgrowth 4- best, 1-worst
AD31	positive	1%	2%	2%	4%	10%	12%	65%	1
AD32	positive	2%	6%	30%	3%	28%	27%	82%	4
AD33	positive	4%	9%	13%	1%	18%	12%	71%	3
AD34	positive	0%	2%	36%	5%	18%	20%	79%	2
AD35	negative	5%	14%	13%	5%	32%	29%	83%	2
AD36	positive	2%	6%	23%	8%	30%	30%	82%	3
AD37	inconclusive	7%	8%	13%	3%	26%	26%	83%	2
AD38	positive	8%	10%	16%	5%	39%	37%	85%	4

Table 3.3 Analysis of infection properties of PBLs from different blood donors. Different donors (AD31-AD38) were analysed to determine their EBV status using ELISA, and then by flow cytometry to determine: percentage of B cells (using CD20 marker) before infection and at day 5, 7 after infection with WT EBV. Additionally, infected cells were tested for: percentage of GFP positive cells, EBNA-2 positive cells and proliferation at day 5 and 7 after infection. Finally, they were scored (1-4, where 4 is the fastest and 1 is the slowest) based on the time taken to establish LCLs. The donors with the highest and lowest values in each column were marked in blue and pink respectively.

3.3.3 Expression of activation markers on EBV-infected B cells

To assess whether the enlargement and clumping of B cells induced by LP-KO ^{i} represents the activation of infected B cells, the expression of activation markers was tested. This was also intended to identify markers of EBV infection that are expressed early after infection (as by day 10 most of the LP-KO ^{i}-infected B cells are already dead (Fig.3.19)) to sort infected cells for downstream analysis.

CD23 has been identified as an early activation marker after infection with EBV (Azim et al., 1990). More recently, it was reported that EBV-infected cells co-expressing high levels of CD23 together with CD58 were likely to be proliferating, as the population of $CD23^{+high}CD58^{+}$ was doubling each day from day 4 onwards (Megyola et al., 2011). Therefore, we wanted to test whether combined analysis of CD23 and CD58 may be a good marker for EBV-infected B cells. It was also reported that CD23/CD58 can be used to identify EBV-infected cells as early as 3 days after infection, although the data to support this statement were unconvincing (Megyola et al., 2011).

To assess the pattern of CD23/CD58 expression in our studies, infected B cells were stained with antibodies against CD23 and CD58 (previously titrated on LCLs- for antibodies see table 2.3) at different time points after infection of primary B cells and analysed using flow cytometry. As can be seen from Figure 3.21, there is no detectable increase in CD23 or CD58 signal until approximately 5 days after infection with WT EBV in comparison to non-infected or E2-KO-infected B cells. Therefore, CD28 and CD58 are not sufficiently early markers of EBV-induced activation to be used to identify populations of infected cells before they begin dividing. B cells infected with mutant viruses that are slower in establishing LCLs (LP-REV ^{i} and Y1Y2-KO), also express CD23/CD58 somewhat later (around 1-2 weeks post infection) than WT EBV (Fig.3.21). Also the populations of $CD23^{+}CD58^{+}$ cells in the LP-REV ^{i} and Y1Y2-KO infections do not increase in numbers as rapidly as in the case of infection with WT or other revertants (notably, at day 3 after infection, the population of $CD23^{+}CD58^{+}$ cells is very similar for LP-REV ^{i}, Y1Y2-KO and E2-REV infections, but the population of E2-REV increases much faster over time than LP-REV ^{i}, Y1Y2-KO). At this point (2 weeks post infection) there are very few remaining EBV-positive cells infected with LP-KO ^{i}. This delay in up-regulation of CD23 and CD58 in the cell populations that expand less efficiently makes the early identification of cells infected with (and activated by) mutant viruses impossible using these markers of activation. The increasing proportion of $CD23^{+}CD58^{+}$ in uninfected and E2-KO-infected B cells over those 2 weeks may suggest that previously activated B cells survive longer in culture than non-activated ones (especially considering extremely low number of live cells in those samples). This experiment was also done with the CD23 marker only (not shown).

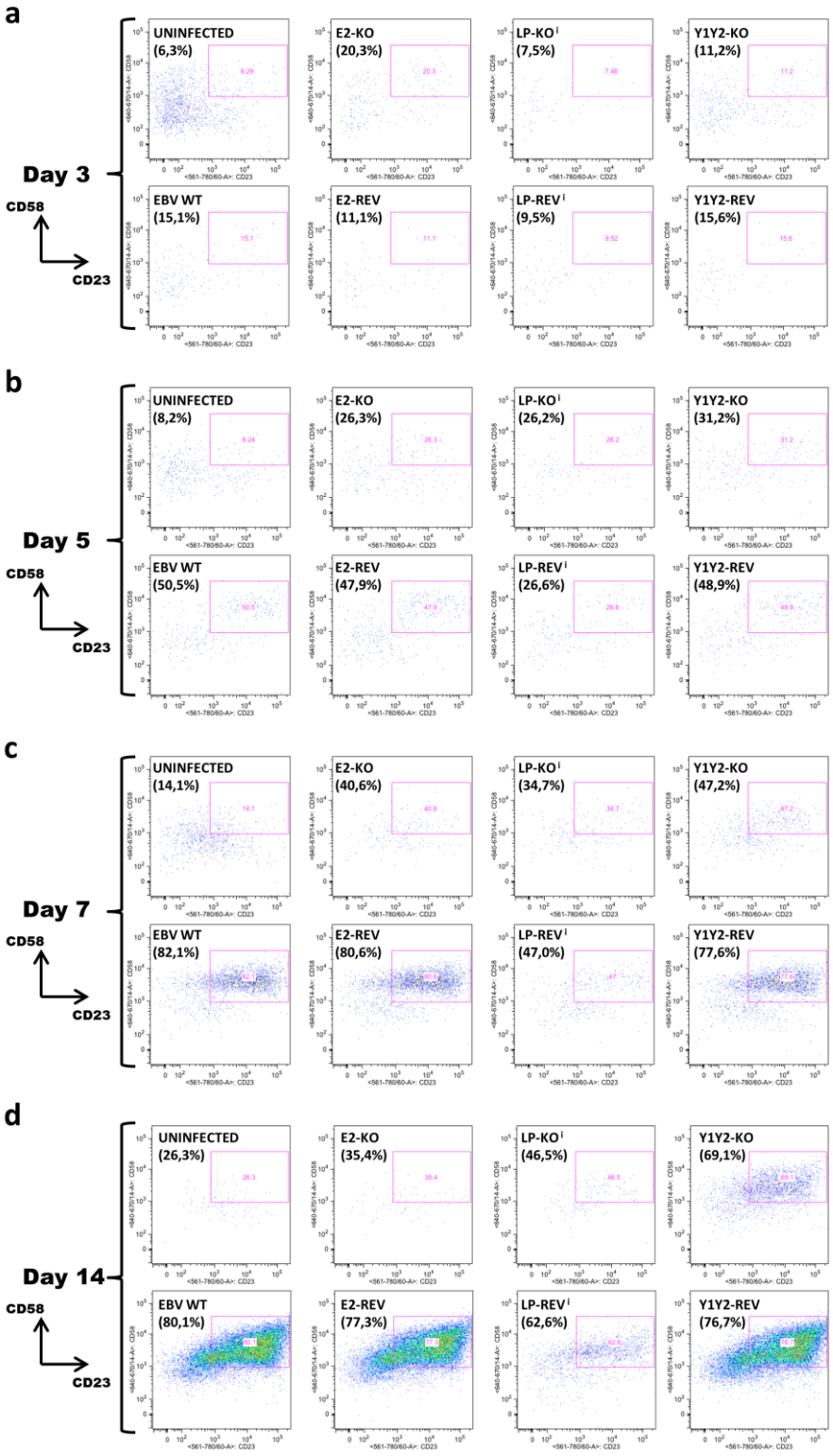

Fig. 3.21 Activation of primary B cells infected with different EBV mutants using CD23 and CD58 as markers. Primary B cells were infected with different EBV recombinants. Proportion (1/4) of infected cells was harvested and stained with live/dead dye and antibodies for extracellular markers: CD23 and CD58 at day: **a.** 3, **b.** 5, **c.** 7 and **d.** 14 post infection. After the staining cells were analyzed using flow cytometry. Dot plots show the characteristics of cells after gating out debris, cell doublets and dead cells. The x-axis shows CD23 signal, while the y-axis shows CD58 signal. The pink square is the gate defining $CD23^{+}CD58^{+}$ cells. The percentage of $CD23^{+}CD58^{+}$ cells is shown in brackets under each recombinant's name.

3.3.4 LP-KO ^{i}- infected B cells can undergo limited proliferation

To assess whether the B cells infected with LP-KO ^{i} are able to proliferate rather than simply aggregate but not divide, proliferation was assayed using flow cytometry to analyze the dilution of Cell Trace Violet signal at different time points after infection (a representative example is shown in Figure 3.22). By day 3 after infection no cell proliferation has been induced by any of the viruses (Fig. 3.22a), confirming observations reported by Nikitin et al., (2010). By day 5, B cells infected with viruses have begun proliferating (Fig.3.22b). The number of divided cells after LP-KO ^{i} infection is lower than induced by wild type or revertant virus infections, but higher than in EBNA-2 knockout or uninfected cells, which show no evidence of any proliferation having occurred. Y1Y2-KO is less efficient at inducing proliferation than WT virus: fewer Y1Y2-KO- infected cells have started proliferating but those that do undergo similar number of divisions. LP-REV ^{i}- infected cells appear to proliferate to a similar extent as Y1Y2-KO-infected: slower than WT. Proliferation induced by E2-REV and Y1Y2-REV is indistinguishable from WT. This analysis was repeated with or without co-culture of infected B cells on irradiated MRC5 feeder cells with very similar results (not shown).

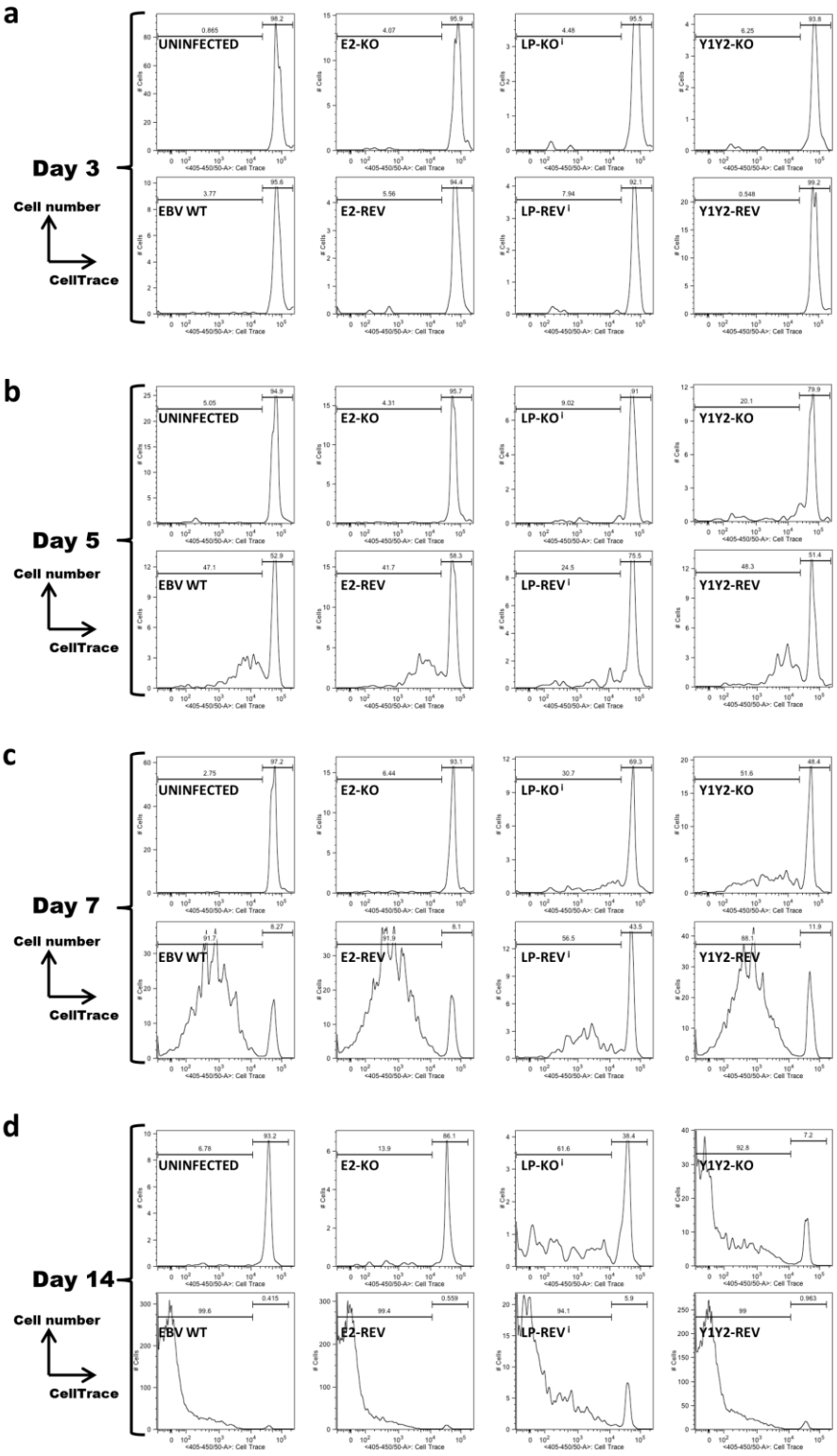

Fig. 3.22 Representative results from proliferation of primary B cells infected with different EBV mutants using CellTrace Violet. Primary B cells were stained with CellTrace Violet just before infection with different EBV recombinants. Cells were additionally stained with live/dead dye at day: **a.** 3, **b.** 5, **c.** 7 and **d.** 14 post infection. After the staining cells were analyzed using flow cytometry. Graphs show the cells after gating out debris, cell doublets and dead cells. The x-axis shows CellTrace fluorescence, while the y-axis shows number of cells counted. A bright, homogenous fluorescent signal (that can be seen in samples collected 3 days after infection) originates from the initial population of non-proliferated cells. Subsequent cell divisions result in signal dilution (each with half the fluorescence intensity of its parent cell) and is represented by the peaks on the left side of the initial peak.

3.3.4.1 Batch variations of CellTrace violet cause toxicity for B cells

Because of the failure to find a good marker of early B cell infection, we hoped to use CellTrace violet as a marker of dividing cells, and to then sort infected cells based on their division to explore further the mechanism of proliferation driven by EBNA-LP. However, with different batches of this chemical, a big variation in the total number of EBNA-2 positive cells measured by flow cytometry was observed. To address this issue, different batches of CellTrace violet were tested on newly infected PBLs. Those cells were additionally stained for EBNA-2 (to distinguish infected cells from non-infected) and with live/dead stain 5 days after infection. The cells were analyzed by flow cytometry; first by gating for live cells and then assessing the percentage of infected cells by drawing the gate around EBNA-2 positive cells. The results showed more than 4 times decrease in percentage of infected (EBNA-2 positive) cells when cell trace was used (Fig.3.23a). The overall PBL population showed a 3-fold increase in the percentage of dead cells when CellTrace was used. This indicates that CellTrace is toxic for cells rather than it interferes/ inhibits EBV-infection of previously stained B cells. This experiment was repeated with 3 different lots of CellTrace with similar effects. The degree of toxicity even varied between different tubes of CellTrace violet from the same lot. Halving the concentration of stain that is recommended by the supplier did not decrease cell death (not shown).

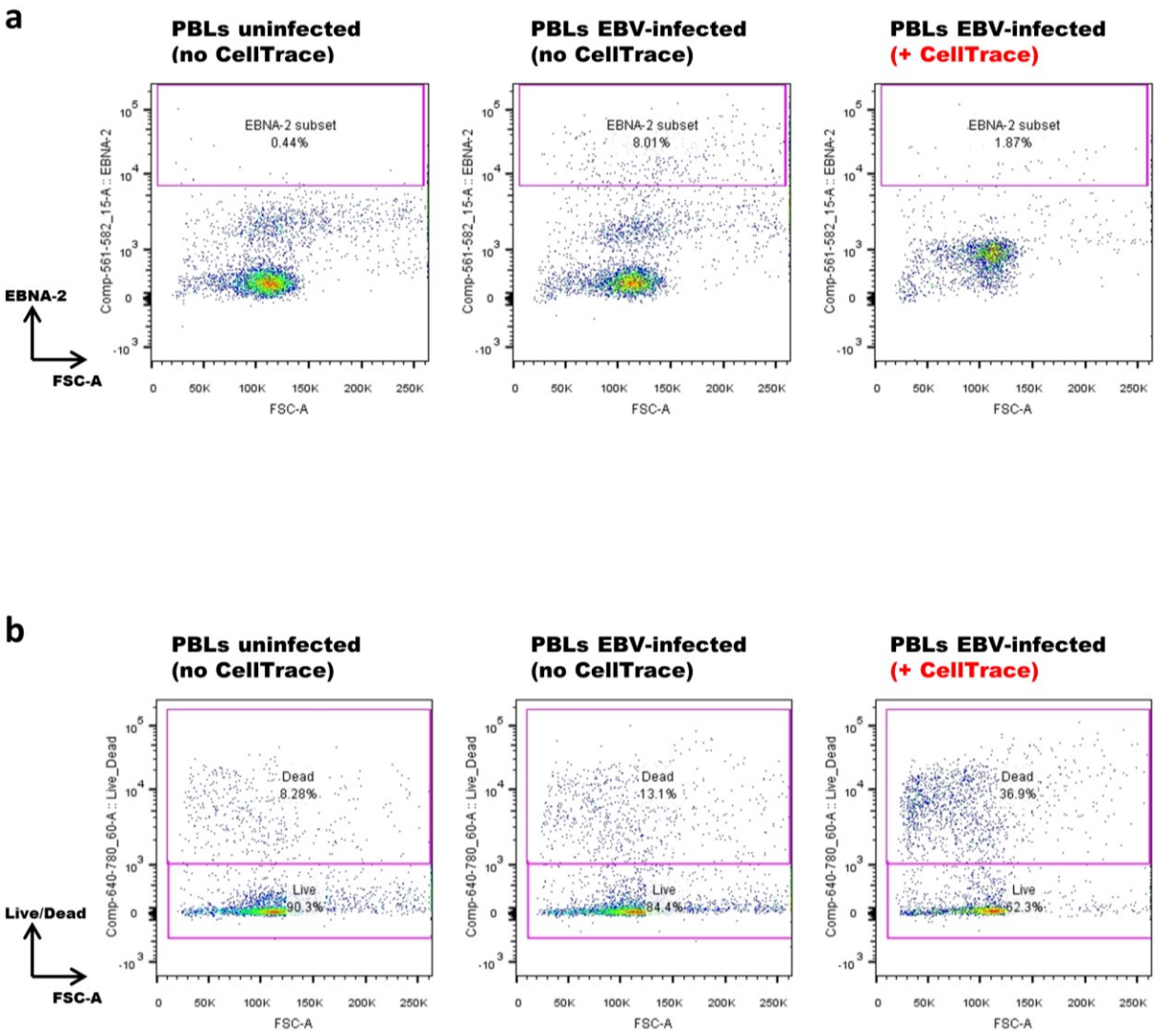

Fig. 3.23 Flow cytometry of PBLs after staining with CellTrace violet. PBLs were stained with CellTrace violet (or incubated with PBS only as a control) then infected with WT EBV. After 5 days cells were harvested and stained for EBNA-2 and dead cells and analyzed using flow cytometry. Dot plots show the population of cells after gating out cell doublets. The x-axis shows the forward scatter area, the y-axis shows: **a.** EBNA-2-PE fluorescence of live cells only, or **b.** live/dead stain fluorescence of all single cells.

3.3.5 LP-KO ^{i}- infected B cells express EBNA-2

The very limited proliferation observed in LP-KO ^{i}-infected B cells raised the question of whether primary B cells are able to express EBNA-2 after infection with a virus that lacks EBNA-LP. To answer this question and to identify infected cells, intracellular staining for flow cytometry was optimized using 3 different fixation/permeabilization conditions: 4% PFA/Triton-X100, 4% PFA/saponin, 80% EtOH (Fig.3.24). The staining showed that both PFA+Triton-X100 and 80% ethanol work well, so they were used in further experiments as described in the relevant figure legends.

As can be seen from Figure 3.25, LP-KO ^{i}-infected adult (Fig.3.25a) and cord blood (Fig.3.25b) B cells can express EBNA-2 at a similar level to WT-infected B cells.

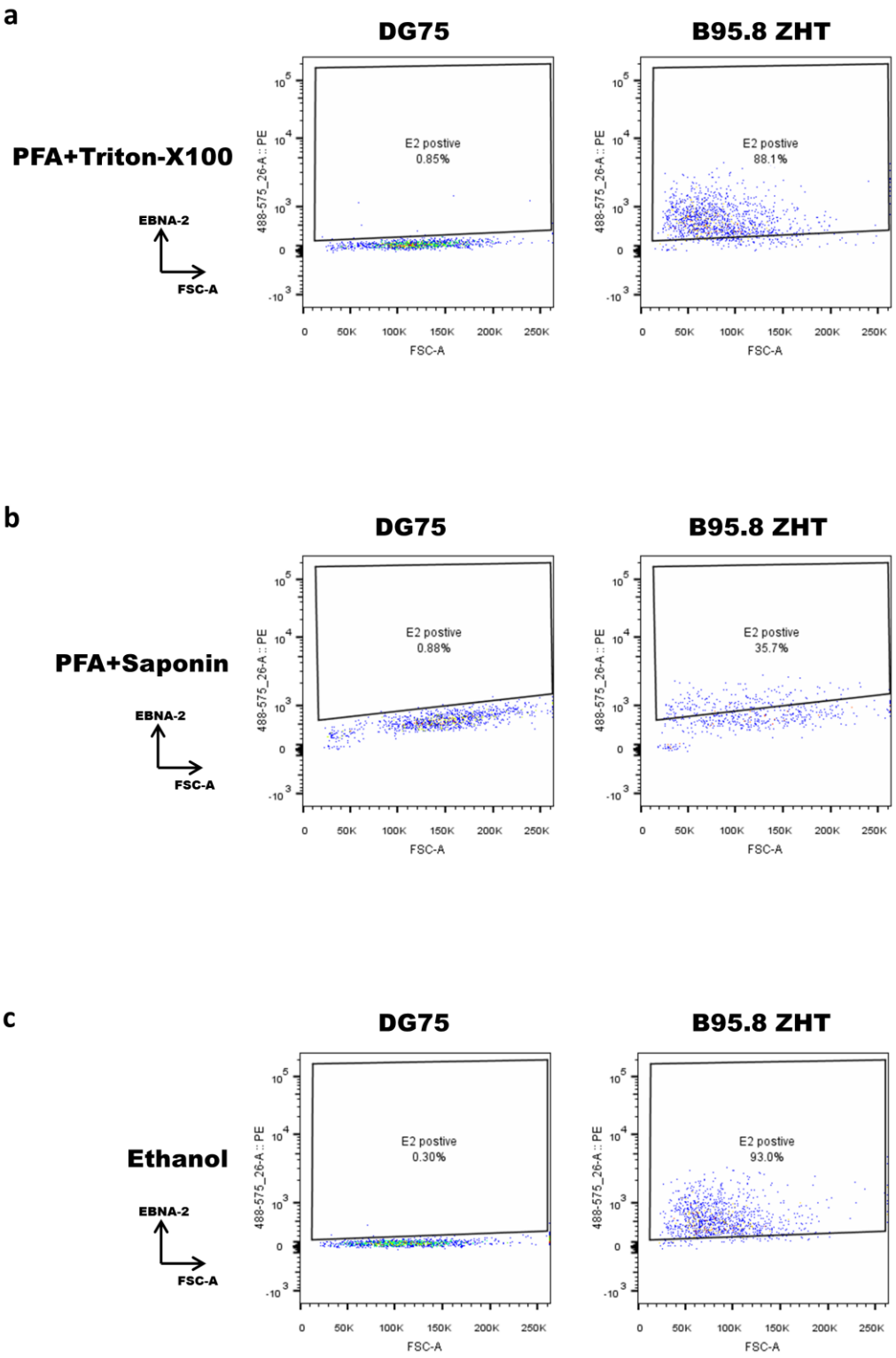

Fig. 3.24 Optimization of intracellular EBNA-2 staining. An EBV-negative B cell line (DG75) and an EBV-positive B cell line (B95.8 ZHT) were stained with fixable live/dead stain and fixed with either **a-b**. 4% PFA or **c.** 80% ethanol. Cells fixed with PFA were additionally permeabilized with either **a.** Triton-X100 or **b.** saponin. After this treatment cells were incubated with mouse anti-EBNA-2 (clone PE2) primary antibody followed by incubation with PE-anti-mouse secondary antibody. Cells were analyzed by flow cytometry. Dot plots show the population of cells after gating to remove debris, cell doublets and dead cells. The x-axis indicates forward scatter area and the y-axis indicates PE fluorescence. Black shapes are the gates that indicate the percentage of EBNA-2 positive cells.

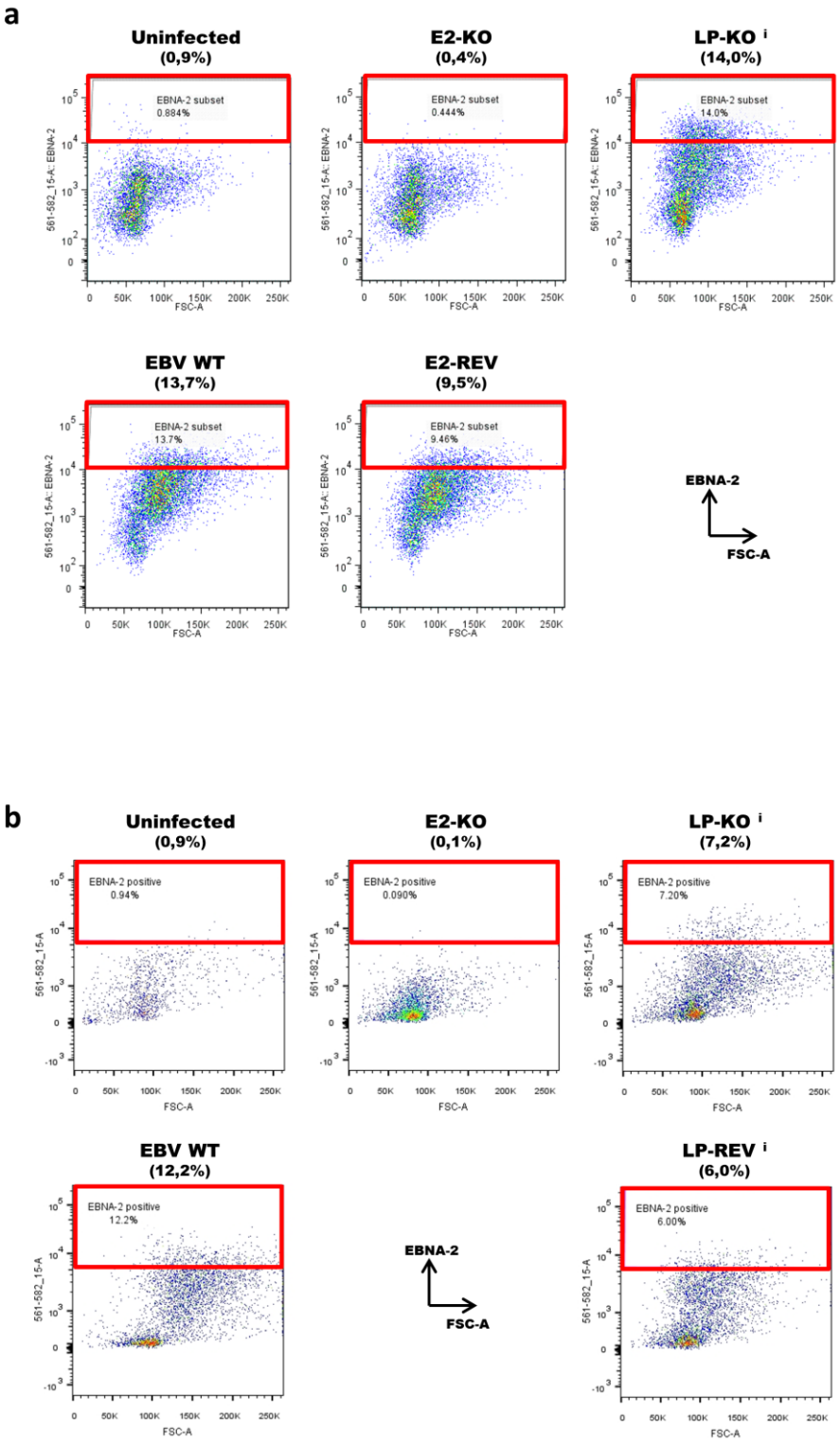

Fig. 3.25 Representative results from expression of EBNA-2 after different mutant EBV infections of: a. adult PBLs, **b.** cord blood PBLs. Isolated PBLs were infected with different mutant viruses, fixed with ethanol, stained for EBNA-2 and analyzed using flow cytometry at day 6 after infection. Dot plots represent population of cell after gating out cell doublets. The x-axis indicates forward scatter area, the y-axis indicates EBNA2-PE fluorescence. Red gates show the population of EBNA-2 positive cells. Percentage of EBNA-2 positive cells is indicated in bracket under the name of each recombinant virus.

3.3.6 Percentage of LP-KO ^{i}-infected B cells progressing to S and G2 phase in the cell cycle is much lower than in WT infection

Optimization of EBNA-2 staining allowed for the identification of infected cells and has become a useful tool in performing experiments that require analysis of only the infected cell population to give meaningful results. One of these experiments was assessment of the progression of infected cell in the cell cycle to establish whether the limited proliferation of LP-KO ^{i}- infected cells is caused by arrest in one of the cell cycle phases. After fixable live/dead staining and ethanol fixation (which gives better DNA staining than PFA), cells were stained with DAPI (DNA-intercalating dye) and anti-EBNA-2 antibody, and analyzed using flow cytometry by first identifying the population of infected (EBNA-2 positive) cells and then assessing the cell cycle profile on this population (Fig.3.26).

As can be seen from Figure 3.26a, on day 6 after infection of adult B cell, the cell cycle profile for WT-infected and revertant-infected B cells are very similar. The percentage of LP-KO ^{i}-infected B cells in both S phase and G2/M is much lower (approximately 1.5 times lower for S phase and 2 times lower for G2/M) than in WT infection (Fig.3.26a), and is similar to that of Y1Y2-KO-infection (Fig.3.26a) which may indicate that B cells infected with those mutants do not enter the cell cycle as efficiently as WT-infected cells. These data are largely consistent with the proliferation results obtained on days 5-7 after infection, which showed much lower percentage of divided cells infected with LP-KO ^{i} and Y1Y2-KO in comparison to WT/REV infections (Fig.3.22). However, the more defective division phenotype of LP-KO ^{i}, which proliferated less than Y1Y2-KO (Fig.3.22), is not reflected in the cell cycle profile, in which there is no obvious difference between Y1Y2-KO and LP-KO ^{i} (Fig. 3.26a).

In cord blood infection, the difference in cell cycle profile between WT and LP-KO ^{i}-infected B cells in both S phase and G2/M is more striking than for adult cells (Fig.3.26b). In

the LP-REV ^{i}-infected B cells, that are somewhat defective in driving cells to divide (Fig. 3.22), a reduction of cells in S phase can be observed, but this reduction is not as great as in LP-KO i-infection. However there is no deficit in G2/M- indeed it is higher than in WT infection (Fig.3.26b), which may suggest a restriction in progression into S phase (or speeds up progression through S phase) and therefore explain the slower proliferation and outgrowth of LP-REV ^{i}-infected cells in comparison to WT.

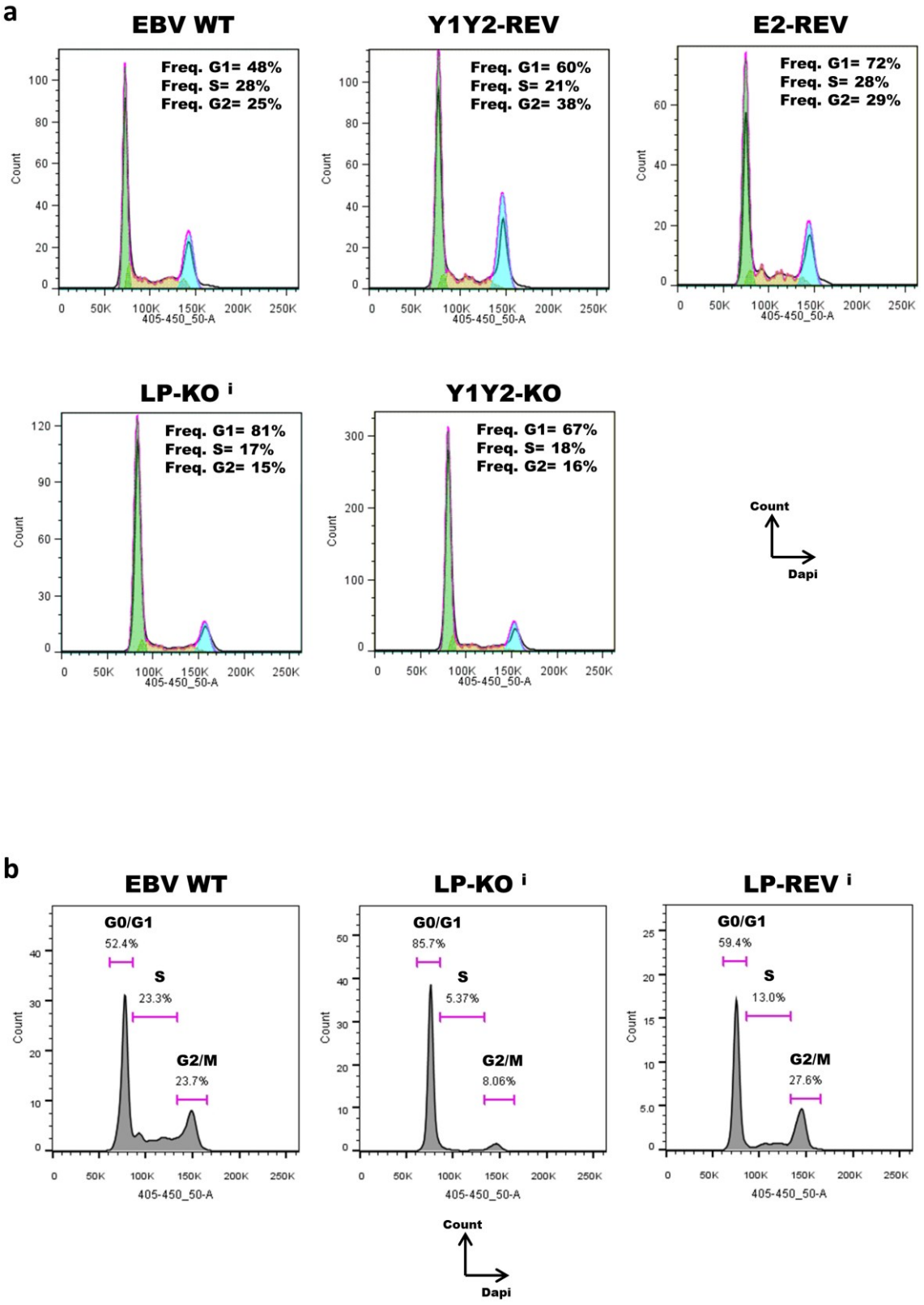

Fig. 3.26 Cell cycle analysis using flow cytometry. Cells were harvested at day 6 after infection, stained with fixable live/dead stain, fixed with ethanol, stained with DAPI and for EBNA-2 and analyzed using flow cytometry. Histograms show population of EBNA-2 positive cells. The x-axis indicated DAPI fluorescence, the y-axis indicates cell count. **a.** Adult PBLs were analyzed using the Watson Cell cycle model (FlowJo). **b.** Cord blood PBLs were analyzed using manual gating.

3.3.7 Attempt to assess role of EBNA-LP in hypoxia

The transformation of B cells by EBV has been reported to lead to the stabilization of hypoxia-inducible factor 1 alpha (HIF1α) and consequent activation of the aerobic glycolytic pathway, permitting a high rate of glycolysis in the cytosol (Warburg effect) (Denko, 2008). EBNA-LP and EBNA-3A have been reported to bind to prolylhydroxylase 1 (PHD1, encoded by *EGLN2*) and prolylhydroxylase 2 (PHD2, encoded by *EGLN1*) respectively. This is theorised to prevent HIF1α hydroxylation by the PHDs and thereby block its consequent degradation. The stabilized HIF1α translocates to the nucleus and transactivates genes involved in aerobic glycolysis (Darekar et al., 2012). To establish whether EBNA-LP is required for activation of aerobic glycolytic pathway and thus establishing LCLs, we attempted to assay primary B cells infected with LP-KO ^{i} for HIF1α stabilization. However, optimization experiments using both flow cytometry and immunofluorescence with 3 different antibodies, including those previously published as detecting HIF1α in EBV-infected B cells (for antibodies see table 2.2 and 2.3) failed to detect any significant accumulation of HIF1α in WT-infected primary B cells early after infection (not shown).

3.3.8 Assessment of Smart Flare RNA detection technology to allow early sorting of live LP-KO ^{i}-infected B cells

Because EBNA-LP is the earliest latent protein expressed after infection, and is readily detectable only a few hours after B cell infection (see section 1.9.2), we hypothesise that the protein may play its most significant role(s) just at the beginning of establishing latency by EBV. Additionally, to assess the importance of EBNA-LP, the knockout needs to be compared with the wild-type and revertant viruses. Since there is a large discrepancy in proliferation induced by the viruses, any global analyses of differences between ENBA-LP knockout and wild-type infected cells are likely to be dominated by cell proliferation-associated differences

if the cells are analysed after day 3. Therefore, the ideal situation would be to identify and analyze infected cells around day 2-3 before they start to proliferate. The most useful would be a method that allows for isolation of a homogenous population of infected-only cells.

As our tests on CD23 and CD58 revealed that they are a relatively late marker of EBV infection (for activation markers see section 3.3.3), we decided to investigate whether SmartFlare technology (Merck Millipore) could be used to identify infected cells. The Smart Flare RNA detection probe is a novel tool that can be used to detect any RNA in live cells. The probe consists of a nanoparticle attached to a double stranded oligonucleotide, where one strand contains a fluorophore that is quenched by the nanoparticle. In principle, the probe enters the cells by endocytosis. Then, when the probe binds to the targeted RNA, the "fluorophore strand" is released from the nanoparticle, resulting in its fluorescence, which can be detected using flow cytometry.

To establish whether this technology can be used in a particular cell system, it needs to be tested for uptake of probes and specificity of the fluorescence. To assess uptake efficiency, the "uptake control" probe (a probe that does not need to bind a target for its fluorophore to be "on") was used: CD19 positive primary B cells (uninfected and infected with WT EBV) were incubated with different concentrations of probe at 3-7 days post infection. As can be seen from Figure 3.27a, most cells (both uninfected and infected B cells) were able to take up the probe and become fluorescent. To then assess the integrity and specificity of nanoparticles entering the B cells, a "scrambled control" probe (a probe that theoretically does not recognize any sequence within the cell and therefore acts as a baseline control for the fluorescence) and a probe against *HPRT* as a "housekeeping" probe (a probe that recognizes an mRNA expressed at a consistent level in the cell) were used as controls for RNA detection. *HPRT* has previously been used as an endogenous control gene in qPCR experiments in our lab, and shows consistent and abundant transcripts in both infected and uninfected primary B cells (not

shown). CD19 positive primary B cells (uninfected and infected with WT EBV) were incubated with different concentrations of probes at 3-7 days post infection. As can be seen from Figure 3.27b, there is no difference in signal between “scrambled” and “housekeeping” control for either uninfected or EBV-infected primary B cells (the manufacturer recommends that the signal from the “housekeeping” control has to be at least one log higher than the “scrambled” control). This suggests that SmartFlare probes (or at least the “scrambled” control) are either disrupted prematurely by B cells or binds to non-specific targets in B cells. At this stage we decided against attempting the expensive design and synthesis of an EBV-specific SmartFlare RNA sequence, since the chances of success were limited.

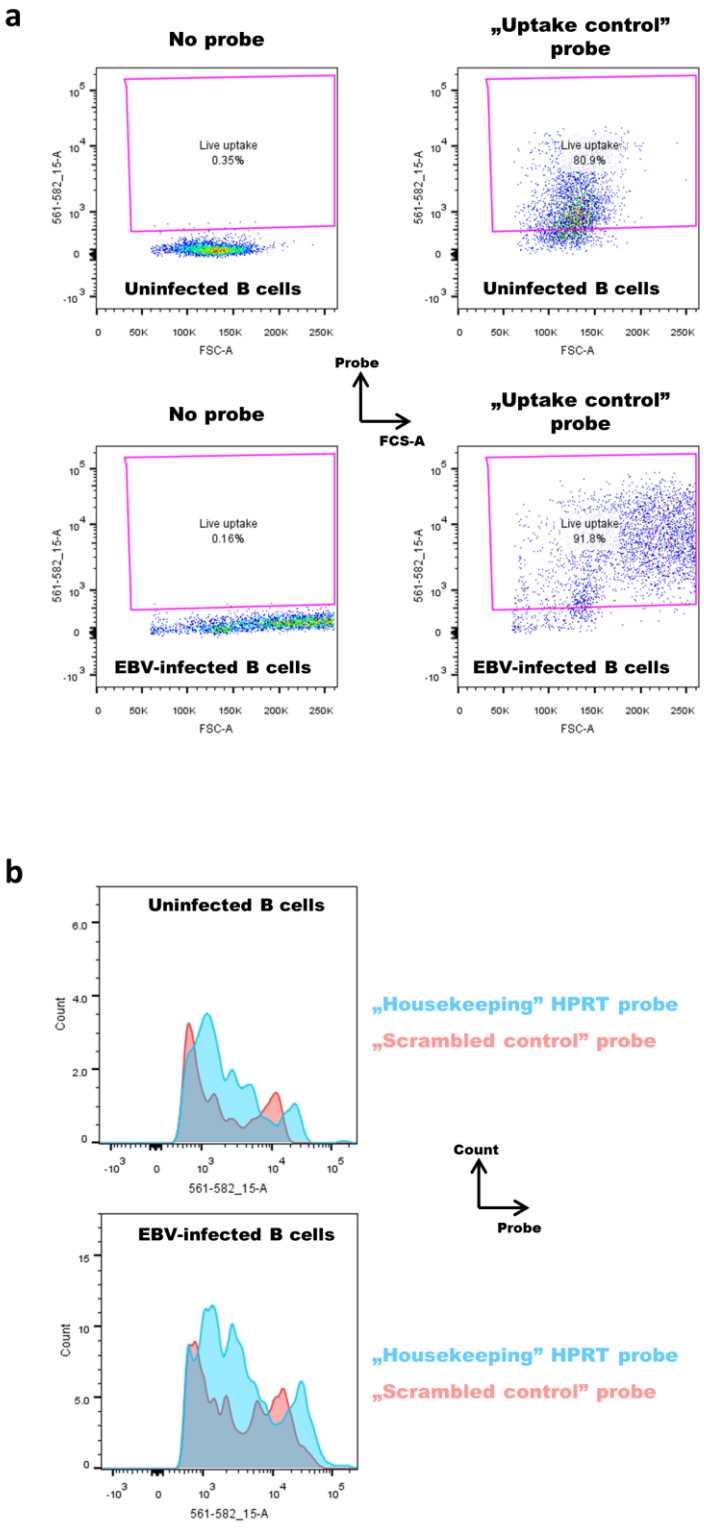

Fig. 3.27 SmartFlare RNA technology in primary B cells. CD19-isolated primary B cells (uninfected or infected with WT EBV) were tested for: **a.** Uptake of a SmartFlare probe. Cells were incubated with 500 pM of "uptake" probe and analyzed using flow cytometry. The x-axis shows the forward scatter area, the y-axis shows fluorescence of the probe. **b.** The difference in signal between "scrambled" and "housekeeping" control to assess the specificity of the SmartFlare assay. Cells were incubated with 400pM control (scrambled) probe or HPRT-specific probe and analysed using flow cytometry. Histograms show only the cells that were able to uptake the probes. The x-axis shows fluorescence of the probe, the y-axis shows cell count. The „scrambled" control is represented by pink histograms, while the „housekeeping" *HPRT* control is represented by the blue histogram.

3.4 Overview of observations made about first generation EBNA-LP mutants EBV

3.4.1 Summary of LP-KO ^{i} observations

Our LP-KO ^{i} is able to express EBV genes to normal levels in BL31, and shows no change in EBNA-2 expression early after infection of B cells by flow cytometry. In BL31 cells, EBNA-LP is not required for the sustained transactivation of host genes regulated by EBNA-2, as indicated by microarray analysis. We have also established that EBNA-LP does not play a role in the EBV-induced resistance to apoptosis induced by staurosporine, ionomycin or camptothecin.

In primary B cells, LP-KO ^{i} is able to activate infected B cells and lead to their limited proliferation. The decrease in proliferation is associated with a reduced percentage of cells in S and G2/M phases of the cell cycle in comparison to WT, perhaps as a result of failure to exit G0/G1 or possibly cell death during S or G2/M. The LP-KO ^{i} virus is not able to establish continuously proliferating LCLs after infection of either adult or cord B cells, even when using feeder cells to support outgrowth.

Most worryingly, however, both independently generated revertants of the two EBNA-LP-knockouts exhibited a partially defective transformation phenotype, that led us to re-examine the basis and construction of our mutant repeat arrays.

3.4.2 Mutations identified in the W repeat of our EBV recombinants

Sequencing analysis of the W repeat used to generate the LP-KO ^{i} and the LP-REV ^{i} repeat arrays identified 4 point mutations/changes relative to the published B95.8 sequence (Ba Abdullah et al, manuscript in preparation). One of the mutations produces a STOP codon

at the end of exon W1 (which was not transferred into our recombinants because it was replaced during the cloning process with a de novo synthesized W1 sequence used to introduce the EBNA-LP-deleting and BsmBI mutations- see section 3.1.1), while the other three are towards the end of the BWRF1 ORF (Fig.3.28). Analysis of the sequence of the B95.8 BAC and the parental virus (in B95.8 itself, a B95.8 derived LCL and in the B95.8-related virus X50-7) suggests that these sequence variations all occur once in a single repeat unit within the W repeats of the viral genome (Mohammed Ba Abdullah, manuscript in preparation), suggesting that our use of this repeat unit as the basis of our recombinants was simply bad luck. The STOP codon in one per six W repeats in B95.8 may explain the reduced levels of longer EBNA-LP forms in cell lines established with the B95.8 strain in comparison to other EBV strains (and the LP-REV ^{i}-infected cells). Analysis of the sequence also identified an additional variant in the hairpin that is in about half of the W repeats in both parental and BAC-derived B95.8 strains. However, we have not confirmed the state of this variant in the repeat unit as the hairpin appears to inhibit the passage of the polymerase during Sanger sequencing of whole repeats.

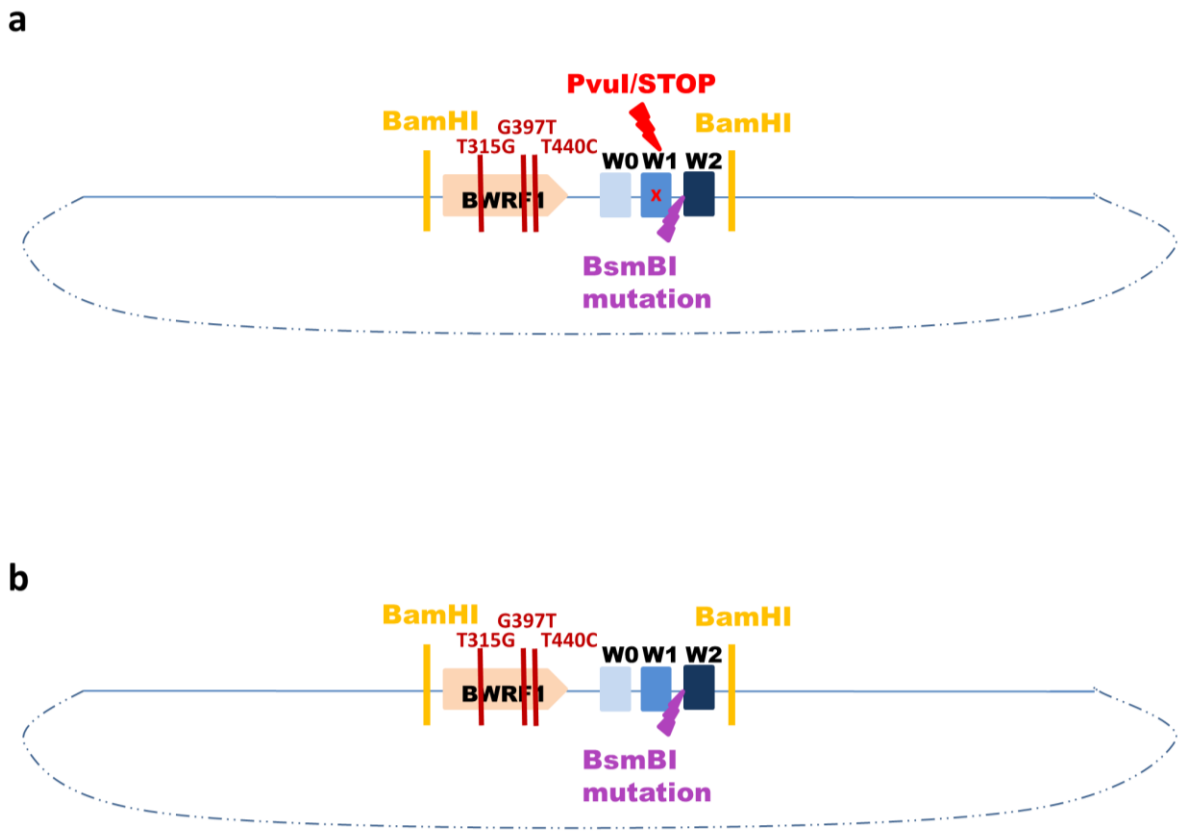

Fig. 3.28 Schematic of a single W repeat used to generate an array of a. LP-KO ^{i} and b. LP-REV ^{i}. BWRF1 open reading frame with discovered mutations in pink. W exons are represented by blue rectangles. BamHI sites are represented by yellow lines. Introduced STOP codon and PvuI mutation in bright red, BsmBI mutation in purple. Discovered mutations in BWRF1 indicated by dark red lines.

3.4.3 Stable intronic RNAs derived from BamW

Recently, stable RNAs derived from BamW introns have been reported as potentially functional based on their structure, stability and conservation (for details see section 1.8.3.4). EBV sisRNA-1 is generated by the 81 nucleotide intron between exon W1 and W2 in which we have point-mutated the BsmBI site. EBV sisRNA-2 is generated from the intron containing the BWRF1 ORF and large hairpin, although the nature of this RNA (i.e. whether it is further processed and what it contains) has not been well defined. Therefore both of these RNAs may potentially be altered in LP-KO ^{i} and LP-REV ^{i} (sisRNA-1 by the BsmBI mutation and sisRNA-2 by the use of the minor variants of BWRF1).

3.4.4 Issues with the current LP-KO ^{i}/ LP-REV ^{i} and B95-8 BAC viruses

The identification of the undesired mutations (or introduced mutations that may alter the expression of sisRNAs) left several possibilities as to why the LP-REV ^{i} (and perhaps by extension LP-KO ^{i}) may be more defective than expected. Any one (or a combination) of the 3 different mutations/changes in the long intron in BWRF1, the BsmBI mutation in the sisRNA-1 intron could cause the defect in LP-REV ^{i}. Alternatively, the lack of heterogeneity of the BamW repeat (e.g. lack of STOP codon in single W1) could be detrimental, as it is not known if B95.8 may benefit from combination of full length and truncated EBNA-LP, improving transformation efficiency. There is also a possibility of another (second site) mutation in the repeat array used to generate LP-REV ^{i}, or in the BACs outside the repeat array, although the latter seems unlikely as the same phenotype was observed for duplicate LP-KO ^{i} and LP-REV ^{i} viruses. Any of these mutations may cause the decreased efficiency of transformation by LP-REV ^{i} that we observed, and in combination with lack of EBNA-LP may be a reason for inability to transform B cells by LP-KO ^{i}.

3.4.5 Conclusion

Because we were not able to establish whether the observed phenotype of LP-KO ^{i} is due to purely the lack of EBNA-LP or if it is due to the combination of lack of EBNA-LP and the mutation(s) that also impair the revertant, we decided to generate new LP-KO EBV using a different strategy to avoid mutating the sisRNA-1 intron and using a “wild type” BamW repeat unit (the one that constitutes the majority of W repeats in B95.8).

4 RESULTS II: ANALYSIS OF THE SECOND GENERATION EBNA-LP MUTANT EBV

To troubleshoot the problems described in section 3.4.4, Dr. White generated two new repeat arrays, one using a completely wild-type W repeat unit, and the other containing the EBNA-LP knockout mutation shown in Figure 3.1 but lacking the intronic mutations.

The repeats were combined using Gibson assembly, a method that allows the assembly of multiple DNA fragments independent of fragment length. The method combines three different enzyme activities: exonuclease, DNA polymerase, and DNA ligase, which allows for joining multiple overlapping DNA fragments in a single isothermal reaction. Because of the nature of the Gibson assembly strategy, the mutation of the BsmBI restriction site was not needed to generate arrays of W repeats.

The new arrays of W repeats were used to generate EBV-BACs: WT ^{w} 1.1 (where "w" stands for "wild-type" W repeats: no W1 STOP codon; no intronic mutations; no heterogeneity in contrast to previously used B95.8 BAC, which will be still called WT EBV in this chapter) and two independent EBNA-LP KOs: LP-KO ^{w} 2.2 and LP-KO ^{w} 4.1 (where "w" again stands for the true wild-type W repeats: no intronic mutations, but the knockout mutation in LP-KO ^{w} is the same as in LP-KO ^{i}), were recombined into the previously generated W-KO BAC (which was used for generating LP-KO ^{i} 2.6) (Fig.4.1). The recombinant BAC DNAs were transfected into HEK 293 cells, EBV-producing cell lines were established and recombinant viruses produced as described in section 3.1.4.

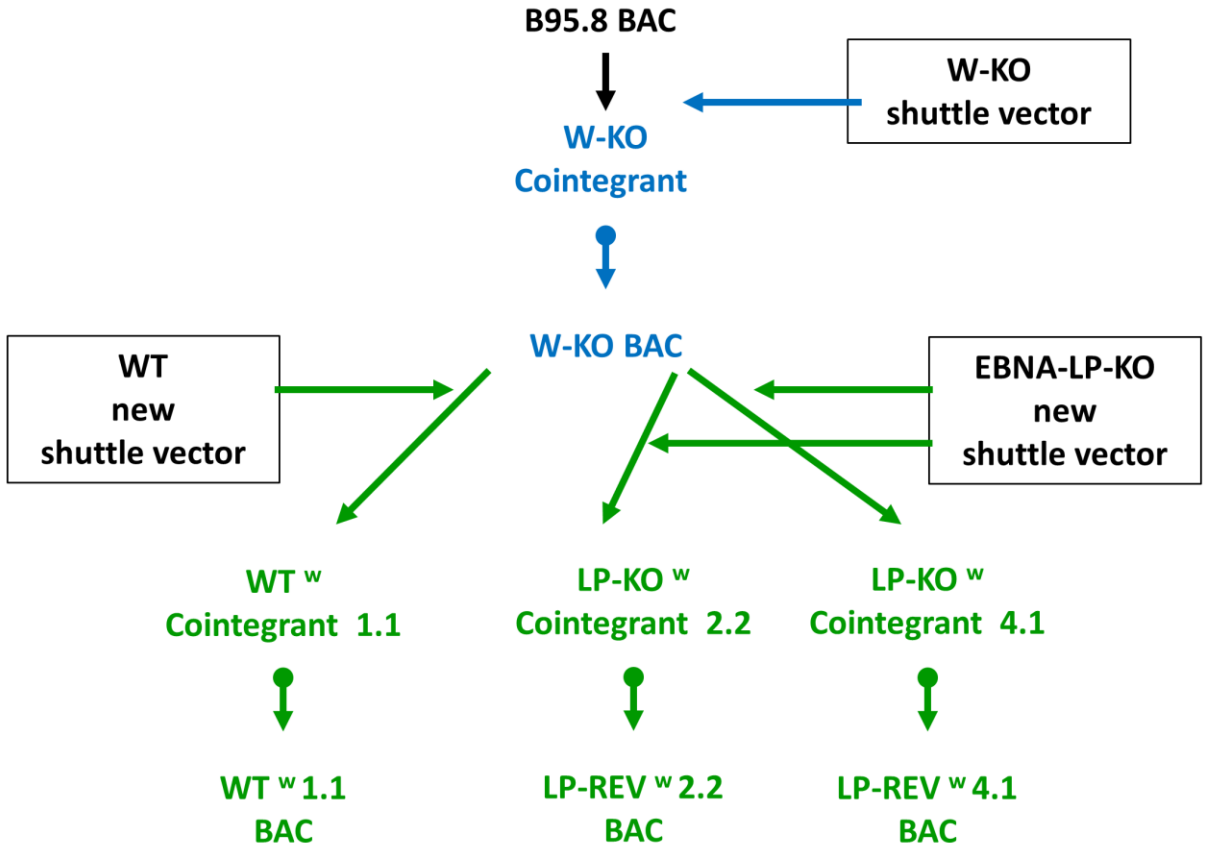

Fig. 4.1 Schematic of generation of new LP-KO ^{w} and WT ^{w} BACs. Shuttle vectors used in recombination in black rectangles. Recombination represented by regular arrows, cointegrants resolving step represented by arrows with round start. Previous recombination that was performed by Dr.White in blue, new recombination performed by Dr.White in green.

4.1 Primary B cells experiments

Because of time limitations we did not analyze the new recombinants in BL31 cells: the new viruses were titrated and used directly to infect primary B cells to address both whether these 'improved' EBNA-LP knockouts (i.e. more representative of wild-type EBVs and with no additional mutations in the W repeats) are able to transform B cells, and to compare the parental WT B95.8 BAC (which contains a STOP codon in one of its W1 exons) to the WT ^{w}, whose *EBNA-LP* is intact. The protocol for B cell infection was same as described in section 3.3.

4.1.1 EBNA-LP is not required for transformation of adult B cells

To assess if the previously observed phenotype of LP-KO ^{i} virus and its inability to establish LCLs is caused exclusively by its lack of EBNA-LP, primary B cells were infected with the complete panel of recombinant viruses (including new LP-KO ^{w} as a true EBNA-LP knockout (without additional mutations) and LP-KO ^{i} for comparison). The characteristics of outgrowth of LP-KO ^{w} 2.2 and LP-KO ^{w} 4.1 were very similar to WT EBV up to day 5 after infection: the cells became activated, aggregated together and the clusters started enlarging. Around day 5, when the WT/REV-infected clumps of cells are still getting bigger, the LP-KO ^{w}-infected cultures stop expanding and remain static until approximately 15 days post infection, when the expansion of the culture appears to begin again. From there they are able to establish LCLs (without feeder cells). This indicates that EBNA-LP is not essential for transformation of adult B cells. Overall, the experiment was repeated 4 times (2 independent LP-KO ^{w} in 5 different donors) with similar results (except in one donor, in which the culture was frequently sampled, involving regular disruption of the clusters of cells, where LP-KO ^{w} 4.1-infected cells died around day 15 post infection, while the second knockout (LP-KO ^{w} 2.2) was able to establish LCLs: see section 4.3). In contrast, cells infected with the new WT ^{w} 1.1 subjectively seemed to establish LCLs a little bit faster than the original WT and revertants. Cells infected with LP-KO ^{i} in these experiments were not able to establish LCLs as reported in the previous chapter.

To confirm that the LCLs established after infection with LP-KO ^{w} do not contain any EBNA-LP, protein was extracted from these cells and Western blotted using anti EBNA-LP antibodies JF186 (B95.8- type specific) and 4D3 (able to detect all known forms of EBNA-LP). LCLs obtained after infection with LP-KO ^{w}, do not express any EBNA-LP, confirming that LP-KO ^{w} alone is able to transform B cells into LCLs (Fig.4.2). Additionally, LCLs obtained after infection with WT ^{w} 1.1 tend to express both more EBNA-LP protein and

longer isoforms than previous WT EBV (Fig.4.2 and 4.5). Similarly, longer and more abundant forms of EBNA-LP were also often observed in spontaneous LCLs and LP-REV [i] LCLs (see Fig. 3.20a and Fig. 4.5), which suggests that the STOP codon present in one of the W repeat in B95.8 may reduce both the expression levels and size of EBNA-LP isoforms.

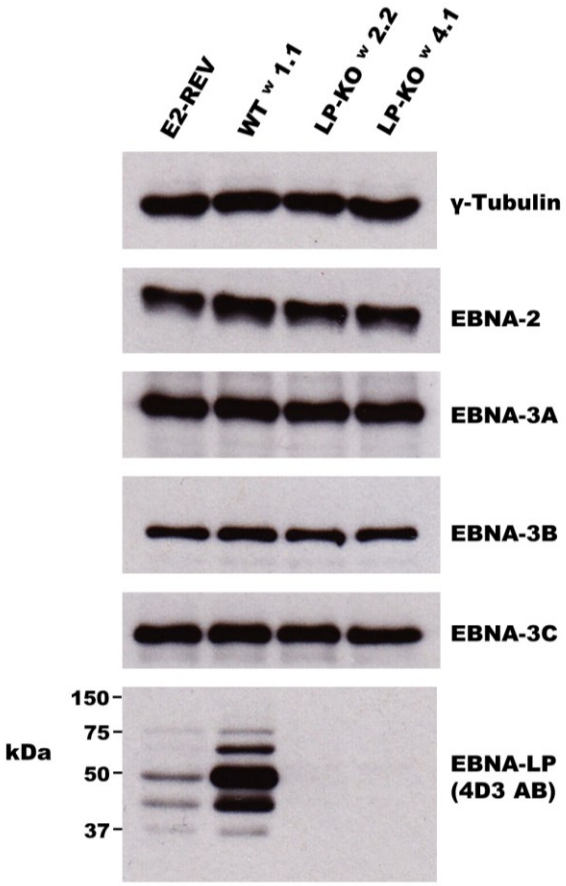

Fig. 4.2 Western blot analysis of protein extracted from LCL obtained after infection of one of donors' B cells with E2-REV, WT [w] and LP-KO [w]. Proteins extracted from LCLs were separated by SDS–PAGE (12% gel for EBNA-LP and 7.5% gels for other proteins) followed by Western blotting with antibodies against EBV latent proteins. 4D3 antibody was used to detect any known form of EBNA-LP. γ-tubulin was used as a loading control.

4.1.2 EBNA-LP is required to transform cord blood B cells

In contrast to adult B cell infection, when the outgrowth experiment was performed by infecting PBLs isolated from cord blood, we were not able to produce LCLs after infection

with either LP-KO ^{w} or Y1Y2-KO, even when cultured on irradiated MRC5 feeder cells. In contrast, positive controls like WTs, Y1Y2-REV and even the defective LP-REV ^{i} EBV were able to transform cord blood PBLs into LCLs in every experiment. Cord blood PBLs infected with WT ^{w} 1.1 were able to establish LCLs consistently faster than WT EBV. The cord blood infections were repeated 3 times (using 2 independent LP-KO ^{w} and Y1Y2-KO EBVs in 4 different donors). All of these results suggest that the presence of full length EBNA-LP is essential for transformation of cord blood B cells.

4.1.3 EBNA-LP improves B cell proliferation early after infection

To compare the proliferation of LP-KO ^{w}-infected B cells with other recombinant viruses, a proliferation assay based on CellTrace Violet signal dilution measured by flow cytometry was performed at different time points after infection (Fig.4.3). As in the previous experiments (section 3.3.4), B cells infected with different recombinant viruses (except E2-KO) start proliferating between day 3 and 5. The number of divided cells after LP-KO ^{w} infection is lower when compared to WT but clearly higher than in LP-KO ^{i} infection (Fig.4.3). In contrast, proliferation induced by WT ^{w} 1.1 is a little bit faster than of WT in this experiment (Fig.4.3), although I have not had time to confirm whether this difference is consistently observed. The proliferation experiment was repeated twice with LP-KO ^{w} and WT (in 3 different donors).

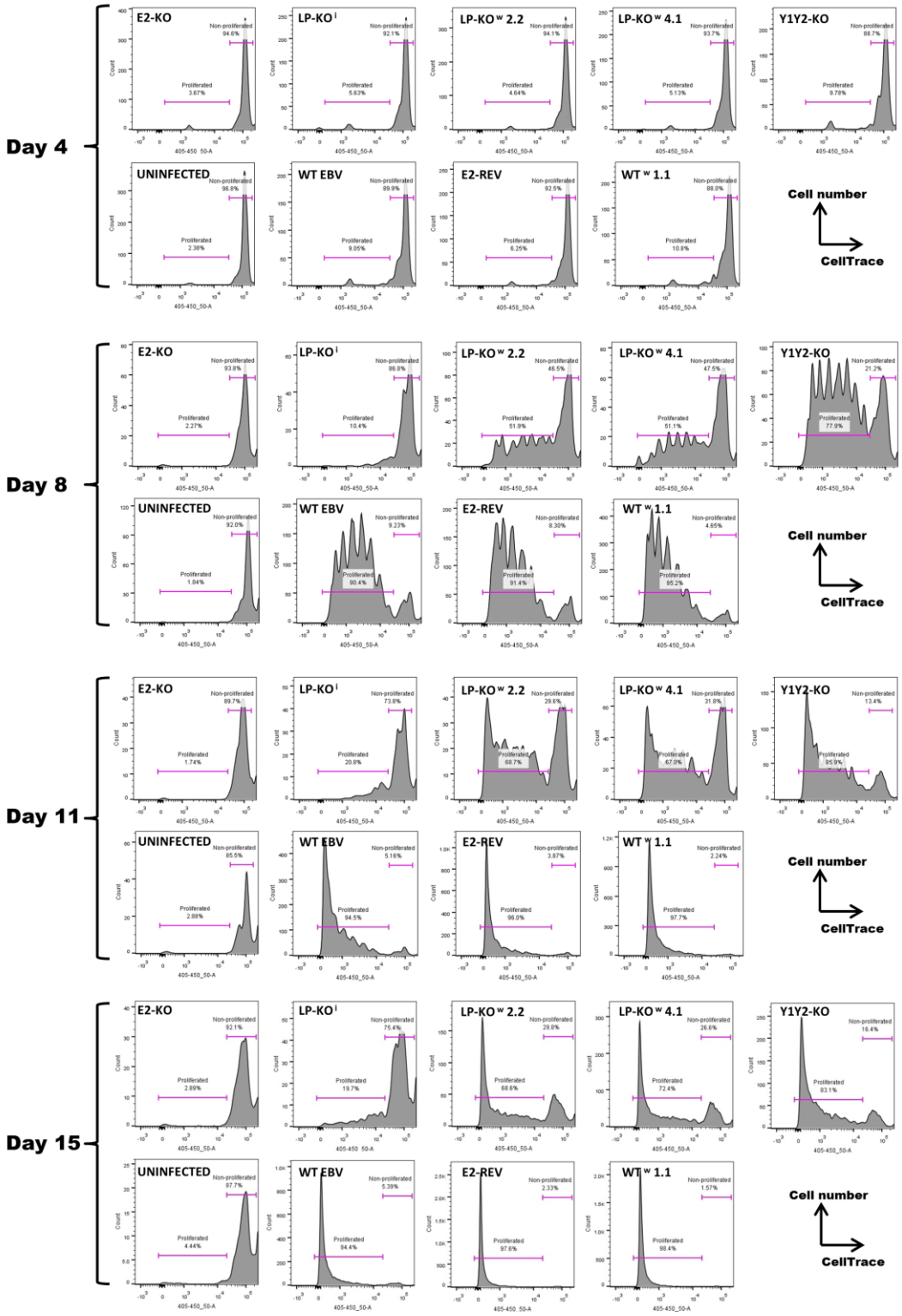

Fig. 4.3 Representative results of proliferation of primary B cells infected with whole panel of EBV mutants using CellTrace Violet. Primary B cells were stained with CellTrace Violet just before infection with different EBV recombinants. Cells were additionally stained with live/dead dye after harvesting on days 4, 8, 11 and 15 post-infection and analyzed by flow cytometry. Histograms show the fluorescence from CellTrace after gating out debris, cell doublets and dead cells. The x-axis shows CellTrace fluorescence, while the y-axis indicates the accumulated number of cells counted. The lower a cell's fluorescence, the more cell divisions it has undergone.

4.1.4 Expression of CD38 on infected B cells

It was previously reported that Y1Y2-KO-infected B cells have increased cytoplasmic immunoglobulin expression (Mannick et al., 1991), suggesting that they may differentiate into plasma cells. To assess whether this is the case and reason for slower proliferation, infected cells were going to be tested for CD38 expression (a plasma cell markers). CD38 antigen is not plasma cell specific as it is expressed by a variety of other cells (i.e. T cells, monocytes, early B cells), however, a very bright signal coming from its higher expression on plasma cells in comparison to other cells, makes it a reasonably specific marker for identification of plasma cells using flow cytometry (Kumar et al., 2010). However, microarray data (White et al., 2010) show that CD38 is also highly transcribed by EBV transformed LCLs. To assess whether CD38 could be used as a marker of early infection, staining for CD38 and flow cytometry was performed. As can be seen from Figure 4.4a, CD38 shows similar expression kinetics to CD23 and CD58, which we assessed previously as candidate activation markers (see section 3.3.3). By analyzing the cells that have already proliferated (Fig.4.4b), it is apparent that by day 11, most of the proliferated EBV-infected cells express CD38 (ranging from 73% for LP-KO ^{i}-infected to 97% for WT-infected).

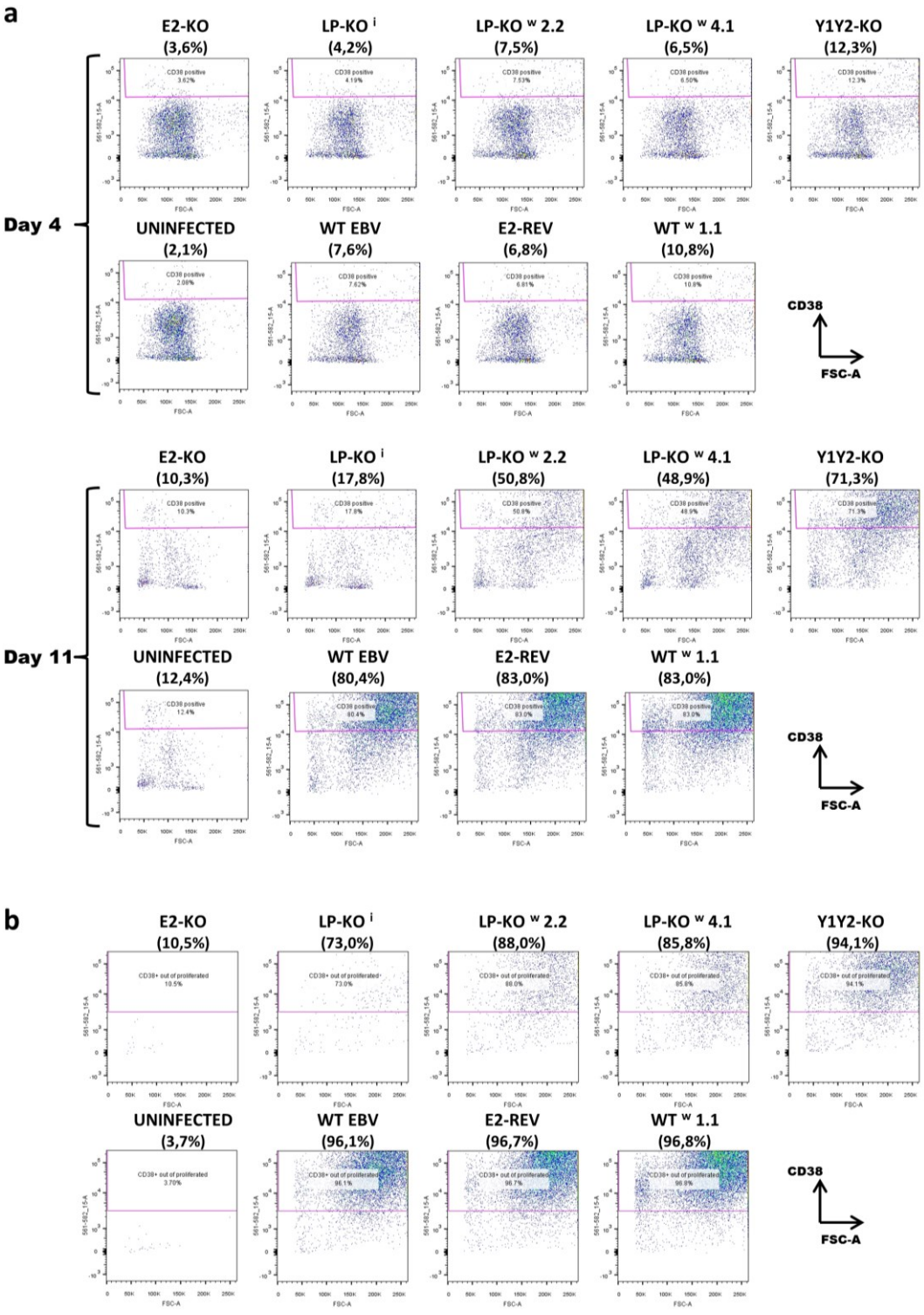

Fig. 4.4 Expression of CD38 marker on B cells infected by different EBV recombinants. Primary B cells were infected with different EBV recombinants and stained with live/dead dye and antibody for the extracellular marker CD38 at day: 4 and 11 post infection. After staining the cells were analyzed using flow cytometry. **a.** Dot plots show population of cell after gating out debris, cell doublets and dead cells. **b.** Dot plots show only the cells that divided at least once by day 11 (based on dilution of the CellTrace Violet signal). The x-axis shows forward scatter, while the y-axis shows CD38 signal. Percentages of CD38 positive cells in pink gates are indicated under the name of each mutant.

4.1.5 Reduced levels of truncated EBNA-LP are not caused by proteosomal degradation

Since the levels of the truncated EBNA-LP are very low in Y1Y2-KO cells (Fig.3.12) and the previously used WT, E2-REV and Y1Y2-REV (all containing the STOP codon in one of their W1 exons) do not express longer forms of EBNA-LP when compared to WT ^{w} and spontaneous LCLs (Fig.4.2 and 3.20a), we speculated that truncated EBNA-LP may be degraded. Therefore, we tested whether these truncated forms are actively targeted to proteasome by treatment of LCLs (established by infection with different recombinant viruses) with a proteasome inhibitor (MG-132).

There is no significant difference in EBNA-LP protein levels between MG-132- and DMSO-treated LCLs (Fig.4.5), therefore these truncated EBNA-LP forms do not seem to be sent for degradation by the proteasome. MG132-treated LCLs were also assessed using immunostaining for EBNA-LP and Sp100, and visualization by confocal microscopy but again no difference in the levels or localization of these proteins was observed between MG-132- and DMSO-treated cell lines (not shown).

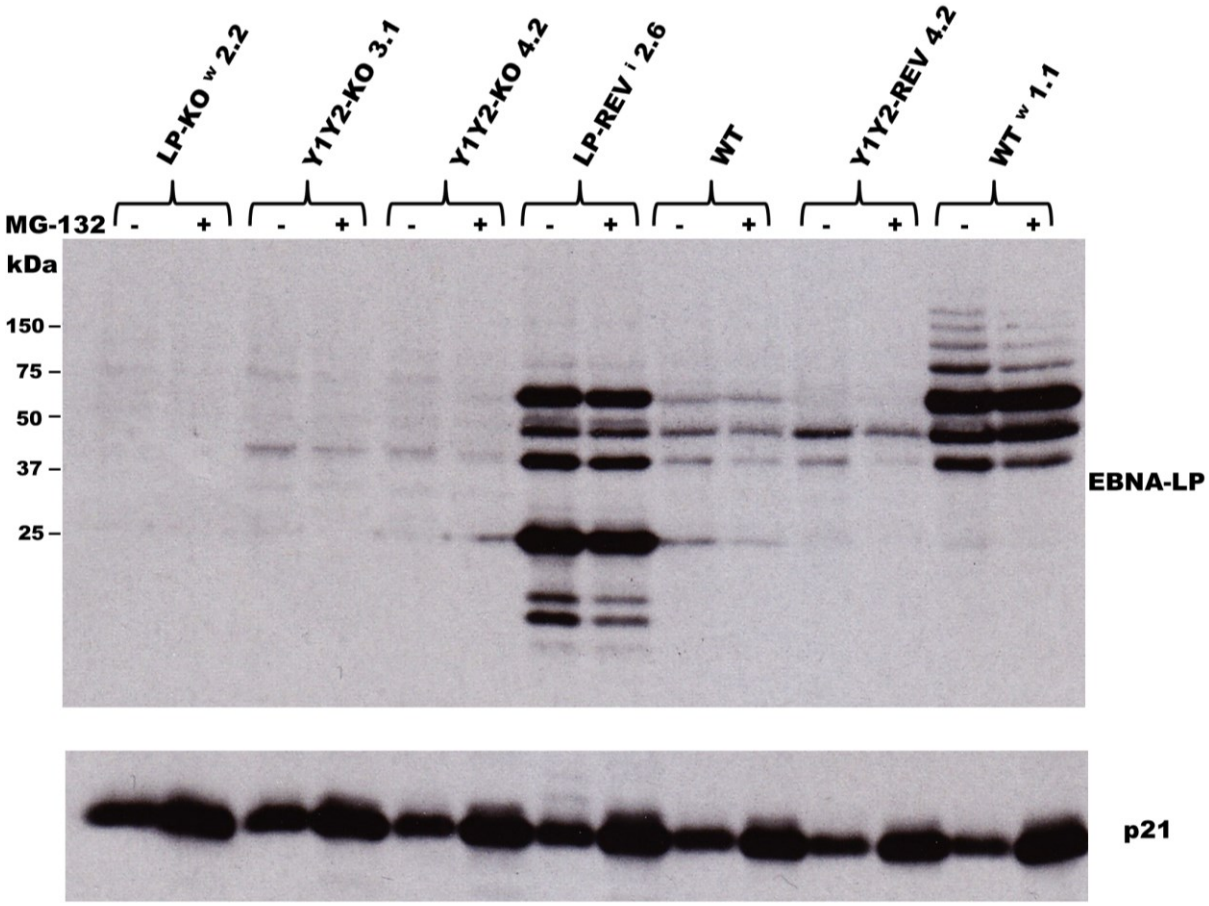

Fig. 4.5 Western blot analysis of protein extracted from LCLs obtained after infection with different recombinant EBVs with (+) or without (-) treatment with MG-132. LCLs were treated with either MG-132 or DMSO (as a carrier control) for 8h. After that time proteins were extracted from LCLs and separated by SDS–PAGE in a 12% gel followed by Western blotting and detection with antibodies against EBNA-LP or p21 (as a positive control for protein accumulation after MG-132 treatment).

4.2 Fluorescence microscopy investigations into EBNA-LP functions

In order to further investigate the functions of EBNA-LP in primary B cell infections, we analysed the abundance and localisation of EBV antigens and host proteins potentially targeted by EBNA-LP using immunofluorescence confocal microscopy. We mostly focused on EBNA-LP's best characterised interaction partner, Sp100.

4.2.1 Pattern of EBNA-LP expression early after infection with EBV recombinants

To assess the levels and localization of EBV nuclear antigens early after infection, primary B cells were infected with a panel of EBV recombinants, and at 48 hours (Fig.4.6) and 7 days (Fig.4.7) after infection, cells were fixed, permeabilized and stained with antibodies against EBNA-2 (rat) and EBNA-LP (mouse).

As expected, all infected cells (as defined by EBNA-2 positivity) also express EBNA-LP (except the LP-KO-infected) and all cells that are positive for EBNA-LP also express EBNA-2 (except the E2-KO-infected). As previously reported for wild type EBV (Ling et al., 2005), EBNA-LP is abundant and homogenous within the nucleus at day 2 (Fig.4.6) and localizes to foci in the nucleus by day 7 (white arrows in Figure 4.7). The two exceptions are E2-KO-infected cells at day 7, whose expression of EBNA-LP is very high in the whole nucleus (Fig.4.7), and the truncated EBNA-LP in Y1Y2-KO-infected cells, which is expressed at a very low level and only within the nucleolus at both day 2 and day 7 after infection (yellow arrows in Figure 4.6 and 4.7). This low abundance of EBNA-LP by Y1Y2-KO is consistent with our Western blot data showing very low EBNA-LP levels in Y1Y2-KO-infected BL31 cells and LCLs (Fig.3.12 and 4.5).

Imaging was complicated by an abundant non-specific signal in the EBNA-LP staining observed as foci outside the cells (purple arrows in Figure 4.6 and 4.7). This phenomenon was noticed in all stained samples (including the uninfected control), but was much worse (more and brighter signals) around infected cells 2 days after infection (which can also be seen from Figure 4.6 and 4.7) and slowly decreased in quantity with time after infection. We therefore tested the secondary antibodies alone, eventually trying six different anti-mouse fluorescent antibodies conjugated with different fluorophores and coming from different companies, 2 different anti-rat and 4 different anti-rabbit (see table 2.5). All of the anti-mouse

secondary antibodies tested, but none of the anti-rat or anti-rabbit secondaries, bound to these foci outside the cells (not shown). We have tried different blocking protocols and different sera but we were not able to eliminate this non-specific binding from our stainings.

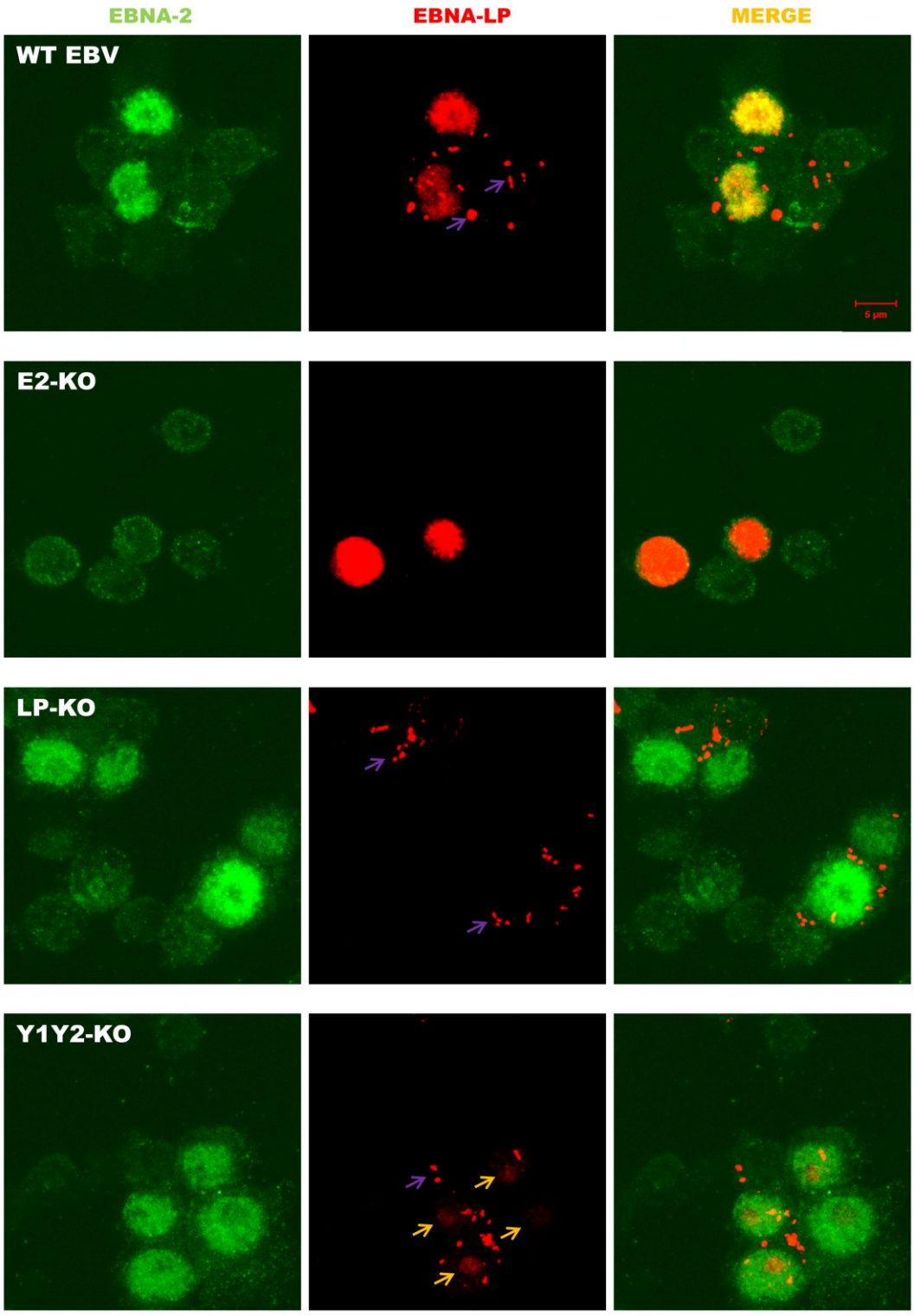

Fig. 4.6 Representative immunofluorescence staining of primary B cells 48h after infection with different EBV recombinants. Cells were fixed with 4% PFA and permeabilized with either Triton X-100 or acetone and stained 48h after infection with the viruses indicated. Images were taken using 63x objective, 4 x software zoom and a projection of z-stack of 1µm sections. EBNA-2 staining uses the rat R3 antibody (green), EBNA-LP staining uses the mouse JF186 antibody (red). The red bar on the merged WT infection picture corresponds to 5 µm. Yellow arrows indicate nucleolar localization. Purple arrows indicate signals due to non-specific binding of secondary anti-mouse antibodies.

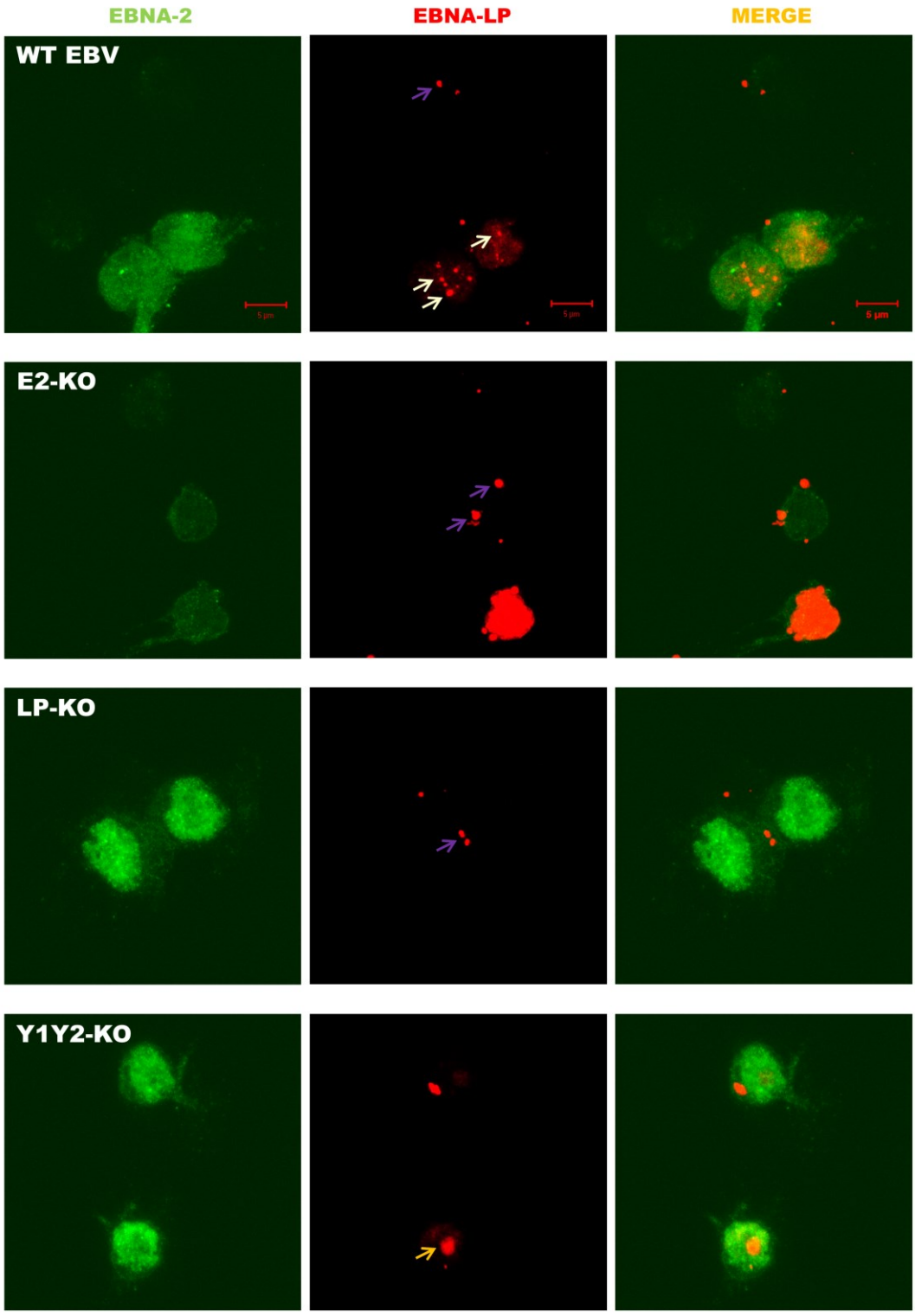

Fig. 4.7 Representative immunofluorescence staining of primary B cells 7 days after infection with different EBV recombinants. Cells were fixed with 4% PFA and permeabilized with either Triton X-100 or acetone and stained 7 days after infection with the viruses indicated. Images were taken using 63x objective, 4 x software zoom and a projection of z-stacks of 1µm sections. EBNA-2 staining uses the rat R3 antibody (green), EBNA-LP staining uses the mouse JF186 antibody (red). The red bar on the merged WT infection picture corresponds to 5 µm. White arrows indicate localization to foci in the nucleus. Yellow arrows indicate nucleolar localization. Purple arrows indicate signals due to non-specific binding of secondary anti-mouse antibodies.

4.2.2 EBV infection does not displace Sp100 from PML NBs

Previous experiments using transient transfection of EBNA-LP into Hep-2 cells suggests that EBNA-LP interacts with Sp100 and displaces it from PML NBs (Ling et al., 2005) and that Sp100 is displaced from PML 48h after EBV infection in primary B cells (Ling et al., 2005) but by 120 hours after infection (and in established LCLs), both EBNA-LP and Sp100 co-localize in PML NBs (Ling et al., 2005). Based on this, we hypothesized that an EBNA-LP knockout virus would fail to displace Sp100 from PML NB.

To test this hypothesis, primary B cells were infected with the panel of EBV recombinants, and analyzed by immunofluorescence microscopy at 48h and 7 days after infection. Cells were stained with antibodies against EBNA-2 (rat) to identify infected cells, EBNA-LP (mouse) and Sp100 (rabbit). The polyclonal antibody initially used to detect Sp100 was a kind gift from Prof. Paul Ling (that we have successfully used to detect Sp100 by Western blotting; not shown).

In contrast to the previously published data, no displacement of Sp100 (using this antibody) was observed 2 days after infection for any of the viruses used, including the wild type B95.8 BAC. Also contrasting with previous observations, the expression of Sp100 was higher in infected than uninfected cells, in which Sp100 was barely detectable (Fig.4.8). Additionally, the signal from this Sp100 antibody also co-localized in most cases with the non-specific staining in the EBNA-LP channel that was attributable to the anti-mouse secondary antibody (Fig.4.8). The experiment using this particular Sp100 antibody was repeated for 5 different donors with consistent results.

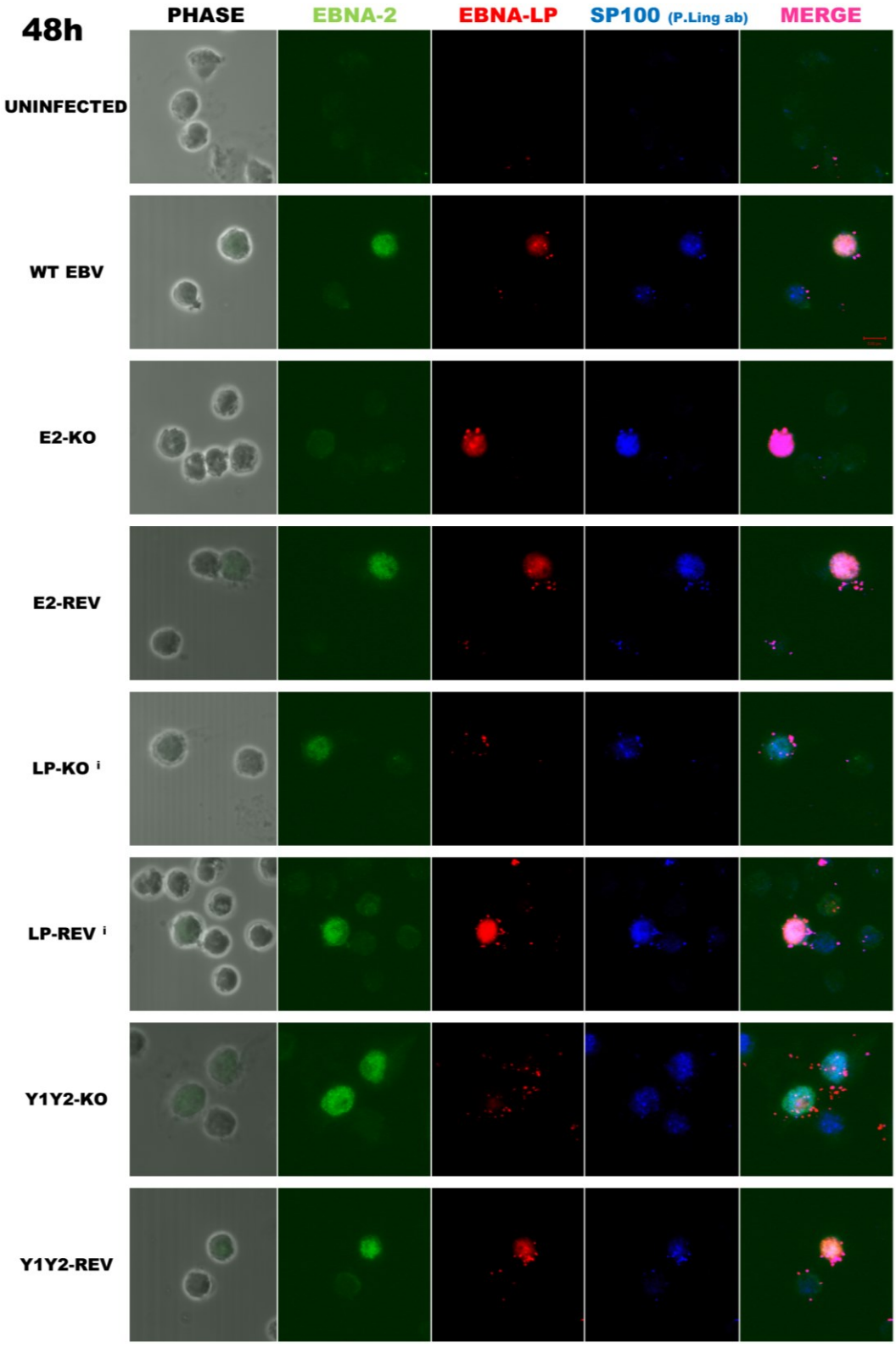

Fig. 4.8 Sp100 staining using the anti-Sp100 antibody obtained from P. Ling and the Triton X-100 permeabilization on primary B cells 48h after infection. Cells were fixed with 4% PFA, permeabilized with Triton X-100 and stained 48h after infection with the viruses indicated. Images were taken using 63x objective, 4 x software zoom and a projection of z-stacks of 1µm sections. EBNA-2 staining uses the rat R3 antibody (green), EBNA-LP staining uses the mouse JF186 antibody (red), Sp100 uses polyclonal rabbit antibody obtained from Paul Ling (blue). The red bar in the WT-infected merged picture corresponds to 5 µm.

Because the staining using Paul Ling's antibody did not show the expected pattern of Sp100 (defined dots/foci in the nucleus), we acquired SpGH, a more widely used and tested polyclonal rabbit anti-Sp100 antibody (kind gift from Prof. Roger Everett). The staining using SpGH antibody is much clearer (Fig.4.9) than the antibody obtained from Prof. Ling. It shows strong nuclear foci without the co-localization with the non-specific extranuclear staining. However, we again did not observe any displacement of Sp100 two days after infection with any strain of EBV (Fig.4.9). By seven days after infection, EBNA-LP co-localizes with Sp100 (as previously published) in most of the mutants, except LP-KO (no EBNA-LP and no change in Sp100 distribution), Y1Y2-KO (where the truncated EBNA-LP again localized in the nucleoli) and E2-KO (which exhibits very high homogenous expression of EBNA-LP) (Fig.4.10). The SpGH antibody was used to test Sp100 localization after infection of 3 different donors with similar results.

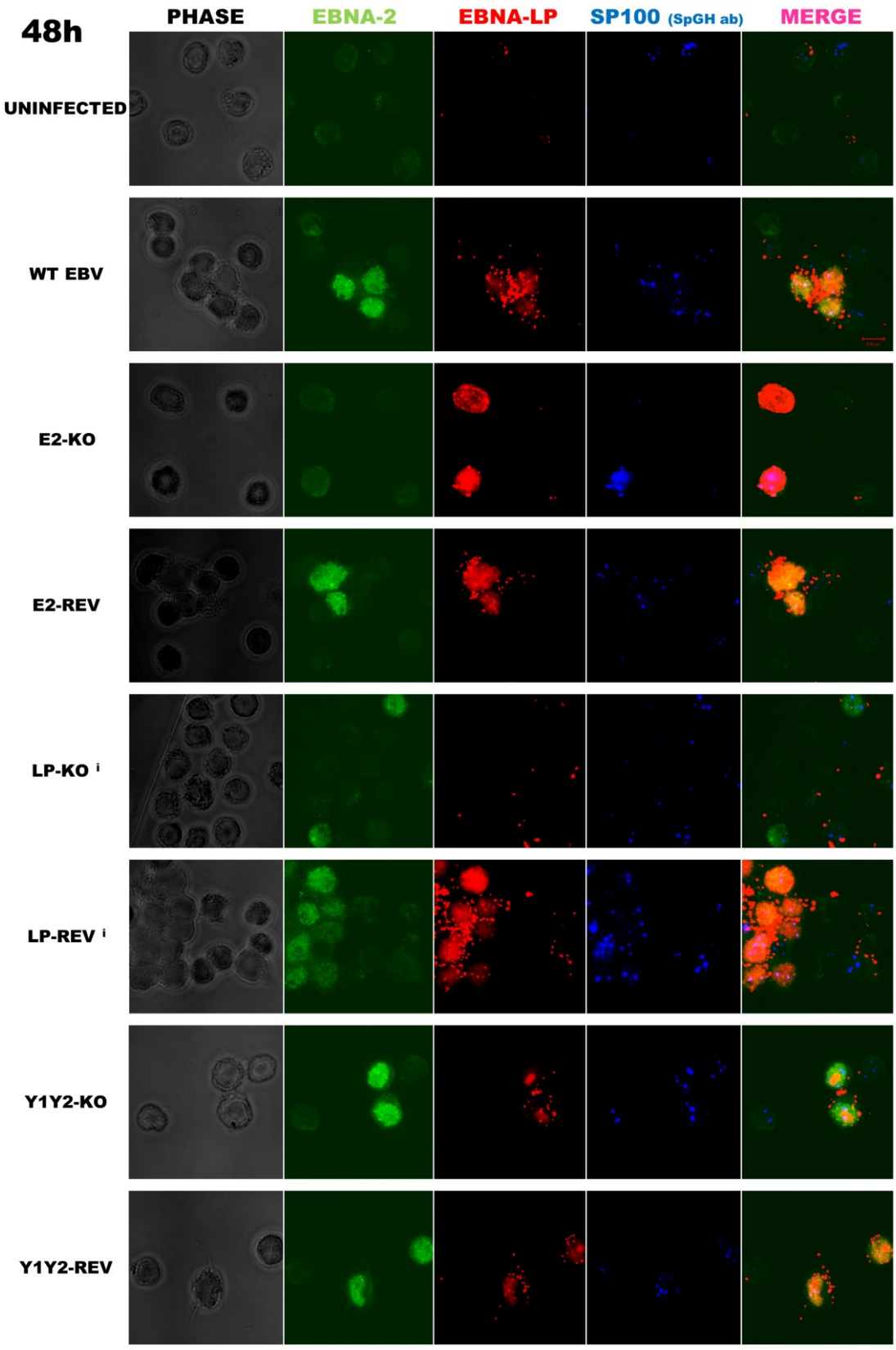

Fig. 4.9 Sp100 staining using the anti-Sp100 (SpGH) antibody and the Triton X-100 permeabilization on primary B cells 48h after infection. Cells were fixed with 4% PFA, permeabilized with Triton X-100 and stained 48h after infection with the viruses indicated. Images were taken as described in Figure 4.8. EBNA-2 staining uses the rat R3 antibody (green), EBNA-LP staining uses the mouse JF186 antibody (red), Sp100 uses the polyclonal rabbit SpGH antibody (blue). The red bar in the WT-infected merged picture corresponds to 5µm.

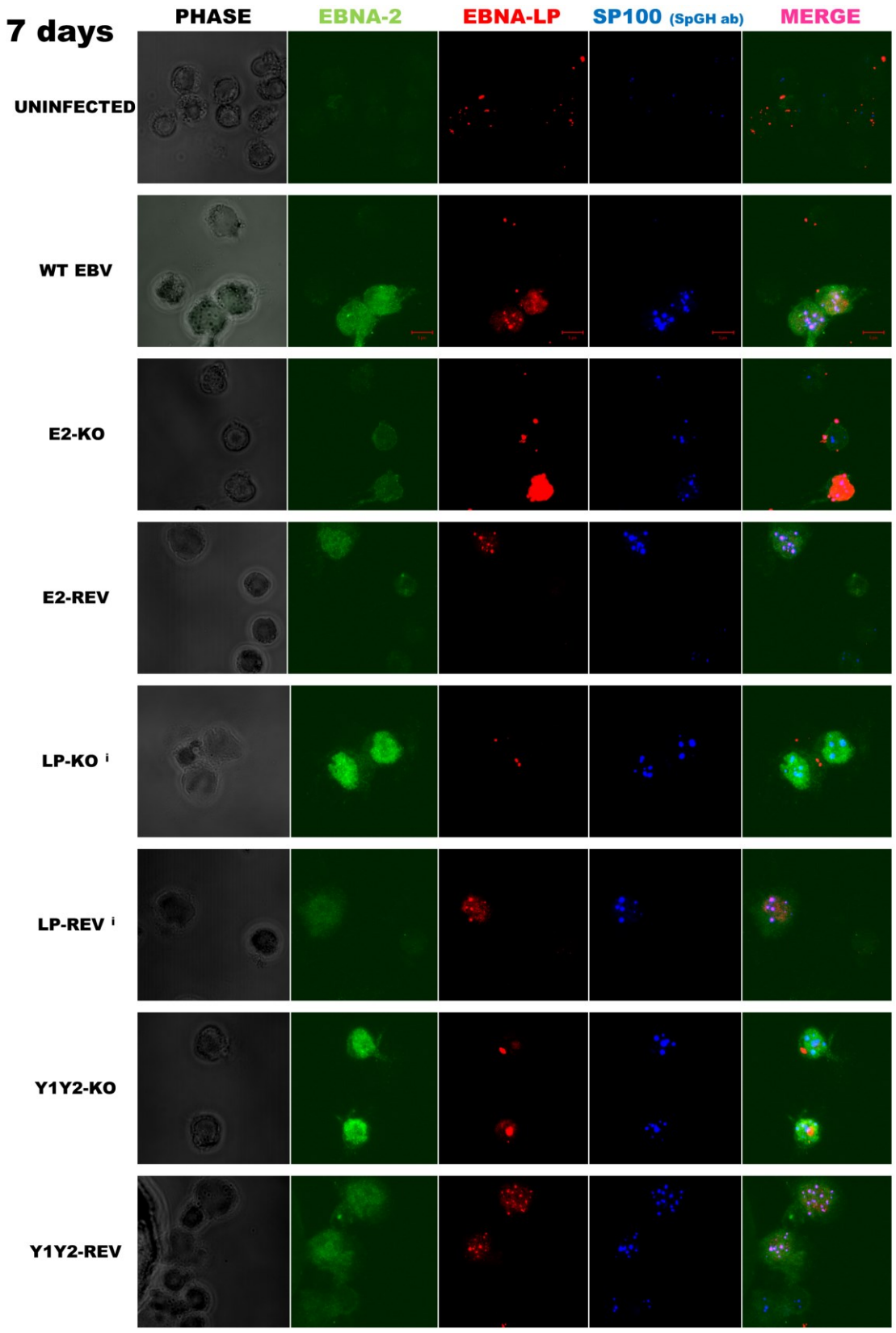

Fig. 4.10 Sp100 staining using the anti-Sp100 (SpGH) antibody and the Triton X-100 permeabilization on primary B cells 7 days after infection. Cells were fixed with 4% PFA, permeabilized with Triton X-100 and stained 48h after infection with the viruses indicated. Images were taken as described in Figure 4.8. EBNA-2 staining uses the rat R3 antibody (green), EBNA-LP staining uses the mouse JF186 antibody (red), Sp100 uses the polyclonal rabbit SpGH antibody (blue). The red bar in the WT-infected merged picture corresponds to 5µm.

To assess whether this lack of Sp100 displacement is a defect of our recombinant EBV strain, we also assessed the ability of the parental B95.8 strain (produced from the B95.8-ZHT cell line (Johannsen et al., 2004)) and M81 EBV (Tsai et al., 2013) to displace Sp100. The M81 strain was used because it has been reported that M81 (in contrast to B95.8) is capable of spontaneous lytic replication in infected cells, which includes robust expression of BZLF1 (Tsai et al., 2013). BZLF1 in turn, has been reported to disrupt PML-NBs (Adamson and Kenney, 2001). However, there was no visible displacement of Sp100 or any difference in Sp100 distribution pattern between these strains and previous experiments (Fig.4.11).

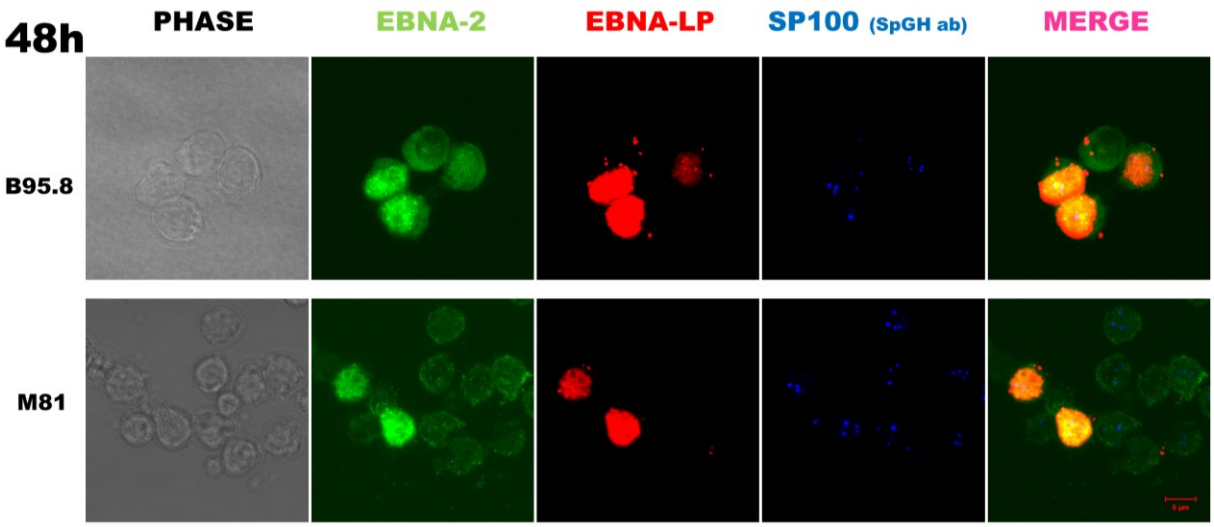

Fig. 4.11 Sp100 staining using the anti-Sp100 (SpGH) antibody and the Triton X-100 permeabilization on primary B cells 48h after infection with alternative EBV strains. Cells were infected with parental B95.8 (produced from B95.8 ZHT cell line) and strain M81 EBVs, and after 48 hours, cells were fixed with 4% PFA, permeabilized with Triton X-100 and stained for EBNA-2 uses the rat R3 antibody (green), for EBNA-LP uses the mouse 4D3 antibody (red) and for Sp100 uses the rabbit SpGH antibody (blue). Images were taken using 63x objective, 4 x software zoom and a projection of z-stacks of 1µm sections. The red bar in the M81-infected merged picture corresponds to 5 µm.

To further investigate whether the lack of Sp100 displacement in our infection is caused by our gentler permeabilization method (we used Triton-X100, while Ling et al., (2005), used acetone), we repeated their protocol which used 4% PFA fixation followed by acetone permeabilization at 48 hours after infection. Again, we did not observe any Sp100 displacement (Fig.4.12). With this fixation, the Sp100 foci seemed to be subjectively a little bit bigger in LP-KO and Y1Y2-KO infections than in WT/REV-infected cells (Fig.4.12), but this needs a more comprehensive computational analysis to assess properly. There is no obvious difference in Sp100 pattern between LP-KO ^{i}- and LP-KO ^{w}- or between WT- and WT ^{w}-infected cells (Fig.4.12).

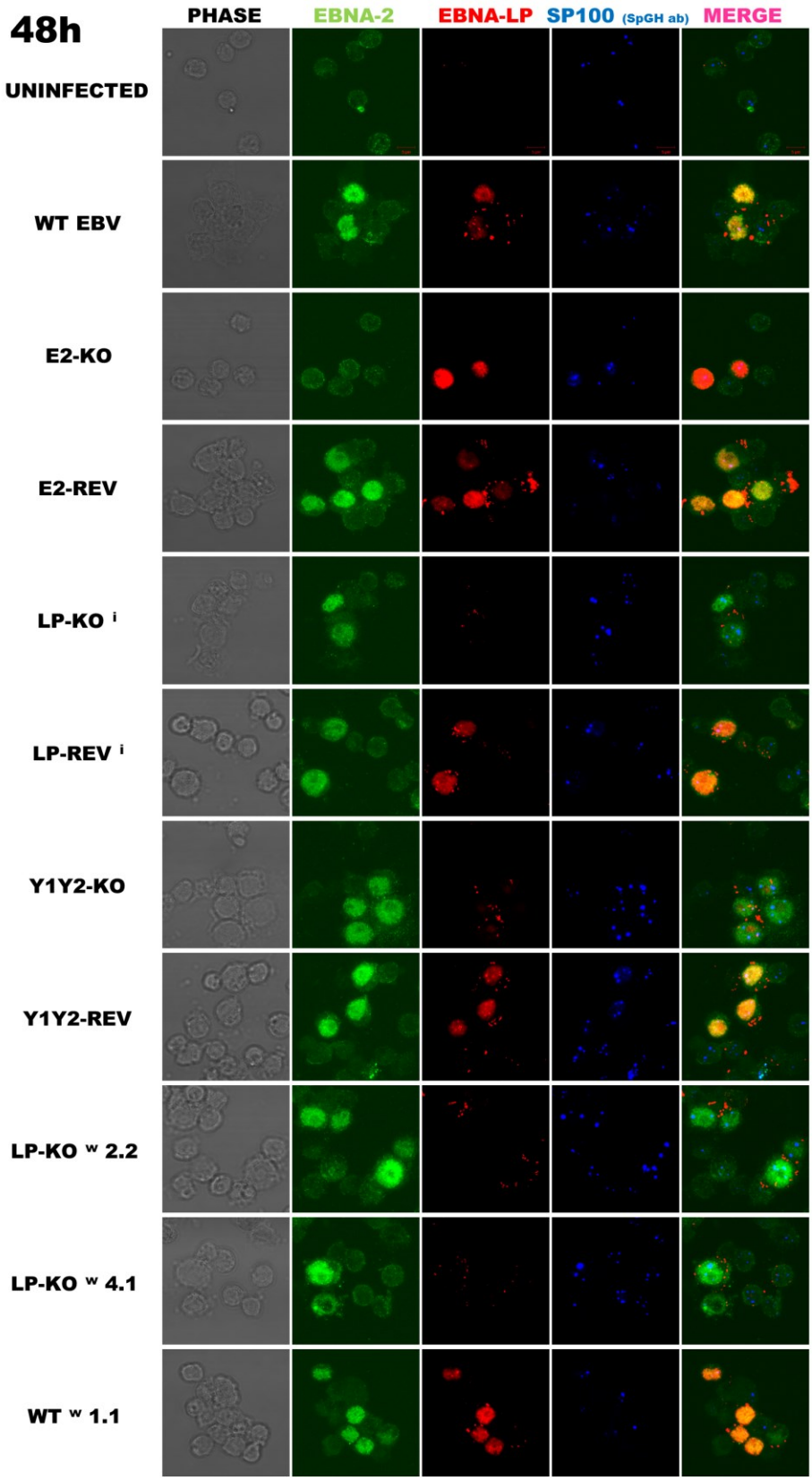

Fig. 4.12 Sp100 staining using the anti-Sp100 (SpGH) antibody and the Acetone permeabilization on primary B cells 48h after infection. Cells were fixed with 4% PFA, permeabilized with acetone and stained 48h after infection with the viruses indicated. Images were taken as described in Figure 4.8. EBNA-2 staining uses the rat R3 antibody (green), EBNA-LP staining uses the mouse JF186 antibody (red), Sp100 uses the polyclonal rabbit SpGH antibody (blue). The red bar in the uninfected pictures corresponds to 5 µm.

4.2.3 The PML staining pattern in primary B cells is similar to Sp100 pattern and does not change after infection with different EBV mutants

Previous research reported that while there was a displacement of Sp100, there was no change in PML pattern after 48h of infection with EBV (Ling et al., 2005). Because we were not able to confirm the Sp100 displacement using the SpGH anti-Sp100 antibody, we wanted to see what happens to PML after EBV infection in our experimental set up, to assess whether there is a size change of PML foci after LP-KO/Y1Y2-KO infection (which appeared to be the case for Sp100 when the cells were permeabilized with acetone (Fig.4.12). Unfortunately, we were not able to combine Sp100 and PML staining, to see if these two proteins are co-localized after EBV infection, because both of the primary antibodies (against Sp100 and PML) are rabbit polyclonal.

The pattern of PML staining in uninfected B cells is very similar to the Sp100 pattern (Fig.4.13); however there are a few more PML foci than Sp100 foci on average per cell and these PML dots are detectable in almost all uninfected B cells in comparison to Sp100 dots which are not detectable in all uninfected cells (Fig.4.12 and 4.13). As for Sp100, there was no change in PML staining pattern 48h after infection with EBV (Fig.4.13). There is also no noticeable difference between different EBV recombinants used and no apparent increase in the size of PML foci was observed after infection with LP-KO/Y1Y2-KO and PFA/acetone fixation/permeabilization (Fig.4.13).

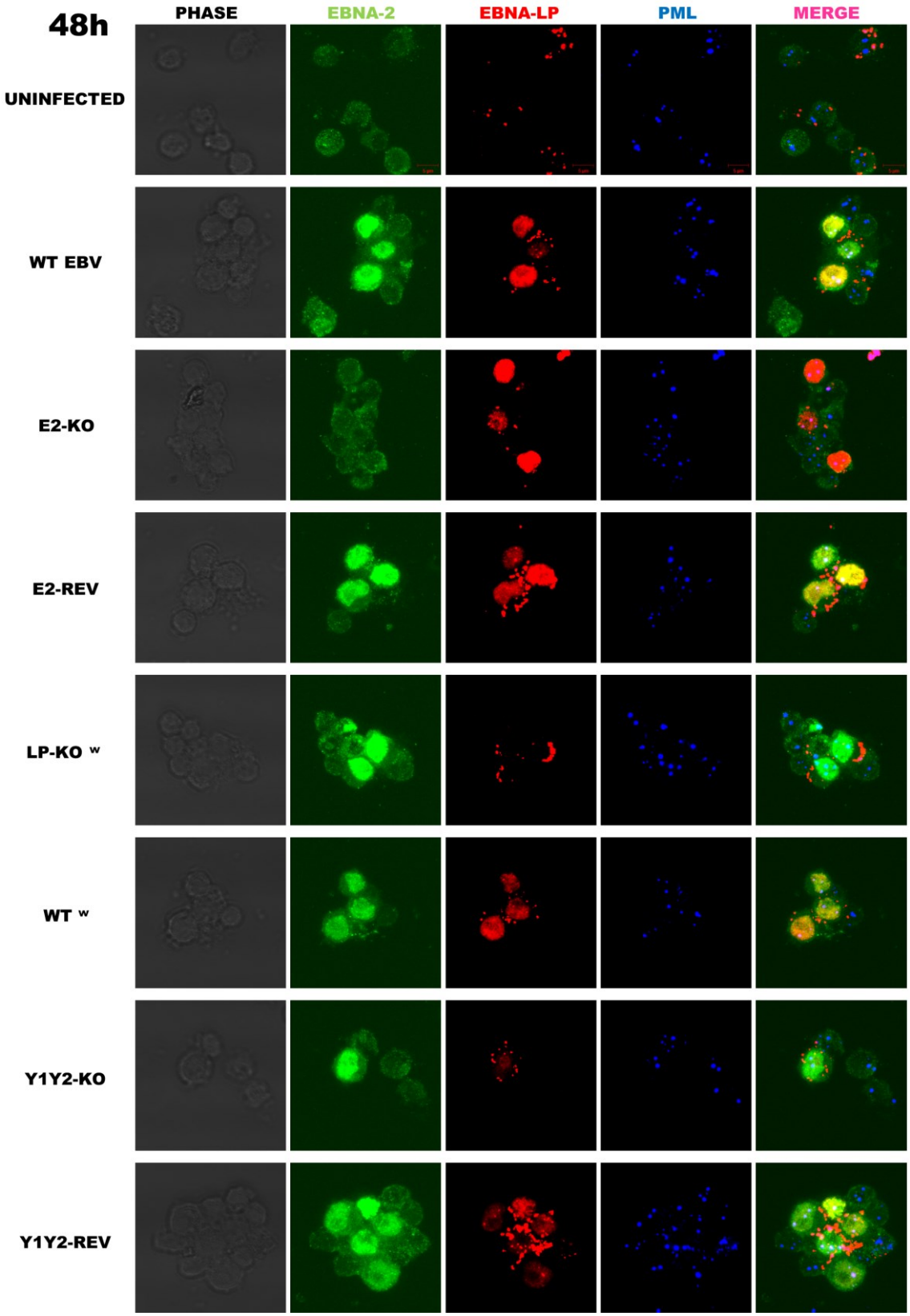

Fig. 4.13 PML staining using the Acetone permeabilization on primary B cells 48h after infection. Cells were fixed with 4% PFA, permeabilized with acetone and stained 48h after infection with the viruses indicated. Images were taken as described in Figure 4.8. EBNA-2 staining uses the rat R3 antibody (green), EBNA-LP staining uses the mouse JF186 antibody (red), PML staining uses rabbit pABah antibody (blue). The red bar in the uninfected pictures corresponds to 5 µm.

4.2.4 EBNA-LP does not play a role in the nuclear export of IFI16

The innate immune responses recognize pathogen-associated molecular patterns (PAMPs), which among others leads to inflammasome induction by interferon inducible protein 16 (IFI16). The KSHV genome has been shown to interact with IFI16, resulting in the nuclear export of IFI16 (Kerur et al., 2011, Singh et al., 2013). It has also been proposed that IFI16 can recognize EBV latent genome and in response, re-localizes from the nucleus to the cytoplasm 48h after infection (Ansari et al., 2013).

Because EBNA-LP is one of the earliest proteins expressed after infection, we hypothesized that it could potentially be responsible for targeting IFI16 and displacing it from the nucleus to the cytoplasm. To test the hypothesis, immunofluorescent staining using antibodies against EBNA-2, EBNA-LP and IFI16 was performed on B cells infected with different EBV recombinants and fixed on days 2 and 6 after infection. As can be seen from Figure 4.14, there is an elevated expression of IFI16 in the nuclei of infected cells for all viruses tested 48h after infection. However, there was no visible redistribution of IFI16 from the nucleus to the cytoplasm after infection with any of the recombinant viruses either 2 days (Fig.4.14) or 6 days (not shown) after infection (note that the EBNA-LP staining in Figure 4.14 is in blue).

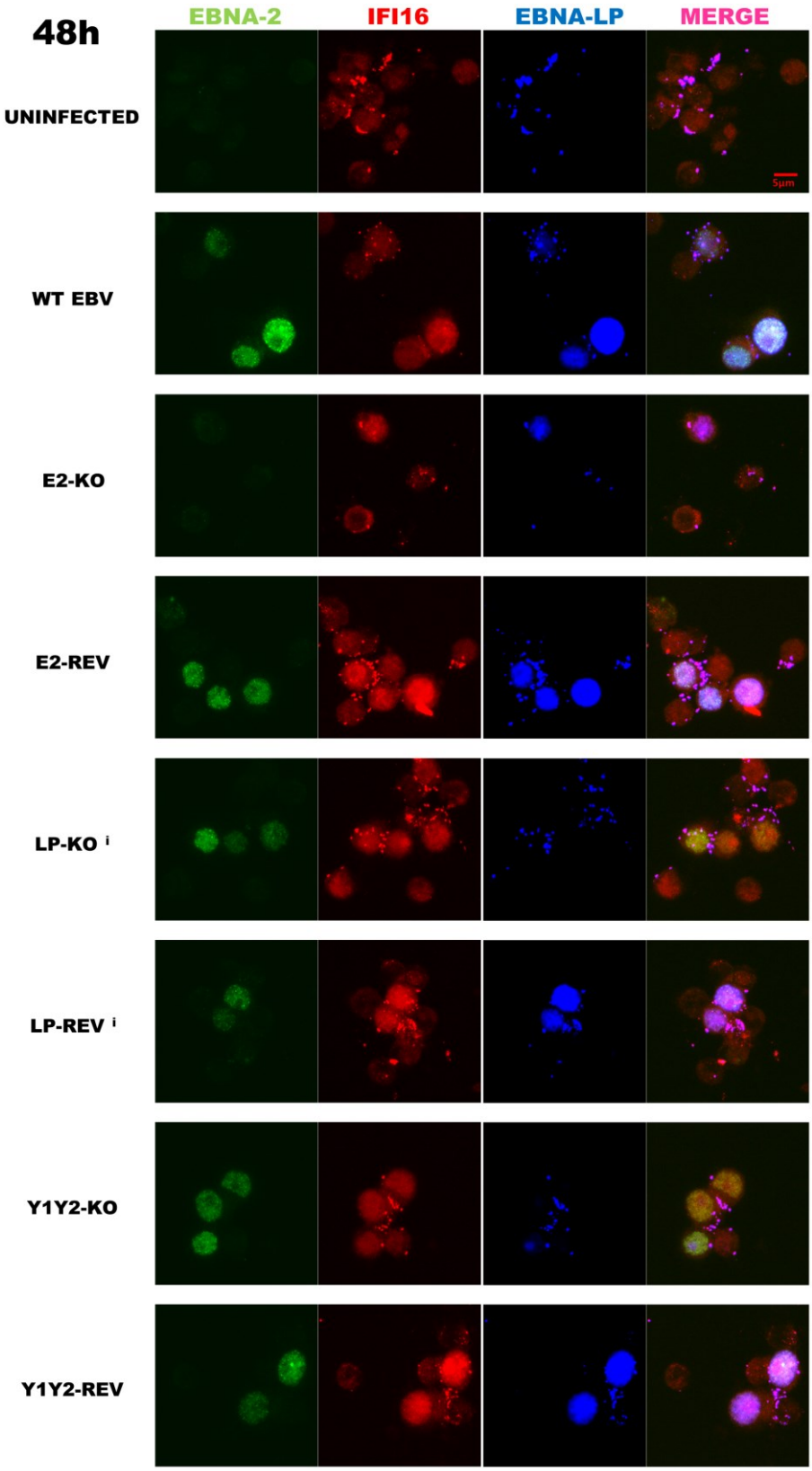

Fig. 4.14 IFI16 in primary B cells 48h after infection with different EBV recombinants. Cells were infected with different EBVs, fixed with 4% PFA and permeabilized with Triton-X100 at 48h after infection and stained for EBNA-2 using rat R3 antibody (green), EBNA-LP using mouse JF186 antibody (blue) and IFI16 using goat C18 antibody (red). Images were taken as described in Figure 4.8. The red bar in the uninfected merged picture corresponds to 5 µm.

4.3 The effect of EBNA-LP on transcription in infected naive B cells

EBNA-LP has previously been reported to enhance the induction of genes by EBNA-2 (see section 1.9.8 for a comprehensive overview). To assess whether this is observable in the early transformation process, and which genes are involved, we assessed the transcription of candidate genes (both cellular and viral genes) that were previously either reported to be co-activated by EBNA-2/EBNA-LP or are known to be important for EBNA-2's induction of the cell cycle in early transformation. A time course experiment after infection of primary CD19-isolated B cells with high titers (MOI=2) of virus was performed: RNA was extracted at 4 different time points post infection (days: 2, 9, 16 and 30) and used in RT-qPCR to assess the expression of potentially relevant host and virus genes. Four housekeeping genes were checked for normalization, of which the best ones were chosen to normalize the results (for details see section 2.6.5).

4.3.1 Normalization and experimental set up

After using housekeeping genes to normalize for differing input cDNA levels (see section 2.6.5), we wanted to add a second normalization process to control for any differences in the relative proportions of EBV-infected and uninfected cells, as this ratio will change both with initial infection efficiency and with differing proliferation rates of EBV-infected cells as the cell lines grow out. For this we checked the suitability of: EBNA-2 (using primers that also amplify EBNA-2-specific transcripts in EBNA-2 KO due to retention of the sequence just downstream of the splice donor site of exon Y3 in our E2-KO), EBNA-3A (using an assay spanning the U exon-EBNA-3A splice junction) and EBER-2 (for TaqMan assays see table 2.8). Since LP-KO and Y1Y2-KO viruses affected transcription in

the same way (see below), the results are grouped and plotted as following: all EBNA-LP knockouts and Y1Y2 knockouts combined as one group and all wild types and revertants together as a second group, to preliminarily assess whether levels of these tested EBV transcripts are independent of EBNA-LP production.

EBNA-2 is the only endogenous transcript that does not appear to be significantly affected by the loss of EBNA-LP and showed the smallest inter-sample variation at all time points (Fig.4.15a). EBNA-3A transcript levels are lower in the EBNA-LP mutant group at day 2 after infection (Fig.4.15b). Surprisingly, EBER-2 expression is also altered by the lack of EBNA-LP; lower for all EBNA-LP mutants at day 2 but higher at day 30 in comparison to WTs and REVs (Fig.4.15c).

Additionally, there is very high level of EBNA-2 transcripts in E2-KO-infected B cells 2 days after infection in comparison to all of the other recombinants (Fig.4.16a). Elevated levels of EBNA-2 transcripts are also seen for LP-REV ^{i} 2.6 on day 30 (Fig.4.16d) in comparison to other recombinants on the same day. Because EBNA-2 seemed to be the most suitable gene to normalize for proportion of infected cells, having no significant inter-sample variation (Fig.4.16) and similar levels in both EBNA-LP mutants and WT-infected cells throughout the time course (Fig.4.15a), the transcription of all genes used in qPCR was analyzed using two normalization strategies: first, normalized to endogenous (housekeeping) controls only, and second, normalized to both endogenous and EBNA-2 gene transcript data. However, it has to be taken into account that while this normalization may be useful for most of the samples, it may distort the results for samples in which EBNA-2 transcript levels are more elevated (i.e. in E2-KO infected cells at day 2 and perhaps LP-REV ^{i} 2.6 at day 30) (Fig.4.15a).

Because of the nature of this experiment (non-infected and EBNA-2 KO-infected primary B cells die within few days as they are not transformed, LP-KO ^{i}-infected B cells die

usually within 14 days after infection), these cells were not analyzed beyond their viable time points. Additionally, one of the LP-KO ^{w}-infected populations of B cells in this experiment (LP-KO ^{w} 4.1) died by approximately 20 days post-infection (this was the only time an LP-KO ^{w} infection of adult cells failed to establish an LCL, perhaps due to the frequent harvesting of the sample).

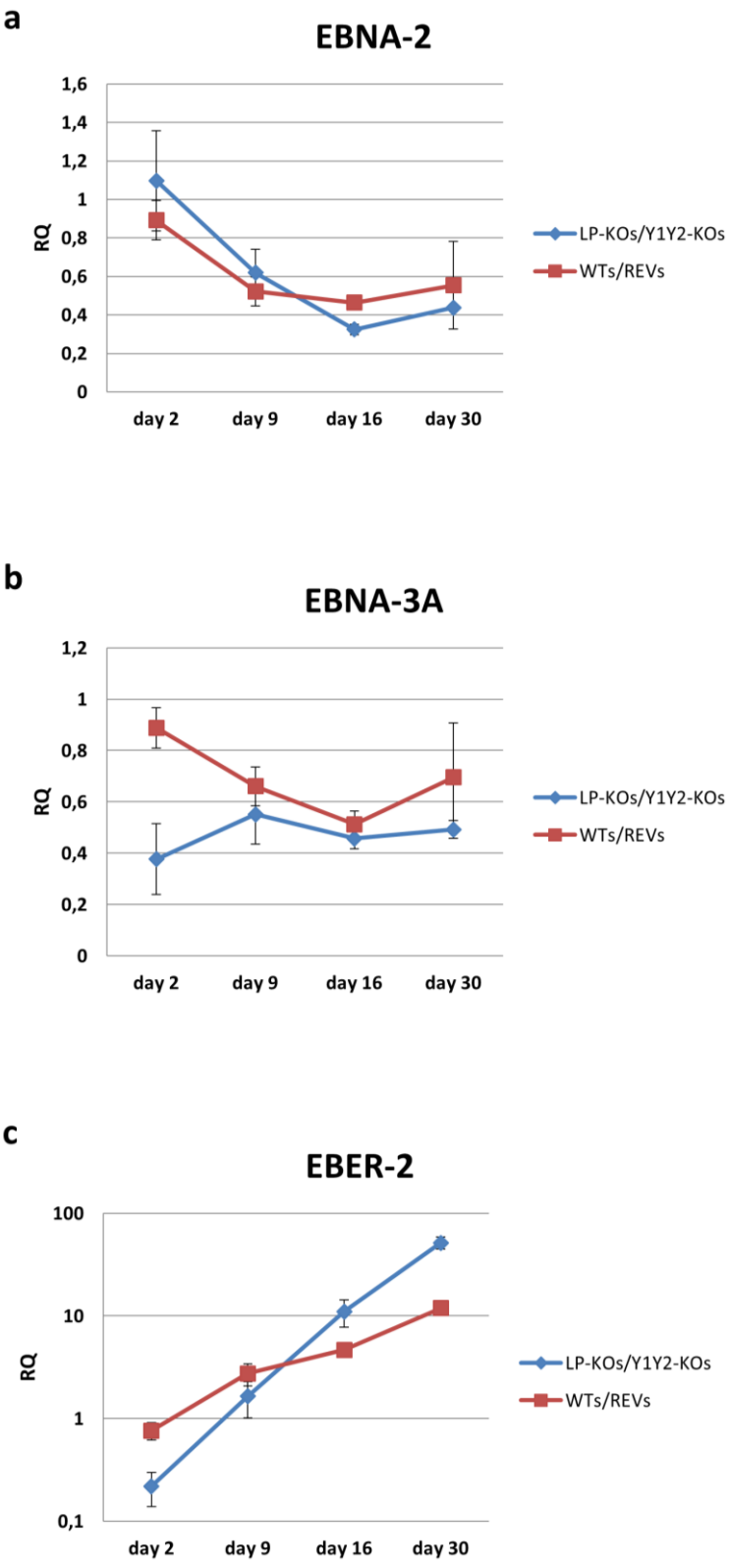

Fig. 4.15 qPCR on genes that were predicted be potentially used as a control for infected cells. cDNA reverse transcribed from RNA extracted at days 2, 9, 16 and 30 after primary B cell infection was quantified by 3 TaqMan qPCR assays: **a.** EBNA-2, **b.** EBNA-3A, **c.** EBER-2 after normalisation to the levels of 2 housekeeping control SYBR green assays (ALAS1 and RPLP0). The mRNA level is shown relative to levels in WT-infected cells (RQ) on day 2 (y-axis). Samples were divided into 2 groups: all LP-KOs and Y1Y2-KOs together (blue line) and all WT and REVs together (red line). The standard deviation was calculated for each group at each time point and is represented by black error bars. The x- axis indicates time post infection (days).

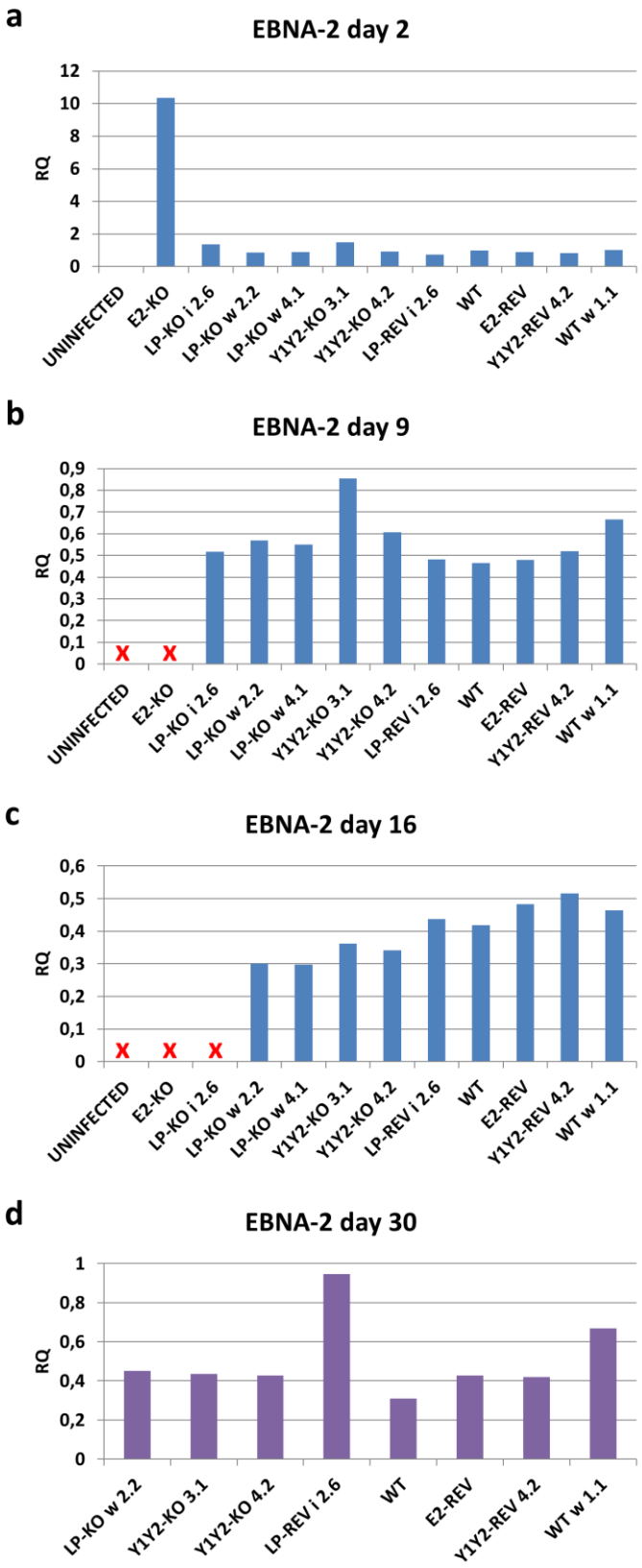

Fig. 4.16 Expression of EBNA-2 in infected B cells. cDNA reverse transcribed from RNA extracted at: **a.** day 2, **b.** day 9, **c.** day 16 and **d.** day 30 after primary B cell infection was quantified by EBNA-2 TaqMan qPCR assay after normalisation to the levels of 2 housekeeping controls. The mRNA level is shown relative to levels in WT-infected cells (RQ) on day 2 (y-axis). The x-axis shows samples infected with different viruses. Cells that did not survive until particular time point are marked by red x on the graphs.

4.3.2 EBNA-3A is expressed at lower levels in EBNA-LP mutants in comparison to WT EBV early after infection

With or without normalizing to EBNA-2, at two days post infection, there are consistently lower levels of EBNA-3A mRNA in all LP-KO- and Y1Y2-KO-infected B cells, when compared to all WT or REV (p-value<0.01) (Fig.4.18a). Those levels become similar for all of the recombinant viruses for the rest of the time course (Fig.4.18b-d). Overall, there is no significant change in the levels of EBNA-3A mRNA throughout the outgrowth of WT-infected cells but there is a delay in reaching this level after infection with EBNA-LP mutants (Fig.4.18e). There is also very high expression level of EBNA-3A transcripts in E2-KO-infected B cells 2 days after infection (Fig.4.17a), which is similar to EBNA-2 transcripts for this particular mutant on day 2 (Fig.4.16a).

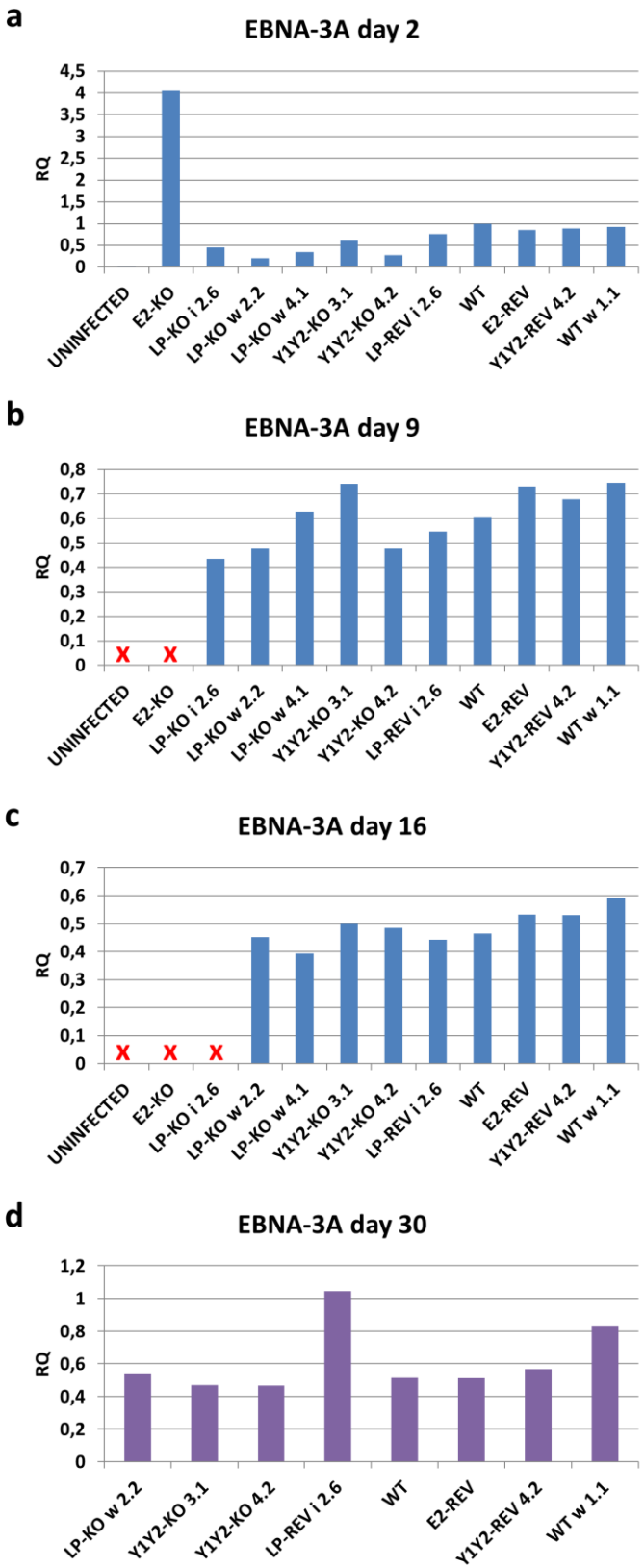

Fig. 4.17 Expression of EBNA-3A in infected B cells. cDNA reverse transcribed from RNA extracted at: **a.** day 2, **b.** day 9, **c.** day 16 and **d.** day 30 after primary B cell infection was quantified by EBNA-3A TaqMan qPCR assay after normalisation to the levels of 2 housekeeping controls. The mRNA level is shown relative to levels in WT-infected cells (RQ) on day 2 (y-axis). The x-axis shows samples infected with different viruses. Cells that did not survive until particular time point are marked by red x on the graphs.

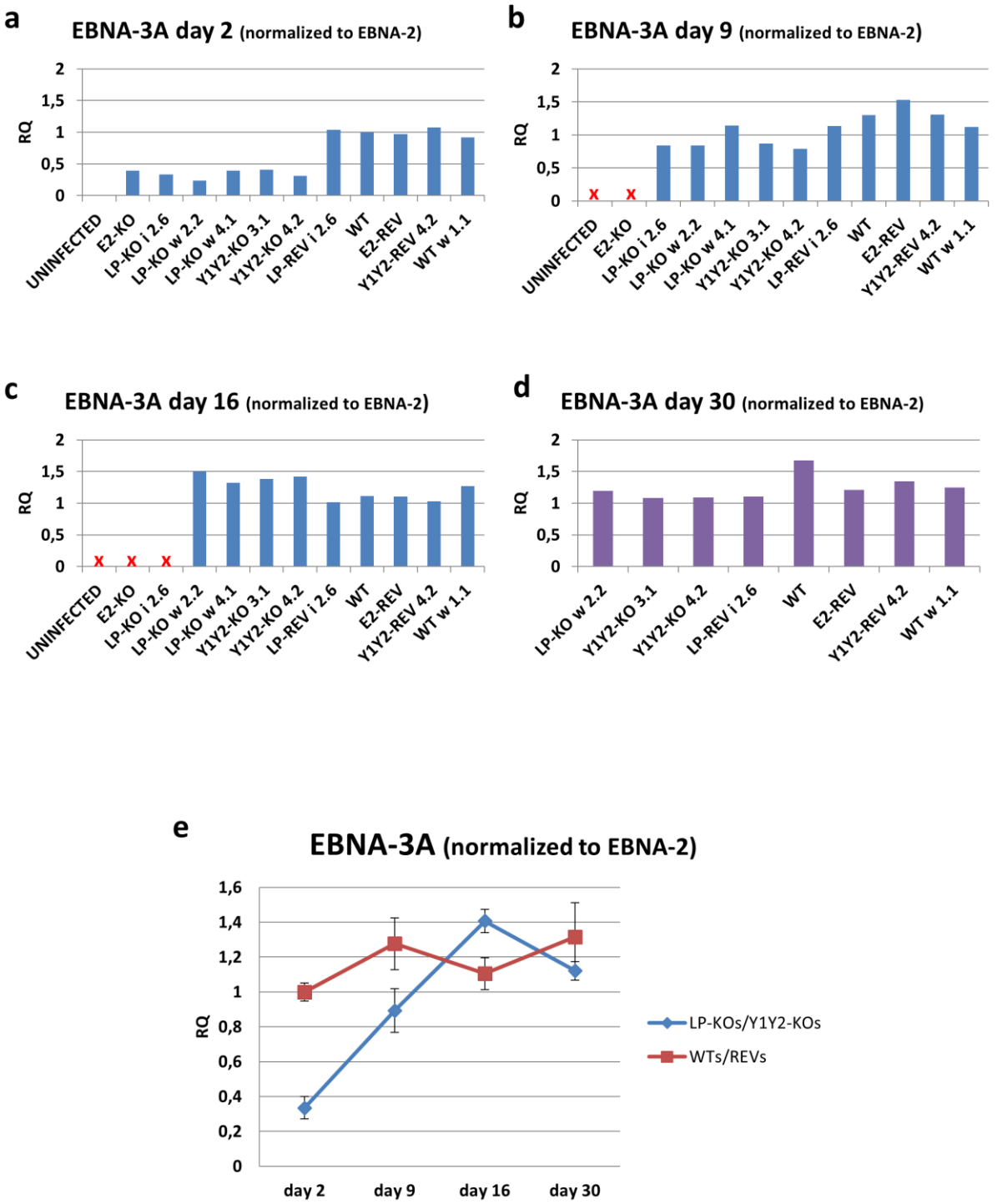

Fig. 4.18 Expression of EBNA-3A in infected B cells after normalization to EBNA-2. Relative levels of EBNA-3A transcripts normalised to housekeeping genes and EBNA-2 levels are presented for **a.** day 2, **b.** day 9, **c.** day 16 and **d.** day 30 after primary B cell infection. The mRNA level is shown relative to levels in WT-infected cells (RQ) on day 2 (y-axis). The x-axis shows samples infected with different viruses. Cells that did not survive until particular time point are marked by red x on the graphs. **e.** Samples were divided into 2 groups: all LP-KOs and Y1Y2-KOs together in one group (blue) and all WT and REVs together (red). Standard deviation was calculated for each group at each time point and is represented by black bars. The x-axis indicates time post infection (days).

4.3.3 EBNA-LP modulates the levels of EBER-2 RNA

Perhaps surprisingly, EBER-2 seems to be the most variable transcript among all of the recombinant viruses (Fig.4.19): EBER-2 levels (for both normalization strategies) change from being consistently 4-5 times lower EBNA-LP mutant-infected to being consistently higher in EBNA-LP mutants by day 16 and 6-fold higher by day 30 when compared to WTs/REVs (Fig.4.20). This is equivalent to an increase of EBER-2 RNA levels in WT-infected cells of approximately 25 times between day 2 and 30 after infection, whereas in EBNA-LP mutant infected cells this increase is approximately 500-fold between day 2 and 30 after infection (Fig.4.20e). Additionally, in E2-KO-infected B cells there is no elevated expression of EBER-2 (Fig.4.19a) in contrast to very high expression levels of both EBNA-2 (Fig.4.16a) and EBNA-3A (Fig.4.17a). This implies that EBNA-2 may be crucial to a transcriptional feedback loop that regulates the transcription of the Cp and/or Wp transcripts.

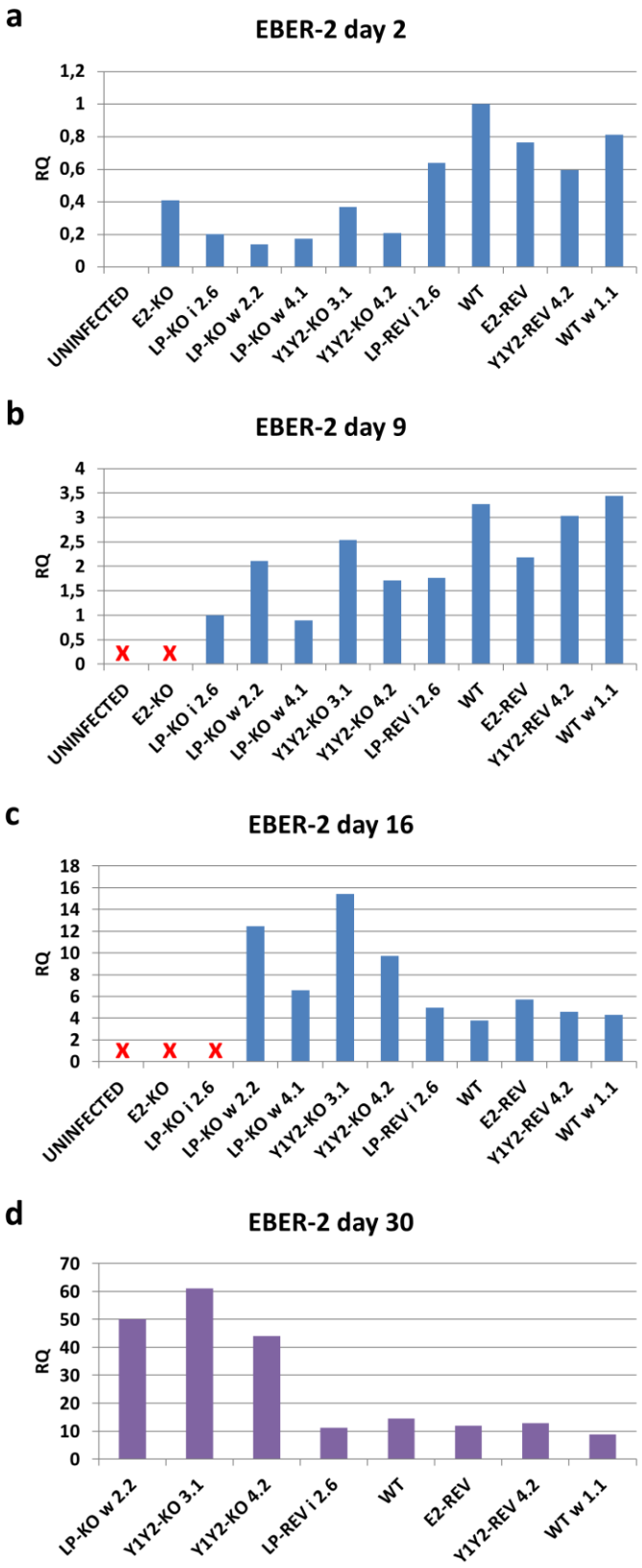

Fig. 4.19 Expression of EBER-2 in infected B cells. cDNA reverse transcribed from RNA extracted at: **a.** day 2, **b.** day 9, **c.** day 16 and **d.** day 30 after primary B cell infection was quantified by EBER-2 TaqMan qPCR assay after normalisation to the levels of 2 housekeeping controls. The RNA level is shown relative to levels in WT-infected cells (RQ) on day 2 (y-axis). The x-axis shows samples infected with different viruses. Cells that did not survive until particular time point are marked by red x on the graphs.

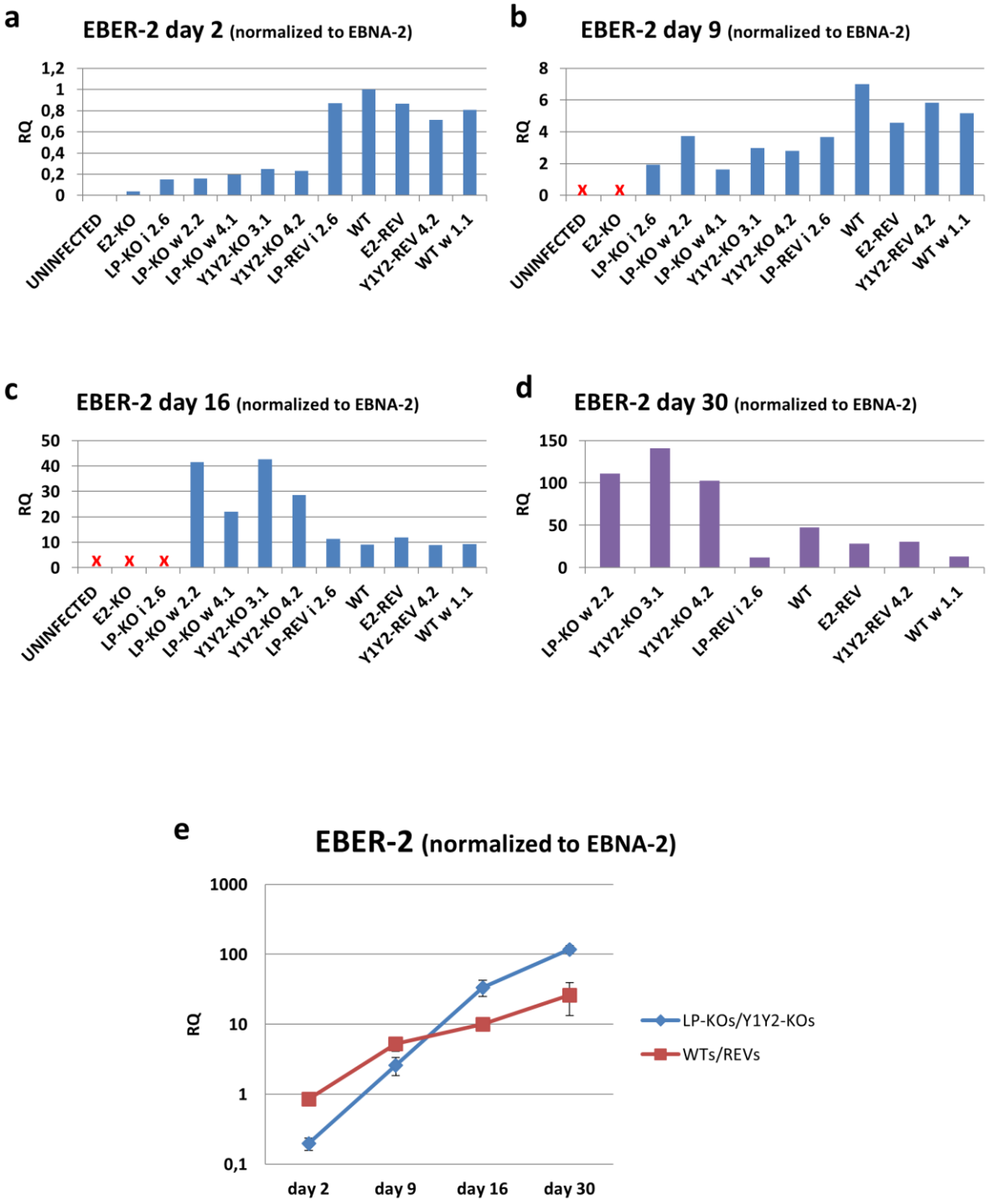

Fig. 4.20 Expression of EBER-2 in infected B cells after normalization to EBNA-2. Relative levels of EBER-2 transcripts normalised to housekeeping genes and EBNA-2 levels are presented for **a.** day 2, **b.** day 9, **c.** day 16 and **d.** day 30 after primary B cell infection. The RNA level is shown relative to levels in WT-infected cells (RQ) on day 2 (y-axis). The x-axis shows samples infected with different viruses. Cells that did not survive until particular time point are marked by red x on the graphs. **e.** Samples were divided into 2 groups: all LP-KOs and Y1Y2-KOs together in one group (blue) and all WT and REVs together (red). Standard deviation was calculated for each group at each time point and is represented by black bars. The x-axis indicates time post infection (days).

4.3.4 EBNA-LP does not interfere with the switch from Wp to Cp promoter

One of possible reason for lower expression of EBNA-3A transcripts (but not EBNA-2 transcripts) in EBNA-LP mutant-infected cells in the first days after infection could be change in the balance of usage of the Wp and Cp promoters (see section 1.9.1). To assess which promoters are active after primary B cell infection with different EBV recombinants, the levels of transcripts initiated from Cp and Wp were analyzed.

There is a similar trend of the promoters' usage for both EBNA-LP mutants and WT-infected groups, with Wp activity decreasing between day 2 and day 16 after infection and Cp activity increasing throughout the tested time points (Fig.4.21), which confirms previously published data for WT EBV (Hutchings et al., 2006). However, the absolute relative abundance of Wp and Cp transcripts cannot be assessed from our data because the mRNA levels are expressed relative to levels in WT-infected cells on day 2, and the efficiency of the two qPCR reactions are not known. There is a slight tendency for EBNA-LP mutants to have higher Wp and lower Cp at day 2 (Fig.4.21). As was seen for EBNA-2 and EBNA-3A transcripts (Fig.4.16a and 4.17a), the E2-KO-infected cells show higher expression from Wp at day 2 in comparison to all other infections (Fig.4.22). This elevated expression is not observed from Cp (not shown). Additionally, Wp transcript levels (but not Cp transcripts) start increasing for LP-REV ^{i} 2.6- infected cells between day 9 and 16 (not shown) and are more than 4 times higher at day 30 in comparison to other LCLs (Fig.4.22), which may suggest that the mutations in BWRF1 and/or sisRNA-1 interfere with Wp silencing.

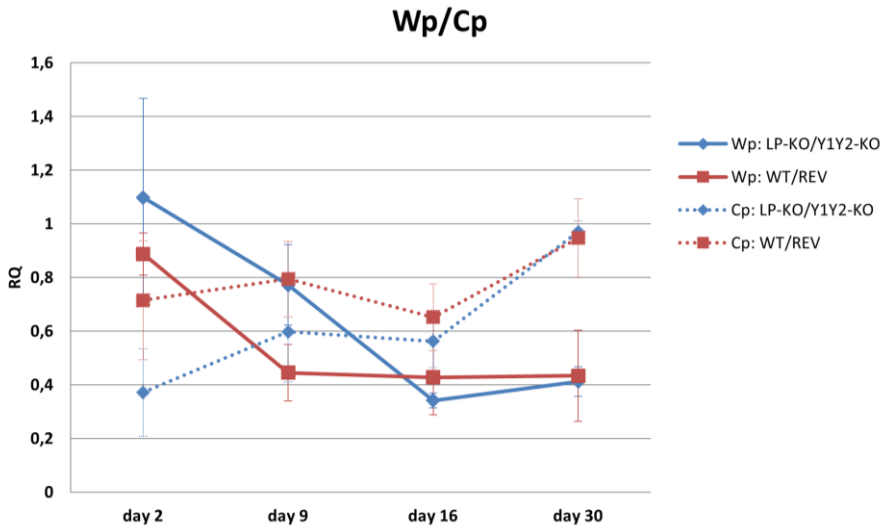

Fig. 4.21 Expression of transcripts generated from Wp and Cp promoters. cDNA reverse transcribed from RNA extracted at day 2, 9, 16 and 30 after primary B cell infection. mRNA level was normalized to housekeeping genes and shown relative to levels in WT-infected cells (RQ) on day 2 (y-axis). Samples were divided into 2 groups: all LP-KOs and Y1Y2-KOs together in one group (blue) and all WT and REVs (except LP-REV ^{i} 2.6) together (red). Standard deviation was calculated for each group at each time point and is represented by black bars. The x-axis indicates time post infection (days).

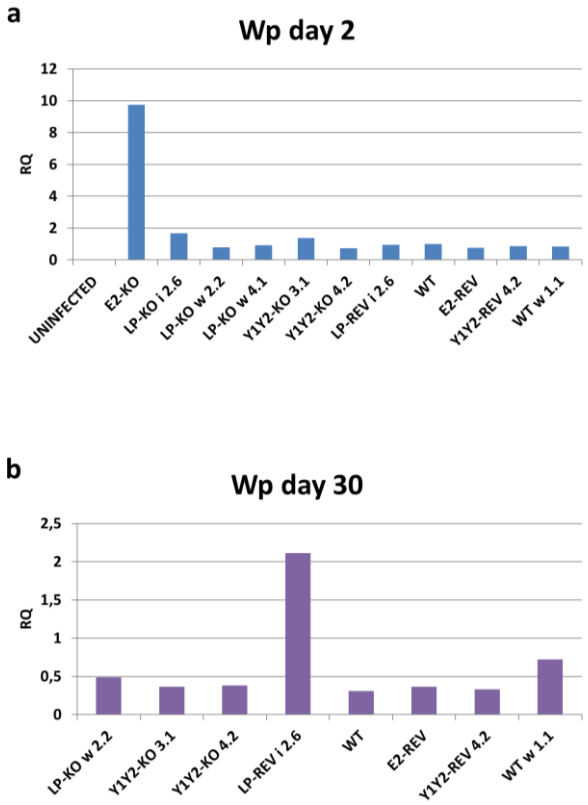

Fig. 4.22 Expression of transcripts generated from Wp on a. day 2 and b. day 30. The mRNA level was normalized to housekeeping genes and shown relative to levels in WT-infected cells (RQ) on day 2 (y-axis). The x-axis shows samples infected with different viruses, the y-axis shows relative quantification (RQ).

4.3.5 EBNA-LP regulates *CCND2* but does not up-regulate *MYC* expression

Previous in vitro co-transfection experiments in primary B cells have suggested that EBNA-2 and EBNA-LP activate the expression of cyclin D2, resulting in the progression of resting B cells into the G1 phase of cell cycle (Sinclair et al., 1994). It is also known that MYC expression can result in increased transcription of cyclin D2 (Bouchard et al., 2001). To test whether this may be the case for the reduced proliferation of LP-KO/Y1Y2-KO-infected B cell, we assessed the levels of *MYC* and *CCND2* (cyclin D2) mRNAs.

CCND2 transcript level is similar among all of the infections (except for uninfected B cells) at day 2 after infection when not normalized to EBNA-2 (not shown). After normalization to EBNA-2, the only sample at day 2 with lower *CCND*2 expression is the E2-KO-infected (Fig.4.23a). However, a difference in *CCND2* levels between the EBNA-LP mutant group and WT group can be seen at day 9, where the expression is lower for LP-KOs/Y1Y2-KOs in comparison to WTs (p-value<0.01) (Fig.4.23a). This reflects the lower expansion rate seen in the outgrowth experiment (section 4.1.1). In the WT-infected group, *CCND2* expression stays at a similar level between day 9 and 30, while for EBNA-LP mutant infected group, it rapidly increases during that time and in early LCLs (day 30) it reaches levels higher than seen in WT LCLs (Fig.4.23a).

In contrast, *MYC* expression levels are very similar among all samples and all time points (except for uninfected and E2-KO-infected B cells) and they do not change their trend after normalization to EBNA-2 (Fig.4.23b).

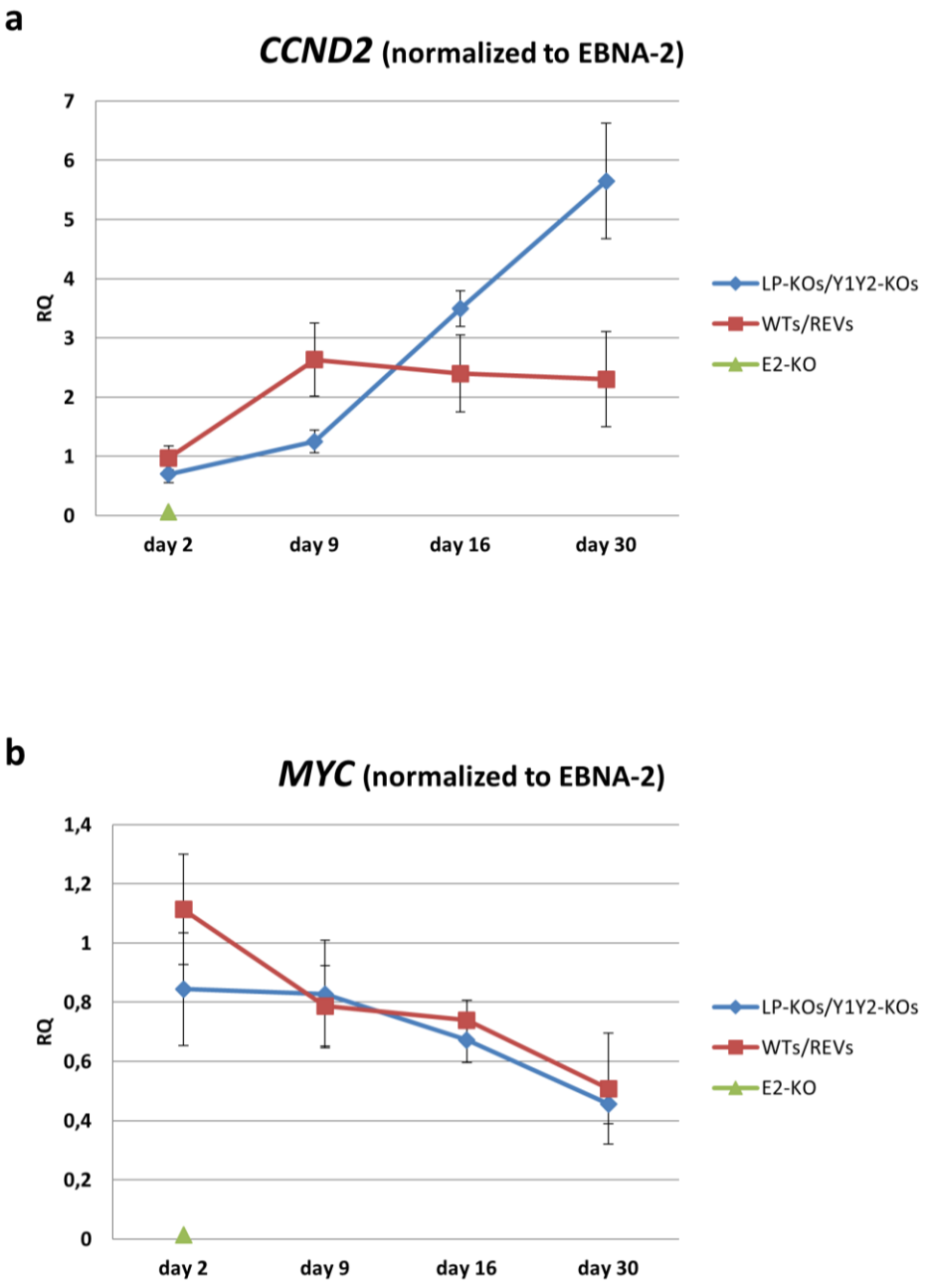

Fig. 4.23 Expression of *CCND2* and *MYC* after normalization to EBNA-2. cDNA reverse transcribed from RNA extracted at day 2, 9, 16 and 30 after primary B cell infection was normalized to housekeeping genes and EBNA-2 levels, and quantified by 2 TaqMan qPCR assays: **a.** *CCND2*, **b.** *MYC*. The mRNA is shown relative to levels in WT-infected cells (RQ) on day 2 (y-axis). Samples were divided into 3 groups: all LP-KOs and Y1Y2-KOs together in one group (blue), all WT and REVs together (red) and E2-KO (green). Standard deviation was calculated for each group at each time point and is represented by black bars. The x-axis indicates time post infection (days).

4.3.6 EBNA-LP may limit EBNA-2 transactivation of host gene *HES1* early after infection

In vitro co-transfection experiments identified EBNA-LP as a co-activator in the activation of the host gene *HES1* by EBNA2, perhaps through its displacement of NCoR and RBPJκ repressive complexes from the *HES1* enhancer (Portal et al., 2011). Another group reported however, that *HES1* transcription is induced by EBNA-2 but shows no further induction after co-expression of EBNA-LP (Peng et al., 2005) (for details see section 1.9.8).

To test how HES1 is regulated in the context of viral infection, qPCR using a *HES1* TaqMan assay was performed. Two days after infection, there is lower level of *HES1* in uninfected and E2-KO-infected B cells (Fig.4.24a). There is a marginal increase in *HES1* transcripts in EBNA-LP mutant infected cells over WT infections at day 2 (Fig.4.24a). When normalized to EBNA-2, however, this small difference diminishes, but by day 9 after infection there is a consistently higher level of *HES1* in EBNA-LP mutant infected cells than in WT-infected cells with both normalization methods (p-value<0.05) (Fig.4.24b and 4.25b). At day 16 and day 30, the levels of *HES1* are relatively similar (and fairly variable) among all of the samples (Fig.4.24c and d and Fig.4.25c and d).

These data show that EBNA-LP does not simply transactivate *HES1* but it is possible that EBNA-LP limits or modulates EBNA-2 in transactivation of this host gene early after infection.

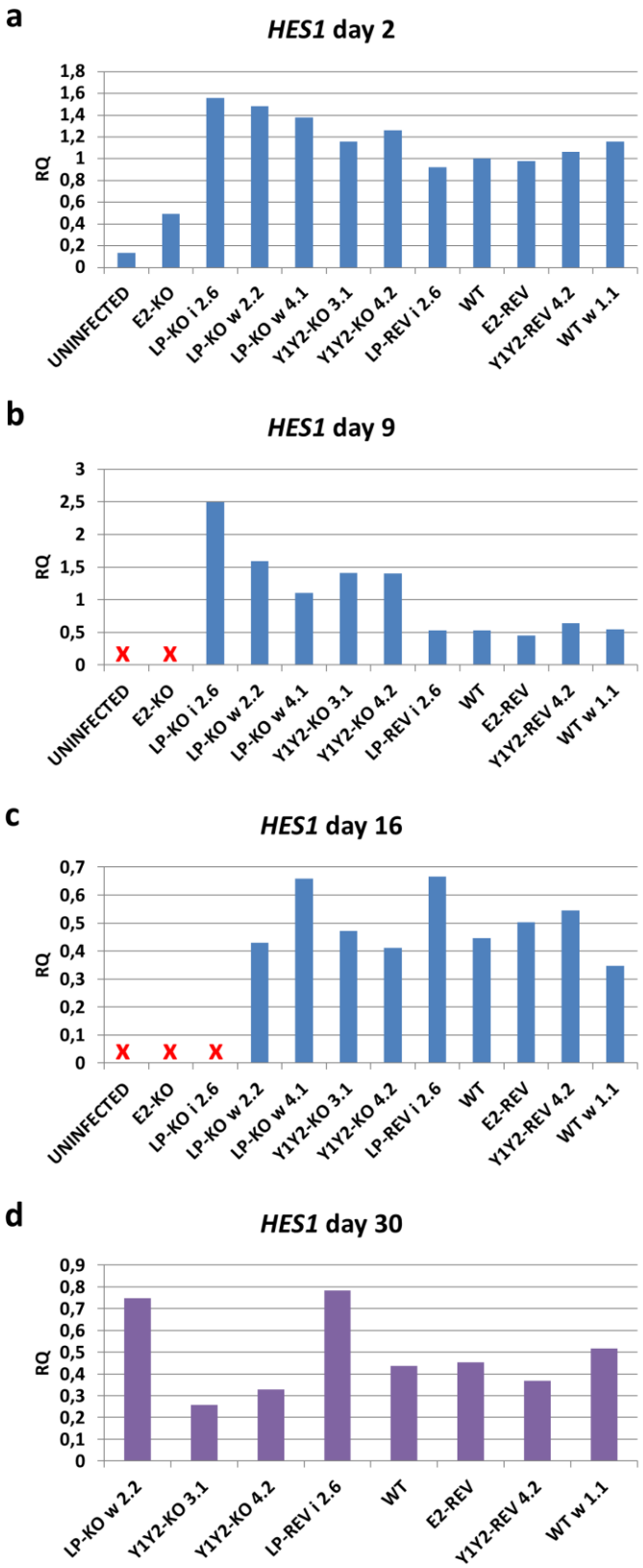

Fig. 4.24 Expression of *HES1* in infected B cells. cDNA reverse transcribed from RNA extracted at: **a.** day 2, **b.** day 9, **c.** day 16 and **d.** day 30 after primary B cell infection was quantified by *HES1* TaqMan qPCR assay after normalisation to the levels of 2 housekeeping controls. The RNA level is shown relative to levels in WT-infected cells (RQ) on day 2 (y-axis). The x-axis shows samples infected with different viruses. Cells that did not survive until particular time point are marked by red x on the graphs.

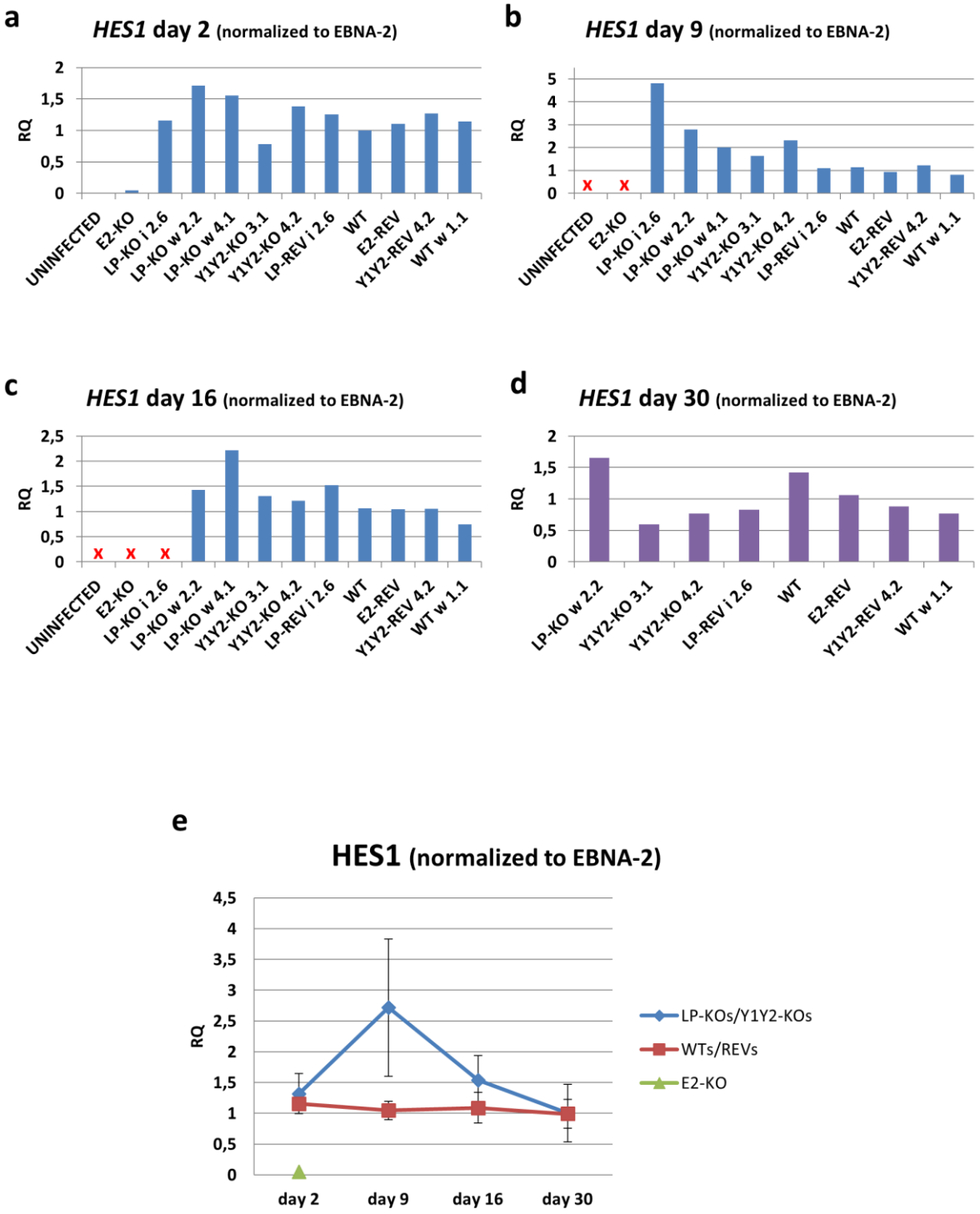

Fig. 4.25 Expression of *HES1* in infected B cells after normalization to EBNA-2. Relative levels of *HES1* transcripts normalised to housekeeping genes and EBNA-2 levels are presented for **a.** day 2, **b.** day 9, **c.** day 16 and **d.** day 30 after primary B cell infection. The RNA level is shown relative to levels in WT-infected cells (RQ) on day 2 (y-axis). The x-axis shows samples infected with different viruses. Cells that did not survive until particular time point are marked by red x on the graphs. **e.** Samples were divided into 3 groups: all LP-KOs and Y1Y2-KOs together in one group (blue), all WT and REVs together (red) and E2-KO (green). Standard deviation was calculated for each group at each time point and is represented by black bars. The x-axis indicates time post infection (days).

4.3.7 EBNA-LP enhances transactivation of the viral LMP-1 and LMP-2 promoters early after infection

It has previously been reported that EBNA-LP can increase EBNA-2 stimulation of the bidirectional *LMP-1*/*LMP-2B* promoter (but not *LMP-2A*) when co-transfected into latency I Burkitt lymphoma cell lines (Nitsche et al., 1997, Peng et al., 2005). To test whether this is also the case in primary B cell infections, qPCR using LMP-1 (Bell et al., 2006) and LMP-2 TaqMan assays was performed on cDNA obtained from RNA extracted from the primary B cell time course experiment.

There is a lower level of LMP-1 mRNA two days after infection with the E2-KO, LP-KO and Y1Y2-KO than with the WT and REV (for both normalization approaches; p-value<0.01) (Fig.4.26a). The levels of LMP-1 mRNA in EBNA-LP mutants rise to become closer to WT on day 9 post infection, but carry on rising to become higher than WT from day 16 to 30 (Fig.4.26c, d). This corresponds to the timings when the restarted expansion of LP-KO is seen in the outgrowth experiments. Interestingly, the cell lines with the lowest levels of LMP-1 at day 9 (LP-KO ^{i} 2.6 and LP-KO ^{w} 4.1) are those that died soon after (Fig.4.26b).

The trend of LMP-2 expression is very similar to LMP-1 for the same samples throughout the time course (Fig.4.27), with 2 noticeable differences: E2-KO infected cells express significantly higher levels of LMP-2 than EBNA-LP mutants at day 2 (Fig.4.27a), and LP-REV ^{i}-infected cells express levels of LMP-2 similar to WTs on day 30 (Fig.4.27d); lower than levels of LMP-1 on the same day (Fig.4.27d). Although, since this analysis has only been performed once, it needs repeating to assess whether it is reproducible.

The transcript levels of both *LMP-1* and *LMP-2* increase significantly with time after infection in all of the samples but the increase is higher in EBNA-LP mutant group than in WT (Fig.4.28).

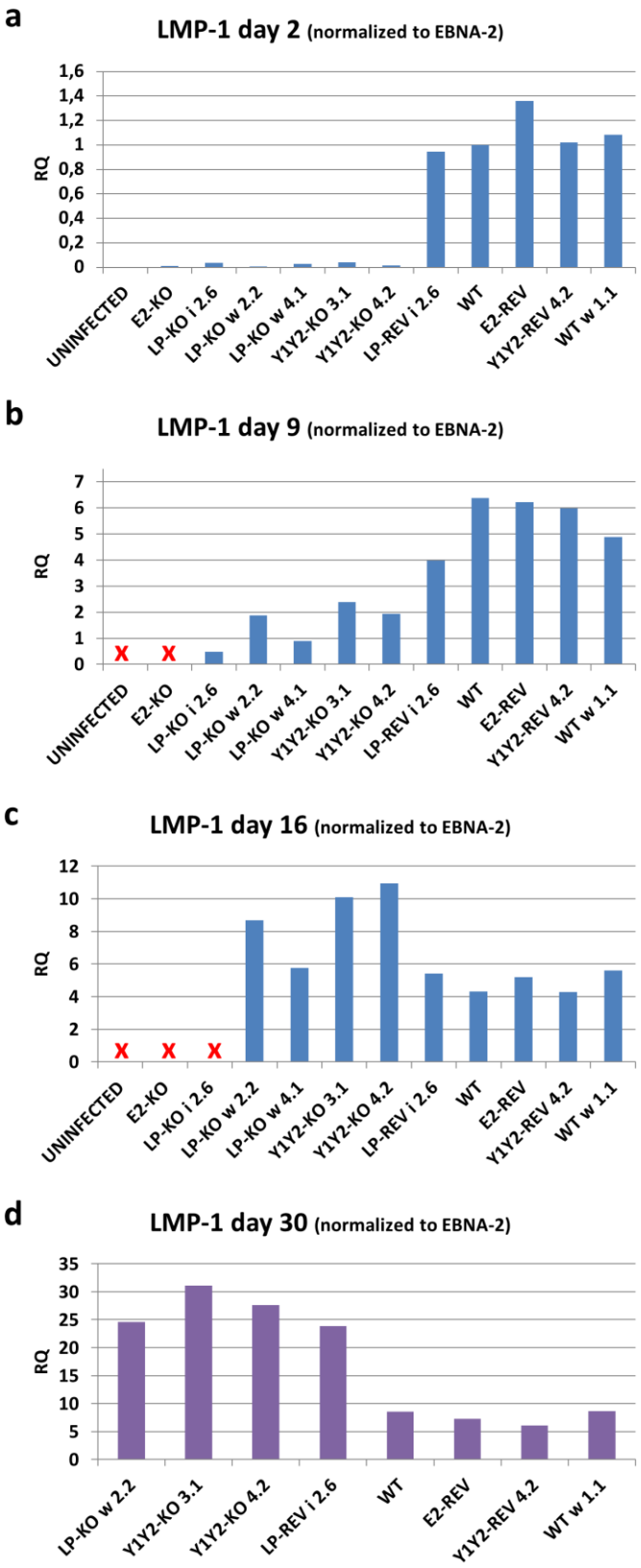

Fig. 4.26 Relative levels of LMP-1 transcripts in infected B cells after normalization to EBNA-2. cDNA reverse transcribed from RNA extracted at: **a.** day 2, **b.** day 9, **c.** day 16 and **d.** day 30 after primary B cell infection was quantified by LMP-1 TaqMan qPCR assay after normalisation to the levels of 2 housekeeping controls. The RNA level is shown relative to levels in WT-infected cells (RQ) on day 2 (y-axis). The x-axis shows samples infected with different viruses. Cells that did not survive until particular time point are marked by red x on the graphs.

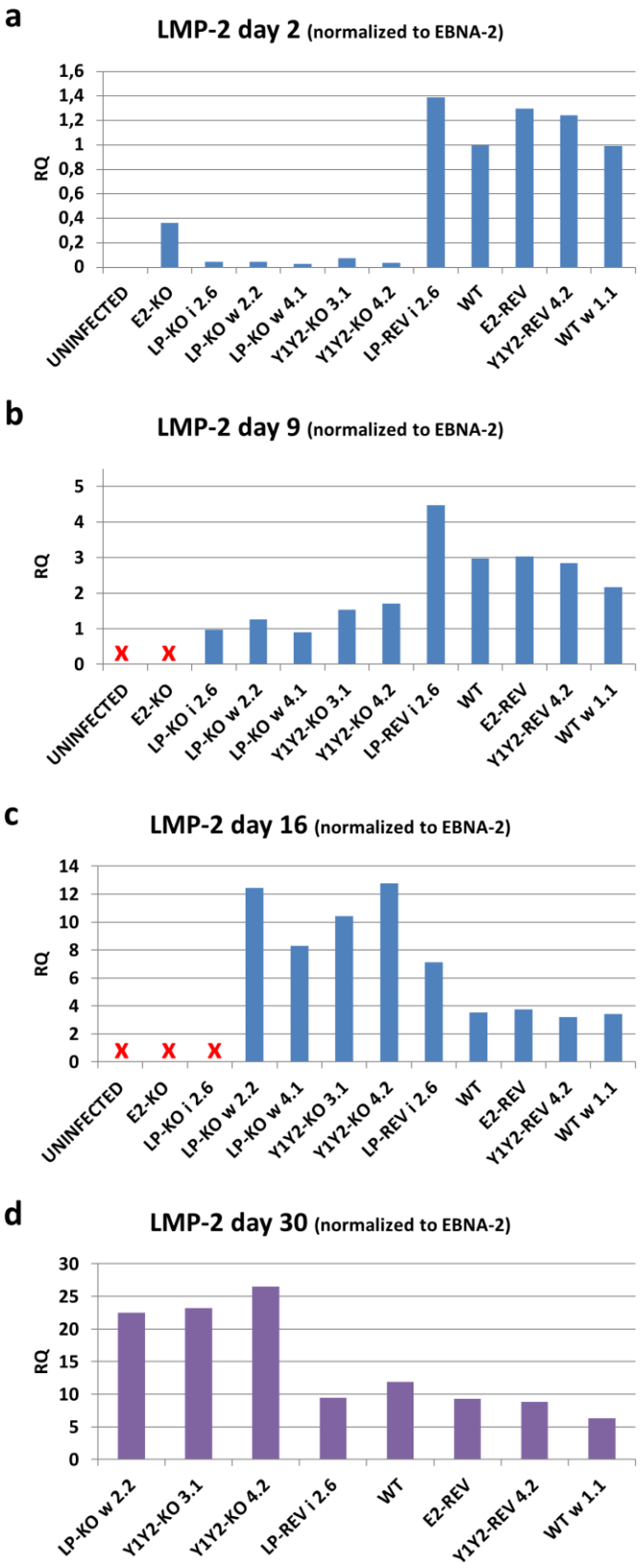

Fig. 4.27 Relative levels of LMP-2 transcripts in infected B cells after normalization to EBNA-2. cDNA reverse transcribed from RNA extracted at: **a.** day 2, **b.** day 9, **c.** day 16 and **d.** day 30 after primary B cell infection was quantified by LMP-2 TaqMan qPCR assay after normalisation to the levels of 2 housekeeping controls. The RNA level is shown relative to levels in WT-infected cells (RQ) on day 2 (y-axis). The x-axis shows samples infected with different viruses. Cells that did not survive until particular time point are marked by red x on the graphs.

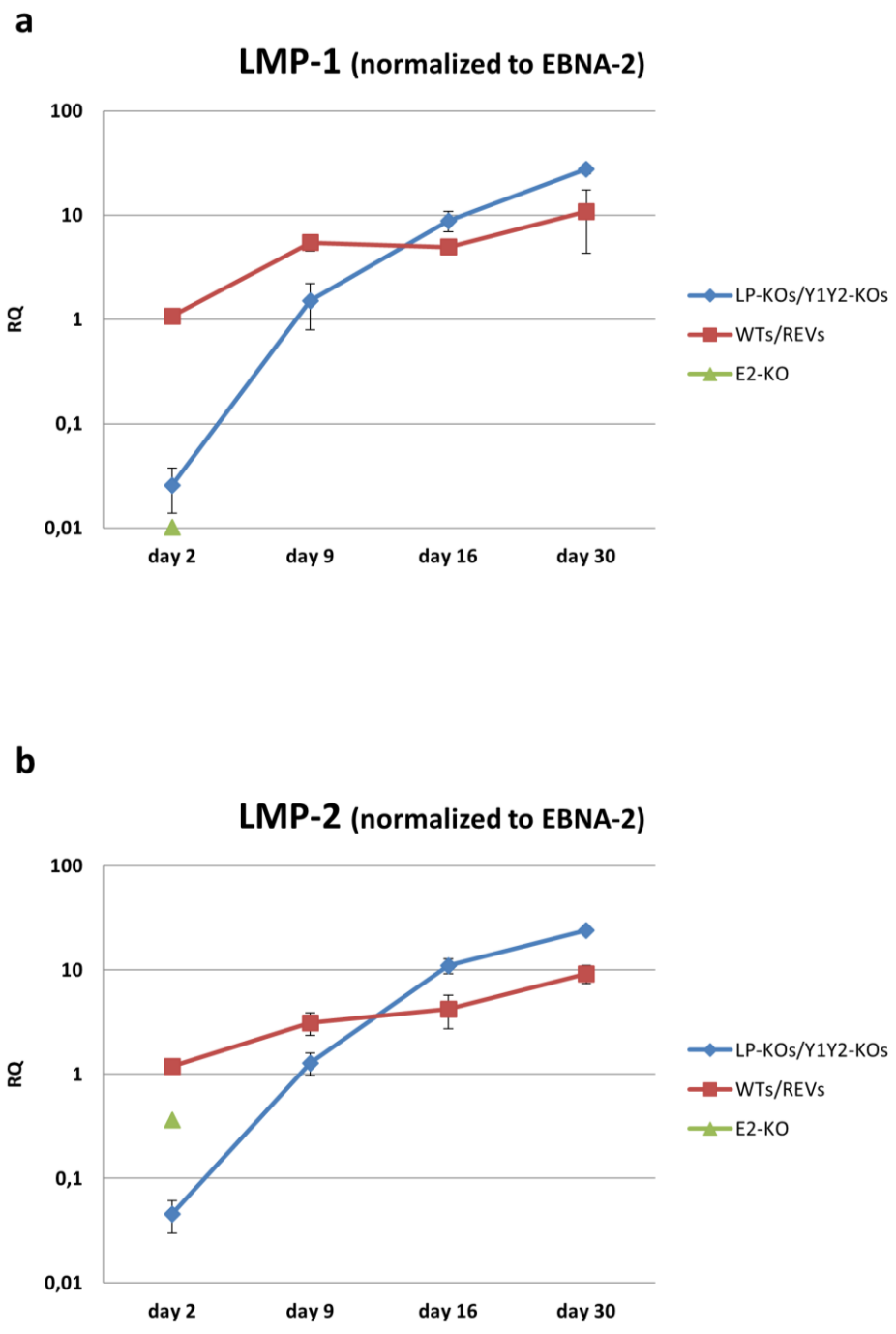

Fig. 4.28 Time course of LMP-1 and LMP-2 mRNA levels after normalization to EBNA-2. cDNA reverse transcribed from RNA extracted at day 2, 9, 16 and 30 after primary B cell infection was normalized to housekeeping genes and EBNA-2 levels, and quantified by TaqMan qPCR assays for **a.** *LMP-1*, and **b.** *LMP-2*. The transcript levels are shown relative to levels in WT-infected cells (RQ) on day 2 (y-axis). Samples were divided into 3 groups: all LP-KOs and Y1Y2-KOs together in one group (blue), all WT and REVs together (red) and E2-KO (green). Standard deviation was calculated for each group at each time point and is represented by black bars. The x-axis indicates time post infection (days).

4.3.8 BsmBI point mutations may up-regulate sisRNA-1 level in cells

Because of the impaired outgrowth and proliferation of LP-KO ^{i} and LP-REV ^{i}-infected B cells, the impact of the point mutations introduced to their introns from which sisRNA-1 and sisRNA-2 are generated was further tested by qPCR (using primers and conditions published by Moss and Steitz, (2013)). Fortunately, both of the qPCR primers hybridize away from the point mutation, so we do not expect the mutation to affect the function of the assay. There is a marginally higher sisRNA-1 level in B cells infected with EBV mutants in which the sisRNAs were mutated (LP-KO ^{i} and LP-REV ^{i}), when compared to viruses which do not contain intronic mutations (for both normalization approaches) (Fig.4.29). This difference increases with the time after infection and is higher in LP-REV ^{i}-infected LCLs by day 30 (Fig.4.29d). However, since this is based on a single cell line, further replicates are required to confirm whether this is consistently the case.

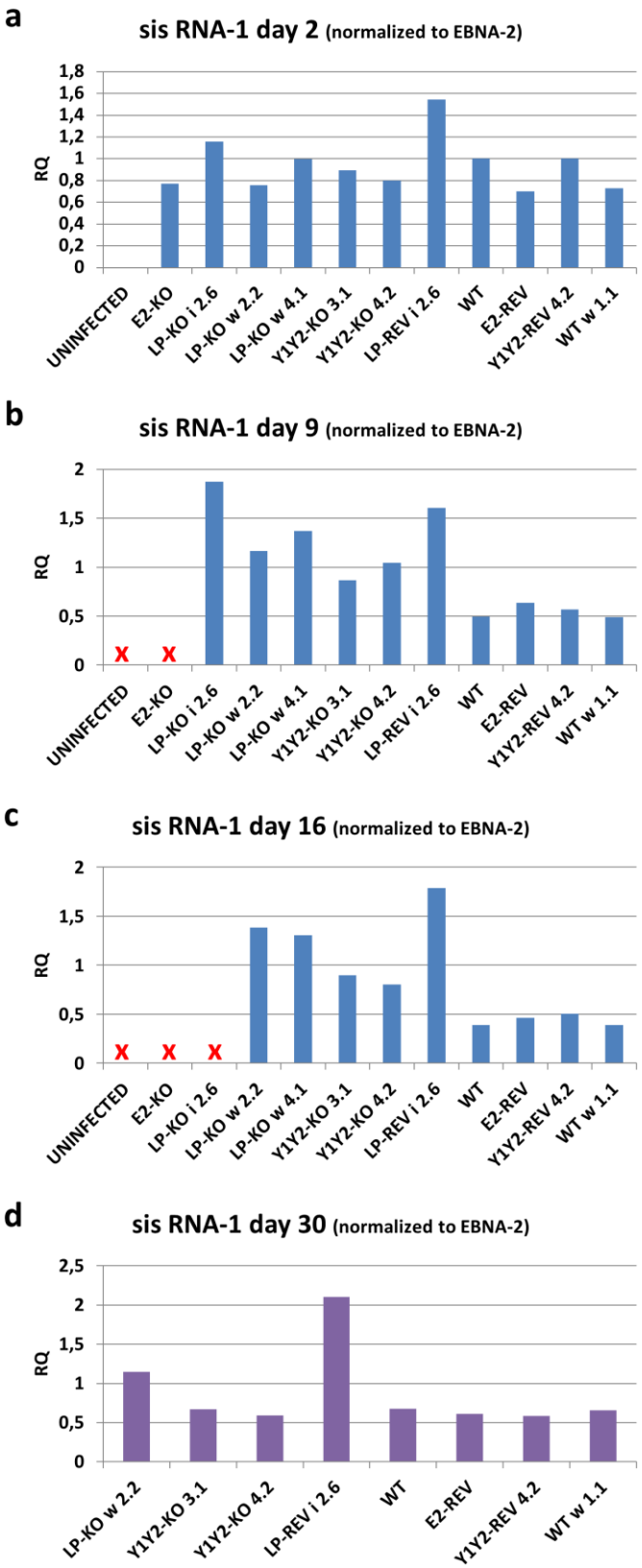

Fig. 4.29 Expression of sisRNA-1 in infected B cells after normalization to EBNA-2. cDNA reverse transcribed from RNA extracted at: **a.** day 2, **b.** day 9, **c.** day 16 and **d.** day 30 after primary B cell infection was quantified by sisRNA-1 qPCR assay after normalisation to the levels of 2 housekeeping controls and EBNA-2. The RNA level is shown relative to levels in WT-infected cells (RQ) on day 2 (y-axis). The x-axis shows samples infected with different viruses. Cells that did not survive until particular time point are marked by red x on the graphs.

4.4 Overview of observations made about second generation EBNA-LP mutant EBVs

Our LP-KO ^{w} virus is able to transform adult B cells but fails in the transformation of cord B cells. In comparison, WT and revertant viruses- including the somewhat defective LP-REV ^{i} virus- transform cord blood B cells with a similar efficiency to adult B cells. Additionally, WT ^{w} virus is better at transforming B cells than the original WT with heterogenous W repeats.

Proliferation of adult B cells after infection with LP-KO ^{w} is less efficient than proliferation of B cells infected with WT, which results in slower expansion and later establishment of LCLs in comparison to WT infections.

Analysis of gene transcription indicates that EBNA-LP contributes to the regulation of several genes. However, the nature of the regulation appears to be more complex than the existing model of assisting EBNA-2 to activate genes. It appears to restrict activation on some genes and at some times, but enhances it at others.

The key phenotypic differences between WT EBV and the first/second generation mutants are summarized in Table 4.1.

Virus	Proliferation of primary B cells	Transformation efficiency of adult B cells	Transformation efficiency of cord B cells	EBV transcript profile early after infection	EBNA-LP protein
WT	+ + + +	+ + + +	+ + + +	"Normal"	Moderate levels/ Short isoforms/ Localized to PML
WT [w]	+ + + + +	+ + + + +	+ + + + +	"Normal"	High levels/ Long isoforms/ Localized to PML
LP-REV [i]	+ + +	+ + +	+ + +	"Normal"	High levels/ Short isoforms/ Localized to PML
Y1Y2-KO	+ +	+ +	-	Reduced EBNA-3A/ EBER-2/ LMPs transcript levels	Very low levels/ Short isoforms/ Localized to nucleoli
LP-KO [w]	+ +	+ +	-	Reduced EBNA-3A/ EBER-2/ LMPs transcript levels	No protein
LP-KO [i]	+	-	-	Reduced EBNA-3A/ EBER-2/ LMPs transcript levels	No protein

Table 4.1 The major phenotypic differences between WT and mutant viruses. The proliferation and transformation efficiency of B cells infected with different recombinant viruses were scored from - to + + + + + (where "-" represents no transformation and "+ + + + +" represents high transformation efficiency/high proliferation).

5 DISCUSSION

5.1 Generation of viruses and an accidental study of the EBV sisRNAs

The results presented in this thesis provide the first demonstration of the role of EBNA-LP in the context of EBV infection. The major challenge with the genetic analysis of this protein during viral infection arises from its complex splicing, which does not allow the simple removal of the EBNA-LP gene from the EBV genome, as that would result in the disruption of other EBNAs' transcripts and the removal of non-coding RNAs arising from EBNA-LP's introns. Indeed an attempt to take this approach revealed that no Wp- or Cp-initiated transcripts and no EBNA-2 or latent BHRF1 transcripts could be detected after infection with virus containing zero W repeats (Tierney et al., 2011). Another challenge in generating an EBNA-LP knockout virus is caused by the repetitive nature of the gene, whereby each repeat unit contains a promoter (Wp) that can initiate an EBNA-LP-encoding transcript and the alternative splicing that allows for (uncharacterized so far) skipping of W repeat exon pairs. Therefore, the introduction of a single STOP codon at the beginning of the EBNA-LP sequence would fail to knock out EBNA-LP, as the W repeat exon with the STOP codon could be skipped (i.e. spliced out) and shorter EBNA-LP protein isoforms lacking this exon could still be expressed. This skipping of a defective W exon and production of shorter isoforms of intact EBNA-LP is apparent in the infections with B95.8-derived WT virus (Fig.4.5), where a STOP codon exists in one of the W1 exons (Ba Abdullah, unpublished data).

Based on these characteristics, we have undertaken a different approach to generate an EBNA-LP knockout, using two different cloning methods. In both cases, it consisted of

introducing a STOP codon into a single W repeat and using this mutated repeat to generate an array of W repeats, where each W repeat has the STOP codon. Therefore, despite the alternative splicing, no single W repeat unit is able to produce EBNA-LP protein.

The first method of generating an array of mutated repeats used type IIS restriction endonucleases, adapting a strategy devised by Grundhoff and Ganem, (2003). This strategy required the introduction of a single point mutation in the intron between W1 and W2 exons, to disrupt an inconvenient restriction site. It is unfortunate that the single W repeat unit that was used to generate these LP-KO ^{i} and LP-REV ^{i} arrays contained additional variations (3 point changes in BWRF1 ORF) that occur in one copy somewhere within the W repeats of the B95.8 virus. As a result the final recombinant EBNA-LP knockout and revertant viruses carry 4 changes of unknown function in each W repeat. These 4 "mutations" are present in the regions where the recently identified sisRNA-1 and sisRNA-2 originate from. Therefore the expression of these sisRNAs may be affected both in LP-KO ^{i} and LP-REV ^{i}.

These additional changes introduced into LP-KO ^{i} and LP-REV ^{i} have a significant meaning with respect to establishing LCLs: LP-KO ^{i} failed completely in establishing LCLs in contrast to LP-KO ^{w}, which was successful (albeit slower than WT) in transforming adult primary B cells into constantly proliferating cells (see section 3.3.1 and 4.1.1). Since LP-REV ^{i} also exhibited a transformation defect relative to the WT, the simplest explanation for the failure of LP-KO ^{i} in transformation is the cumulative effect of the lack of EBNA-LP and the impact of sequence changes in the introns from which sisRNAs are reportedly produced (Moss and Steitz, 2013). Additionally, this additive nature of the sisRNA and EBNA-LP mutations indicates that these two are acting at independent places in the transformation process, which is reinforced by the observation that LP-REV ^{i} is able to establish LCLs from cord B cells, while LP-KO ^{w} is not. However, to distinguish whether the mutation in sisRNA-1, sisRNA-2 or both are causing the reduction in transformation, sisRNA-1 and sisRNA-2

mutant viruses have to be generated. Work is currently being undertaken in our lab to identify and distinguish the role of both sisRNAs in B cell transformation. Preliminary analyses suggest that either deletion of the hairpin region from sisRNA-2 or deletion of the entire sisRNA-1 intron have detrimental effects on transformation (Ana Gali and Sam Correia, unpublished data).

Large stable introns producing RNAs have been previously found in other herpesviruses (Burton et al., 2003). In herpes simplex virus 1 (HSV1), an unstable 8.3 kb latency-associated transcript (LAT) is spliced to produce a stable 2 kb LAT intron that is abundantly expressed in latently infected neurons (Farrell et al., 1991), and recently a second nested 1.5 kb LAT intron (twintron) has been identified to be as stable as the 2 kb LAT (Brinkman et al., 2013). The 2kb LAT was found to be able to suppress apoptosis by inhibition of caspase-induced apoptotic pathways *in vitro* (Henderson et al., 2002) and to protect neuronal cells *in vivo* (Ahmed et al., 2002). It is therefore possible- if their mechanisms of action are similar- that sisRNA-1 and/or sisRNA-2 are required early after infection to help in preventing EBV-infected cells from undergoing apoptosis. Preliminary data obtained by Ana Gali in our lab indicate that sisRNA-1 knockout virus is slower than WT EBV at inducing proliferation in primary B cells and establishing LCLs. The sisRNA-1 point mutation in our LP-KO ^{i} and LP-REV ^{i} viruses is in a position that is conserved in most other species of lymphocryptoviruses (LCVs) (Moss and Steitz, 2013). The evidence for the existence (and nature) of sisRNA-1 is also more clearly defined than for sisRNA-2: sisRNA-1 can be detected by Northern blot whereas sisRNA-2 is only evident from short-read sequencing (Moss and Steitz, 2013). Also, the three point mutations in the sisRNA-2/BWRF1 of LP-KO ^{i} and LP-REV ^{i} are in one of the most polymorphic region of the W repeat, and two of the three changes are also found as single nucleotide polymorphisms (SNPs) in other strains (Ba Abdullah, unpublished data). For these reasons, the sisRNA-1 mutation in our LP-

KO ^{i} and LP-REV ^{i} seems to most likely be the culprit for the observed transformation defect in these viruses.

In the second method for generation of EBNA-LP knockout, the repeats were assembled using Gibson assembly of a W repeat unit that matches the wild type W repeat sequence as it was published (Baer et al., 1984). The STOP codon was introduced to this repeat unit in a same way as in the first assembly method. Additionally, mutation of the sisRNA-1 intron between W1 and W2 was not required for this method to work. Thus, it allowed the generation of an EBNA-LP knockout virus (LP-KO ^{w}) without additional changes in the viral genome. Because, all of the W repeats in this knockout virus are homogeneous (which is not the case for WT B95.8 EBV) an additional WT virus (WT ^{w}) was generated to have homogeneous W repeat units, just as LP-KO ^{w} does, but without STOP codons in any of the W repeats. In contrast, the B95.8 BAC has one of its six W1 exons containing a STOP codon (Ba Abdullah, unpublished data). After establishing LCLs using WT ^{w} virus, we have found that it produces longer and more diverse isoforms of the protein than B95.8 (WT) (Fig.4.5).

5.2 Role of EBNA-LP in B cell transformation

The LP-KO ^{w} mutant viruses (in contrast to LP-KO ^{i} mutants) were able to establish LCLs after infection of adult primary B cells (see section 4.1.1). Also Y1Y2-KO viruses which have been generated in our lab succeeded in establishing LCLs (see section 3.3.1). Interestingly, both LP-KO ^{w} and Y1Y2-KO did not required feeder cells in their outgrowth in contrast to previously generated Y1Y2 mutants (Hammerschmidt and Sugden, 1989, Mannick et al., 1991). This is similar to our experience with EBNA-3A knockout virus, which required feeder cells in its outgrowth when generated and used by Hertle et al., (2009),

but has been able to establish LCLs without feeder cells in our lab (Skalska et al., 2010). One of the differences between our Y1Y2-KO and the Y1Y2-KO generated by Hammerschmidt and Sugden, (1989), is that our knockout was generated in a way to retain the splice acceptor of exon Y1 and splice donor of Y2, whereas the previous knockouts entirely lacked both the Y1 and Y2 exons, which could have altered the splicing of downstream EBNAs. However, the Y1Y2-KO viruses generated by Mannick et al., (1991) also retains the splicing sites and was no different in transforming B cells than the one generated by Hammerschmidt and Sugden, (1989), i.e. feeder cells were required for this mutant to establish LCLs (Mannick et al., 1991). Alternatively, our knockout has defined number (6) of homogenous W repeats, while previous knockouts were generated by recombination between W repeats from type 2 and type 1 EBV, and the total number of W repeats in the virus after recombination was not assessed in any of these cases (Hammerschmidt and Sugden, 1989, Mannick et al., 1991). It is therefore possible that the more impaired transformation phenotype observed in the P3HR1-based mutants when compared to ours, could be a result of a lower number of W repeats, presence of less transforming variants of W exons (as the transformation efficiency between different EBNA-LP variants has never been assessed), incompatibility of the inserted type 1 EBNA-LP/EBNA-2 cassette with the type 2 EBNA-3s of P3HR1, or some other aspect of the P3HR1 backbone that differs from B95.8 (e.g. BARTs).

The main barrier to comparing the impact of deleting just the Y exon domains with knockout of the whole EBNA-LP protein is that the levels of EBNA-LP produced after infection with our Y1Y2-KO are very low (Fig.4.5) and the small amount of protein that is made localizes to nucleoli (Fig 4.6). A combination of the low abundance and altered localization of Y1Y2-KOs may be a reason for similarity to the complete knockout (LP-KO ^{w}) outgrowth after B cell infection. For instance, if the truncated protein is trapped in the nucleolus, it cannot perform functions in the rest of the nucleus/cell. There are no previous

reports of this phenomenon: it has been reported that Y1Y2 -deletion mutants of EBNA-LP express normal nuclear localization when transfected into HeLa cells (McCann et al., 2001) or EBV-positive latency I Burkitt lymphoma cell line (Nitsche et al., 1997), and that low molecular weight (27kDA and 34kDa) EBNA-LP lacking Y1Y2 exons localizes mainly to the cytoplasm in the Daudi and P3HR1 cell lines (Garibal et al., 2007). We have not observed cytoplasmic localization of our Y1Y2-KO EBNA-LP during infection. This may be because longer forms are expressed by our mutant virus, but this is difficult to establish because of the very low expression of this mutated protein, which is barely detectable by Western blot (Fig.4.5). Nucleolar localization signals (NoLS) consists of a high proportion of basic amino acids (especially lysines and arginines) and is usually found in the residues closest to the protein termini, in regions that are easily accessible (Scott et al., 2010). It is therefore possible that we have created or unmasked a nucleolar localization signal when truncating EBNA-LP, as the beginning of the Y1 exon that is kept in our Y1Y2-KO consists of a high number of arginines (Fig.3.5). Recently, it has been also reported that there are specialized ribosomal intergenic spacer noncoding RNAs in the nucleolus that can bind to particular proteins and immobilize them there (Audas et al., 2012). Notably, PML and hsp70 have nucleolar detention sequences (NoDSs) and in certain conditions (for example cellular stress) they can be bound by these noncoding RNAs and immobilized in the nucleolus. Since EBNA-LP binds components of PML domains (Ling et al., 2005) as well as hsp70 (Mannick et al., 1995), it is possible that EBNA-LP can be captured there through a binding partner, and that the Y1Y2 domain is required for modifying these interactions and/or for translocation away from the nucleolus. Alternatively, the conformation of EBNA-LP may change when there is no Y1Y2 domain, which could affect binding to hsp70 and thereby result in nucleolar localization. Another possibility is that the Y1Y2 domain prevents the protein from localizing to the nucleolus. Additionally it has been reported that a proteasome

inhibitor (MG-132) induces nucleolar translocation of EBNA-LP in B95.8-derived LCLs (Pokrovskaja et al., 2001), but we could not reproduce this (not shown). Nor did MG132 increase levels of truncated EBNA-LP (Fig.4.5), suggesting that the low levels of the protein are not due to its targeting to the proteasome. Summarizing, our Y1Y2-KO may behave similarly to LP-KO ^{w} either because of a low abundance of truncated protein or because the truncated protein cannot reach the right part of the cell, so it is functionally knocked out. Either way, Y1Y2-KO does not reflect functionality of a truncated EBNA-LP in the context of viral infection. We cannot tell whether the low level is due to protein instability or relates to the STOP codon in one of the W repeats, reducing protein levels.

There is however, a subtle difference in the dynamics of outgrowth between LP-KO ^{w} and Y1Y2-KO; the Y1Y2-KO outgrowth is slower than WT but similar in its linearity, with cultures showing continual expansion, whereas LP-KO ^{w} has a distinct lag stage between approximately day 5 and 15, when the culture appears to be static but re-enters expansion phase after day 15. We intend to undertake proliferation assays such as 5-ethynyl-2'-deoxyuridine (EdU) incorporation pulses and further cell cycle profiling to assess whether this lag represents a transient arrest in proliferation or an increase in cell death over this time. However, these timings of particular stages coincide with the observation made by the Luftig group on LMP-1 expression, that there is a significant increase in the level of this protein between day 14 and 21 (Price et al., 2012). LMP-1 has been identified to be essential for efficient B cell transformation by EBV both *in vitro* and *in vivo* (Kaye et al., 1993, Dirmeier et al., 2003). In LP-KO ^{w}, the expression of LMP-1 is significantly lower early after infection in comparison to WT-infection but the transcript levels of this protein in LP-KOs infections do not reach the level of those in WT-infections until sometime between day 9 and 16, suggesting that the static phase of LP-KO ^{w} outgrowth might be due to not high enough expression of LMP-1; perhaps once the required level of LMP-1 is achieved, the LP-KO ^{w} re-

enter the expansion phase. LMP-1 knockout viruses were able to establish LCLs only when infected B cells were cultured in the presence of feeder cells (Kaye et al., 1993, Dirmeier et al., 2003, Ahsan et al., 2005). The B cell transformation using LMP-1 knockout virus was significantly impaired in comparison to WT virus but the dynamics of the outgrowth have not been described (Dirmeier et al., 2003). However, based on the transcript levels of other genes (described in further paragraphs of this discussion), the changes in expression of EBER-2, LMP-2 or of host genes whose regulation by EBNA-LP has yet to be characterized, might be responsible or contribute to the delay in outgrowth of LP-KO ^{w}-infected B cells. Another feature of the time when LP-KO ^{w}-infected B cells re-enter expansion is that this is when EBNA-3-regulated genes are properly repressed/induced (e.g. repression of tumor suppressor $p16^{INK4a}$ by EBNA-3A/EBNA-3C (Skalska et al., 2013) or induction of the activation-induced cytidine deaminase (AID) by EBNA-3C (Kalchschmidt et al., 2016a)). It is therefore possible that the action of EBNA-3s in gene regulation could compensate for the lack of EBNA-LP from around two weeks after infection.

In contrast to infections of adult B cells, both LP-KO ^{w} and Y1Y2-KO are unable to establish LCLs from cord blood PBLs. This may be either due to heterologous immunity (or some other aspect of the immune cells co-isolated with the cord B cells) or a function of the immaturity of cord B cells. Heterologous immunity is a theory suggesting that responses to new infections early in life are mostly triggered by naïve T cells, which then become memory T cells (Selin et al., 1998). In this context, the proliferation of naïve T cells is interleukin-2 (IL-2) independent (Tan et al., 2001). Cyclosporin A, which was used in the outgrowth experiments to prevent T cell killing of EBV-infected cells, suppresses the expression of the interleukin 2 gene (Randak et al., 1990). It is therefore a potent inhibitor of T cell activation, but may not inhibit naïve T cells if they can recognize EBV-infected cells, as they can proliferate without IL-2. Were this the case, LP-KO-infected cord blood B cells may not be

able to establish LCLs because they are slower at proliferation and may be killed due to naïve T cells responses or other immune compartments present in the cord blood cell population. However, LP-REV ^{i} which is also slow in establishing LCLs would be predicted to have a similar defect, but it does not, as it transforms cord PBLs into LCLs with a similar efficiency to adult PBLs. It could also be possible that LP-KO ^{w} fails to suppress an innate immune response(s) triggered in cord blood as it is known that the innate immunity differs between adults and neonates (e.g. higher IL-6, IL-10, IL-23 response in neonates when compared to adults) (Basha et al., 2014).

In contrast to T cells, there is only a limited literature on the differences between cord and adult B cells. However, Ha et al., (2008), characterized a defect in signaling via CD40 in cord B cells. They reported that activation of extracellular signal-regulated kinase (ERK) and p38 after CD40 stimulation of cord blood B cells is very inefficient (Ha et al., 2008). The signals that are induced by activation of co-stimulatory B cell receptor CD40 by T helper cells are mimicked by LMP-1 in EBV infected B cells (Kilger et al., 1998). Therefore, in cord blood B cells, other signals (possibly induced by EBNA-LP) that are LMP-1 independent, could be required to establish LCLs.

To test whether the cord blood transformation defect is caused by the immaturity of cord B cells or presence of other cytotoxic immune compartments, the experiments using purified CD19 cord B cells have to be performed. These experiments are more challenging as the volumes of cord blood that we receive are usually not enough to isolate CD19-positive B cells required for EBV infections. However, in the course of writing this thesis, I undertook a preliminary experiment infecting with LP-KO ^{w} after isolation of CD19-positive B cells from cord blood. Since these infections also failed to generate LCLs, it is likely that the reason for LP-KO's failure to transform cord B cells is due to an intrinsic property of the B cell rather than bystander cells. The growth phenotype was very similar to adult B cells until

approximately day 14, however, between day 14 and 17, when the LP-KO-infected adult B cell population begins to expand, the LP-KO infected cord blood B cells died. It is therefore possible that in cord blood B cells, where the CD40 signaling is impaired and cannot be mimicked by LMP-1, the higher levels of LMP-1 can be toxic and instead of driving proliferation, apoptosis is induced. High levels of LMP-1 have been reported previously to cause toxicity to B-lymphoid lines (Hammerschmidt et al., 1989) and to activate apoptosis in B cells via the UPR pathway (Pratt et al., 2012). We know that in LP-KO infections, the levels of LMP-1 rise above the levels found in WT infections between day 9 and 16 (when the LP-KO ^{w}-infected adult cells start expanding again), and keep on increasing for a further 2 weeks, which corresponds to the time when LP-KO-infected cord blood B cells start dying. More experiments on LMP-1-triggered apoptosis in cord blood B cells are required to test this hypothesis and are now being undertaken in our lab.

It has also been reported that the apoptosis induced by LMP-1 can be inhibited by expression of the anti-apoptotic protein, BCL2A1 (Pratt et al., 2012). *BCL2A1* expression is activated by EBNA-2 in BL31 cells (Fig.3.14). It is possible that in primary cord B cells, EBNA-LP co-activates *BCL2A1* and the failure to do so in LP-KO ^{w}-infected cord B cells (but not adult cells) results in LMP-1-triggered apoptosis. However, experiments to test the differences in gene expression between cord- and adult-infected B cells are required. As we now have access to paired samples of cord and maternal blood, we are in a position to do transcriptomic experiments with the minimal possible variation in the genetic background (for such a type of experiment).

It is possible that different B cell subsets respond to EBV infection in different ways (i.e. LP-KO ^{w} may not be able to transform naïve B cells (which constitute 100% of cord blood B cell population), whereas it can transform activated or memory B cells only). Therefore, we are in the process of sorting adult CD19-positive B cells into 4 sub-populations

(naïve, unswitched memory, switched memory and non-naïve non-memory B cells) based on their CD27 and IgD status and infecting them with LP-KO ^{w} and WT ^{w} viruses to assess whether there is a difference in transformation efficiency between these populations.

Because we do not know when cord B cells become mature (i.e. when cord-like phenotype will change to an adult-like phenotype), assessing the ability of LP-KO ^{w} to transform B cells isolated from children and adolescents could be a useful tool to investigate whether these changes can still be observed in children's B cells and should the timing of the change correlate to onset of puberty, could give us some indications why infectious mononucleosis affects only individuals during or after adolescence.

5.3 Role of EBNA-LP in gene regulation

5.3.1 Viral genes

The changes in expression of the viral latency genes may explain some of the phenotypic changes observed in the outgrowth experiments. LMP-1, LMP-2 and EBER-2 are all radically changed, being very low early and very high later after infection with LP-KO (see section 4.3). The more modest change in EBNA-2 to EBNA-3A ratio early after infection seems less likely to affect outgrowth. As mentioned above, LMP-1 is regulated by EBNA-LP, and seems to be important but not mandatory for the generation of LCLs *in vitro* (Dirmeier et al., 2003). The importance of EBNA-LP in the rapid induction of LMP-1 in the first week after infection supports previously published data from co-transfection experiments into latency I Burkitt lymphoma cell lines (Nitsche et al., 1997). It has been suggested however, that LMP-1 is not important early after WT EBV infection because of the very low levels of this protein during the first two weeks of infection (Price et al., 2012). However,

when compared to LP-KO-infections, even this “low level” of LMP-1 transcripts in WT infection on day 2 is 50 times higher than for EBNA-LP mutants (Fig.4.26). As it is not clear what roles are played by the low levels of LMP-1 found early during infection, we cannot exclude its importance at this time. On the other hand, LP-KO-infected cells may be lacking sufficient growth signals until LMP-1 signaling (or a combination of the genes that exhibit the same expression kinetics) reaches a certain threshold (e.g. the levels observed in WT infections at early time points) at which point the cells re-enter expansion phase. It would therefore be interesting to assess the kinetics of early proliferation of LMP-1 knockout-infected B cells as these have not been described in detail (Dirmeier et al., 2003).

While the low level of LMP-1 observed early during infection was predicted by transient transfection experiments, it was not anticipated that LMP-1 transcript levels would be significantly elevated in LP-KO-infected cells later after infection. It has been shown that LMP-1 can be expressed from two different promoters: a proximal promoter (ED-L1) (Hudson et al., 1985) and a distal promoter within the terminal repeats (TR-L1) (Sadler and Raab-Traub, 1995). During latency III, LMP-1 transcription is induced by EBNA-2 (Wang et al., 1990) but in latency II it is EBNA-2-independent. Our qPCR assay spans exon 2 to exon 3, detecting transcripts initiated by both TR-L1 and ED-L1 (Fig.1.3), thus it would be interesting to assess also the expression only from the distal promoter, which we plan to undertake shortly.

Levels of LMP-2 transcripts varied in a very similar way to the LMP-1 transcript levels. It has been previously published that in co-transfection experiments EBNA-LP co-activated LMP-2B but not LMP-2A (Peng et al., 2005). Our current analysis looked only at total LMP-2 transcripts, so it would be useful to distinguish between expression from the three known LMP-2 promoters: LMP-2A, LMP-2B (Sample et al., 1989) and the promoter in the TR (Fox et al., 2010) in our time course, which is now being assessed in our lab.

Another viral gene whose expression is coordinated with the LMPs during B cell outgrowth is EBER-2. A very recent analysis suggests that EBER-1 is similarly regulated. The function of EBERs is still controversial and unclear, with genetic analyses giving different results depending on the virus strain used: there was an impairment in transformation when Akata EBER-KO was used (Yajima et al., 2005), but no impairment when B95.8-BAC or transformation-competent P3HR1 strains lacking EBERs were assessed (Gregorovic et al., 2011, Swaminathan et al., 1991). It is therefore difficult to draw conclusions from these data. However, the levels of EBER-2 seem to be controlled by EBNA-LP and the different effects of this regulation are observed based on time point after infection. Both *EBER*s are transcribed by RNA polymerase III and contain RNA polymerase III intragenic transcription control regions, but also have three upstream promoter elements more typical of polymerase II-transcribed genes (Howe and Shu, 1989). It has been hypothesized that these upstream elements of the *EBER* genes play a role in the transactivation of *EBER* transcription by EBNAs (Howe and Shu, 1989) but no latency protein has been shown to transactivate *EBER* so far.

Because LMP-1, LMP-2A and EBER-2 follow the same kinetics in LP-KO-infections, it seems likely that there may be a common regulatory mechanism, and/or coordinated regulation of the whole locus upstream of oriP, e.g. by DNA loop formation. The CCCTC-binding factor (CTCF) promotes and regulates chromatin looping by inducing chromatin boundary formation and chromatin insulation (Phillips and Corces, 2009). It has been shown that CTCF binds to the EBV genome upstream of the Cp promoter (Tempera et al., 2011), upstream of EBER (Day et al., 2007) and within the first intron of LMP-2A (Chen et al., 2014), which would probably disrupt potential looping of the whole locus. However, it has been suggested that CTCF has a more complex three-dimensional insulator function

(Chen et al., 2014). Therefore, there is a possibility that EBNA-LP displaces or recruits CTCF to some of these sites impacting the transcription of EBV genes.

Our assessment of EBV gene expression by LP-KO also showed a change in the ratio of EBNA-2 to EBNA-3A (and by extension perhaps the other EBNA-3s, although this has not yet been assessed) as EBNA-3A levels are lower in LP-KO than in WT on day 2 (Fig.4.18). Between day 9 and 16, they reach levels similar to those in WT (Fig.4.18); this is the time when LMPs or EBER-2 levels go up as well (Fig.4.28 and 4.20). However, in contrast to previously described genes, EBNA-3A levels do not go above those observed in WT at later stages after infection.

Some interesting observations were also made using the EBNA-2 knockout virus: expression from the Wp promoter (but not Cp) is dramatically (10 fold) higher in E2-KO infected cells than in WTs or other mutant viruses (Fig.4.22a), which results in an elevation of EBNA-2, EBNA-3A and sisRNA-1 transcripts. Such elevated transcript levels are also observed for LMP-2 (but not LMP-1), when the qPCR data are not normalized to EBNA-2 (not shown), and the normalization to EBNA-2 cancels out this effect (Fig.4.27a). A high level of EBNA-LP in E2 KO-infected cells was confirmed by fluorescence microscopy (Fig.4.7), which fits with the elevated levels of EBNA-3A and EBNA-2 transcripts seen by qPCR. A similar observation was made by Tierney et al., (2011), where in EBNA-2 knockout-infected B cells, other EBNAs were detectable by Western blot even earlier than they appeared in wild-type virus infections (Tierney et al., 2011). These observations are also supported by protein expression in Wp-restricted Burkitt lymphomas, which carry an EBNA-2 gene-deleted genome and express EBNA-1, EBNA-3A, EBNA-3B, and EBNA-3C from the Wp promoter (Kelly et al., 2013). This indicates that EBNA-2 plays a role in suppressing Wp perhaps as a negative feedback loop on its own expression. However, because we only used one E2-KO virus, experiments using independently generated E2-KOs should be performed.

It has been previously described that later during infection the switch in Wp/Cp promoter usage in WT infections is due to extensive Wp methylation (Hutchings et al., 2006). Despite this, Wp is never completely silenced in LCLs (Hutchings et al., 2006), which can be observed from our results. However, in LP-REV ^{i}-infected cells on day 30 the Wp transcript level is significantly higher than in other LCLs (Fig.4.22b). This suggests that the intronic mutations have a role in Wp regulation. However, since the LP-REV ^{i} observation is based on one data point- no conclusion can be drawn just yet. This idea is currently being tested in a sisRNA-1 knockout virus (i.e. a virus completely lacking the small intron between exons W1 and W2).

To better characterize the correlations in expression of viral genes in LP-KO-infected cells and to obtain more information about the mechanism by which EBNA-LP regulates particular genes, a broader panel of viral genes will be analyzed in a new time course, but was not accomplished in time for inclusion in this thesis.

5.3.2 Host genes

A role for EBNA-LP in modulating host gene transcription is not as clear as for viral genes. In a previous study, transfection of EBNA-2 by itself could not induce expression of *cyclin D2* and only when EBNA-2 and EBNA-LP were electroporated together into gp340-primed primary B cells, *cyclin D2* transcripts were detectable at 24h post-transfection (Sinclair et al., 1994). *Cyclin D2* expression was predicted to be lower in LP-KOs early after infection and therefore the main reason for decreased proliferation based on previous research (Sinclair et al., 1994). In our time course however, the levels of *cyclin D2* turned out to be similar 2 days after infection with EBNA-LP-mutant viruses when compared to WT infections (Fig.4.23). A significant difference however, was observed at day 9 post infection, which corresponds to the time when LP-KO-infected B cells appear static (non-proliferative)

(Fig.4.23). It is therefore possible that to enter further efficient proliferation the expression of cyclin D2 has to reach particular levels, which is happening between day 9 and 16 for LP-KOs. However, it is difficult to assess with these experiments whether reduced cyclin D2 expression has caused a reduction in proliferation, or if a block in proliferation has reduced the cyclin D2 expression. Because *cyclin D2* expression is also activated by MYC (Bouchard et al., 2001), we looked at MYC expression, and found it to be the same between WT and LP-KO at all time points (Fig.4.23b), which fits with the absence of literature to suggest that MYC expression is regulated by EBNA-LP. The difference between our and previous experiment on cyclin D2 regulation is that we introduced the whole virus (instead of single plasmids expressing individual proteins) into the cells and the combined action of different EBV proteins/RNAs may induce or co-activate expression of *cyclin D2* in the absence of EBNA-LP. Interestingly, the expression of *cyclin D2* is significantly higher in LP-KO-established early LCLs, perhaps suggesting selection for an elevated CCND2 level may allow expansion of LCLs in the absence of EBNA-LP, or reflecting a mechanism similar to that which leads to elevated LMP levels at thirty days post infection (Fig.4.23a).

HES1 is a host gene whose induction by EBNA-2 has been reported both to be enhanced by EBNA-LP (Portal et al., 2011) and not altered by EBNA-LP (Peng et al., 2005). From our experiments it looks like EBNA-LP does not enhance its transcription, but may limit its transactivation, albeit only early after infection (Fig.4.24). These data are additionally supported by our ChIP results (see section below).

To characterize more host genes whose expression is influenced by EBNA-LP, we are planning to perform RNAseq analysis at two days after infection, when the effect of EBNA-LP on viral target genes is easily measured, but before differences in proliferation rate, cell cycle entry or cell death (or of other EBV genes) are likely to interfere with the analysis. This

would enable us to determine whether there are significant changes in the transcript levels of other host genes when EBNA-LP is absent and give more indications on the mechanism(s) of action of EBNA-LP. Our attempts to determine the gene expression changes in BL31 cells infected with different virus mutants (including LP-KO ^{i} and Y1Y2-KO) did not show any significant changes in levels of proteins that are known to be regulated by EBNA-2 (Fig.3.14). This may be due to the fact that BL31 cells are already transformed and have the MYC translocation characteristic of Burkitt lymphoma cell lines which may mask any effect or pathway triggered by EBNA-LP or because the effect of EBNA-LP regulation is settled in established cell lines in a similar way as it appears in primary B cells infections. The analysis was further compromised by the apparent failure of two of the wild-type controls to express longer isoforms of EBNA-LP and higher levels of EBNA-2 (Fig.3.13). In the PCA these two controls clustered with the LP-KOs, which suggests that they may behave like EBNA-LP knockouts. Having taken these changes into account, the most interesting observation made using this model system, was the change in expression of genes involved in mitochondrial function (e.g. *LYRM7, MRPS17*). LYRM7 is an assembly factor that enables formation of the main enzyme complex in the mitochondrial respiratory chain (complex III or CIII) (Sánchez et al., 2013). Mutations in this gene are associated with lactic acidosis in patients (Invernizzi et al., 2013). Lactic acidosis has been also reported as a result of cancer cells switching their metabolism from an oxidative phosphorylation towards glycolysis, phenomenon known as the Warburg effect (Claudino et al., 2015). Our data suggest that EBNA-LP down-regulates *LYRM7* (Fig.3.13), which could be consistent with inducing the Warburg effect. The association with mitochondria (and by inference, potentially with metabolism) is of particular interest, because EBNA-LP has been already reported to lead to the stabilization of HIF1α and activation of the aerobic glycolytic pathway, permitting a Warburg effect (Darekar et al., 2012). However, our initial attempts to assess HIF1α stabilization, by flow cytometry and

immunofluorescence microscopy were not successful, so we did not pursue this further. The expression of genes engaged in metabolic switch could be analyzed in primary B cell infection using RNAseq experiments and the difference in metabolism between LP-KO- and WT-infected cells will be assessed soon using oxygen consumption assays.

5.3.3 Mechanism of gene regulation by EBNA-LP

To further assess the mechanism of action of EBNA-LP in gene regulation based on the interesting results obtained for LMP-1 and HES1 transcription, ChIP analysis has been performed on infected primary B cells in our lab by Richard Palermo, to look at EBNA-2, and a transcription factor associated with its binding sites, RBPJ. Attempts to ChIP EBNA-LP failed to conclusively identify any binding at EBNA-2 binding sites on day 2, and since we have no positive control for EBNA-LP binding, it is not clear whether this ChIP even worked. A previously published EBNA-LP ChIP (Portal et al., 2013), showed rather poor signal strength, with the reported signal only marginally different from background binding across the genome. The observed background may be due to the JF186 EBNA-LP antibody, which may not be suitable to perform ChIP analysis, or to the possibility that EBNA-LP does not bind to the chromatin at these locations (or indeed at any locations).

However, ChIP performed for EBNA-2 in primary infections (comparing WT ^{w} with LP-KO ^{w} infections) revealed that while there are strong signals for EBNA-2 binding at the LMP-1 and LMP-2A transcription start sites in WT ^{w}-infected B cells on day 2 (Fig.5.1a), there is no signal (above the IgG control) for EBNA-2 at these sites in LP-KO ^{w}-infected cells. EBNA-2 is slowly recruited (taking two weeks or more) to the sites at later time points in the infection (Richard Palermo, unpublished data).

In contrast, there was abundant EBNA-2 binding at the HES1 transcriptional start site in both LP-KO ^{w}- infected and WT ^{w}-infected B cells on day 2 (Fig.5.1a). EBNA-2 binding at *HES1* (and other host genes) is consistently a little higher in LP-KO ^{w}-infected cells, which correlates with the qPCR data showing higher levels of HES1 transcripts in LP-KO ^{w} than in WT ^{w} early after infection (Fig.4.25). This suggests that while EBNA-LP is required for EBNA-2's rapid recruitment to the LMP locus after infection, it is not required for EBNA-2 binding at HES1 locus, but may have a role in modulating (i.e. limiting) its recruitment. Therefore, there is possibility that EBNA-LP is much more important for allowing the recruitment of transcription factors to the naked (or freshly chromatinised) DNA of the virus genome compared to host DNA, i.e. setting up the incoming viral genome for transcription.

It has been recently published that EBNA-2 drives formation of new chromatin binding sites for transcription factors RBPJ and EBF1 (Lu et al., 2016). However, ChIP for RBPJ (performed in our lab by Richard Palermo) showed no difference in RBPJ levels between LP-KO ^{w}-infected and WT ^{w}-infected B cells on day 2 at any of the checked sites (Fig.5.1b). It is therefore possible, that the recruitment of RBPJ by EBNA-2 reported by Lu et al., (2016), is only true for RBPJ-dependent (and perhaps also EBNA-LP-independent) binding to chromatin and that the EBNA-2 binding to LMP-1/LMP-2A sites at day 2 after primary infection is RBPJ-independent and depends on EBNA-LP instead or that RBPJ alone is not sufficient to recruit EBNA-2 at these sites. However, at this stage, there are many other possibilities of the mechanism through which LMP-1/LMP-2A are activated early after infection. It may be that EBNA-LP recruits EBNA-2 via other transcription factors like EBF1, PU.1, PAX5 and many others that have been previously described as important in LMP-1 activation (Price et al., 2012, Lu et al., 2016). EBF1 is an especially interesting candidate as its depletion alters EBNA-2 binding to *LMP-1* but not *HES1* and it is also found at *EBER* locus (Lu et al., 2016). An alternative reason may be interaction of EBNA-LP with

repressive complexes like NCoR (Portal et al., 2011) or HDACs (Portal et al., 2006) that has been reported previously, and removing them from the EBNA-2 binding sites, which we are planning to characterize now in our lab. Additionally, the EBNA-LP action does not have to be direct; lack of expression of EBNA-LP may decrease/inhibit expression of transcription factors, or regulate them in a post-translational manner, altering the localization or modification of factors. Our planned RNAseq experiment will characterize the effect of EBNA-LP depletion on the expression of genes (both viral and host) that we have not assessed by qPCR.

It is interesting to ask what recruits EBNA-2 to these sites. We know that the fully repressed state of EBNA-3s-regulated genes is only achieved by around 30 days (Kalchschmidt et al., 2016a, Skalska et al., 2010), but we do not understand why gene regulation by EBNA-3s take place over such a long period of time. In contrast, the activation of genes by EBNA-2 is generally invoked quite rapidly (Spender et al., 2001). It is therefore possible that EBNA-2 by itself requires more time to induce changes in gene expression and only in the presence of EBNA-LP its rapid action is enabled. We also do not yet understand why the levels of LMP-1 are much higher in LP-KO ^{w}-infected cells than in WT ^{w}-infected cells at the later time points. It is possible that something drives the limited expression of LMP-1 early after infection with LP-KO ^{w} that would be removed by EBNA-LP, and when EBNA-2 finally binds to its LMP-1 transcription site, the effect is additive. Therefore, we observe a higher maximum level of LMP-1 transcripts at later times after infection.

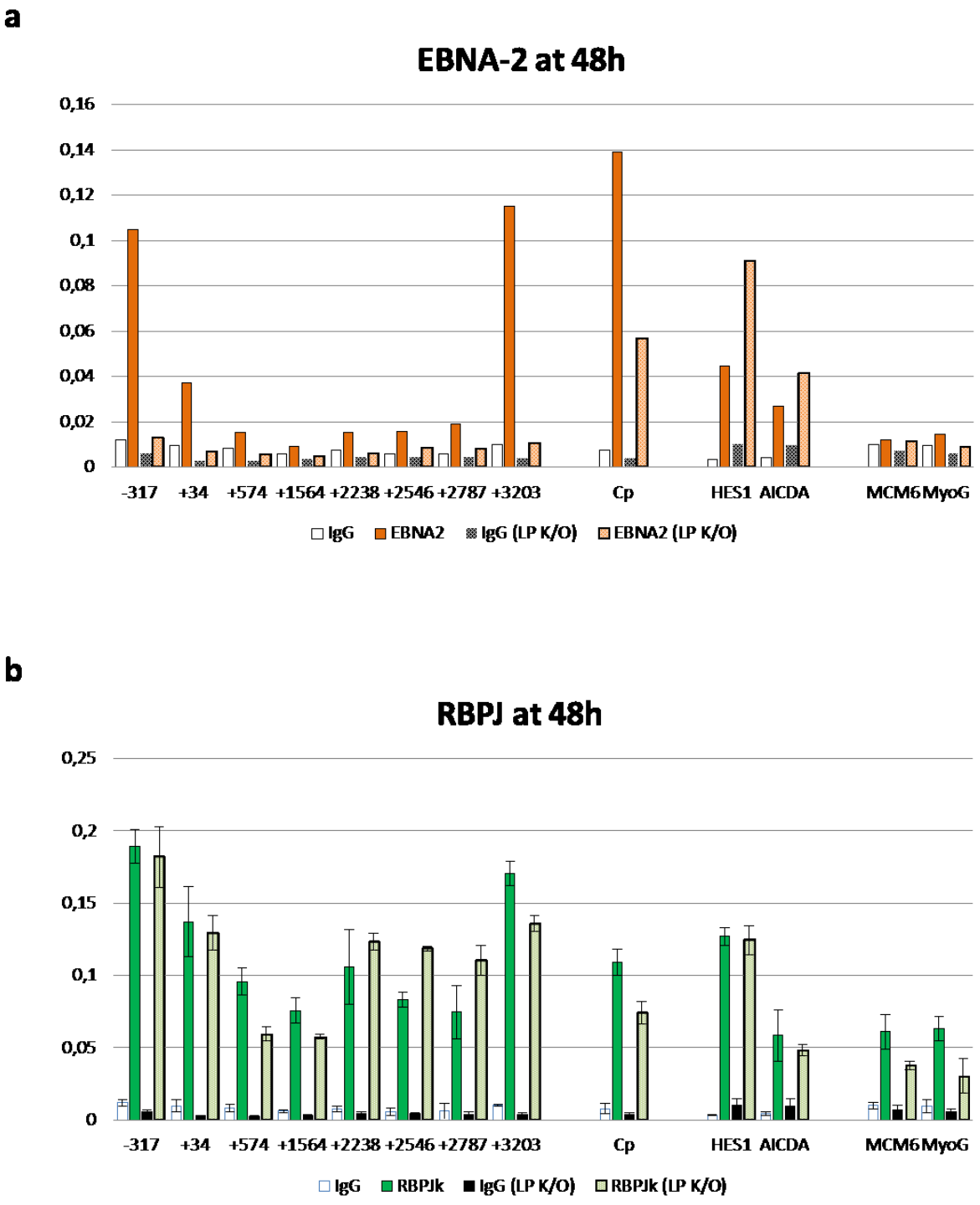

Fig. 5.1 Binding of EBNA-2 and RBPJ at transcription sites two days after primary B cell infection. The x-axis indicates the positions amplified by the qPCR assays. The numbers represent distance of the assay from the LMP-1 transcriptional start site: The EBNA-2 binding sites in the LMP-1 promoter is at -317 and in the LMP-2A promoter at +3203. Promoter-proximal binding sites in Cp, HES1 and AICDA. As controls without RBPJ or EBNA-2 binding sites, MCM6 and MyoG promoter primers were used. Darker bars represent ChIPs from WT ^{w} infections; lighter bars represent LP-KO ^{w} infections. Non-specific species-matched IgG ChIP (black/white bars) was performed as a negative control. Experimental data and figure were produced by Richard Palermo.

5.3.4 Association with Sp100

As mentioned above, it is not known how EBNA-LP co-regulates EBNA2's activation of genes. In addition to NCoR and HDAC4/5, Sp100 has also been theorized as a mediator of EBNA-2 transcriptional enhancement (see section 1.9.9.1). Sp100 and other components of PML NBs that are able to act as antiviral restriction factors have been shown in multiple contexts to be manipulated or targeted for degradation by a number of different DNA viruses in order to allow viral gene expression or replication (Everett et al., 2006). For instance, PML NBs are disrupted by the HSV protein ICP0, which then leads to the degradation of PML and Sp100 (Everett, 2001), and by CMV proteins IE1 and IE2, which displace PML and Sp100 from PML NBs (Ahn et al., 1998). Displacement of Sp100 from nuclear bodies by EBV was reported two days after B cell infection, and attributed to EBNA-LP based on a series of transfection experiments in HeLa cells (Ling et al., 2005). We did not attempt to reproduce the displacement by overexpression of EBNA-LP alone. However, we were not able to reproduce the previously reported pattern in primary B cells (i.e. Sp100 localized to multiple (~10) very small but well defined foci in uninfected cells but no detectable Sp100 foci were seen in EBV-infected cells (Ling et al., 2005)), despite using different fixation conditions, different antibodies and different EBV strains and mutants.

We were not able to establish which anti-Sp100 antibody was used in the previous study; the polyclonal serum sent to us by the Ling group did not reproduce the previously observed pattern of Sp100 distribution in the cells: Sp100 was barely detectable in uninfected cells, showed a mostly dispersed nuclear localization in EBV-infected cells and was prone to bind to background extracellular foci that were also bound by several secondary anti-mouse antibodies (Fig.4.8). A second antibody (SpGH received from Professor Everett that has been widely used to detect Sp100 in a variety of different contexts) gave us the clear expected (localized to foci) pattern, but no displacement of Sp100 after infection with EBV was seen

(Fig.4.9). On the contrary, Sp100 was more readily detected in infected than uninfected cells: this may be either because of the state of uninfected cell, which start dying due to lack of survival signals or because of an innate immune activation triggering the up-regulation of Sp100 in infected cells. The only difference that we were able to attribute to EBNA-LP was a subjectively slightly bigger size of Sp100 foci in LP-KO-infected B cells on day 2 when acetone permeabilization was used (Fig.4.12). It is therefore possible that maybe EBNA-LP (through its interaction with Sp100) makes the whole nuclear body structure less tight, reducing the affinity between Sp100 and PML, such that when a more stringent permeabilization is used, this structure may be more easily disrupted, decreasing the size of Sp100 dots in WT-infected cells on day 2; if extended permeabilization with acetone was used in the previous study it could possibly cause the complete disruption of Sp100 dots.

There are several Sp100 splice variants that have been identified (Guldner et al., 1999) as well as different modified forms of Sp100 based on their sumoylation (Müller and Dejean, 1999). Various Sp100 splice variant have different patterns of localization, e.g. Sp100A localizes to PML NBs, while Sp100B, Sp100C and Sp100HMG are mostly dispersed (Negorev et al., 2006). It has been reported that only these dispersed isoforms of Sp100 are responsible for suppressing the HSV immediate early (IE) proteins expression (Negorev et al., 2006). It is therefore possible that the antibodies we used recognize different forms of Sp100 from the antibody used in the previous study. Also, if the antibody received from Paul Ling's group recognizes the more dispersed isoforms of Sp100, this could explain the observed up-regulation after EBV infection as a result of cell defense mechanisms to suppress the expression of viral proteins and no change observed in the Sp100 pattern when SpGH antibody is used. Additionally, different anti-Sp100 antibodies (including an antibody that recognizes only sumoylated Sp100) have been tested in our group for western blotting in

different cell types, but because of the challenges of infecting cells in large enough numbers for Western blotting, we have not yet analyzed them in primary infections.

Another difference between our methodology and the Ling lab's experiment is the way of infecting the cells. In our experiments cells were infected for 2-3h with virus-containing supernatant (the supernatant was either obtained by transfection of producer HEK293 cell lines or by 4-hydroxytamoxifen (HT) induction of B95.8 ZHT and culturing both of them for 4 days), then the virus was removed and cells resuspended in fresh primary B cell media with suitable for their growth FCS. The previous study used virus-containing supernatant derived from B95.8 cells (obtained by culturing B95.8 to saturation for 9-12 days) and cells were infected and incubated in this supernatant until fixation for microscopy staining. It is therefore possible that something produced by the stressed B95.8 cells (as they were kept for so long in the same medium to induce virus production as a stress response) may have contributed to the displacement of Sp100 by EBV, which did not occur in our system. Conversely, it is possible that HT and the two different chemicals used for transfection of producer cell lines could prevent the dispersal of Sp100 by EBV. For instance, Sp100 is induced by interferon (Grötzinger et al., 1996) so any stimulus that induces interferon could mask the dispersal of Sp100 by EBNA-LP.

Another interferon-inducible protein that has been shown as a critical antiviral factor and sensor of viral DNA is IFI16 (Diner et al., 2015). It has been reported that during early HSV infection, IFI16 is targeted for degradation (Diner et al., 2015), after KSHV infection it localizes mostly to the cytoplasm (Kerur et al., 2011) but after vaccinia infection it remains in the nucleus (Kerur et al., 2011). It has also been reported that IFI16 can recognize EBV latent genome and re-localizes from the nucleus to the cytoplasm 48h after infection (Ansari et al., 2013). We did not observe the re-localization of IFI16 in our experiments, although Ansari et al., (2013), used a different primary antibody (raised in mice), which we have not tested

because it could not be combined with EBNA-LP staining. Also, maybe our viruses trigger a different innate immune activation from theirs, for reasons we do not understand.

In future work different approaches can be taken to further investigate association of EBNA-LP with different PML components, e.g. making new detection reagents (Affimers) against different Sp100 isoforms, looking at different ways of preparing and analyzing the cells, such as image-associated flow cytometry to further investigate and quantify the change in size and number of Sp100 foci.

5.4 Identification of infected cells

One of our aims was to comprehensively analyze the changes in the cell induced by EBNA-LP, which entails global analyses of cellular properties. A lot of the analyses that could be performed in primary B cell infections (particularly protein mass spectometry) and would give us answers about the role of EBNA-LP, require or would give clearer data with a homogenous population of latently infected cells. This is very difficult to achieve by infection alone with the virus titers that we can produce. As has been reported previously, even when primary B cells are infected with EBV at MOI=100, only 80% cells become infected (Shannon-Lowe et al., 2005). Similarly, where different recombinant viruses induce different proliferation efficiencies (as seen with the LP-KOs), the transcriptome and proteome differences between the cells would become dominated by cell cycle-associated factors, and it is likely that the underlying causes would become lost in this experimental noise. Therefore, it would be ideal to be able to identify and sort for the population of infected cells before they start to proliferate.

The CD23 and CD58 molecules have been identified previously as markers expressed at early times after EBV infection (Megyola et al., 2011). However, we did not see a

significant or consistent increase in CD23 or CD58 signal until approximately 5-7 days post infection with WT EBV (when the cells are already proliferating) over the signal from uninfected or E2-KO-infected B cells. We have not excluded the possibility that use of a different antibody against these proteins, changing the quality or source of the B cells (especially reducing unwanted activation), using different fluorophore or other technical variables could improve these signals. However, there was some inconsistency in the time points in the previously published experiments (see Megyola et al., (2011): Fig.1), as they reported 45% CD23 positive B cells at 44h post infection but only 30% at 66h post infection.

Our attempt to use Smart Flare technology with the intention of detecting latent transcripts by day 3 was prevented by the high background of the negative control, limiting further investigation and development of a useful probe.

Sorting cells based on whether they have proliferated could be achieved using CellTrace violet. This technique permits the sorting of infected cells based on whether they have divided and explore further the mechanism of proliferation driven by EBNA-LP (Nikitin et al., 2010). However, based on our experience with a high rate of cell death triggered by CellTrace, this experimental approach is not without a risk, even if the differing proliferation rates were not problematic.

In the future it would potentially be very useful to perform a cell surface proteome experiment to identify robustly up-regulated cell surface markers that could be used to isolate these early infected cells.

5.5 Summary

The experiments presented in this thesis provide the first identification of the role of EBNA-LP in early B cell infection and transformation and highlighted different aspects of its significance. We have found that EBNA-LP is not critical for transformation of adult B cells but is required to transform cord B cells. This difference in phenotype between LP-KO-infected neonatal and adult cells provokes questions about the functional differences between mature and immature B cells, between adult, neonatal and childhood immune cells, and their responses to EBV infection, which could have a clinical relevance to age-associated pathology such as infectious mononucleosis. EBNA-LP regulation of both viral and host genes gave us direction to investigate the impact of EBNA-LP at the chromatin level and resulted in discovering its importance of recruiting EBNA-2 to EBV genome. The potential importance of sisRNAs in transformation has also been demonstrated- albeit unintentionally- by our study. Generation of sisRNAs mutants and combining the data with those obtained from LP-KO-infections will allow us for better understanding of a complex action of EBV early after B cell infection and in establishing latency.

6 REFERENCES

Abbot, S.D., M. Rowe, K. Cadwallader, A. Ricksten, J. Gordon, F. Wang, L. Rymo, and A.B. Rickinson. 1990. Epstein-Barr virus nuclear antigen 2 induces expression of the virus-encoded latent membrane protein. *J. Virol.* 64:2126–34.

Adams, A. 1987. Replication of Latent Epstein-Barr Virus Genomes in Raji Cells. *J. Virol.* 61:1743–1746.

Adams, J.M., A.W. Harris, C.A. Pinkert, L.M. Corcoran, W.S. Alexander, S. Cory, R.D. Palmiter, and R.L. Brinster. 1985. The c-myc oncogene driven by immunoglobulin enhancers induces lymphoid malignancy in transgenic mice. *Nature*. 318:533–8.

Adamson, a L., and S. Kenney. 2001. Epstein-barr virus immediate-early protein BZLF1 is SUMO-1 modified and disrupts promyelocytic leukemia bodies. *J. Virol.* 75:2388–99. doi:10.1128/JVI.75.5.2388-2399.2001.

Adler, B., E. Schaadt, B. Kempkes, U. Zimber-Strobl, B. Baier, and G.W. Bornkamm. 2002. Control of Epstein-Barr virus reactivation by activated CD40 and viral latent membrane protein 1. *Proc. Natl. Acad. Sci. U. S. A.* 99:437–42. doi:10.1073/pnas.221439999.

Ahmed, M., M. Lock, C.G. Miller, and N.W. Fraser. 2002. Regions of the herpes simplex virus type 1 latency-associated transcript that protect cells from apoptosis in vitro and protect neuronal cells in vivo. *J. Virol.* 76:717–29. doi:10.1128/JVI.76.2.717-729.2002.

Ahmed, W., P.S. Philip, S. Tariq, and G. Khan. 2014. Epstein-Barr virus-encoded small RNAs (EBERs) are present in fractions related to exosomes released by EBV-transformed cells. *PLoS One*. 9. doi:10.1371/journal.pone.0099163.

Ahn, J.H., E.J. Brignole, and G.S. Hayward. 1998. Disruption of PML subnuclear domains by the acidic IE1 protein of human cytomegalovirus is mediated through interaction with PML and may modulate a RING finger-dependent cryptic transactivator function of PML. *Mol. Cell. Biol.* 18:4899–4913.

Ahsan, N., T. Kanda, K. Nagashima, and K. Takada. 2005. Epstein-Barr Virus Transforming Protein LMP1 Plays a Critical Role in Virus Production Epstein-Barr Virus Transforming Protein LMP1 Plays a Critical Role in Virus Production. *J. Virol.* 79:4415–4424. doi:10.1128/JVI.79.7.4415.

Allday, M.J. 2009. How does Epstein-Barr virus (EBV) complement the activation of Myc in the pathogenesis of Burkitt's lymphoma? *Semin. Cancer Biol.* 19:366–376. doi:10.1016/j.semcancer.2009.07.007.

Allday, M.J., D.H. Crawford, and B.E. Griffin. 1989. Epstein-Barr virus latent gene expression during the initiation of B cell immortalization. *J. Gen. Virol.* 70:1755–1764. doi:10.1099/0022-1317-70-7-1755.

Ambinder, R.F., W. a Shah, D.R. Rawlins, G.S. Hayward, and S.D. Hayward. 1990. Definition of the sequence requirements for binding of the EBNA-1 protein to its palindromic target sites in Epstein-Barr virus DNA. *J. Virol.* 64:2369–2379.

Anderson, L.J., and R. Longnecker. 2008. An auto-regulatory loop for EBV LMP2A involves activation of Notch. *Virology*. 371:257–266. doi:10.1016/j.virol.2007.10.009.

Anderton, E., J. Yee, P. Smith, T. Crook, R.E. White, and M.J. Allday. 2008. Two Epstein-Barr virus (EBV) oncoproteins cooperate to repress expression of the proapoptotic tumour-suppressor Bim: clues to the pathogenesis of Burkitt's lymphoma. *Oncogene*. 27:421–433. doi:10.1038/sj.onc.1210668.

Ansari, M.A., V.V. Singh, S. Dutta, M.V. Veettil, D. Dutta, L. Chikoti, J. Lu, D. Everly, and B. Chandran. 2013. Constitutive interferon-inducible protein 16-inflammasome activation during Epstein-Barr virus latency I, II, and III in B and epithelial cells. *J. Virol.* 87:8606–23. doi:10.1128/JVI.00805-13.

Audas, T.E., M.D. Jacob, and S. Lee. 2012. Immobilization of Proteins in the Nucleolus by Ribosomal Intergenic Spacer Noncoding RNA. *Mol. Cell*. 45:147–157. doi:10.1016/j.molcel.2011.12.012.

Azim, T., M.J. Allday, and D.H. Crawford. 1990. Immortalization of Epstein-Barr virus-infected CD23-negative B lymphocytes by the addition of B cell growth factor. *J. Gen. Virol.* 71:665–671.

Baer, R., A.T. Bankier, M.D. Biggin, P.L. Deininger, P.J. Farrell, T.J. Gibson, G. Hatfull, G.S. Hudson, S.C. Satchwell, and C. Séguin. 1984. 1984-Nature-Baer-DNA sequence and expression of the B95-8 Epstein-Barr virus genome. *Nature*. 310:207–11. doi:10.1038/310207a0.

Bakacs, T., E. Svedmyr, E. Klein, L. Rombo, and D. Weiland. 1978. EBV-related cytotoxicity of Fc receptor negative T lymphocytes separated from the blood of

infectious mononucleosis patients. *Cancer Lett.* 4:185–189. doi:10.1016/S0304-3835(78)94347-1.

Balfour, H.H., O.A. Odumade, D.O. Schmeling, B.D. Mullan, J.A. Ed, J.A. Knight, H.E. Vezina, W. Thomas, and K.A. Hogquist. 2013. Behavioral, virologic, and immunologic factors associated with acquisition and severity of primary epstein-barr virus infection in university students. *J. Infect. Dis.* 207:80–88. doi:10.1093/infdis/jis646.

Balfour, H.H.J., S.K. Dunmire, and K.A. Hogquist. 2015. Infectious mononucleosis. *Clin. Transl. Immunol.* 4:e33. doi:10.1038/cti.2015.1.

Bandobashi, K., a Maeda, N. Teramoto, N. Nagy, L. Székely, H. Taguchi, I. Miyoshi, G. Klein, and E. Klein. 2001. Intranuclear localization of the transcription coadaptor CBP/p300 and the transcription factor RBP-Jk in relation to EBNA-2 and -5 in B lymphocytes. *Virology*. 288:275–82. doi:10.1006/viro.2001.1103.

Barth, S., T. Pfuhl, A. Mamiani, C. Ehses, K. Roemer, E. Kremmer, C. Jäker, J. Höck, G. Meister, and F.A. Grässer. 2008. Epstein-Barr virus-encoded microRNA miR-BART2 down-regulates the viral DNA polymerase BALF5. *Nucleic Acids Res.* 36:666–675. doi:10.1093/nar/gkm1080.

Basha, S., N. Surendran, and M. Pichichero. 2014. Immune responses in neonates. *Expert Rev. Clin. Immunol.* 10:1171–84. doi:10.1586/1744666X.2014.942288.

van Beek, J., A.A.T.P. Brink, M.B.H.J. Vervoort, M.J.M. van Zijp, C.J.L.M. Meijer, A.J.C. van del Brule, and J.M. Middledorp. 2003. In vivo transcription of the Epstein-Barr virus (EBV) BamHI-A region without associated in vivo BARFO protein expression in multiple EBV-associated disorders. *J. Gen. Virol.* 84:2647–2659. doi:10.1099/vir.0.19196-0.

Bell, A.I., K. Groves, G.L. Kelly, D. Croom-Carter, E. Hui, A.T.C. Chan, and A.B. Rickinson. 2006. Analysis of Epstein-Barr virus latent gene expression in endemic Burkitt's lymphoma and nasopharyngeal carcinoma tumour cells by using quantitative real-time PCR assays. *J. Gen. Virol.* 87:2885–2890. doi:10.1099/vir.0.81906-0.

Bell, P., P.M. Lieberman, and G.G. Maul. 2000. Lytic but not latent replication of epstein-barr virus is associated with PML and induces sequential release of nuclear domain 10 proteins. *J. Virol.* 74:11800–11810. doi:10.1128/JVI.74.24.11800-11810.2000.

Bemark, M., and M.S. Neuberger. 2000. The c-MYC allele that is translocated into the IgH

locus undergoes constitutive hypermutation in a Burkitt's lymphoma line. *Oncogene*. 19:3404–3410. doi:10.1038/sj.onc.1203686.

Bhende, P.M., W.T. Seaman, H.-J. Delecluse, and S.C. Kenney. 2004. The EBV lytic switch protein, Z, preferentially binds to and activates the methylated viral genome. *Nat. Genet.* 36:1099–1104. doi:10.1038/ng1424.

Bodescot, M., and M. Perricaudet. 1986. Epstein-Barr virus mRNAs produced by alternative splicing. *Nucleic Acids Res.* 14:7103–14.

Bornkamm, G.W., and W. Hammerschmidt. 2001. Molecular virology of Epstein-Barr virus. *Philos. Trans. R. Soc. Lond. B. Biol. Sci.* 356:437–59. doi:10.1098/rstb.2000.0781.

Borza, C.M., and L.M. Hutt-Fletcher. 2002. Alternate replication in B cells and epithelial cells switches tropism of Epstein-Barr virus. *Nat. Med.* 8:594–599. doi:10.1038/nm0602-594.

Bouchard, C., O. Dittrich, A. Kiermaier, K. Dohmann, A. Menkel, M. Eilers, and B. Lüscher. 2001. Regulation of cyclin D2 gene expression by the Myc/Max/Mad network: Myc-dependent TRRAP recruitment and histone acetylation at the cyclin D2 promoter. *Genes Dev.* 15:2042–2047. doi:10.1101/gad.907901.

Brady, G., G.J. MacArthur, and P.J. Farrell. 2007. Epstein-Barr virus and Burkitt lymphoma. *J. Clin. Pathol.* 60:1397–402. doi:10.1136/jcp.2007.047977.

Brinkman, K.K., P. Mishra, and N.W. Fraser. 2013. The half-life of the HSV-1 1.5 kb LAT intron is similar to the half-life of the 2.0 kb LAT intron. *J. Neurovirol.* 19:102–108. doi:doi:10.1007/s13365-012-0146-6.

Burton, E. a, C.-S. Hong, and J.C. Glorioso. 2003. The stable 2.0-kilobase intron of the herpes simplex virus type 1 latency-associated transcript does not function as an antisense repressor of ICP0 in nonneuronal cells. *J. Virol.* 77:3516–3530. doi:10.1128/JVI.77.6.3516-3530.2003.

Cahir-McFarland, E.D., K. Carter, A. Rosenwald, J.M. Giltnane, S.E. Henrickson, L.M. Staudt, and E. Kieff. 2004. Role of NF-kappa B in cell survival and transcription of latent membrane protein 1-expressing or Epstein-Barr virus latency III-infected cells. *J. Virol.* 78:4108–19. doi:10.1128/JVI.78.8.4108.

Cai, X., A. Schäfer, S. Lu, J.P. Bilello, R.C. Desrosiers, R. Edwards, N. Raab-Traub, and B.R. Cullen. 2006. Epstein-Barr virus microRNAs are evolutionarily conserved and

differentially expressed. *PLoS Pathog.* 2:e23. doi:10.1371/journal.ppat.0020023.

Chen, H.-S., K. a Martin, F. Lu, L.N. Lupey, J.M. Mueller, P.M. Lieberman, and I. Tempera. 2014. Epigenetic deregulation of the LMP1/LMP2 locus of Epstein-Barr virus by mutation of a single CTCF-cohesin binding site. *J. Virol.* 88:1703–13. doi:10.1128/JVI.02209-13.

Chen, M.-R. 2011. Epstein-barr virus, the immune system, and associated diseases. *Front. Microbiol.* 2:5. doi:10.3389/fmicb.2011.00005.

Chesnokova, L.S., and L.M. Hutt-Fletcher. 2014. Epstein-Barr virus infection mechanisms. *Chin. J. Cancer*. 33:545–548. doi:10.5732/cjc.014.10168.

Chijioke, O., A. Müller, R. Feederle, M.H.M. Barros, C. Krieg, V. Emmel, E. Marcenaro, C.S. Leung, O. Antsiferova, V. Landtwing, W. Bossart, A. Moretta, R. Hassan, O. Boyman, G. Niedobitek, H.J. Delecluse, R. Capaul, and C. Münz. 2013. Human natural killer cells prevent infectious mononucleosis features by targeting lytic epstein-barr virus infection. *Cell Rep.* 5:1489–1498. doi:10.1016/j.celrep.2013.11.041.

Claudino, W.M., A. Dias, W. Tse, and V.R. Sharma. 2015. Type B lactic acidosis: a rare but life threatening hematologic emergency. A case illustration and brief review. *Am. J. Blood Res.* 5:25–9.

Clute, S.C., Y.N. Naumov, L.B. Watkin, N. Aslan, J.L. Sullivan, K. Luzuriaga, R.M. Welsh, and R. Puzone. 2013. NIH Public Access. 185:6753–6764. doi:10.4049/jimmunol.1000812.Broad.

Clute, S.C., L.B. Watkin, M. Cornberg, Y.N. Naumov, J.L. Sullivan, K. Luzuriaga, R.M. Welsh, and L.K. Selin. 2005. Cross-reactive influenza virus – specific CD8 + T cells contribute to lymphoproliferation in Epstein-Barr virus – associated infectious mononucleosis. *J. Clin. Invest.* 115. doi:10.1172/JCI25078.3602.

Cohen, J.I., F. Wang, J. Mannick, and E. Kieff. 1989. Epstein-Barr virus nuclear protein 2 is a key determinant of lymphocyte transformation. *Proc. Natl. Acad. Sci. U. S. A.* 86:9558–62. doi:10.1073/pnas.86.23.9558.

Cooper, A., E. Johannsen, S. Maruo, E. Cahir-McFarland, D. Illanes, D. Davidson, and E. Kieff. 2003. EBNA3A association with RBP-Jkappa down-regulates c-myc and Epstein-Barr virus-transformed lymphoblast growth. *J. Virol.* 77:999–1010. doi:10.1128/JVI.77.2.999-1010.2003.

Darekar, S., K. Georgiou, M. Yurchenko, S.P. Yenamandra, G. Chachami, G. Simos, G. Klein, and E. Kashuba. 2012. Epstein-barr virus immortalization of human B-cells leads to stabilization of hypoxia-induced factor 1 alpha, congruent with the Warburg effect. *PLoS One*. 7:1–8. doi:10.1371/journal.pone.0042072.

Day, L., C.M. Chau, M. Nebozhyn, A.J. Rennekamp, M. Showe, and P.M. Lieberman. 2007. Chromatin profiling of Epstein-Barr virus latency control region. *J. Virol.* 81:6389–6401. doi:10.1128/JVI.02172-06.

Delecluse, H.J., and W. Hammerschmidt. 2000. The genetic approach to the Epstein-Barr virus: from basic virology to gene therapy. *Mol. Pathol.* 53:270–9. doi:10.1136/mp.53.5.270.

Delecluse, H.-J., T. Hilsendegen, D. Pich, R. Zeidler, and W. Hammerschmidt. 1998. Propagation and recovery of intact, infectious Epstein-Barr virus from prokaryotic to human cells. *Proc. Natl. Acad. Sci. U. S. A.* 95:8245–8250.

Demetriades, C., and G. Mosialos. 2009. The LMP1 promoter can be transactivated directly by NF-kappaB. *J. Virol.* 83:5269–77. doi:10.1128/JVI.00097-09.

Denko, N.C. 2008. Hypoxia, HIF1 and glucose metabolism in the solid tumour. TL - 8. *Nat. Rev. Cancer*. 8 VN-re:705–713. doi:10.1038/nrc2468.

Dillner, J., B. Kallin, H. Alexander, I. Ernberg, M. Uno, Y. Ono, G. Klein, and R.A. Lerner. 1986. An Epstein-Barr virus (EBV)-determined nuclear antigen (EBNA5) partly encoded by the transformation-associated Bam WYH region of EBV DNA: preferential expression in lymphoblastoid cell lines. *Proc. Natl. Acad. Sci. U. S. A.* 83:6641–5. doi:10.1073/pnas.83.17.6641.

Diner, B.A., K.K. Lum, and I.M. Cristea. 2015. The emerging role of nuclear viral DNA sensors. *J. Biol. Chem.* 290:26412–26421. doi:10.1074/jbc.R115.652289.

Dirmeier, U., B. Neuhierl, E. Kilger, H.B. Cells, E. Virus, G. Reisbach, M.L. Sandberg, and W. Hammerschmidt. 2003. Latent Membrane Protein 1 Is Critical for Efficient Growth Transformation of Human B Cells by Epstein-Barr Virus Latent Membrane Protein 1 Is Critical for Efficient Growth Transformation of. 2982–2989.

Dong, Y.L., and B. Sugden. 2008. The LMP1 oncogene of EBV activates PERK and the unfolded protein response to drive its own synthesis. *Blood*. 111:2280–2289. doi:10.1182/blood-2007-07-100032.

Draborg, A.H., K. Duus, and G. Houen. 2013. Epstein-Barr virus in systemic autoimmune diseases. *Clin. Dev. Immunol.* 2013:535738. doi:10.1155/2013/535738.

Dufva, M., M. Olsson, and L. Rymo. 2001. Epstein-Barr virus nuclear antigen 5 interacts with HAX-1, a possible component of the B-cell receptor signalling pathway. *J. Gen. Virol.* 82:1581–1587.

Ehlin-Henriksson, B., J. Gordon, and G. Klein. 2003. B-lymphocyte subpopulations are equally susceptible to Epstein-Barr virus infection, irrespective of immunoglobulin isotype expression. *Immunology*. 108:427–430. doi:10.1046/j.1365-2567.2003.01601.x.

Epstein, M.A., G. Henle, B.G. Achong, and Y.M. Barr. 1965. Morphological and Biological Studies on a Virus in Cultured Lymphoblasts From Burkitt'S Lymphoma. *J. Exp. Med.* 121:761–70. doi:10.1084/jem.121.5.761.

Everett, R.D. 2001. DNA viruses and viral proteins that interact with PML nuclear bodies. *Oncogene*. 20:7266–7273. doi:10.1038/sj.onc.1204759.

Everett, R.D. 2006. Interactions between DNA viruses, ND10 and the DNA damage response. *Cell. Microbiol.* 8:365–374. doi:10.1111/j.1462-5822.2005.00677.x.

Everett, R.D., S. Rechter, P. Papior, N. Tavalai, T. Stamminger, and A. Orr. 2006. PML contributes to a cellular mechanism of repression of herpes simplex virus type 1 infection that is inactivated by ICP0. *J. Virol.* 80:7995–8005. doi:10.1128/JVI.00734-06.

Fadeel, B., and E. Grzybowska. 2009. HAX-1: A multifunctional protein with emerging roles in human disease. *Biochim. Biophys. Acta - Gen. Subj.* 1790:1139–1148. doi:10.1016/j.bbagen.2009.06.004.

Falk, K.I., and I. Ernberg. 1999. Demethylation of the Epstein-Barr virus origin of lytic replication and of the immediate early gene BZLF1 is DNA replication independent. *Arch. Virol.* 144:2219–2227. doi:10.1007/s007050050636.

Farrell, M.J., A.T. Dobson, and L.T. Feldman. 1991. Herpes simplex virus latency-associated transcript is a stable intron. *Proc. Natl. Acad. Sci. U. S. A.* 88:790–4. doi:10.1073/pnas.88.3.790.

Feederle, R., E.J. Bartlett, and H.-J. Delecluse. 2010. Epstein-Barr virus genetics: talking about the BAC generation. *Herpesviridae*. 1:6. doi:10.1186/2042-4280-1-6.

Finke, J., M. Rowe, B. Kallin, I. Ernberg, A. Rosén, J. Dillner, and G. Klein. 1987.

Monoclonal and polyclonal antibodies against Epstein-Barr virus nuclear antigen 5 (EBNA-5) detect multiple protein species in Burkitt's lymphoma and lymphoblastoid cell lines. *J. Virol.* 61:3870–8.

Found, C., and D.A. Thorley-lawson. 2001. Epstein-Barr virus : exploiting the immune system. 1.

Fox, C.P., T.A. Haigh, G.S. Taylor, H.M. Long, S.P. Lee, C. Shannon-Lowe, S. O'Connor, C.M. Bollard, J. Iqbal, W.C. Chan, A.B. Rickinson, A.I. Bell, and M. Rowe. 2010. A novel latent membrane 2 transcript expressed in Epstein-Barr virus-positive NK- and T-cell lymphoproliferative disease encodes a target for cellular immunotherapy. *Blood*. 116:3695–3704. doi:10.1182/blood-2010-06-292268.

Fruehling, S., R. Swart, K.M. Dolwick, E. Kremmer, and R. Longnecker. 1998. Tyrosine 112 of latent membrane protein 2A is essential for protein tyrosine kinase loading and regulation of Epstein-Barr virus latency. *J. Virol.* 72:7796–806.

Gahn, T. a, and B. Sugden. 1995. An EBNA-1-dependent enhancer acts from a distance of 10 kilobase pairs to increase expression of the Epstein-Barr virus LMP gene. *J. Virol.* 69:2633–2636.

Garibal, J., E. Hollville, A.I. Bell, G.L. Kelly, B. Renouf, Y. Kawaguchi, A.B. Rickinson, and J. Wiels. 2007. Truncated form of the Epstein-Barr virus protein EBNA-LP protects against caspase-dependent apoptosis by inhibiting protein phosphatase 2A. *J. Virol.* 81:7598–607. doi:10.1128/JVI.02435-06.

Gatto, D., and R. Brink. 2013. B cell localization: Regulation by EBI2 and its oxysterol ligand. *Trends Immunol.* 34:336–341. doi:10.1016/j.it.2013.01.007.

Gregorovic, G., R. Bosshard, C.E. Karstegl, R.E. White, S. Pattle, A.K.S. Chiang, O. Dittrich-Breiholz, M. Kracht, R. Russ, and P.J. Farrell. 2011. Cellular gene expression that correlates with EBER expression in Epstein-Barr Virus-infected lymphoblastoid cell lines. *J. Virol.* 85:3535–45. doi:10.1128/JVI.02086-10.

Grossman, S.R., E. Johannsen, X. Tong, R. Yalamanchili, and E. Kieff. 1994. The Epstein-Barr virus nuclear antigen 2 transactivator is directed to response elements by the J kappa recombination signal binding protein. *Proc. Natl. Acad. Sci. U. S. A.* 91:7568–72. doi:10.1073/pnas.91.16.7568.

Grötzinger, T., K. Jensen, and H. Will. 1996. The interferon (IFN)-stimulated gene Sp100

promoter contains an IFN-γ activation site and an imperfect IFN-stimulated response element which mediate type I IFN inducibility. *J. Biol. Chem.* 271:25253–25260. doi:10.1074/jbc.271.41.25253.

Grundhoff, A., and D. Ganem. 2003. The Latency-Associated Nuclear Antigen of Kaposi ' s Sarcoma-Associated Herpesvirus Permits Replication of Terminal The Latency-Associated Nuclear Antigen of Kaposi ' s Sarcoma-Associated Herpesvirus Permits Replication of Terminal Repeat-Containing Plasm. 77:2779–2783. doi:10.1128/JVI.77.4.2779.

Guldner, H.H., C. Szostecki, P. Schröder, U. Matschl, K. Jensen, C. Lüders, H. Will, and T. Sternsdorf. 1999. Splice variants of the nuclear dot-associated Sp100 protein contain homologies to HMG-1 and a human nuclear phosphoprotein-box motif. *J. Cell Sci.* 112 (Pt 5:733–747.

Ha, Y.J., Y.-C. Mun, C.-M. Seong, and J.R. Lee. 2008. Characterization of phenotypically distinct B-cell subsets and receptor-stimulated mitogen-activated protein kinase activation in human cord blood B cells. *J. Leukoc. Biol.* 84:1557–1564. doi:10.1189/jlb.0706457.

Hammerschmidt, W., and B. Sugden. 1988. Identification and Characterization of Orilyt, A Lytic Origin of Dna-Replication of Epstein-Barr Virus. *Cell*. 55:427–433.

Hammerschmidt, W., and B. Sugden. 1989. Genetic analysis of immortalizing functions of Epstein-Barr virus in human B lymphocytes. *Nature*. 340:393–7. doi:10.1038/340393a0.

Hammerschmidt, W., B. Sugden, and V. Baichwal. 1989. The transforming domain alone of the latent membrane protein of Epstein- Barr virus is toxic to cells when expressed at high levels. *J Virol*. 63:2469–2475.

Harada, S., and E. Kieff. 1997. Epstein-Barr virus nuclear protein LP stimulates EBNA-2 acidic domain-mediated transcriptional activation. *J. Virol.* 71:6611–8.

Hart, S.L., L. Collins, K. Gustafsson, and J.W. Fabre. 1997. Integrin-mediated transfection with peptides containing arginine-glycine-aspartic acid domains. *Gene Ther.* 4:1225–1230.

Hayakawa, T., T. Haraguchi, H. Masumoto, and Y. Hiraoka. 2003. Cell cycle behavior of human HP1 subtypes: distinct molecular domains of HP1 are required for their centromeric localization during interphase and metaphase. *J. Cell Sci.* 116:3327–3338.

doi:10.1242/jcs.00635.

Henderson, G., W. Peng, L. Jin, G.-C. Perng, A.B. Nesburn, S.L. Wechsler, and C. Jones. 2002. Regulation of caspase 8- and caspase 9-induced apoptosis by the herpes simplex virus type 1 latency-associated transcript. *J. Neurovirol.* 8 Suppl 2:103–11. doi:10.1080/13550280290101085.

Hertle, M.L., C. Popp, S. Petermann, S. Maier, E. Kremmer, R. Lang, J. Mages, and B. Kempkes. 2009. Differential gene expression patterns of EBV infected EBNA-3A positive and negative human B lymphocytes. *PLoS Pathog.* 5. doi:10.1371/journal.ppat.1000506.

Heslop, H.E. 2005. Biology and treatment of Epstein-Barr virus-associated non-Hodgkin lymphomas. *Hematology Am. Soc. Hematol. Educ. Program*. 260–6. doi:10.1182/asheducation-2005.1.260.

Hicks, M.R., S.S. Al-mehairi, and A.J. Sinclair. 2003. The Zipper Region of Epstein-Barr Virus bZIP Transcription Factor Zta Is Necessary but Not Sufficient To Direct DNA Binding The Zipper Region of Epstein-Barr Virus bZIP Transcription Factor Zta Is Necessary but Not Sufficient To Direct DNA Binding. *J. Virol.* 77:8173–8177. doi:10.1128/JVI.77.14.8173.

Hjalgrim, H., J. Askling, K. Rostgaard, S. Hamilton-Dutoit, M. Frisch, J.-S. Zhang, M. Madsen, N. Rosdahl, H.B. Konradsen, H.H. Storm, and M. Melbye. 2003. Characteristics of Hodgkin's lymphoma after infectious mononucleosis. *N. Engl. J. Med.* 349:1324–1332. doi:10.1056/NEJMoa023141.

Hopwood, P., and D.H. Crawford. 2000. The role of EBV in post-transplant malignancies: a review. *J. Clin. Pathol.* 53:248–54. doi:10.1136/jcp.53.4.248.

Howe, J.G., and M. Di Shu. 1989. Epstein-Barr virus small RNA (EBER) genes: Unique transcription units that combine RNA polymerase II and III promoter elements. *Cell*. 57:825–834. doi:10.1016/0092-8674(89)90797-6.

Hsieh, J., T. Henkel, P. Salmon, E. Robey, M. Peterson, and S. Hayward. 1996. Truncated mammalian Notch1 activates CBF1/RBPJk-repressed genes by a mechanism resembling that of Epstein-Barr virus EBNA2. *Mol Cell Biol*. 16:952–959. doi:10.1128/MCB.16.3.952.

Hudson, G.S., P.J. Farrell, and B.G. Barrell. 1985. Two related but differentially expressed

potential membrane proteins encoded by the EcoRI Dhet region of Epstein-Barr virus B95-8. *J. Virol.* 53:528–35.

Humme, S., G. Reisbach, R. Feederle, H.-J. Delecluse, K. Bousset, W. Hammerschmidt, and A. Schepers. 2003. The EBV nuclear antigen 1 (EBNA1) enhances B cell immortalization several thousandfold. *Proc. Natl. Acad. Sci. U. S. A.* 100:10989–10994.

Hutchings, I. a, R.J. Tierney, G.L. Kelly, J. Stylianou, A.B. Rickinson, and A.I. Bell. 2006. Methylation status of the Epstein-Barr virus (EBV) BamHI W latent cycle promoter and promoter activity: analysis with novel EBV-positive Burkitt and lymphoblastoid cell lines. *J. Virol.* 80:10700–10711. doi:10.1128/JVI.01204-06.

Hwang, A.E., A.S. Hamilton, M.G. Cockburn, R. Ambinder, J. Zadnick, E.E. Brown, T.M. Mack, and W. Cozen. 2012. Evidence of genetic susceptibility to infectious mononucleosis: a twin study. *Epidemiol. Infect.* 140:2089–95. doi:10.1017/S0950268811002457.

Iizasa, H., A. Nanbo, J. Nishikawa, M. Jinushi, and H. Yoshiyama. 2012. Epstein-barr virus (EBV)-associated gastric carcinoma. *Viruses*. 4:3420–3439. doi:10.3390/v4123420.

Inman, G.J., and P.J. Farrell. 1995. Epstein-Barr virus EBNA-LP and transcription regulation properties of pRB, p107 and p53 in transfection assays. *J. Gen. Virol.* 76:2141–2149.

Invernizzi, F., M. Tigano, C. Dallabona, C. Donnini, I. Ferrero, M. Cremonte, D. Ghezzi, C. Lamperti, and M. Zeviani. 2013. A Homozygous Mutation in LYRM7/MZM1L Associated with Early Onset Encephalopathy, Lactic Acidosis, and Severe Reduction of Mitochondrial Complex III Activity. *Hum. Mutat.* 34:1619–1622. doi:10.1002/humu.22441.

Jayasooriya, S., T.I. de Silva, J. Njie-jobe, C. Sanyang, A.M. Leese, A.I. Bell, K.A. McAulay, P. Yanchun, H.M. Long, T. Dong, H.C. Whittle, A.B. Rickinson, S.L. Rowland-Jones, A.D. Hislop, and K.L. Flanagan. 2015. Early Virological and Immunological Events in Asymptomatic Epstein-Barr Virus Infection in African Children. *PLoS Pathog.* 11:1–18. doi:10.1371/journal.ppat.1004746.

Jenson, H., P. Farrell, and G. Miller. 1987. Sequences of the Epstein-Barr Virus (EBV) large internal repeat form the center of a 16-kilobase-pair palindrome of EBV (P3HR-1) heterogeneous DNA [published erratum appears in J Virol 1987 Sep;61(9):2950]. *J Virol*. 61:1495–1506.

de Jesus, O., P.R. Smith, L.C. Spender, C.E. Karstegl, H.H. Niller, D. Huang, and P.J. Farrell. 2003. Updated Epstein-Barr virus (EBV) DNA sequence and analysis of a promoter for the BART (CST, BARFO) RNAs of EBV. *J. Gen. Virol.* 84:1443–1450. doi:10.1099/vir.0.19054-0.

Jiménez-Ramírez, C., A.J. Brooks, L.P. Forshell, K. Yakimchuk, B. Zhao, T.Z. Fulgham, and C.E. Sample. 2006. Epstein-Barr virus EBNA-3C is targeted to and regulates expression from the bidirectional LMP-1/2B promoter. *J. Virol.* 80:11200–8. doi:10.1128/JVI.00897-06.

Jochner, N., D. Eick, U. Zimber-Strobl, M. Pawlita, G.W. Bornkamm, and B. Kempkes. 1996. Epstein-Barr virus nuclear antigen 2 is a transcriptional suppressor of the immunoglobulin mu gene: implications for the expression of the translocated c-myc gene in Burkitt's lymphoma cells. *EMBO J.* 15:375–82. doi:8617212.

Johannsen, E., M. Luftig, M.R. Chase, S. Weicksel, E. Cahir-McFarland, D. Illanes, D. Sarracino, and E. Kieff. 2004. Proteins of purified Epstein-Barr virus. *Proc. Natl. Acad. Sci. U. S. A.* 101:16286–91. doi:10.1073/pnas.0407320101.

Joseph, a M., G.J. Babcock, and D. a Thorley-Lawson. 2000. Cells expressing the Epstein-Barr virus growth program are present in and restricted to the naive B-cell subset of healthy tonsils. *J. Virol.* 74:9964–9971. doi:10.1128/JVI.74.21.9964-9971.2000.

Kaiser, C., G. Laux, D. Eick, N. Jochner, G.W. Bornkamm, and B. Kempkes. 1999. The proto-oncogene c-myc is a direct target gene of Epstein-Barr virus nuclear antigen 2. *J. Virol.* 73:4481–4484.

Kalchschmidt, J.S., R. Bashford-Rogers, K. Paschos, A.C.T. Gillman, C.T. Styles, P. Kellam, and M.J. Allday. 2016a. Epstein-Barr virus nuclear protein EBNA3C directly induces expression of AID and somatic mutations in B cells. *J. Exp. Med.* jem.20160120. doi:10.1084/jem.20160120.

Kalchschmidt, J.S., A.C.T. Gillman, K. Paschos, Q. Bazot, B. Kempkes, and M.J. Allday. 2016b. EBNA3C Directs Recruitment of RBPJ (CBF1) to Chromatin during the Process of Gene Repression in EBV Infected B Cells. *PLoS Pathog.* 12:1–30. doi:10.1371/journal.ppat.1005383.

Kalla, M., A. Schmeinck, M. Bergbauer, D. Pich, and W. Hammerschmidt. 2010. AP-1 homolog BZLF1 of Epstein-Barr virus has two essential functions dependent on the

epigenetic state of the viral genome. *Pnas*. 107:850–855. doi:10.1073/pnas.0911948107.

Kanda, T., M. Yajima, N. Ahsan, M. Tanaka, and K. Takada. 2004. Production of High-Titer Epstein-Barr Virus Recombinants Derived from Akata Cells by Using a Bacterial Artificial Chromosome System Production of High-Titer Epstein-Barr Virus Recombinants Derived from Akata Cells by Using a Bacterial Artificial Chromosom. doi:10.1128/JVI.78.13.7004.

Kanzler, H., R. Küppers, M.L. Hansmann, and K. Rajewsky. 1996. Hodgkin and Reed-Sternberg cells in Hodgkin's disease represent the outgrowth of a dominant tumor clone derived from (crippled) germinal center B cells. *J. Exp. Med.* 184:1495–1505. doi:10.1084/jem.184.4.1495.

Kashuba, E., K. Mattsson, K. Pokrovskaja, C. Kiss, M. Protopopova, B. Ehlin-Henriksson, G. Klein, and L. Szekely. 2003. EBV-encoded EBNA-5 associates with P14ARF in extranucleolar inclusions and prolongs the survival of P14ARF-expressing cells. *Int. J. Cancer*. 105:644–653. doi:10.1002/ijc.11124.

Kashuba, E., M. Yurchenko, K. Szirak, J. Stahl, G. Klein, and L. Szekely. 2005. Epstein-Barr virus-encoded EBNA-5 binds to Epstein-Barr virus-induced Fte1/S3a protein. *Exp. Cell Res.* 303:47–55. doi:10.1016/j.yexcr.2004.08.025.

Kashuba, E., M. Yurchenko, S.P. Yenamandra, B. Snopok, L. Szekely, B. Bercovich, A. Ciechanover, and G. Klein. 2011. Epstein-Barr virus-encoded EBNA-5 forms trimolecular protein complexes with MDM2 and p53 and inhibits the transactivating function of p53. *Int. J. Cancer*. 128:817–825. doi:10.1002/ijc.25414.

Kawaguchi, Y., K. Nakajima, M. Igarashi, T. Morita, M. Tanaka, M. Suzuki, A. Yokoyama, G. Matsuda, K. Kato, M. Kanamori, and K. Hirai. 2000. Interaction of Epstein-Barr virus nuclear antigen leader protein (EBNA-LP) with HS1-associated protein X-1: implication of cytoplasmic function of EBNA-LP. *J Virol*. 74:10104–10111. doi:10.1128/JVI.74.21.10104-10111.2000.

Kaye, K.M., K.M. Izumi, and E. Kieff. 1993. Epstein-Barr virus latent membrane protein 1 is essential for B-lymphocyte growth transformation. *Proc. Natl. Acad. Sci. U. S. A.* 90:9150–4. doi:10.1073/pnas.90.19.9150.

Kelly, G.L., H.M. Long, J. Stylianou, W.A. Thomas, A. Leese, A.I. Bell, G.W. Bornkamm, J. Mautner, A.B. Rickinson, and M. Rowe. 2009. An epstein-barr virus anti-apoptotic

protein constitutively expressed in transformed cells and implicated in burkitt lymphomagenesis: The Wp/BHRF1 link. *PLoS Pathog.* 5. doi:10.1371/journal.ppat.1000341.

Kelly, G.L., A.E. Milner, R.J. Tierney, D.S.G. Croom-carter, M. Altmann, A.I. Bell, A.B. Rickinson, and W. Hammerschmidt. 2005. Epstein-Barr Virus Nuclear Antigen 2 (EBNA2) Gene Deletion Is Consistently Expression in Burkitt ' s Lymphoma Cells and with Increased Resistance to Apoptosis Epstein-Barr Virus Nuclear Antigen 2 (EBNA2) Gene Deletion Is Consistently Linked with EBNA3. 2. doi:10.1128/JVI.79.16.10709.

Kelly, G.L., J. Stylianou, J. Rasaiyaah, W. Wei, W. Thomas, D. Croom-Carter, C. Kohler, R. Spang, C. Woodman, P. Kellam, A.B. Rickinson, and A.I. Bell. 2013. Different Patterns of Epstein-Barr Virus Latency in Endemic Burkitt Lymphoma (BL) Lead to Distinct Variants within the BL-Associated Gene Expression Signature. *J. Virol.* 87:2882–2894. doi:10.1128/JVI.03003-12.

Kerur, N., M.V. Veettil, N. Sharma-Walia, V. Bottero, S. Sadagopan, P. Otageri, and B. Chandran. 2011. IFI16 Acts as a Nuclear Pathogen Sensor to Induce the Inflammasome in Response to Kaposi Sarcoma-Associated Herpesvirus Infection. *Cell Host Microbe*. 9:363–375. doi:10.1016/j.chom.2011.04.008.

Kilger, E., A. Kieser, M. Baumann, and W. Hammerschmidt. 1998. Epstein-Barr virus-mediated B-cell proliferation is dependent upon latent membrane protein 1, which simulates an activated CD40 receptor. *EMBO J.* 17:1700–1709. doi:10.1093/emboj/17.6.1700.

Kirchmaier, a L., and B. Sugden. 1998. Rep*: a viral element that can partially replace the origin of plasmid DNA synthesis of Epstein-Barr virus. *J. Virol.* 72:4657–4666.

Kitay, M.K., and D.T. Rowe. 1996a. Protein-protein interactions between Epstein-Barr virus nuclear antigen-LP and cellular gene products: binding of 70-kilodalton heat shock proteins. *Virology*. 220:91–99. doi:10.1006/viro.1996.0289.

Kitay, M.K., and D.T. Rowe. 1996b. Cell Cycle Stage-Specific Phosphorylation of the Epstein-Barr Virus Immortalization Protein EBNA-LP. *J. Virol.* 70:7885–7893.

Klein, U., G. Klein, B. Ehlin-Henriksson, K. Rajewsky, and R. Küppers. 1995. Burkitt's lymphoma is a malignancy of mature B cells expressing somatically mutated V region genes. *Mol. Med.* 1:495–505.

Knowles, D.M., E. Cesarman, a Chadburn, G. Frizzera, J. Chen, E. a Rose, and R.E. Michler. 1995. Correlative morphologic and molecular genetic analysis demonstrates three distinct categories of posttransplantation lymphoproliferative disorders. *Blood*. 85:552–565.

Kulwichit, W., R.H. Edwards, E.M. Davenport, J.F. Baskar, V. Godfrey, and N. Raab-Traub. 1998. Expression of the Epstein-Barr virus latent membrane protein 1 induces B cell lymphoma in transgenic mice. *Proc. Natl. Acad. Sci. U. S. A.* 95:11963–8. doi:10.1073/pnas.95.20.11963.

Kumar, S., T. Kimlinger, and W. Morice. 2010. Immunophenotyping in multiple myeloma and related plasma cell disorders. *Best Pract. Res. Clin. Haematol.* 23:433–451. doi:10.1016/j.beha.2010.09.002.

Küppers, R., and K. Rajewsky. 1998. The origin of Hodgkin and Reed/Sternberg cells in Hodgkin's disease. *Annu. Rev. Immunol.* 16:471–493. doi:10.1146/annurev.immunol.16.1.471.

Kutz, H., G. Reisbach, U. Schultheiss, and A. Kieser. 2008. The c-Jun N-terminal kinase pathway is critical for cell transformation by the latent membrane protein 1 of Epstein-Barr virus. *Virology*. 371:246–256. doi:10.1016/j.virol.2007.09.044.

Lai, E.C. 2002. Keeping a good pathway down: Transcriptional repression of Notch pathway target genes by CSL proteins. *EMBO Rep.* 3:840–845. doi:10.1093/embo-reports/kvf170.

Laichalk, L.L., and D. a Thorley-Lawson. 2005. Terminal Differentiation into Plasma Cells Initiates the Replicative Cycle of Epstein-Barr Virus In Vivo Terminal Differentiation into Plasma Cells Initiates the Replicative Cycle of Epstein-Barr Virus In Vivo. *J. Virol.* 79:1296–1307. doi:10.1128/JVI.79.2.1296.

Lallemand-Breitenbach, V., and H. de Thé. 2010. PML nuclear bodies. *Cold Spring Harb. Perspect. Biol.* 2:1–17. doi:10.1101/cshperspect.a000661.

Lee, N., W.N. Moss, T.A. Yario, and J.A. Steitz. 2015. EBV noncoding RNA binds nascent RNA to drive host PAX5 to viral DNA. *Cell*. 160:607–618. doi:10.1016/j.cell.2015.01.015.

Lerner, M.R., N.C. Andrews, G. Miller, and J.A. Steitz. 1981. Two small RNAs encoded by Epstein-Barr virus and complexed with protein are precipitated by antibodies from

patients with systemic lupus erythematosus. *Proc. Natl. Acad. Sci. U. S. A.* 78:805–9. doi:10.1073/pnas.78.2.805.

Levitskaya, J., M. Coram, V. Levitsky, S. Imreh, P.M. Steigerwald-Mullen, G. Klein, M.G. Kurilla, and M.G. Masucci. 1995. Inhibition of antigen processing by the internal repeat region of the Epstein-Barr virus nuclear antigen-1. *Nature*. 375:685–8. doi:10.1038/375685a0.

Liang, C.L., J.L. Chen, Y.P.P. Hsu, J.T. Ou, and Y.S. Chang. 2002. Epstein-Barr virus BZLF1 gene is activated by transforming growth factor-β through cooperativity of smads and c-Jun/c-Fos proteins. *J. Biol. Chem.* 277:23345–23357. doi:10.1074/jbc.M107420200.

Lindahl, T., A. Adams, G. Bjursell, G. Bornkamm, C. Kaschka-Dierich, and U. Jehn. 1976. Covalently closed circular duplex DNA of Epstein-Barr virus in a human lymphoid cell line. *J Mol Biol*. 102:511–530. doi:10.1016/0022-2836(76)90331-4.

Ling, P.D., R.S. Peng, A. Nakajima, J.H. Yu, J. Tan, S.M. Moses, W.-H. Yang, B. Zhao, E. Kieff, K.D. Bloch, and D.B. Bloch. 2005. Mediation of Epstein-Barr virus EBNA-LP transcriptional coactivation by Sp100. *EMBO J.* 24:3565–75. doi:10.1038/sj.emboj.7600820.

Ling, P.D., J. Tan, and R. Peng. 2009. Nuclear-cytoplasmic shuttling is not required for the Epstein-Barr virus EBNA-LP transcriptional coactivation function. *J. Virol.* 83:7109–7116. doi:10.1128/JVI.00654-09.

Liu, Y.J., D.E. Joshua, G.T. Williams, C.A. Smith, J. Gordon, and I.C. MacLennan. 1989. Mechanism of antigen-driven selection in germinal centres. *Nature*. 342:929–31. doi:10.1038/342929a0.

Longnecker, R., C.L. Miller, X.Q. Miao, B. Tomkinson, and E. Kieff. 1993. The last seven transmembrane and carboxy-terminal cytoplasmic domains of Epstein-Barr virus latent membrane protein 2 (LMP2) are dispensable for lymphocyte infection and growth transformation in vitro. *J. Virol.* 67:2006–13.

Lu, F., H.S. Chen, A. V. Kossenkov, K. DeWispeleare, K.J. Won, and P.M. Lieberman. 2016. EBNA2 Drives Formation of New Chromosome Binding Sites and Target Genes for B-Cell Master Regulatory Transcription Factors RBP-jκ and EBF1. *PLoS Pathog.* 12:1–24. doi:10.1371/journal.ppat.1005339.

Lupton, S., and a J. Levine. 1985. Mapping genetic elements of Epstein-Barr virus that facilitate extrachromosomal persistence of Epstein-Barr virus-derived plasmids in human cells. *Mol. Cell. Biol.* 5:2533–2542. doi:10.1128/MCB.5.10.2533.

Lynch, D.T., J.S. Zimmerman, and D.T. Rowe. 2002. Epstein-Barr virus latent membrane protein 2B (LMP2B) co-localizes with LMP2A in perinuclear regions in transiently transfected cells. *J. Gen. Virol.* 83:1025–1035. doi:10.1099/0022-1317-83-5-1025.

Mackey, D., and B. Sugden. 1999. The linking regions of EBNA1 are essential for its support of replication and transcription. *Mol. Cell. Biol.* 19:3349–3359.

Mancao, C., and W. Hammerschmidt. 2007. Epstein-Barr virus latent membrane protein 2A is a B-cell receptor mimic and essential for B-cell survival. *Blood*. 110:3715–21. doi:10.1182/blood-2007-05-090142.

Manet, E., H. Gruffat, M.C. Trescol-Biemont, N. Moreno, P. Chambard, J.F. Giot, and A. Sergeant. 1989. Epstein-Barr virus bicistronic mRNAs generated by facultative splicing code for two transcriptional trans-activators. *EMBO J.* 8:1819–26.

Mannick, J.B., J.I. Cohen, M. Birkenbach, a Marchini, and E. Kieff. 1991. The Epstein-Barr virus nuclear protein encoded by the leader of the EBNA RNAs is important in B-lymphocyte transformation. *J. Virol.* 65:6826–6837.

Mannick, J.B., X. Tong, A. Hemnes, and E. Kieff. 1995. The Epstein-Barr virus nuclear antigen leader protein associates with hsp72/hsc73. *J Virol*. 69:8169–8172.

Maruo, S., Y. Wu, S. Ishikawa, T. Kanda, D. Iwakiri, and K. Takada. 2006. Epstein-Barr virus nuclear protein EBNA3C is required for cell cycle progression and growth maintenance of lymphoblastoid cells. *Proc. Natl. Acad. Sci. U. S. A.* 103:19500–5. doi:10.1073/pnas.0604919104.

McCann, E.M., G.L. Kelly, A.B. Rickinson, and A.I. Bell. 2001. Genetic analysis of the Epstein-Barr virus-coded leader protein EBNA-LP as a co-activator of EBNA2 function. *J. Gen. Virol.* 82:3067–3079.

Megyola, C., J. Ye, and S. Bhaduri-McIntosh. 2011. Identification of a sub-population of B cells that proliferates after infection with Epstein-Barr virus. *Virol. J.* 8:84. doi:10.1186/1743-422X-8-84.

Miller, G., and M. Lipman. 1973. Release of infectious Epstein-Barr virus by transformed marmoset leukocytes. *Proc. Natl. Acad. Sci. U. S. A.* 70:190–4.

doi:10.1073/pnas.70.1.190.

Moss, W.N., N. Lee, G. Pimienta, and J. a Steitz. 2014. RNA families in Epstein-Barr virus. *RNA Biol.* 11:10–7. doi:10.4161/rna.27488.

Moss, W.N., and J. a Steitz. 2013. Genome-wide analyses of Epstein-Barr virus reveal conserved RNA structures and a novel stable intronic sequence RNA. *BMC Genomics*. 14:543. doi:10.1186/1471-2164-14-543.

Müller, S., and A. Dejean. 1999. Viral immediate-early proteins abrogate the modification by SUMO-1 of PML and Sp100 proteins, correlating with nuclear body disruption. *J. Virol.* 73:5137–43.

Negorev, D.G., O. V. Vladimirova, A. Ivanov, F. Rauscher, and G.G. Maul. 2006. Differential Role of Sp100 Isoforms in Interferon-Mediated Repression of Herpes Simplex Virus Type 1 Immediate-Early Protein Expression. *J. Virol.* 80:8019–8029. doi:10.1128/JVI.02164-05.

Neuhierl, B., R. Feederle, W. Hammerschmidt, and H.J. Delecluse. 2002. Glycoprotein gp110 of Epstein-Barr virus determines viral tropism and efficiency of infection. *Proc. Natl. Acad. Sci. U. S. A.* 99:15036–41. doi:10.1073/pnas.232381299.

Niedobitek, G. 2000. Epstein-Barr virus infection in the pathogenesis of nasopharyngeal carcinoma. *Mol. Pathol.* 53:248–54. doi:10.1007/s12250-015-3592-5.

Nikitin, P.A., C.M. Yan, E. Forte, A. Bocedi, J.P. Tourigny, R.E. White, M.J. Allday, A. Patel, S.S. Dave, W. Kim, K. Hu, J. Guo, D. Tainter, E. Rusyn, and M.A. Luftig. 2010. An ATM/Chk2-mediated DNA damage-responsive signaling pathway suppresses Epstein-Barr virus transformation of primary human B cells. *Cell Host Microbe*. 8:510–22. doi:10.1016/j.chom.2010.11.004.

Ning, S., A.M. Hahn, L.E. Huye, and J.S. Pagano. 2003. Interferon regulatory factor 7 regulates expression of Epstein-Barr virus latent membrane protein 1: a regulatory circuit. *J. Virol.* 77:9359–68. doi:10.1128/JVI.77.17.9359.

Nitsche, F., A. Bell, A. Rickinson, F. Nitsche, and A. Bell. 1997. Epstein-Barr virus leader protein enhances EBNA-2-mediated transactivation of latent membrane protein 1 expression : a role for the W1W2 repeat domain . Epstein-Barr Virus Leader Protein Enhances EBNA-2- Mediated Transactivation of Latent Membrane Protein.

Noda, C., T. Murata, T. Kanda, H. Yoshiyama, A. Sugimoto, D. Kawashima, S. Saito, H.

Isomura, and T. Tsurumi. 2011. Identification and characterization of CCAAT enhancer-binding protein (C/EBP) as a transcriptional activator for Epstein-Barr virus oncogene latent membrane protein 1. *J. Biol. Chem.* 286:42524–42533. doi:10.1074/jbc.M111.271734.

Nonkwelo, C., J. Skinner, A. Bell, A. Rickinson, and J. Sample. 1996. Transcription start sites downstream of the Epstein-Barr virus (EBV) Fp promoter in early-passage Burkitt lymphoma cells define a fourth promoter for expression of the EBV EBNA-1 protein. *J. Virol.* 70:623–627.

Palser, A.L., N.E. Grayson, R.E. White, C. Corton, S. Correia, M.M. Ba Abdullah, S.J. Watson, M. Cotten, J.R. Arrand, P.G. Murray, M.J. Allday, A.B. Rickinson, L.S. Young, P.J. Farrell, and P. Kellam. 2015. Genome diversity of Epstein-Barr virus from multiple tumor types and normal infection. *J. Virol.* 89:5222–37. doi:10.1128/JVI.03614-14.

Parker, B.D., A. Bankier, S. Satchwell, B. Barrell, and P.J. Farrell. 1990. Sequence and transcription of Raji Epstein-Barr virus DNA spanning the B95-8 deletion region. *Virology*. 179:339–346. doi:10.1016/0042-6822(90)90302-8.

Parkin, D.M. 2006. The global health burden of infection-associated cancers in the year 2002. *Int. J. Cancer*. 118:3030–3044. doi:10.1002/ijc.21731.

Paulson, E.J., and S.H. Speck. 1999. Differential methylation of Epstein-Barr virus latency promoters facilitates viral persistence in healthy seropositive individuals. *J. Virol.* 73:9959–9968.

Pegtel, D.M., K. Cosmopoulos, D.A. Thorley-Lawson, M.A.J. van Eijndhoven, E.S. Hopmans, J.L. Lindenberg, T.D. de Gruijl, T. Würdinger, and J.M. Middeldorp. 2010. Functional delivery of viral miRNAs via exosomes. *Proc. Natl. Acad. Sci. U. S. A.* 107:6328–33. doi:10.1073/pnas.0914843107.

Peng, C.-W., Y. Xue, B. Zhao, E. Johannsen, E. Kieff, and S. Harada. 2004. Direct interactions between Epstein-Barr virus leader protein LP and the EBNA2 acidic domain underlie coordinate transcriptional regulation. *Proc. Natl. Acad. Sci. U. S. A.* 101:1033–8. doi:10.1073/pnas.0307808100.

Peng, C.W., B. Zhao, H.C. Chen, M.L. Chou, C.Y. Lai, S.Z. Lin, H.Y. Hsu, and E. Kieff. 2007. Hsp72 up-regulates Epstein-Barr virus EBNALP coactivation with EBNA2.

Blood. 109:5447–5454. doi:10.1182/blood-2006-08-040634.

Peng, R., A. V Gordadze, E.M. Fuentes Pananá, F. Wang, J. Zong, G.S. Hayward, J. Tan, and P.D. Ling. 2000a. Sequence and functional analysis of EBNA-LP and EBNA2 proteins from nonhuman primate lymphocryptoviruses. *J. Virol.* 74:379–389. doi:10.1128/JVI.74.1.379-389.2000.

Peng, R., S.C. Moses, J. Tan, E. Kremmer, and P.D. Ling. 2005. The Epstein-Barr virus EBNA-LP protein preferentially coactivates EBNA2-mediated stimulation of latent membrane proteins expressed from the viral divergent promoter. *J. Virol.* 79:4492–505. doi:10.1128/JVI.79.7.4492-4505.2005.

Peng, R., J. Tan, and P.D. Ling. 2000b. Conserved Regions in the Epstein-Barr Virus Leader Protein Define Distinct Domains Required for Nuclear Localization and Transcriptional Cooperation with EBNA2. *J. Virol.* 74:9953–9963. doi:10.1128/JVI.74.21.9953-9963.2000.

Petti, L., C. Sample, and E. Kieff. 1990. Subnuclear localization and phosphorylation of Epstein-Barr virus latent infection nuclear proteins. *Virology*. 176:563–574. doi:10.1016/0042-6822(90)90027-O.

Phillips, J.E., and V.G. Corces. 2009. CTCF: master weaver of the genome. *Cell*. 137:1194–211. doi:10.1016/j.cell.2009.06.001.

Pokrovskaja, K., K. Mattsson, E. Kashuba, G. Klein, and L. Szekely. 2001. Proteasome inhibitor induces nucleolar translocation of Epstein-Barr virus-encoded EBNA-5. *J. Gen. Virol.* 82:345–358.

Portal, D., a Rosendorff, and E. Kieff. 2006. Epstein-Barr nuclear antigen leader protein coactivates transcription through interaction with histone deacetylase 4. *Proc. Natl. Acad. Sci. U. S. A.* 103:19278–83. doi:10.1073/pnas.0609320103.

Portal, D., B. Zhao, M. a Calderwood, T. Sommermann, E. Johannsen, and E. Kieff. 2011. EBV nuclear antigen EBNALP dismisses transcription repressors NCoR and RBPJ from enhancers and EBNA2 increases NCoR-deficient RBPJ DNA binding. *Proc. Natl. Acad. Sci. U. S. A.* 108:7808–13. doi:10.1073/pnas.1104991108.

Portal, D., H. Zhou, B. Zhao, P. V Kharchenko, E. Lowry, L. Wong, J. Quackenbush, D. Holloway, S. Jiang, Y. Lu, and E. Kieff. 2013. Epstein-Barr virus nuclear antigen leader protein localizes to promoters and enhancers with cell transcription factors and EBNA2.

Proc. Natl. Acad. Sci. U. S. A. 110:18537–42. doi:10.1073/pnas.1317608110.

Pratt, Z.L., J. Zhang, and B. Sugden. 2012. The latent membrane protein 1 (LMP1) oncogene of Epstein-Barr virus can simultaneously induce and inhibit apoptosis in B cells. *J. Virol.* 86:4380–93. doi:10.1128/JVI.06966-11.

Price, a. M., J.P. Tourigny, E. Forte, R.E. Salinas, S.S. Dave, and M. a. Luftig. 2012. Analysis of Epstein-Barr Virus-Regulated Host Gene Expression Changes through Primary B-Cell Outgrowth Reveals Delayed Kinetics of Latent Membrane Protein 1-Mediated NF- B Activation. *J. Virol.* 86:11096–11106. doi:10.1128/JVI.01069-12.

Radkov, S. a, M. Bain, P.J. Farrell, M. West, M. Rowe, and M.J. Allday. 1997. Epstein-Barr virus EBNA3C represses Cp, the major promoter for EBNA expression, but has no effect on the promoter of the cell gene CD21. *J. Virol.* 71:8552–62.

Ragoczy, T., and G. Miller. 1999. Role of the epstein-barr virus RTA protein in activation of distinct classes of viral lytic cycle genes. *J. Virol.* 73:9858–66.

Randak, C., T. Brabletz, M. Hergenröther, I. Sobotta, and E. Serfling. 1990. Cyclosporin A suppresses the expression of the interleukin 2 gene by inhibiting the binding of lymphocyte-specific factors to the IL-2 enhancer. *EMBO J.* 9:2529–2536.

Reusch, J.A., D.M. Nawandar, K.L. Wright, S.C. Kenney, and J.E. Mertz. 2015. Cellular differentiation regulator BLIMP1 induces Epstein-Barr virus lytic reactivation in epithelial and B cells by activating transcription from both the R and Z promoters. *J. Virol.* 89:1731–43. doi:10.1128/JVI.02781-14.

Rickinson, A.B., L.S. Young, and M. Rowe. 1987. Influence of the Epstein-Barr Virus Nuclear Antigen EBNA 2 on the Growth Phenotype of Virus-Transformed B Cells. *J. Virol.* 61:1310–1317.

Robertson, E.S., J. Lin, and E. Kieff. 1996. 1996-J Virol-Robertson-The amino-terminal domains of Epstein-Barr virus nuclear proteins 3A 3B and 3C interact with RBPJ(kappa). *J. Virol.* 70:3068–74.

Robertson, E.S., B. Tomkinson, and E. Kieff. 1994. An Epstein-Barr virus with a 58-kilobase-pair deletion that includes BARF0 transforms B lymphocytes in vitro. *J. Virol.* 68:1449–1458.

Rogers, R.P., M. Woisetschlaeger, and S.H. Speck. 1990. Alternative splicing dictates translational Epstein -Barr virus transcripts start in. 9:2273–2277.

Ropero, S., and M. Esteller. 2007. The role of histone deacetylases (HDACs) in human cancer. *Mol. Oncol.* 1:19–25. doi:10.1016/j.molonc.2007.01.001.

Roughan, J.E., and D. a Thorley-Lawson. 2009. The intersection of Epstein-Barr virus with the germinal center. *J. Virol.* 83:3968–76. doi:10.1128/JVI.02609-08.

Rovedo, M., and R. Longnecker. 2007. Epstein-barr virus latent membrane protein 2B (LMP2B) modulates LMP2A activity. *J. Virol.* 81:84–94. doi:10.1128/JVI.01302-06.

Rowe, D.T. 1999. [Frontiers in Bioscience 4, d346-371, March 15, 1999] EPSTEIN-BARR VIRUS IMMORTALIZATION AND LATENCY David T. Rowe. 346–371.

Rowe, M., L. Fitzsimmons, and A.I. Bell. 2014. Epstein-Barr virus and Burkitt lymphoma. *Chin. J. Cancer*. 33:609–619. doi:10.5732/cjc.014.10190.

Rowe, M., L.S. Young, K. Cadwallader, L. Petti, E. Kieff, and A.B. Rickinson. 1989. Distinction between Epstein-Barr virus type A (EBNA 2A) and type B (EBNA 2B) isolates extends to the EBNA 3 family of nuclear proteins. *J. Virol.* 63:1031–9.

Sadler, R.H., and N. Raab-Traub. 1995. The Epstein-Barr virus 3.5-kilobase latent membrane protein 1 mRNA initiates from a TATA-Less promoter within the first terminal repeat. *J. Virol.* 69:4577–81.

Sample, J., M. Hummel, D. Braun, M. Birkenbach, and E. Kieff. 1986. Nucleotide sequences of mRNAs encoding Epstein-Barr virus nuclear proteins : A probable transcriptional initiation site. 83:5096–5100.

Sample, J., D. Liebowitz, and E. Kieff. 1989. Two related Epstein-Barr virus membrane proteins are encoded by separate genes. *J. Virol.* 63:933–7.

Sánchez, E., T. Lobo, J.L. Fox, M. Zeviani, D.R. Winge, and E. Fernández-Vizarra. 2013. LYRM7/MZM1L is a UQCRFS1 chaperone involved in the last steps of mitochondrial Complex III assembly in human cells. *Biochim. Biophys. Acta*. 1827:285–93. doi:10.1016/j.bbabio.2012.11.003.

Schepers, A., D. Pich, and W. Hammerschmidt. 1996. Activation of oriLyt, the lytic origin of DNA replication of Epstein-Barr virus, by BZLF1. *Virology*. 220:367–376. doi:10.1006/viro.1996.0325.

Scott, M.S., F.M. Boisvert, M.D. McDowall, A.I. Lamond, and G.J. Barton. 2010. Characterization and prediction of protein nucleolar localization sequences. *Nucleic*

Acids Res. 38:7388–7399. doi:10.1093/nar/gkq653.

Selin, L.K., S.M. Varga, I.C. Wong, and R.M. Welsh. 1998. Protective heterologous antiviral immunity and enhanced immunopathogenesis mediated by memory T cell populations. *J. Exp. Med.* 188:1705–15. doi:10.1084/jem.188.9.1705.

Shaku, F., G. Matsuda, R. Furuya, C. Kamagata, M. Igarashi, M. Tanaka, M. Kanamori, Y. Nishiyama, N. Yamamoto, and Y. Kawaguchi. 2005. Development of a Monoclonal Antibody against Epstein-Barr Virus Nuclear Antigen Leader Protein (EBNA-LP) That Can Detect EBNA-LP Expressed in P3HR1 Cells. 49:477–483.

Shannon-Lowe, C., G. Baldwin, R. Feederle, A. Bell, A. Rickinson, and H.J. Delecluse. 2005. Epstein-Barr virus-induced B-cell transformation: Quantitating events from virus binding to cell outgrowth. *J. Gen. Virol.* 86:3009–3019. doi:10.1099/vir.0.81153-0.

Shannon-Lowe, C.D., B. Neuhierl, G. Baldwin, A.B. Rickinson, and H.-J. Delecluse. 2006. Resting B cells as a transfer vehicle for Epstein-Barr virus infection of epithelial cells. *Proc. Natl. Acad. Sci. U. S. A.* 103:7065–70. doi:10.1073/pnas.0510512103.

Sinclair, a J., and P.J. Farrell. 1995. Host cell requirements for efficient infection of quiescent primary B lymphocytes by Epstein-Barr virus. *J. Virol.* 69:5461–5468.

Sinclair, a J., I. Palmero, G. Peters, and P.J. Farrell. 1994. EBNA-2 and EBNA-LP cooperate to cause G0 to G1 transition during immortalization of resting human B lymphocytes by Epstein-Barr virus. *EMBO J.* 13:3321–3328.

Singh, V. V, N. Kerur, V. Bottero, S. Dutta, S. Chakraborty, M. a Ansari, N. Paudel, L. Chikoti, and B. Chandran. 2013. Kaposi's Sarcoma-Associated Herpesvirus Latency in Endothelial and B cells Activates Interferon Gamma-Inducible Protein 16 (IFI16) Mediated Inflammasomes. *J Virol*. 87:4417–4431. doi:10.1128/jvi.03282-12.

Skalska, L., R.E. White, M. Franz, M. Ruhmann, and M.J. Allday. 2010. Epigenetic repression of p16INK4A by latent epstein-barr virus requires the interaction of EBNA3A and EBNA3C with CtBP. *PLoS Pathog.* 6. doi:10.1371/journal.ppat.1000951.

Skalska, L., R.E. White, G.A. Parker, A.J. Sinclair, K. Paschos, and M.J. Allday. 2013. Induction of p16INK4a Is the Major Barrier to Proliferation when Epstein-Barr Virus (EBV) Transforms Primary B Cells into Lymphoblastoid Cell Lines. *PLoS Pathog.* 9. doi:10.1371/journal.ppat.1003187.

Skalsky, R.L., and B.R. Cullen. 2013. NIH Public Access. *Annu Rev Microbiol*. 64:123–141.

doi:10.1146/annurev.micro.112408.134243.Viruses.

Skare, J., and J.L. Strominger. 1980. Cloning and mapping of BamHI endonuclease fragments of DNA from the transforming B95-8 strain of Epstein-Barr virus (recombinant DNA/blot hybridization). *Biochemistry*. 77:3860–3864.

Smith, P.R., O. de Jesus, D. Turner, M. Hollyoake, C.E. Karstegl, B.E. Griffin, L. Karran, Y. Wang, S.D. Hayward, and P.J. Farrell. 2000. Structure and coding content of CST (BART) family RNAs of Epstein-Barr virus. *J. Virol.* 74:3082–3092. doi:10.1128/JVI.74.7.3082-3092.2000.

Spender, L.C., G.H. Cornish, B. Kempkes, P.J. Farrell, and B. Rowland. 2001. Direct and Indirect Regulation of Cytokine and Cell Cycle Proteins by EBNA-2 during Epstein-Barr Virus Infection Direct and Indirect Regulation of Cytokine and Cell Cycle Proteins by EBNA-2 during Epstein-Barr Virus Infection. 75:3537–3546. doi:10.1128/JVI.75.8.3537.

Strang, G., and A.B. Rickinson. 1987. In vitro expansion of Epstein-Barr virus-specific HLA-restricted cytotoxic T cells direct from the blood of infectious mononucleosis patients. *Immunology*. 62:647–654.

Sugden, B., and N. Warren. 1989. A promoter of Epstein-Barr virus that can function during latent infection can be transactivated by EBNA-1, a viral protein required for viral DNA replication during latent infection. *J. Virol.* 63:2644–9.

Sugimoto, M., Y. Furuichi, T. Ide, and M. Goto. 1999. Incorrect us of “immortalization” for B-lymphoblastoid cell lines transformed by Epstein-Barr virus. *J. Virol.* 73:9690–1.

Swaminathan, S., B. Tomkinson, and E. Kieff. 1991. Recombinant Epstein-Barr virus with small RNA (EBER) genes deleted transforms lymphocytes and replicates in vitro. *Proc. Natl. Acad. Sci. U. S. A.* 88:1546–50. doi:10.1073/pnas.88.4.1546.

Szekely, L., K. Pokrovskaja, W.Q. Jiang, H. de The, N. Ringertz, and G. Klein. 1996. The Epstein-Barr virus-encoded nuclear antigen EBNA-5 accumulates in PML-containing bodies. *J. Virol.* 70:2562–8.

Szekely, L., G. Selivanova, K.P. Magnusson, G. Klein, and K.G. Wiman. 1993. EBNA-5, an Epstein-Barr virus-encoded nuclear antigen, binds to the retinoblastoma and p53 proteins. *Proc. Natl. Acad. Sci. U. S. A.* 90:5455–9.

Takada, K., and Y. Ono. 1989. Synchronous and sequential activation of latently infected

Epstein-Barr virus genomes. *J. Virol.* 63:445–449.

Tan, J.T., E. Dudl, E. LeRoy, R. Murray, J. Sprent, K.I. Weinberg, and C.D. Surh. 2001. IL-7 is critical for homeostatic proliferation and survival of naive T cells. *Proc. Natl. Acad. Sci. U. S. A.* 98:8732–7. doi:10.1073/pnas.161126098.

Tempera, I., M. Klichinsky, and P.M. Lieberman. 2011. EBV latency types adopt alternative chromatin conformations. *PLoS Pathog.* 7. doi:10.1371/journal.ppat.1002180.

Thorley-Lawson, D.A., and A. Gross. 2004. Persistence of the Epstein–Barr Virus and the Origins of Associated Lymphomas. *N. Engl. J. Med.* 350:1328–1337. doi:10.1056/NEJMra032015.

Thorley-Lawson, D., and G. Babcock. 1999. A model for persistent infection with Epstein-Barr virus: the stealth virus of human B cells. *Life Sci.* 65:1433–1453.

Tierney, R.J., K.-Y.K. Kao, J.K. Nagra, and A.B. Rickinson. 2011. Epstein-Barr Virus BamHI W Repeat Number Limits EBNA2 / EBNA-LP Coexpression in Newly Infected B Cells and the Efficiency of B-Cell Transformation : a Rationale for the Multiple W Repeats in Wild-Type Virus Strains Epstein-Barr Virus BamHI W Repeat Number. *J. Virol.* 85:12362–12375. doi:10.1128/JVI.06059-11.

Tobollik, S., L. Meyer, M. Buettner, S. Klemmer, B. Kempkes, E. Kremmer, G. Niedobitek, and B. Jungnickel. 2006. Epstein-Barr virus nuclear antigen 2 inhibits AID expression during EBV-driven B-cell growth. *Blood*. 108:3859–3864. doi:10.1182/blood-2006-05-021303.

Tomkinson, B., and E. Kieff. 1992. Use of second-site homologous recombination to demonstrate that Epstein-Barr virus nuclear protein 3B is not important for lymphocyte infection or growth transformation in vitro. *J. Virol.* 66:2893–903.

Tomkinson, B., E. Robertson, and E. Kieff. 1993. Epstein-Barr virus nuclear proteins EBNA-3A and EBNA-3C are essential for B-lymphocyte growth transformation. *J. Virol.* 67:2014–2025.

Touitou, R., M. Hickabottom, G.A. Parker, M.J. Allday, and T.I.M. Crook. 2001. Physical and Functional Interactions between the Corepressor CtBP and the Epstein-Barr Virus Nuclear Antigen Physical and Functional Interactions between the Corepressor CtBP and the Epstein-Barr Virus Nuclear Antigen EBNA3C. *J. Virol.* 75:7749–55. doi:10.1128/JVI.75.16.7749.

Tsai, M.-H., A. Raykova, O. Klinke, K. Bernhardt, K. Gärtner, C.S. Leung, K. Geletneky, S. Sertel, C. Münz, R. Feederle, and H.-J. Delecluse. 2013. Spontaneous lytic replication and epitheliotropism define an Epstein-Barr virus strain found in carcinomas. *Cell Rep.* 5:458–70. doi:10.1016/j.celrep.2013.09.012.

Turro, E., A. Lewin, A. Rose, M.J. Dallman, and S. Richardson. 2010. MMBGX: A method for estimating expression at the isoform level and detecting differential splicing using whole-transcript affymetrix arrays. *Nucleic Acids Res.* 38:1413. doi:10.1093/nar/gkq071.

Tzellos, S., P.B. Correia, C.E. Karstegl, L. Cancian, J. Cano-Flanagan, M.J. McClellan, M.J. West, and P.J. Farrell. 2014. A single amino acid in EBNA-2 determines superior B lymphoblastoid cell line growth maintenance by Epstein-Barr virus type 1 EBNA-2. *J. Virol.* 88:8743–53. doi:10.1128/JVI.01000-14.

Vockerodt, M., F.Z. Cader, C. Shannon-Lowe, and P. Murray. 2014. Epstein-Barr virus and the origin of hodgkin lymphoma. *Chin. J. Cancer*. 33:591–597. doi:10.5732/cjc.014.10193.

Voss, T.C., I. a Demarco, C.F. Booker, and R.N. Day. 2005. Functional interactions with Pit-1 reorganize co-repressor complexes in the living cell nucleus. *J. Cell Sci.* 118:3277–3288. doi:10.1242/jcs.02450.

Wang, F., S.F. Tsang, M.G. Kurilla, J.I. Cohen, and E. Kieff. 1990. Epstein-Barr virus nuclear antigen 2 transactivates latent membrane protein LMP1. *J. Virol.* 64:3407–16.

White, R.E., M.A. Calderwood, and A. Whitehouse. 2003. Generation and precise modification of a herpesvirus saimiri bacterial artificial chromosome demonstrates that the terminal repeats are required for both virus production and episomal persistence. *J. Gen. Virol.* 84:3393–403. doi:10.1099/vir.0.19387-0.

White, R.E., I.J. Groves, E. Turro, J. Yee, E. Kremmer, and M.J. Allday. 2010. Extensive co-operation between the Epstein-Barr virus EBNA3 proteins in the manipulation of host gene expression and epigenetic chromatin modification. *PLoS One*. 5:e13979. doi:10.1371/journal.pone.0013979.

White, R.E., P.C. Rämer, K.N. Naresh, S. Meixlsperger, L. Pinaud, C. Rooney, B. Savoldo, R. Coutinho, C. Bödör, J. Gribben, H.A. Ibrahim, M. Bower, J.P. Nourse, M.K. Gandhi, J. Middeldorp, F.Z. Cader, P. Murray, C. Münz, and M.J. Allday. 2012. EBNA3B-deficient EBV promotes B cell lymphomagenesis in humanized mice and is found in

human tumors. *J. Clin. Invest.* 122:1487–1502. doi:10.1172/JCI58092.

White, R.E., R. Wade-Martins, and M.R. James. 2001. Sequences adjacent to oriP improve the persistence of Epstein-Barr virus-based episomes in B cells. *J Virol*. 75:11249–11252. doi:10.1128/JVI.75.22.11249-11252.2001.

Wilda, M., K. Busch, I. Klose, T. Keller, W. Woessmann, J. Kreuder, J. Harbott, and A. Borkhardt. 2004. Level of MYC overexpression in pediatric Burkitt's lymphoma is strongly dependent on genomic breakpoint location within the MYC locus. *Genes Chromosom. Cancer*. 41:178–182. doi:10.1002/gcc.20063.

Woellmer, A., J.M. Arteaga-Salas, and W. Hammerschmidt. 2012. BZLF1 Governs CpG-Methylated Chromatin of Epstein-Barr Virus Reversing Epigenetic Repression. *PLoS Pathog.* 8. doi:10.1371/journal.ppat.1002902.

Woellmer, A., and W. Hammerschmidt. 2014. NIH Public Access. 3:260–265. doi:10.1016/j.coviro.2013.03.005.Epstein-Barr.

Woisetschlaeger, M., J.L. Strominger, and S.H. Speck. 1989. Mutually exclusive use of viral promoters in Epstein-Barr virus latently infected lymphocytes. *Proc. Natl. Acad. Sci. U. S. A.* 86:6498–502.

Woisetschlaeger, M., C.N. Yandava, L.A. Furmanski, J.L. Strominger, and S.H. Speck. 1990. Promoter switching in Epstein-Barr virus during the initial stages of infection of B lymphocytes. 87:1725–1729.

Wysokenski, D. a, and J.L. Yates. 1989. Multiple EBNA1-binding sites are required to form an EBNA1-dependent enhancer and to activate a minimal replicative origin within oriP of Epstein-Barr virus. *J. Virol.* 63:2657–2666.

Xia, T., A.O. Hara, I. Araujo, J. Barreto, E. Carvalho, J. Bahia, J.C. Ramos, E. Luz, C. Pedroso, M. Manrique, L. Ngoc, C. Brites, D.P. Dittmer, and W.J.H. Jr. 2010. NIH Public Access. 68:1436–1442. doi:10.1158/0008-5472.CAN-07-5126.EBV.

Xie, J., H. Wu, C. Dai, Q. Pan, Z. Ding, D. Hu, B. Ji, Y. Luo, and X. Hu. 2014. Beyond Warburg effect--dual metabolic nature of cancer cells. *Sci. Rep.* 4:4927. doi:10.1038/srep04927.

Xing, L., and E. Kieff. 2007. Epstein-Barr virus BHRF1 micro- and stable RNAs during latency III and after induction of replication. *J. Virol.* 81:9967–75. doi:10.1128/JVI.02244-06.

Yajima, M., T. Kanda, and K. Takada. 2005. Critical Role of Epstein-Barr Virus (EBV) -Encoded RNA in Efficient EBV-Induced B-Lymphocyte Growth Transformation Critical Role of Epstein-Barr Virus (EBV) -Encoded RNA in Efficient EBV-Induced B-Lymphocyte Growth Transformation. 79:4298–4307. doi:10.1128/JVI.79.7.4298.

Yates, J.L., S.M. Camiolo, and J.M. Bashaw. 2000. The minimal replicator of Epstein-Barr virus oriP. *J. Virol.* 74:4512–4522. doi:10.1128/JVI.74.10.4512-4522.2000.

Ye, J., L. Gradoville, D. Daigle, and G. Miller. 2007. De novo protein synthesis is required for lytic cycle reactivation of Epstein-Barr virus, but not Kaposi's sarcoma-associated herpesvirus, in response to histone deacetylase inhibitors and protein kinase C agonists. *J. Virol.* 81:9279–91. doi:10.1128/JVI.00982-07.

Yee, J., R.E. White, E. Anderton, and M.J. Allday. 2011. Latent Epstein-Barr virus can inhibit apoptosis in B cells by blocking the induction of NOXA expression. *PLoS One*. 6:e28506. doi:10.1371/journal.pone.0028506.

Yokoyama, A., M. Tanaka, G. Matsuda, K. Kato, M. Kanamori, H. Kawasaki, H. Hirano, I. Kitabayashi, M. Ohki, K. Hirai, and Y. Kawaguchi. 2001. Identification of major phosphorylation sites of Epstein-Barr virus nuclear antigen leader protein (EBNA-LP): ability of EBNA-LP to induce latent membrane protein 1 cooperatively with EBNA-2 is regulated by phosphorylation. *J. Virol.* 75:5119–5128. doi:10.1128/JVI.75.11.5119-5128.2001.

Young, L.S., and C.W. Dawson. 2014. Epstein-Barr virus and nasopharyngeal carcinoma. *Chin. J. Cancer*. 33:581–590. doi:10.5732/cjc.014.10197.

Zhao, B., J. Zou, H. Wang, E. Johannsen, C. Peng, J. Quackenbush, J.C. Mar, C.C. Morton, M.L. Freedman, S.C. Blacklow, J.C. Aster, B.E. Bernstein, and E. Kieff. 2011. Epstein-Barr virus exploits intrinsic B-lymphocyte transcription programs to achieve immortal cell growth. *Proc. Natl. Acad. Sci. U. S. A.* 108:14902–7. doi:10.1073/pnas.1108892108.

Zimmermann, J., and W. Hammerschmidt. 1995. Structure and role of the terminal repeats of Epstein-Barr virus in processing and packaging of virion DNA. *J. Virol.* 69:3147–3155.